Impact of climate change on arctic shipping : Vessel damage and regulations

Kubat, Ivana; Collins, Anne; Gorman, Bob; Timco, Garry

https://doi.org/10.4224/12340992
Technical Report, 2006-02

CANADIAN HYDRAULICS CENTRE
CENTRE D'HYDRAULIQUE CANADIEN

Impact of Climate Change on Arctic Shipping: Vessel Damage and Regulations

Ivana Kubat, Anne Collins, Bob Gorman and Garry Timco

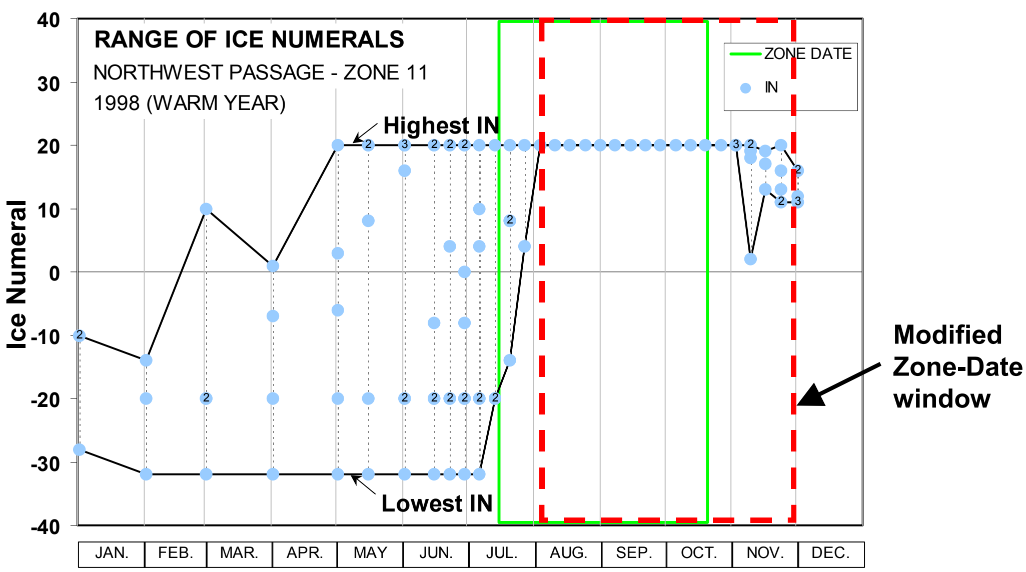

Technical Report CHC-TR-038

February 2006

National Research Council Canada
Conseil national de recherches Canada

CANADIAN HYDRAULICS CENTRE
CENTRE D'HYDRAULIQUE CANADIEN

Impact of Climate Change on Arctic Shipping: Vessel Damage and Regulations

Ivana Kubat, Anne Collins, Bob Gorman and Garry Timco

Technical Report CHC-TR-038

February 2006

National Research Council Canada
Conseil national de recherches Canada

CANADIAN HYDRAULICS CENTRE
CENTRE D'HYDRAULIQUE CANADIEN

Impact of Climate Change on Arctic Shipping: Vessel Damage and Regulations

Ivana Kubat[1], Anne Collins[1], Bob Gorman[2] and Garry Timco[1]

[1]Canadian Hydraulics Centre
National Research Council of Canada
Ottawa, Ont. K1A 0R6
Canada

[2]Enfotec
25 Tapiola Cres. Suite 206
Ottawa, Ont. K1P 2J7
Canada

Technical Report
CHC-TR-038

February 2006

ABSTRACT

The purpose of this project was to assess the impact of climate change on the likelihood and severity of damage to vessels operating in Artic waters, and address the impacts of climate change on the pollution prevention regulations governing ship traffic in the Arctic. Transport Canada has the responsibility for regulating Arctic shipping in Canada as part of the Arctic Shipping Pollution Prevention Regulations. A Zone/Date System (ZDS) is used North of the 60° latitude. The ZDS is based on historical data of ice conditions up to the early 1970's and on the premise that the ice conditions are consistent from year-to-year. The ZDS consists of sixteen geographic regions (Zones) and an associated Table that indicates the dates that each class of vessel is allowed in each geographical region. The Arctic Ice Regime Shipping System (AIRSS) is used by vessels wishing to access the Arctic Control Zones outside permissible dates for the vessels. The AIRSS, in contrast, allows shipping based on the actual, not historical, ice conditions.

In this project a methodology to evaluate Canada's Arctic shipping Regulations was developed. Length of the shipping season in the Northwest Passage and Hudson Strait for a colder than normal and a warmer than normal year was analyzed by both the ZDS and the AIRSS, and both systems were then compared. The ice conditions in the North West Passage (NWP) shipping lanes and the access routes to the Port of Churchill in Hudson Strait were analyzed and a potential of damage to vessels was assessed. Based on this study advice will be provided to Transport Canada regarding the need for regulatory reform in the Arctic due to climate change.

TABLE OF CONTENTS

LIST OF FIGURES

LIST OF TABLES

Impact of Climate Change on Arctic Shipping: Vessel Damage and Regulations

1. Introduction and Objectives

Canada has established the Climate Change Action Fund (CCAF) and Action Plan 2000 (AP 2000) to encourage projects and activities that will contribute to Canada's ability to meet its climate change obligations. The Climate Change Impacts and Adaptation Directorate (CCIAD), Natural Resources Canada coordinates the climate change impacts and adaptation activities in the CCAF/AP 2000. The Canadian Hydraulics Centre (CHC), of the National Research Council Canada, submitted a proposal to study impact of the climate change on Arctic shipping with respect to vessel damage and Regulations and obtained funding for the study.

The project was a two-year project, funded partially by the Climate Change Impact Adaptation Directorate and partially by Transport Canada. The project team was comprised of members of Transport Canada (TC) that have the authority for setting regulatory standards and for regulating Arctic shipping, the Canadian Hydraulics Centre (CHC) that has been working with Transport Canada for several years to ensure that the regulations have a solid scientific basis (Timco and Frederking 1996; Timco et al. 1997) and Enfotec Ltd. (a subsidiary of Fednav Limited of Montreal) that has been specializing in the provision of ice navigation support services to shipping companies. The CHC also closely worked with Canadian Ice Service (CIS) during the project.

The objectives of the project are to assess the impacts of climate change on the likelihood and severity of damage to vessels operating in Arctic waters, and to address the impacts of climate change on the pollution prevention regulations governing ship traffic in the Arctic. Advice will be provided to Transport Canada on whether the regulations can be adapted to meet climate change while maintaining reasonable access for ships to the Arctic with minimal impact on the environment.

This study will help to identify areas of concern for shipping in the north due to climate change. It will provide information which shipping companies can use to evaluate the length of the shipping season and to evaluate the type of ice-strengthened vessels that they will need to meet the pollution regulations.

2. Review of Previous Climate Change Work in the Arctic

Many studies investigating the climate trend have been done. The majority of them indicate that the perennial sea ice cover in the Arctic is declining. Comiso (2002) points out that the satellite data from 1978 to 2000 indicate a decline in sea ice cover in the Arctic as 9% per decade. The Canadian Centre for Climate Modelling and Analysis coupled global climate model (CGCM) projects the long-term decreasing trend in the annual mean sea-ice extent (Flato and Boer, 2001). Cavalieri et al. (1997) analyzed passive microwave satellite observations from 1978 to 1996 and found that the sea ice cover in the Arctic decreased by 3% per decade. The interannual variations are 2.3% of the annual mean with the 5-year period. The 3% per decade reduction in ice extents has also been reported for the Arctic Ocean with the greatest reduction occurring during the spring and summer period (Parkinson et al., 1999). The Parkinson et al. study found the greatest reduction in ice extent occurring in the Sea of Okhotsk and the Russian Arctic with increases in Baffin Bay, the Labrador Coast and in the Gulf of St. Lawrence. However, the study period of only 18 years coincided with heavier than normal ice conditions in the Canadian Arctic Archipelago (1978) and ended with historically higher than normal ice conditions in the Gulf of St.Lawrence and the Labrador Coast (1990-1995). It is likely that these results would show different patterns had it run over a longer period. There was no trend discernible within the Canadian Archipelago in their analysis.

Zhang et al. (2000) show a warming trend for the fall season across the Queen Elizabeth Islands in daily maximum and daily minimum temperatures for the period from 1950-1998. In other seasons the trends are less obvious. Flato and Brown (1996) investigated the sensitivity of land-fast ice to potential climate change and found that warming causes a decrease in maximum ice thickness and an increase in the length of the open water season. Rothrock et al. (1999) analyzed ice draft data obtained from the submarine cruises between 1958 and 1976 and compared it to data obtained from submarine cruises in 1990. They found that ice draft in 1990 was over 1 meter thinner than that measured between 1958 and 1976. The ice draft decreased the most in the central and eastern part of the Arctic Ocean. The authors also compared 1990s data to ice draft obtained from submarine cruises between 1993 and 1997 and found a declining trend at a rate of 0.1 m per year.

On the other hand, the results of Parkinson's study (Parkinson, 1992) indicate that sea ice extent increases in Hudson Bay, Baffin Bay/ Davis Strait, and in the Arctic Ocean. In this study Parkinson analyzed the Nimbus 7 scanning multichannel microwave radiometer (SMMR) data set covering period from October 24, 1978 to August 20, 1987. It is interesting to note that year 1986 was very cold year on record and that the trend in the Canadian Arctic air temperature between years 1979 and 1986 is decreasing. Parkinson's analysis shows that there is a trend toward milder conditions in the eastern Arctic and more severe ice conditions in the western Arctic for period 1979-1986. The interannual fluctuations in the length of the sea ice season are high.

Earlier findings of Arctic ice thinning up to 40% over the past 40 years have been largely discounted as inaccurate (Holloway and Sou, 2001).

A number of studies exist, which indicate that there is apparent trend in first-year (FY) ice melt in the Canadian Arctic Archipelago (Wilson et al. 2004, Howel and Yackel 2004, Melling 2002, Falkingham et al. 2001).

A study by Melling (2002) on the ice of the Svedrup Basin region of Archipelago noted that ice melts more rapidly within the Arctic Islands than over the Arctic Ocean due to the lack of the cold halocline within the Islands and the influence of the Atlantic warm water layer in this area. The study supports the theory that it is the ice plugs of the northern Svedrup that prevent the Arctic Ocean Old Ice from penetrating the Islands and that when these melt out in warm summers more Old Ice from Arctic Ocean invades into Canadian shipping channels. This ice will be thicker and more heavily ridged as a result of being exposed to oceanic heat flux for a shorter time in transit.

The ice plugs in the Nansen Sound and the Svedrup Channel of Queen Elizabeth Islands (QEI) broke only in years 1962 and 1998 (Agnew 2001, Jeffers et al. 2001). Year 1998 was one of the warmest years on record in the Canadian Arctic history. Maslanik et al. (1999) examined the 1998 sea ice glitch considering the preceding year ice conditions and the roles of atmospheric circulation. They analyzed the 1953-1997 data set.

Wilson et al. (2004) point out that after year 1998 the import of MY ice into the NWP increased and by year 2003 the region was covered by MY ice similar to conditions preceding the warm year 1998. The authors also indicate that there is an apparent trend in FY ice melt in the Canadian Arctic Archipelago, which will allow more MY ice to reach the NWP and the Beaufort Sea pack ice to shift south. This scenario will make shipping in the NWP equivalently challenging and hazardous to nowadays even if the climate warms.

Howell and Yackel (2004) assessed ship navigation variability from 1969-2001 for the western part of the NWP. As of now, the NWP is not feasible to uphold intercontinental shipping activities. The major drawback of future navigation in the NWP will be the invasion of MY into the NWP routes as a result of increased FY ice melt. Falkingham et al. (2001, 2002) also support the fact that an increase of MY ice drift into the NWP caused by reduction of FY ice will make shipping through the NWP more difficult and hazardous.

DF Dickins Associates Ltd. (1998) reviewed the historical ice conditions along the deep draft approach routes to the Beaufort/Coronation regions from the East (Parry Channel) and the West (Chukchi Sea) and determined the approximate level of reliability that could be expected for different vessels under extreme conditions that may have affected the completion of a successful sealift.

The most complete work in context of the Canadian north is the analysis of ice conditions by the Canadian Ice Service over the period 1969-2001 (Falkingham et al. 2001, 2002).

Conclusions of their study are that the sea ice cover in the Canadian Arctic decreased by about 15% over the period of 1969-2001, with considerable regional variation. In the Hudson Bay, the sea ice coverage during summer decreased by 40% over period 1971-2001 and 72% in the Labrador Sea over the same period. The average annual temperature measured at Resolute Bay meteorological station located in the centre of the NWP rose 1.3°C since 1969 or 2.5% per decade. Length of the shipping season (season with less than 5% ice cover) in the Hudson Bay has increased by about two weeks since 1971 (Falkingham, 2002). The authors indicate that period of three decades is an extremely short time to make any conclusions in the climatological sense. Their study is based on the Canadian Ice Service Digital database (Crocker and Carrieres 2000a, 2000b). The 32-year dataset (1969-2001) analyzed by Crocker et al. (in press) shows a large variability in sea ice conditions. The authors indicate that the short length of the dataset and the high natural variability make it difficult to extract patterns and trends. In cold years the ice cover can almost double while in warm years it can decrease by 50%. In summary they found a trend in ice cover decrease and increase in the length of the shipping season.

Polyakov et al. (2003) analyzed the long-term ice variability in Arctic and support the finding that a definitive conclusion cannot be made due to the lack of long-term observation. Their study was focused on examining the fast ice thickness and ice extent in Kara, Laptev, Siberian, and Chukchi Seas.

Brown and Cote (1992) investigated interannual variability of land-fast ice thickness and snow cover at four sites in the Canadian Arctic Islands, Alert Inlet, Eureka, Mould Bay, and Resolute, for period 1950-1989. The data shows a large fluctuation from one year to the next. The trends in maximum ice thickness and snow depth vary by location. There is no evidence of significant trends for Eureka and Mould Bay. Measurements obtained at Alert show trend of decreasing ice thickness, while at Resolute the trend is an increase of ice thickness. The authors point out that the snow cover, which acts as an insulation, is the most important factor influencing 30-60% of the variance in maximum land-fast ice thickness. The annual variation in air temperature influences less than 4% of the variance in maximum land-fast ice thickness.

Melling and Riedel (2005) summarized findings of continuous observations by sub-sea sonar from a 12-year draft record for seasonal pack ice in the Beaufort Sea. They found that there is a thinning trend, however the trend has low significance because the seasonal and inter-annual variability are large. Much longer time series than those presently available are required for climate change impact definitive evidence. The snow cover, ice circulation and ridging influence the variability and trend in the thickness and extent of seasonal ice.

Dumas et al. (2004) used meteorological data from Tuktoyaktuk station and a one-dimensional thermodynamic sea ice model (Flato and Brown, 1996) for simulating the ice thickness and land-fast ice duration under possible climate change scenarios. They found that the annual temperature increase of 4°C would decrease the ice duration by 3 weeks. They also investigated the influence of the snow cover on the ice duration and found that the snow accumulation plays also a large role in affecting the ice cover duration.

Comiso (2002) indicates that the Arctic system is a complex system controlled by many variables such as the Arctic Oscillation, the North Atlantic Oscillation (NAO), and the Pacific Decadal Oscillation, the effects which should be also considered. Also Parkinson et al. (1999) explain that the changes in the Arctic ice cover are tied to the large-scale atmospheric patterns of the NAO.

Mysak and Manak (1989) and Barnett (1980) noticed a 4-6 year fluctuation in the ice severity conditions in the western Arctic. They believe that 4-6 year cycle may be related to the natural interannual variability in the North Pacific sea-level pressure. The time-scale of the sea-ice anomaly fluctuations varies from region to region within the High Arctic.

There is much discussion in the literature on the existence of the Arctic Oscillation (AO) and the influence this has on the climate of the Arctic region (Dickson et al. 2000, Mysak and Manak 1989, Mysak 1986).

The existing work suggests that the climate change will influence the ice conditions in the Canadian Arctic shipping lanes. The volume of vessel traffic and vessel speed will increase with the predicted ice cover extent decrease, which will result in higher potential for vessel damage and pollution. The existing work, however, is not of sufficient detail to detect any regional differences across the NWP. It was found that the existing studies lack the detail required for the analysis specific to each of the shipping control zones that cover the Northwest Passage and that there is little use of the historical temperature data from stations in the Canadian Arctic in the analysis. Therefore this project focused on analyzing Melting degree days to determine if there are any differences or similarities among regions and to find if any pattern or relationship exists between number of melting degree days and melt of the Old Ice. Length of the shipping season based on the melting degree-days was analyzed for communities located along the NWP and approaches to Churchill. The two existing Regulatory Shipping Systems were compared. The focus of this study was on the portion of the Canadian Arctic that covers the Northwest Passage as well as the access to the port of Churchill through Hudson Strait.

3. Regulatory Shipping Systems

Transport Canada has the responsibility for regulating Arctic shipping in Canada as part of the Arctic Shipping Pollution Prevention Regulations (ASPPR). The Canadian Government drafted the ASPPR in 1972 to regulate navigation in Canadian waters north of 60°N latitude. This is done using a Zone/Date System (ZDS), which is based on the premise that nature is consistent from year-to-year. It consists of sixteen geographic regions (Zones) and an associated Table that indicates the dates that each class of vessel is allowed in each geographical region, Figure 1 and Table 1, respectively. The ship types and classes in the system are:
Arctic Class: 10, 8, 7, 6, 4, 3, 2, 1A, 1
Type Ships: A, B, C, D, E

The Arctic Class was normally but not accurately described as the thickness in feet of level ice that the vessel would have the power and strength to break. The Type ships represent the Classifications Societies' designation of ice-capable ships that are in turn equivalent to the Baltic Rules. The severity of ice conditions in the Zones is determined by a number assigned to each Zone, having the most severe Zone numbered 1 and the least severe Zone numbered 16 (Figure 1). The Zones and Dates are based on historical data on ice conditions up to early 1970's. The ZDS is described in detail in ASPPR (1989). Climate change could have a significant influence on the veracity of the Zones and Dates.

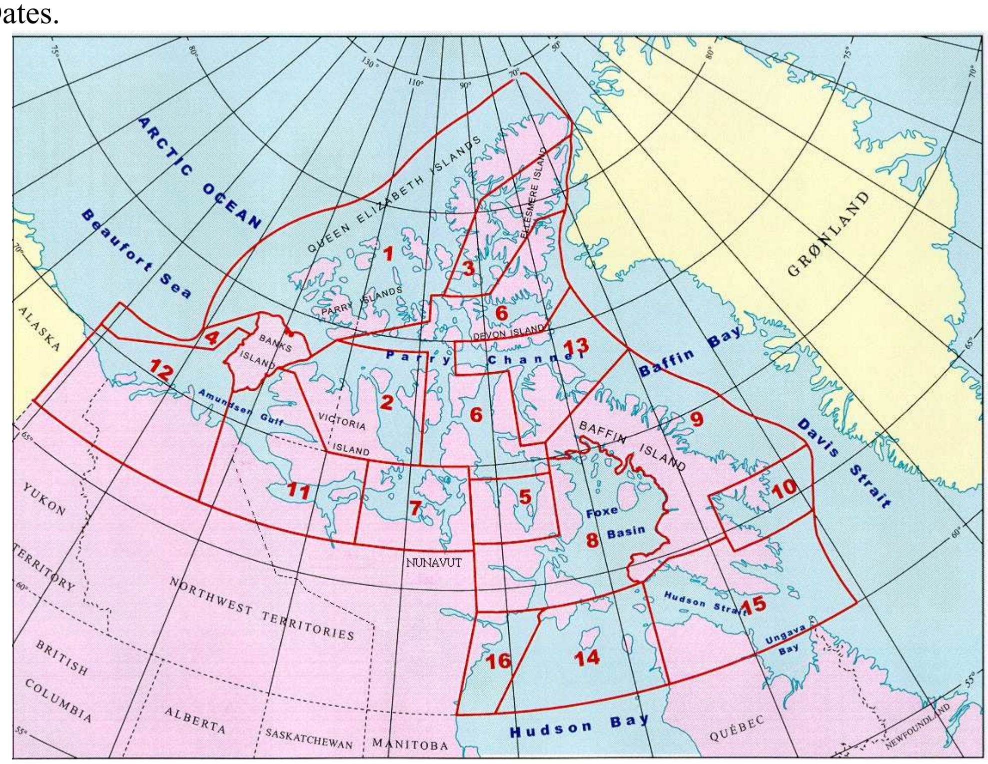

Figure 1: Shipping Safety Control Zones in Canada (as per Zone/Date System) (ASPPR, 1989)

Table 1: Table X: Zone/Date Table (ASPPR, 1989)

Item	Category	Zone 1	Zone 2	Zone 3	Zone 4	Zone 5	Zone 6	Zone 7	Zone 8	Zone 9	Zone 10	Zone 11	Zone 12	Zone 13	Zone 14	Zone 15	Zone 16
1.	Arctic Class 10	All Year	All Year	All Year	All Year	All Year	All Year	All Year	All Year	All Year	All Year	All Year	All Year	All Year	All Year	All Year	All Year
2.	Arctic Class 8	July 1 to	All Year	All Year	All Year	All Year	All Year	All Year	All Year	All Year	All Year	All Year	All Year	All Year	All Year	All Year	All Oct. 15
3.	Arctic Class 7	Aug. 1 to Sept. 30	Aug. 1 to Nov. 30	July 1 to Dec. 31	July 1 to Dec. 15	July 1 to Dec. 15	All Year	All Year	All Year	All Year	All Year	All Year	All Year	All Year	All Year	All Year	All Year
4.	Arctic Class 6	Aug. 15 to Sept. 15	Aug. 1 to Oct. 31	July 15 to Nov. 30	July 15 to Nov. 30	Aug. 1 to Oct. 15	July 15 to Feb. 28	July 1 to Mar. 31	July 1 to Mar. 31	All Year	All Year	July 1 to Mar. 31	All Year	All Year	All Year	All Year	All Year
5.	Arctic Class 4	Aug. 15 to Sept. 15	Aug. 15 to Oct. 15	July 15 to Oct. 31	July 15 to Nov. 15	Aug. 15 to Sept. 30	July 20 to Dec. 31	July 15 to Jan. 15	July 15 to Jan. 15	July 10 to Mar. 31	July 10 to Feb. 28	July 5 to Jan. 15	June 1 to Jan. 31	June 1 to Feb. 15	June 15 to Feb. 15	June 15 to Mar. 15	June 1 to Feb. 15
6.	Arctic Class 3	Aug. 20 to Sept. 15	Aug. 20 to Sept. 30	July 25 to Oct. 15	July 20 to Nov. 5	Aug. 20 to Sept. 25	Aug. 1 to Nov. 30	July 20 to Dec. 15	July 20 to Dec. 31	July 20 to Jan. 20	July 15 to Jan. 25	July 5 to Dec. 15	June 10 to Dec. 31	June 10 to Dec. 31	June 20 to Jan. 10	June 20 to Jan. 31	June 5 to Jan. 10
7.	Arctic Class 2	No Entry	No Entry	Aug. 15 to Sept. 30	Aug. 1 to Oct. 31	No Entry	Aug. 15 to Nov. 20	Aug. 1 to Nov. 20	Aug. 1 to Nov. 30	Aug. 1 to Dec. 20	July 25 to Dec. 20	July 10 to Nov. 20	June 15 to Dec. 5	June 25 to Nov. 22	June 25 to Dec. 10	June 25 to Dec. 20	June 10 to Dec. 10
8.	Arctic Class 1A	No Entry	No Entry	Aug. 20 to Sept. 15	Aug. 20 to Sept. 30	No Entry	Aug. 25 to Oct. 31	Aug. 10 to Nov. 5	Aug. 10 to Nov. 20	Aug. 10 to Dec. 10	Aug. 1 to Dec. 10	July 15 to Nov. 10	July 1 to Nov. 10	July 15 to Oct. 31	July 1 to Nov. 30	July 1 to Dec. 10	June 20 to Nov. 30
9.	Arctic Class 1	No Entry	No Entry	No Entry	No Entry	No Entry	Aug. 25 to Sept. 30	Aug. 10 to Oct. 15	Aug. 10 to Oct. 31	Aug. 10 to Oct. 31	Aug. 1 to Oct. 31	July 15 to Oct. 20	July 1 to Oct. 31	July 15 to Oct. 15	July 1 to Nov. 30	July 1 to Nov. 30	June 20 to Nov. 15
10.	Type A	No Entry	No Entry	Aug. 20 to Sept. 10	Aug. 20 to Sept. 20	No Entry	Aug. 15 to Oct. 15	Aug. 1 to Oct. 25	Aug. 1 to Nov. 10	Aug. 1 to Nov. 20	July 25 to Nov. 20	July 10 to Oct. 31	June 15 to Nov. 10	June 25 to Oct. 22	June 25 to Nov. 30	June 25 to Dec. 5	June 20 to Nov. 20
11.	Type B	No Entry	No Entry	Aug. 20 to Sept. 5	Aug. 20 to Sept. 15	No Entry	Aug. 25 to Sept. 30	Aug. 10 to Oct. 15	Aug. 10 to Oct. 31	Aug. 10 to Oct. 31	Aug. 1 to Oct. 31	July 15 to Oct. 20	July 1 to Oct. 25	July 15 to Oct. 15	July 1 to Nov. 30	July 1 to Nov. 30	June 20 to Nov. 10
12.	Type C	No Entry	No Entry	No Entry	No Entry	No Entry	Aug. 25 to Sept. 25	Aug. 10 to Oct. 10	Aug. 10 to Oct. 25	Aug. 10 to Oct. 25	Aug. 1 to Oct. 25	July 15 to Oct. 15	July 1 to Oct. 25	July 15 to Oct. 10	July 1 to Nov. 25	July 1 to Nov. 25	June 20 to Nov. 10
13.	Type D	No Entry	No Entry	No Entry	No Entry	No Entry	No Entry	Aug. 10 to Oct. 5	Aug. 15 to Oct. 20	Aug. 15 to Oct. 20	Aug. 5 to Oct. 20	July 15 to Oct. 10	July 1 to Oct. 20	July 30 to Sept. 30	July 10 to Nov. 10	July 5 to Nov. 10	July 1 to Oct. 31
14.	Type E	No Entry	No Entry	No Entry	No Entry	No Entry	No Entry	Aug. 10 to Sept. 30	Aug. 20 to Oct. 20	Aug. 20 to Oct. 15	Aug. 10 to Oct. 20	July 15 to Sept. 30	July 1 to Oct. 20	Aug. 15 to Sept. 20	July 20 to Oct. 31	July 20 to Nov. 5	July 1 to Oct. 31

Transport Canada, in consultation with Stakeholders, has made extensive revisions to the Regulations through the introduction of the Ice Regime System (ASPPR 1989; Canadian Gazette 1996; Equivalent Standards 1995; AIRSS 1996). The changes are designed to reduce the risk of structural damage to ships which could lead to the release of pollution into the environment, yet provide the necessary flexibility to Shipowners by making use of actual ice conditions, as seen by the Master to determine transit. Arctic Ice Regime Shipping System (AIRSS) is a Regulatory Standard of the ASPPR. It allows shipping based on the actual, not historical, ice conditions. At the present time, it is used exclusively outside the ZDS (i.e. for the access of the Arctic Control Zones outside permissible dates for vessel), with special requirements for its use.

In this new system, an "Ice Regime", which is a region of generally consistent ice conditions, is defined at the time the vessel enters that specific geographic region, or it is defined in advance for planning and design purposes. The Arctic Ice Regime Shipping System (AIRSS) is based on a simple arithmetic calculation that produces an "**Ice Numeral**" that combines the ice regime and the vessel's ability to navigate safely in that region. The Ice Numeral (IN) is based on the quantity of hazardous ice with respect to the ASPPR classification of the vessel (see Table 2). The Ice Numeral is calculated from

$$IN = [C_a \, x \, IM_a] \quad + \quad [C_b \, x \, IM_b] \quad + ... \qquad [1]$$

where

IN = Ice Numeral

C_a = Concentration in tenths of ice type "*a*"

IM_a = **Ice Multiplier** for ice type "*a*" and Ship Category (from Table 2)

The term on the right hand side of the equation (*a, b, c,* etc.) is repeated for as many ice types as may be present, including open water. The values of the Ice Multipliers are adjusted to take into account the decay or ridging of the ice by adding or subtracting a correction of 1 to the multiplier, respectively (see Table 2). The Ice Numeral is therefore unique to the particular ice regime and ship operating within its boundaries.

The vessel class is defined in terms of vessels that are designed to operate in severe ice conditions for both transit and icebreaking (Canadian Arctic Class - **CAC**) as well as vessels designed to operate in more moderate first-year ice conditions (**Type** ships). The classes were developed based on a "nominal" ice type, which were correlated to the World Meteorological Organization (WMO) classification for sea ice as given in Table 3. (ASPPR 1989).

The Ice Regime System determines whether or not a given vessel should proceed through that particular ice regime. If the Ice Numeral is negative, the ship is *not* allowed to proceed. However, if the Ice Numeral is zero or positive, the ship is allowed to proceed into the ice regime. Responsibility to plan the route, identify the ice, and carry out this numeric calculation rests with the Ice Navigator who could be the Master or Officer of the Watch. Due care and attention of the mariner, including avoidance of hazards, is vital to the successful application of the Ice Regime System. Authority by the Regulator

(Pollution Prevention Officer) to direct ships in danger, or during an emergency, remains unchanged.

At the present time, there is only partial application of the Ice Regime System, exclusively outside of the "Zone/Date" System. That is, vessel traffic is regulated by the Zone/Date System, but is allowed to proceed into a (normally) restricted zone if the ice conditions are such that the Ice Regime System gives a positive Ice Numeral. For this, the vessel must have an Ice Navigator onboard and initially send an *Ice Regime Routing Message* to the CCG-NORDREG office in Iqaluit indicating a positive ice regime. Following the voyage, an *After Action Report* must be submitted to Transport Canada. Full details are found in the applicable regulatory standards guidelines.

Table 2: Table of the Ice Multipliers (IM) for the Ice Regime System

Ice Types			Ice Multipliers						
			Type **E**	Type **D**	Type **C**	Type **B**	Type **A**	CAC **4**	CAC **3**
Old / Multi-Year Ice.................	(MY)		-4	-4	-4	-4	-4	-3	-1
Second Year Ice....................	(SY)		-4	-4	-4	-4	-3	-2	1
Thick First Year Ice................	(TFY)	> 120 cm	-3	-3	-3	-2	-1	1	2
Medium First Year Ice.............	(MFY)	70-120 cm	-2	-2	-2	-1	1	2	2
Thin First Year Ice................ Thin First Year Ice - 2nd Stage	(FY)	30-70 cm 50-70 cm	-1	-1	-1	1	2	2	2
Thin First Year Ice - 1st Stage		30-50 cm	-1	-1	1	1	2	2	2
Grey-White Ice......................	(GW)	15-30 cm	-1	1	1	1	2	2	2
Grey Ice..............................	(G)	10-15 cm	1	2	2	2	2	2	2
Nilas, Ice Rind		< 10 cm	2	2	2	2	2	2	2
New Ice..............................	(N)	< 10 cm	"	"	"	"	"	"	"
Brash (ice fragments < 2 m across)			"	"	"	"	"	"	"
Bergy Water			"	"	"	"	"	"	"
Open Water			"	"	"	"	"	"	"

Ice Decay: If MY, SY, TFY or MFY ice has Thaw Holes or is Rotten, add 1 to the IM for that ice type.

Ice Roughness: If the total ice concentration is 6/10s or greater and more than one-third of an ice type is deformed, subtract 1 from the IM for the deformed ice type.

Table 3: Vessel Class for the Ice Regime System

CATEGORY	OPERATING ROLE	ICE TYPE
CAC 1	Unrestricted	Multiyear Ice
CAC 2	Transit or controlled icebreaking	Multiyear Ice
CAC 3	Transit or controlled icebreaking	Second Year Ice
CAC 4	Transit or controlled icebreaking	Thick First Year Ice
Type A	Transit	Medium First Year Ice
Type B	Transit	Thin First Year Ice - 2nd Stage
Type C	Transit	Thin First Year Ice - 1st Stage
Type D	Transit	Grey-White Ice
Type E	Transit	Grey Ice

4. CIS Data – Air Temperatures

Daily air temperatures measured at the meteorological stations were supplied from the Canadian Ice Service. Seven meteorological stations (Tuktoyaktuk, Inuvik, Cambridge Bay, Resolute, Pond Inlet, Iqaluit, and Coral Harbour) representing the communities that lie along the Northwest Passage and in the approaches to Churchill were selected as locations where historical weather data have been collected. These were used to identify the changes that have occurred in the regions over the past 36 years (1968-2004). The stations are shown in Figure 2.

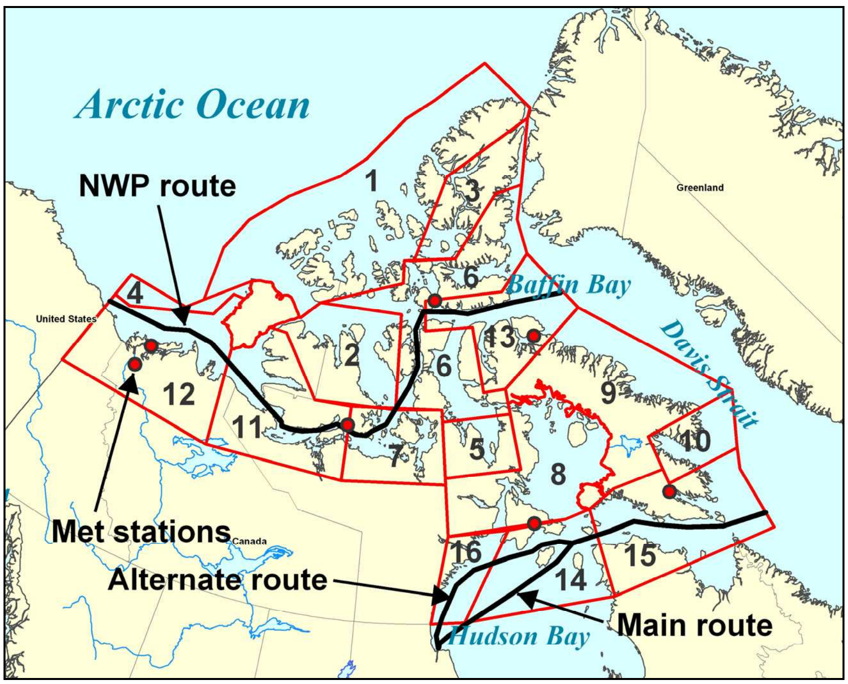

Figure 2: Shipping Safety Control Zones in Canada, Meteorological Stations used for Air Temperature Analysis (from left on NWP route: Inuvik, Tuktoyaktuk, Cambridge Bay, Resolute, Pond Inlet; from left in Hudson Bay: Coral Harbour, Iqaluit), and Shipping Routes in Northwest Passage and in Hudson Bay

4.1 Annual Cumulative Melting Degrees

The files with daily air temperatures data contain information on daily minimum, maximum and mean (average) temperature. Since the files don't include sufficiently detailed data that could have been analyzed on an hourly basis, a "melting degree" approach was used as the indicator for ice melt. The melting degree (MD) was calculated as the reported average temperature greater than or equal to 0°C for each day throughout the year. The cumulative melting degree (CMD) was calculated as a sum of melting degrees for each individual year and was plotted over the 36-year range for each station (Figure 3).

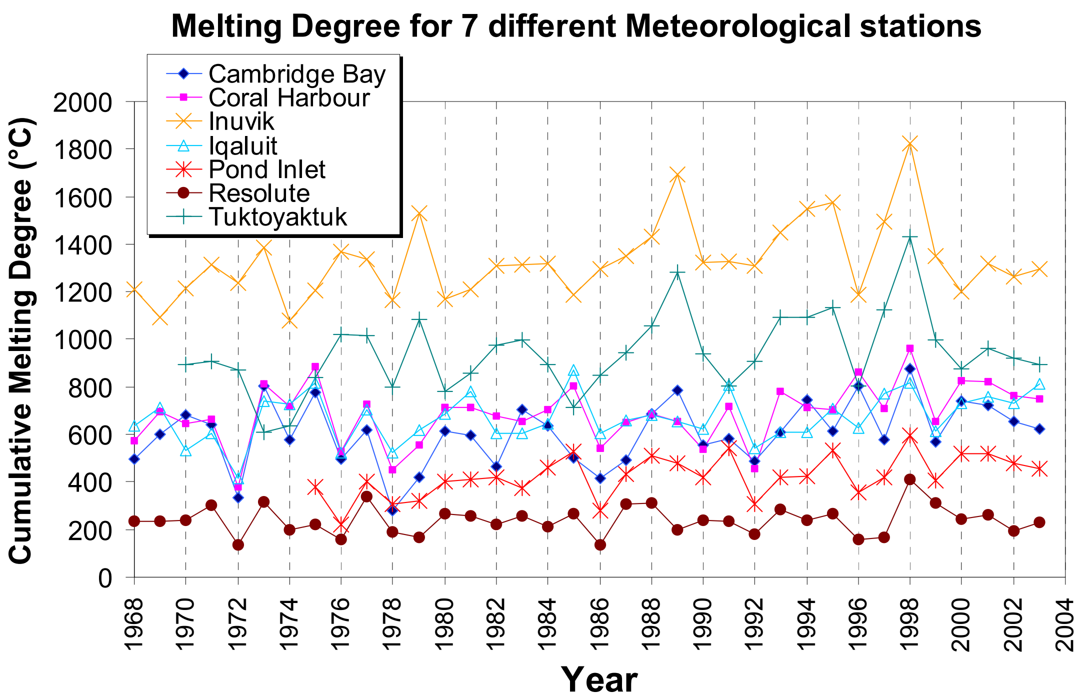

Figure 3: Cumulative Melting Degree (CMD, calculated as Cumulative Air Temperature above 0°C) from selected Met Stations (year 1968 – 2004)

Each station is showing an increase in cumulative melting degrees (CMD) since the late 1960's. The objective was to project expected CMD to 2020 and beyond, and assess the likely range of ice conditions that would impact shipping. These plots are shown in Figure 4 to Figure 10.

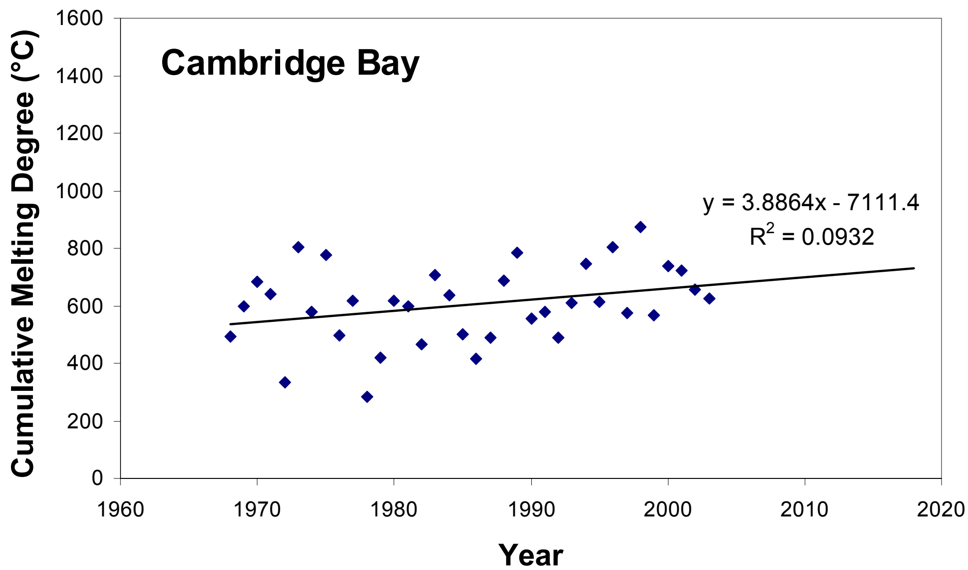

Figure 4: Expected Cumulative Melting Degree trendline at Cambridge Bay projected to year 2020 based on 1968 to 2003 dataset.

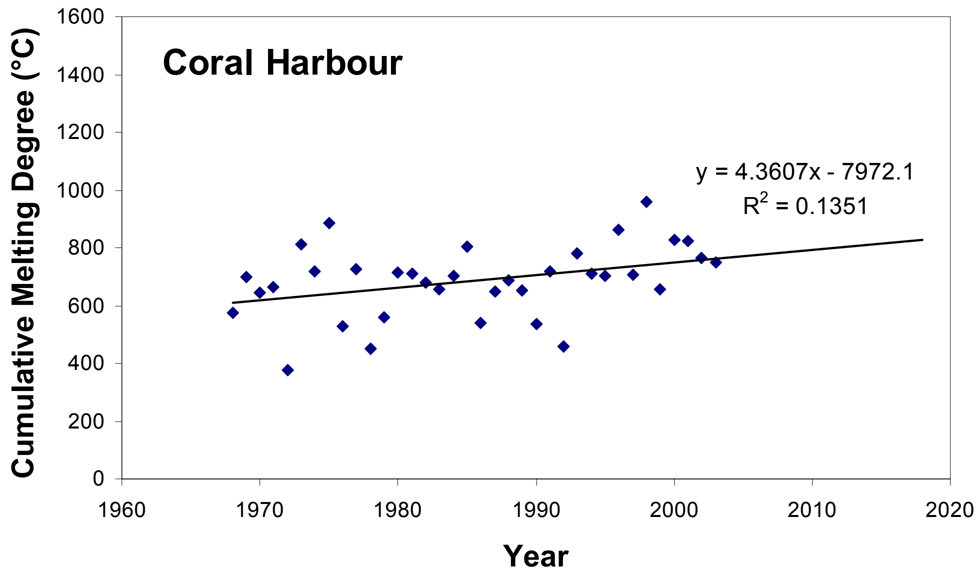

Figure 5: Expected Cumulative Melting Degree trendline at Coral Harbour projected to year 2020 based on 1968 to 2003 dataset.

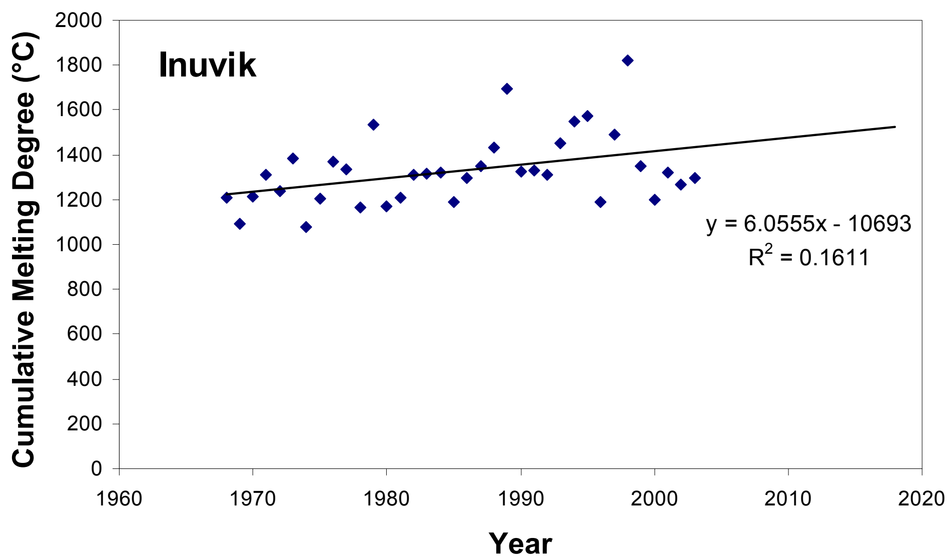

Figure 6: Expected Cumulative Melting Degree trendline at Inuvik projected to year 2020 based on 1968 to 2003 dataset.

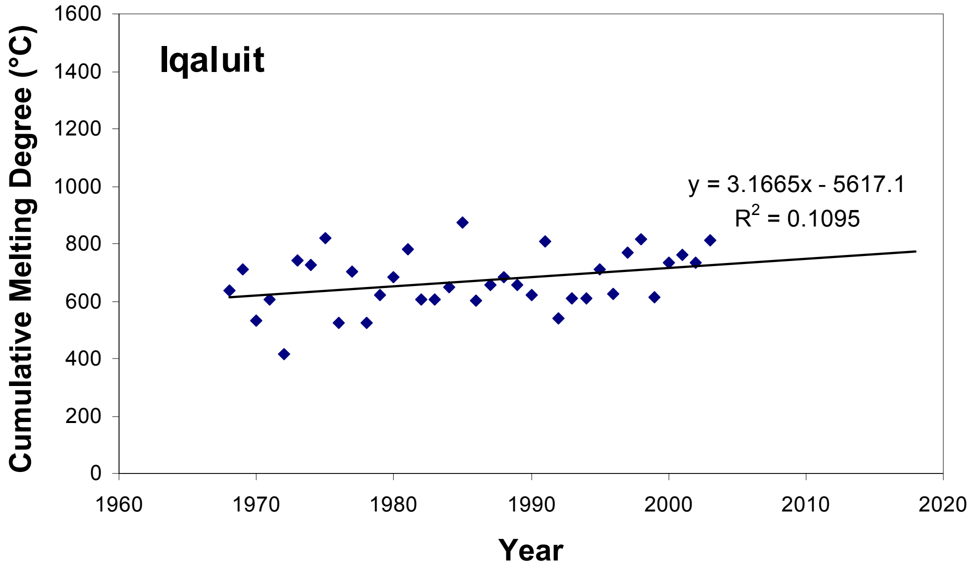

Figure 7: Expected Cumulative Melting Degree trendline at Iqaluit projected to year 2020 based on 1968 to 2003 dataset.

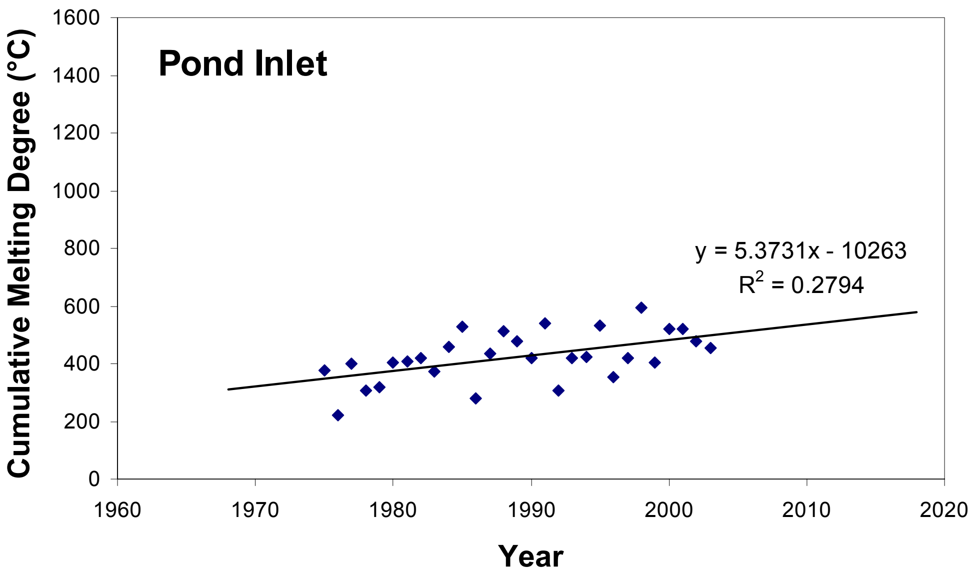

Figure 8: Expected Cumulative Melting Degree trendline at Pond Inlet projected to year 2020 based on 1968 to 2003 dataset.

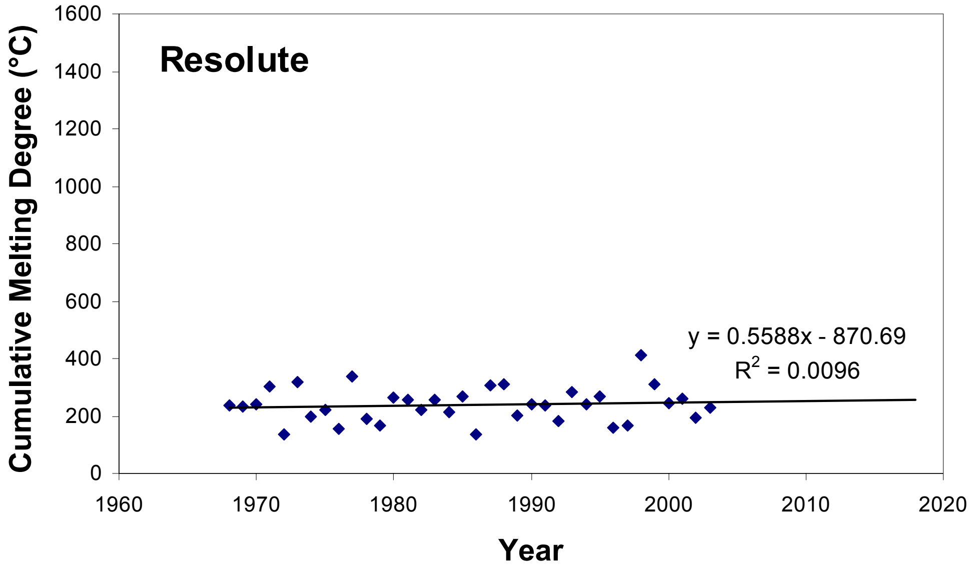

Figure 9: Expected Cumulative Melting Degree trendline at Resolute projected to year 2020 based on 1968 to 2003 dataset.

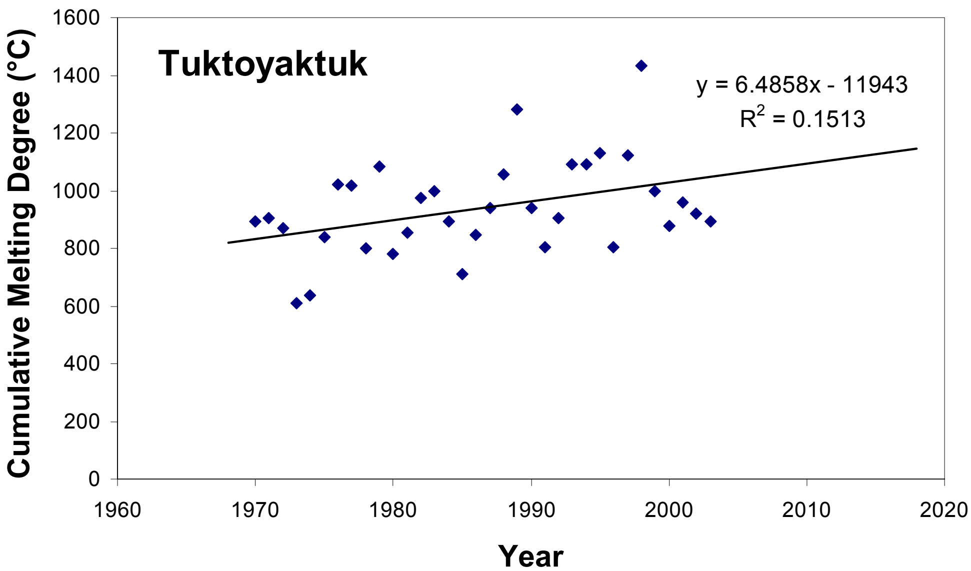

Figure 10: Expected Cumulative Melting Degree trendline at Tuktoyaktuk projected to year 2020 based on 1968 to 2003 dataset.

As can be seen, there is high degree of variance in the data with three standard deviations required to cover all data points within each station. CMDs can vary between 100 to 150% from the lowest to the highest values. R^2 values range from 0.0096 to 0.279 and are all very low indicating high scatter in the data. This scatter reduces confidence in carrying the trend line forward.

Figure 11 to Figure 17 show the Cumulative Melting Degree per decade.

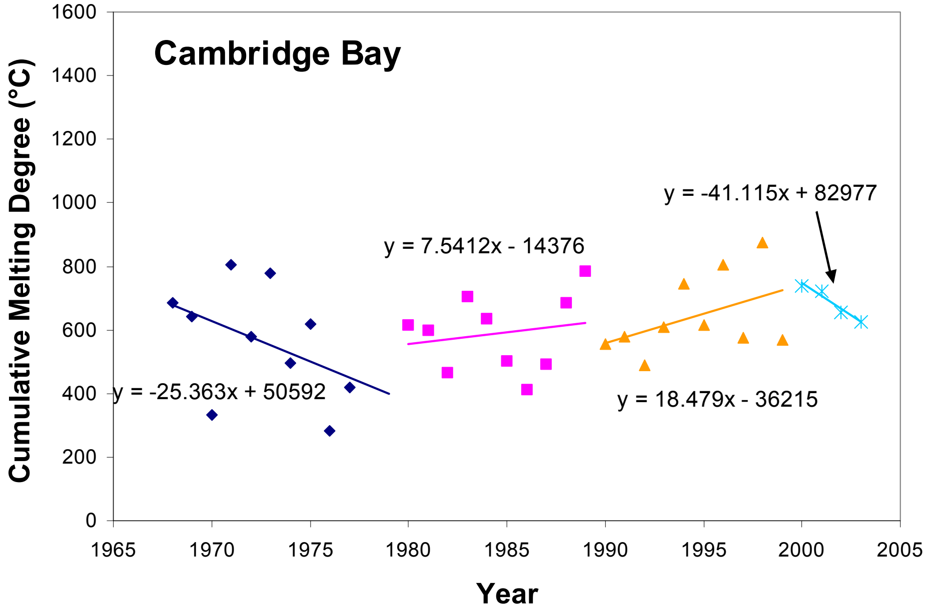

Figure 11: Cumulative melting degree trendline per decade at Cambridge Bay (years 1968–1979, 1980-1989, 1990-2000, above 2000)

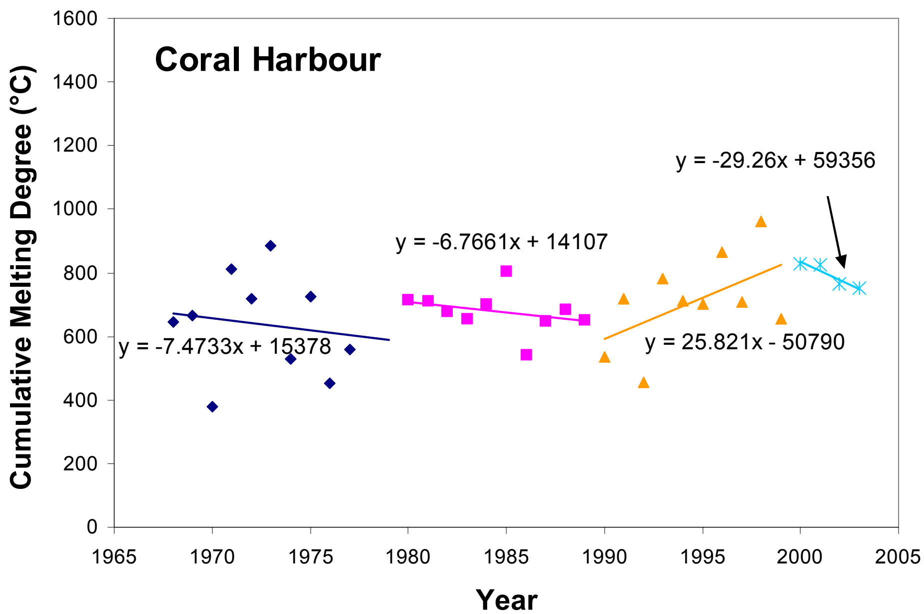

Figure 12: Cumulative melting degree trendline per decade at Coral Harbour (years 1968–1979, 1980-1989, 1990-2000, above 2000)

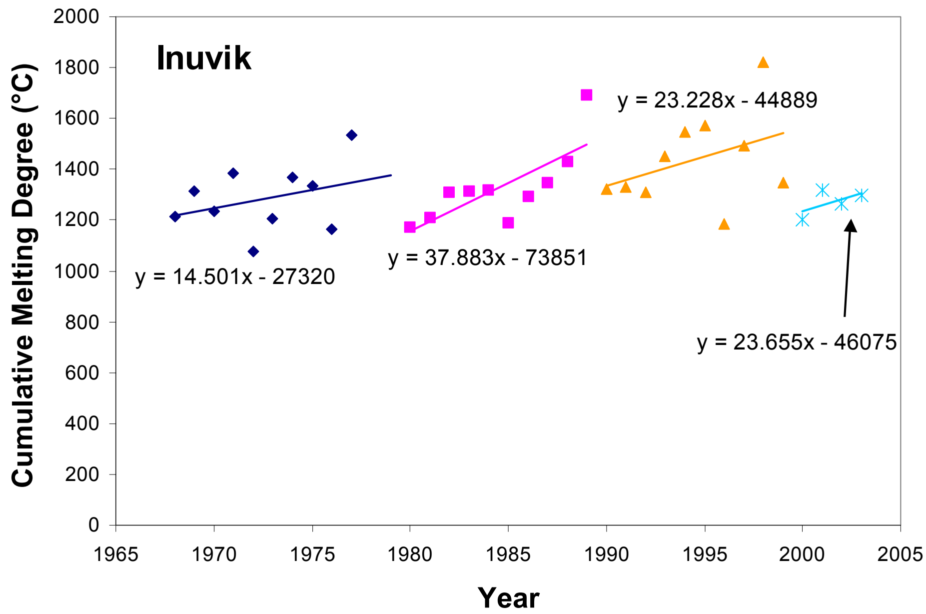

Figure 13: Cumulative melting degree trendline per decade at Inuvik (years 1968–1979, 1980-1989, 1990-2000, above 2000)

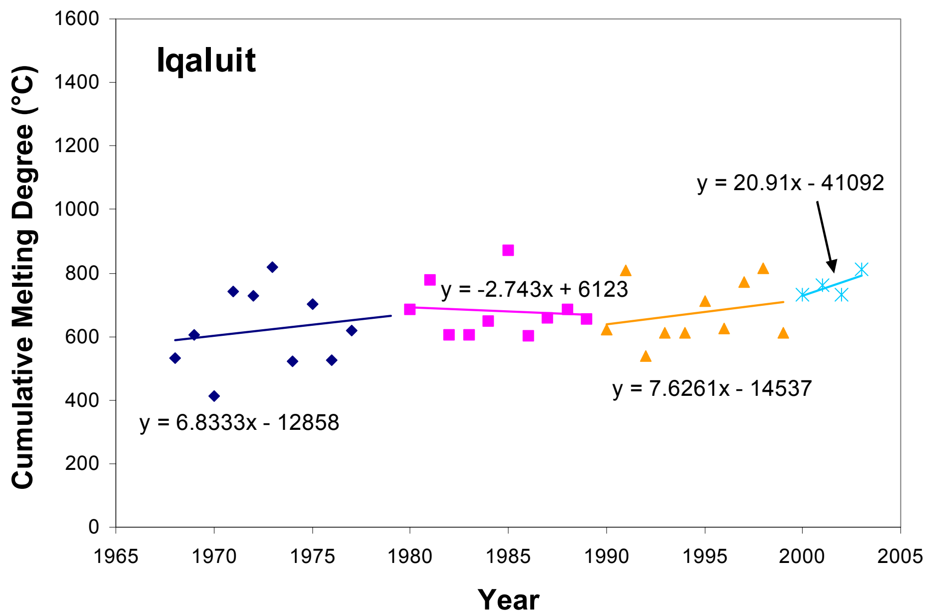

Figure 14: Cumulative melting degree trendline per decade at Iqaluit (years 1968–1979, 1980-1989, 1990-2000, above 2000)

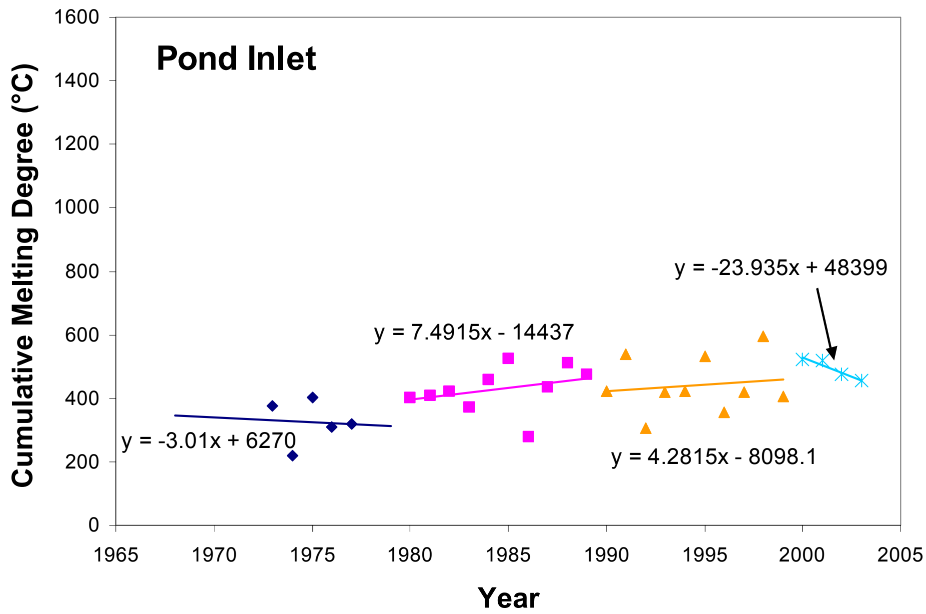

Figure 15: Cumulative melting degree trendline per decade at Pond Inlet (years 1972–1979, 1980-1989, 1990-2000, above 2000)

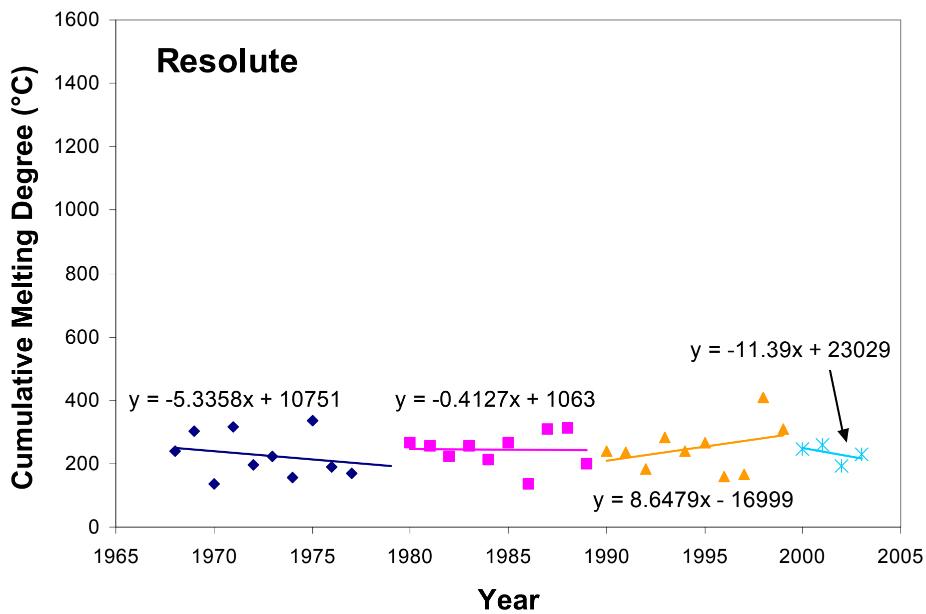

Figure 16: Cumulative melting degree trendline per decade at Resolute (years 1968–1979, 1980-1989, 1990-2000, above 2000)

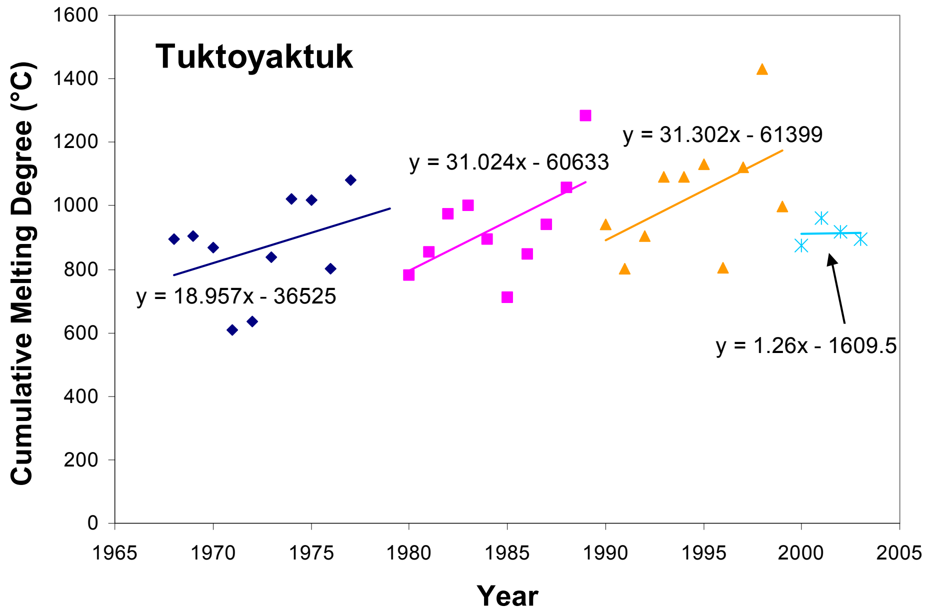

Figure 17: Cumulative melting degree trendline per decade at Tuktoyaktuk (years 1968–1979, 1980-1989, 1990-2000, above 2000)

There is variation within decades with the 1970's being generally a decade of declining temperatures, and with the 1980's and particularly the 1990's being decade of rising temperatures. There is a trend, mainly in the central and high Arctic for declining CMDs during the present decade. This change to cooler temperatures is reflected in the return of the Old Ice in many areas of the high Arctic since its destruction in 1998.

The average annual CMD throughout the period between years 1968 and 2004 was calculated for the whole Arctic (represented by an average CMD of the seven met stations) and plotted in Figure 18. As can be seen, there is high interannual variability in CMD for both the individual stations and the whole Arctic. The high degree of variability from one summer to the next has important implications to marine operations in the Canadian Arctic as ice conditions encountered from one year to the next can also be highly variable. To investigate the effect this interannual variability has on the Zone/Date system for the Northwest Passage, representative "colder than normal" and "warmer than normal" summers across the control zones that compose the Northwest Passage as well as the access routes to the Port of Churchill in Hudson Strait were selected. The warmer than normal summer would also be representative of a warmer Arctic in the future in the case of a warming trend in the climate conditions. Years 1986 (cold year) and 1998 (warm year) were selected for the NWP, and years 1992 (cold year) and 1998 (warm year) for Hudson Strait.

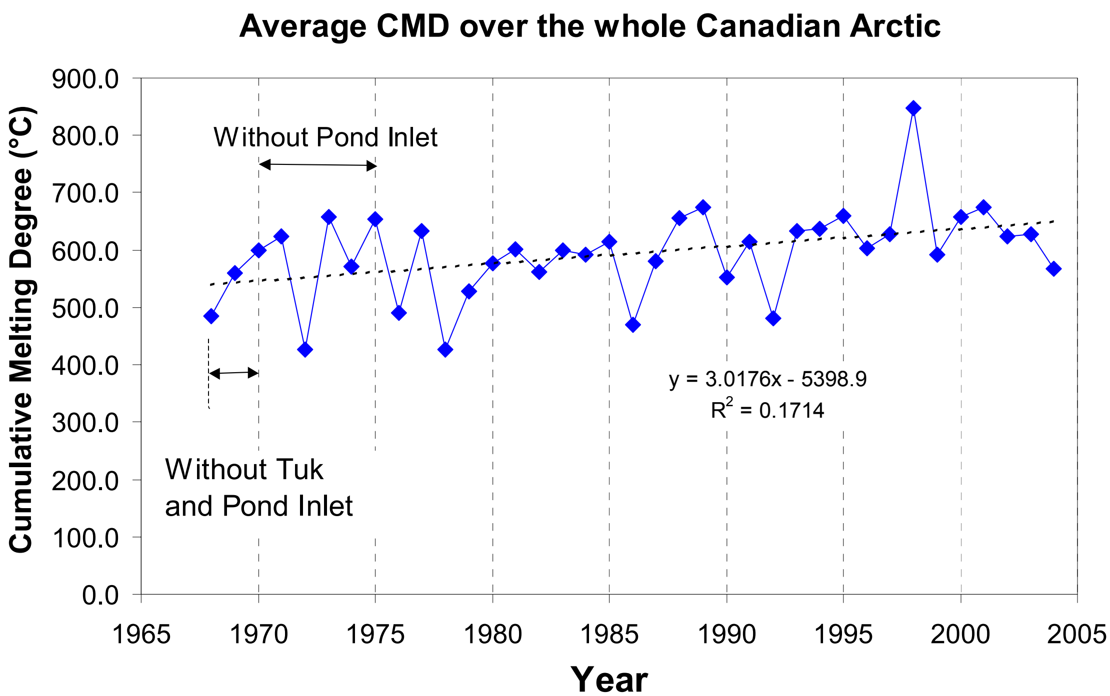

Figure 18: Cumulative Melting Degree (CMD, calculated as Cumulative Air Temperature above 0°C) averaged over the Canadian Arctic

4.2 Length of Melting Season

The length of the melting season was calculated as the sum of days when the air temperature, at the 7 met stations, was greater than –1.8 °C. Table 4 lists the beginning, the end, and the length of the melting season for each year throughout the period between years 1968 and 2004. Statistics such as Mean, Median, Minimum and Maximum are also listed for each location in this Table. Number of days with air temperature above –1.8°C for each of the 7 met station locations are plotted in Figure 19 to Figure 25.

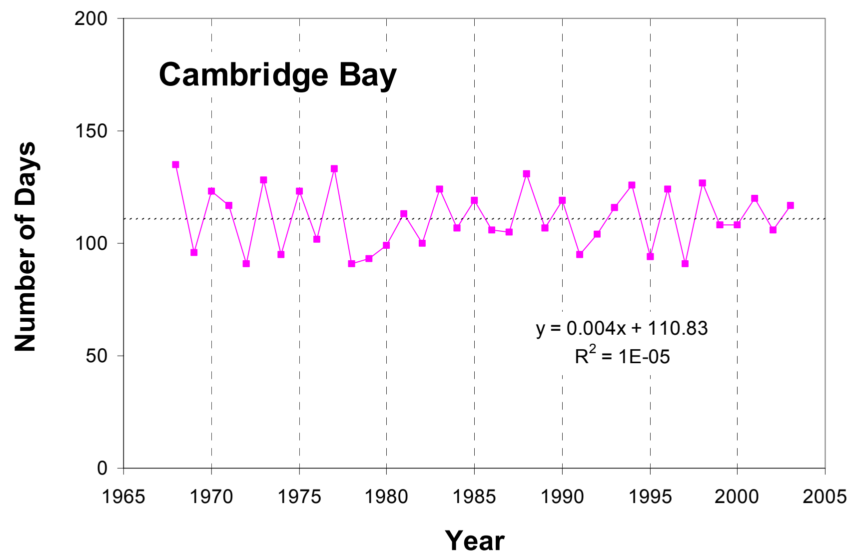

Figure 19: Number of days with air temperature above –1.8°C at Cambridge Bay throughout period of 1968-2003

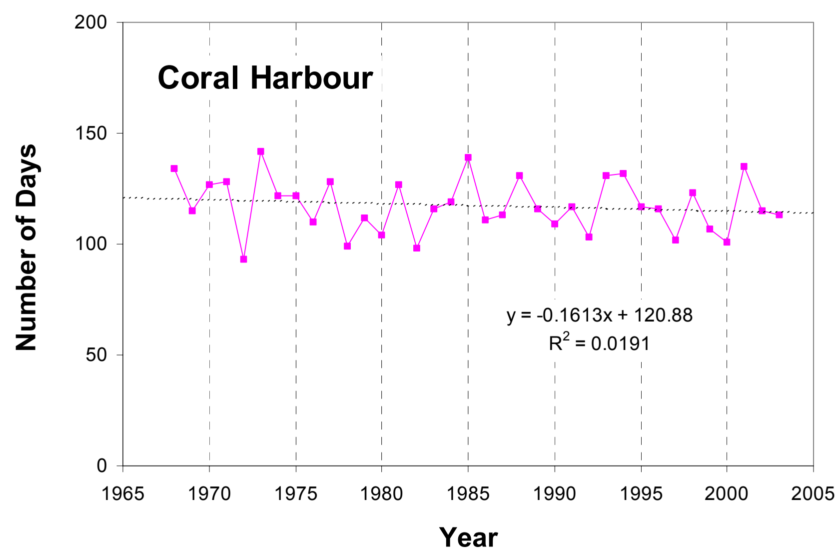

Figure 20: Number of days with air temperature above –1.8°C at Coral Harbour throughout period of 1968-2003

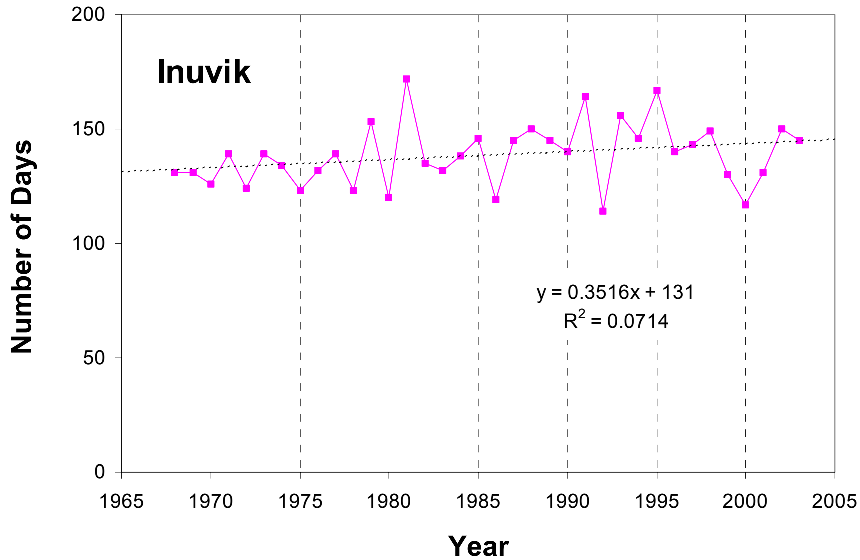

Figure 21: Number of days with air temperature above –1.8°C at Inuvik throughout period of 1968-2003

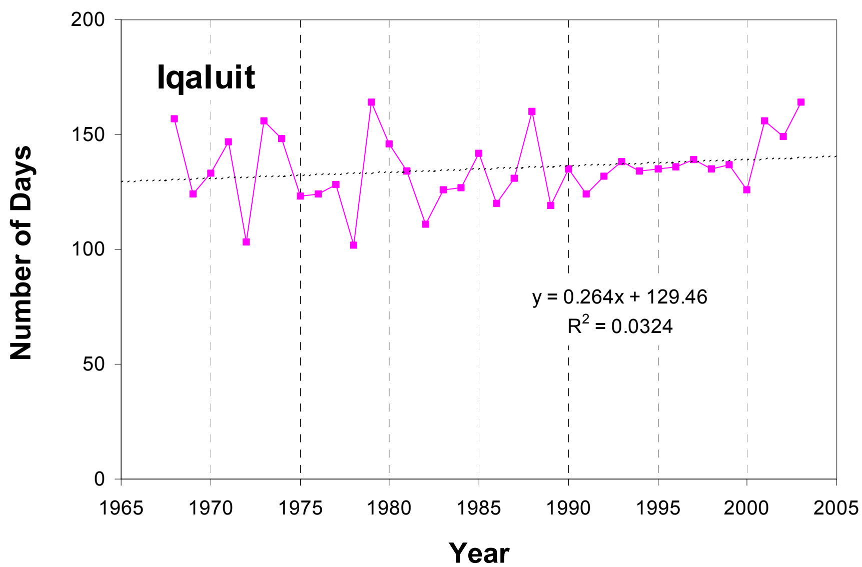

Figure 22: Number of days with air temperature above –1.8°C at Iqaluit throughout period of 1968-2003

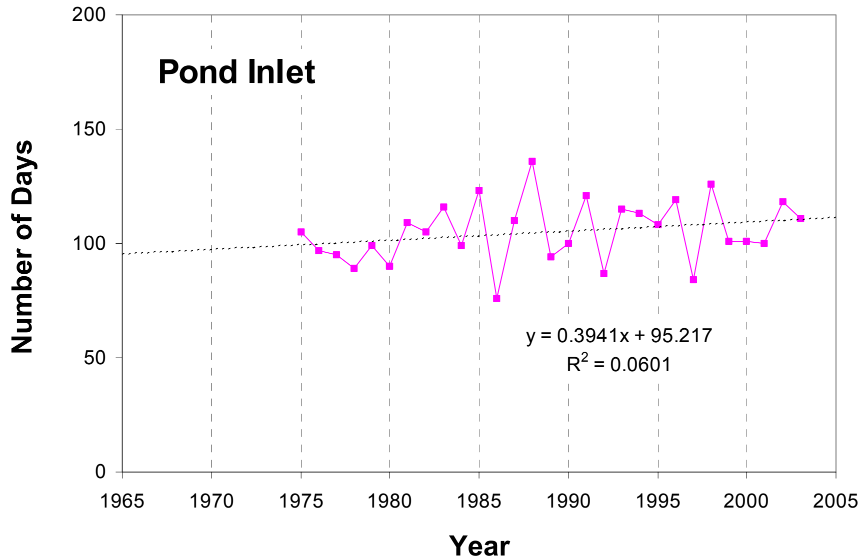

Figure 23: Number of days with air temperature above –1.8°C at Pond Inlet throughout period of 1975-2003

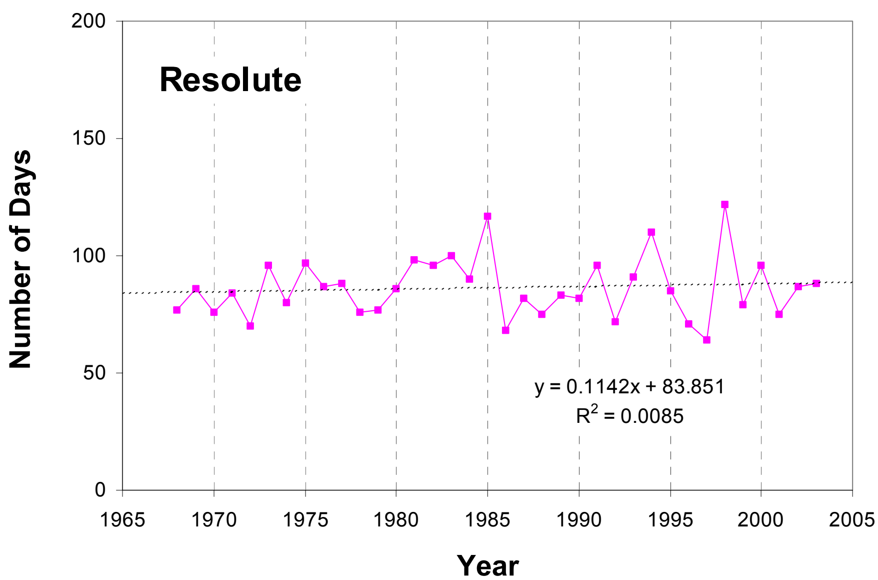

Figure 24: Number of days with air temperature above –1.8°C at Resolute throughout period of 1968-2003

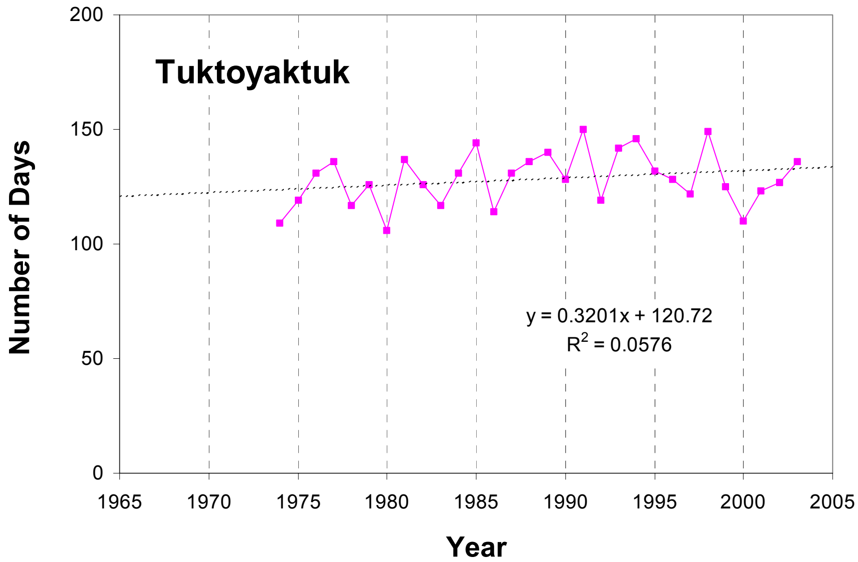

Figure 25: Number of days with air temperature above –1.8°C at Tuktoyaktuk throughout period of 1974-2003

There has been very little change in the number of days with air temperature above -1.8°C calculated from daily air temperature data obtained from the 7 met stations. Some stations show a slight increase (such as in the western Arctic) while others show a slight decrease.

Table 4: Number of days with air temperature above –1.8°C at 7 locations in the Canadian Arctic (based on the air temperature data obtained from the met stations at these locations). Start and End are given in Julian Days.

Year	Cambridge Bay			Coral Harbour			Inuvik			Iqaluit			Pond Inlet			Resolute			Tuktoyaktuk		
	Start (JD)	End (JD)	Length (days)	Start (JD)	End (JD)	Length (days)	Start (JD)	End (JD)	Length (days)	Start (JD)	End (JD)	Length (days)	Start (JD)	End (JD)	Length (days)	Start (JD)	End (JD)	Length (days)	Start (JD)	End (JD)	Length (days)
1968	151	286	135	160	294	134	146	277	131	152	309	157				164	241	77			
1969	166	262	96	156	271	115	157	288	131	147	271	124				166	252	86			
1970	146	269	123	152	279	127	140	266	126	153	286	133				168	244	76			
1971	155	272	117	156	284	128	135	274	139	154	301	147				158	242	84			
1972	160	251	91	170	263	93	146	270	124	164	267	103				171	241	70			
1973	142	270	128	149	291	142	139	278	139	137	293	156				157	253	96			
1974	159	254	95	141	263	122	132	266	134	135	283	148				171	251	80	156	265	109
1975	144	267	123	145	267	122	144	267	123	147	270	123	155	260	105	147	244	97	145	264	119
1976	164	266	102	151	261	110	142	274	132	149	273	124	161	258	97	166	253	87	143	274	131
1977	147	280	133	149	277	128	143	282	139	150	278	128	154	249	95	158	246	88	144	280	136
1978	170	261	91	164	263	99	149	272	123	164	266	102	158	247	89	169	245	76	155	272	117
1979	163	256	93	146	258	112	134	287	153	125	289	164	162	261	99	175	252	77	147	273	126
1980	158	257	99	160	264	104	142	262	120	123	269	146	165	255	90	164	250	86	156	262	106
1981	154	267	113	154	281	127	117	289	172	150	284	134	148	257	109	153	251	98	140	277	137
1982	162	262	100	159	257	98	138	273	135	152	263	111	156	261	105	157	253	96	148	274	126
1983	148	272	124	155	271	116	145	277	132	148	274	126	149	265	116	154	254	100	149	266	117
1984	151	258	107	150	269	119	134	272	138	155	282	127	156	255	99	155	245	90	141	272	131
1985	146	265	119	139	278	139	136	282	146	138	280	142	143	266	123	144	261	117	138	282	144
1986	166	272	106	163	274	111	149	268	119	151	271	120	167	243	76	173	241	68	155	269	114
1987	162	267	105	156	269	113	140	285	145	153	284	131	156	266	110	159	241	82	147	278	131
1988	151	282	131	152	283	131	131	281	150	145	305	160	135	271	136	172	247	75	144	280	136
1989	154	261	107	151	267	116	140	285	145	145	264	119	159	253	94	167	250	83	146	286	140
1990	153	272	119	154	263	109	132	272	140	141	276	135	157	257	100	166	248	82	144	272	128
1991	155	250	95	149	266	117	118	282	164	149	273	124	150	271	121	157	253	96	132	282	150
1992	160	264	104	169	272	103	141	255	114	157	289	132	167	254	87	170	242	72	141	260	119
1993	149	265	116	134	265	131	129	285	156	133	271	138	151	266	115	157	248	91	144	286	142
1994	144	270	126	148	280	132	135	281	146	144	278	134	146	259	113	143	253	110	137	283	146
1995	156	250	94	152	269	117	113	280	167	135	270	135	150	258	108	150	235	85	144	276	132
1996	146	270	124	157	273	116	129	269	140	141	277	136	155	274	119	169	240	71	141	269	128
1997	162	253	91	152	254	102	131	274	143	132	271	139	154	238	84	170	234	64	152	274	122
1998	152	279	127	153	276	123	129	278	149	147	282	135	149	275	126	151	273	122	129	278	149
1999	163	271	108	165	272	107	141	271	130	146	283	137	159	260	101	163	242	79	147	272	125
2000	158	266	108	161	262	101	150	267	117	145	271	126	161	262	101	161	257	96	156	266	110
2001	153	273	120	139	274	135	149	280	131	141	297	156	164	264	100	154	229	75	150	273	123
2002	159	265	106	155	270	115	126	276	150	148	297	149	151	269	118	159	246	87	148	275	127
2003	163	280	117	156	269	113	137	282	145	136	300	164	148	259	111	162	250	88	146	282	136
Mean	155	266	111	153	271	117	137	276	139	145	280	135	155	260	105	161	247	86	146	274	129
Median	155	267	108	154	270	116	139	277	139	147	278	135	155	260	105	162	248	86	146	274	128
Min	142	250	91	134	254	93	113	255	114	123	263	102	135	238	76	143	229	64	129	260	106
Max	170	286	135	170	294	142	157	289	172	164	309	164	167	275	136	175	273	122	156	286	150

JD = Julian Day

5. Annual Variability in Summer Temperatures across the Canadian Arctic

As can be seen from data of annual melting degree accumulations (Figure 3 and Figure 18) all stations show an increase in the air temperatures since the late 1960's. However, there is a high degree of variability from one year to the next. The seasonal temperatures indicate variation of three standard deviations from the mean. At virtually every station, the highest annual accumulation of melting degrees is 100% to 150% more than the lowest value in the record. Often a below or above average year will occur in close succession. Marine operations occur during the short summer season in the Canadian Arctic. This high degree of variability from one summer to the next has important implications to marine operations in the Canadian Arctic as ice conditions encountered from one year to the next can also be highly variable. In assessing the implications of a warming climate on Arctic shipping, we must also consider the possible reasons for this interannual variability as they may be greater than the changes that may come from climate change over the next 20 to 50 years.

The length of the summer period when melting degrees are accumulated is short in the Canadian Arctic, spanning from early June to mid-September for most locations. This short time span makes the summer melting period in many areas in the Canadian Arctic very susceptible to persistent or "blocking" weather systems that may bring several weeks of cold northerly winds or warmer southerly flow in a row, contributing to the wide range of melting degree days experienced from one season to the next. A blocking weather pattern occurs when the transition of weather fronts is very slow or highly repetitive such that the same above or below normal temperature and precipitation pattern persists for several weeks or months at a time. Such blocking patterns sometimes look like the Greek letter Omega, with a strong central high pressure cell and two opposing low pressure cells on each side, also known as an "Omega Block". Another common blocking pattern is a "Rex Block" when two or more strong high and low pressure cells lock in a succession creating an "S" pattern of frontal boundaries.

On the surface these blocking systems appear to be a product of short term "weather" patterns and are not associated with longer term climate change. However, there are elements of the climate of North America that contribute to the creation of these blocking patterns. The juxtaposition of cold ice masses in the Arctic Ocean and Greenland with the warm ocean waters of the North Atlantic and North Pacific create three significant weather systems that affect the climate of North America. These are the "Aleutian Low" pressure cell found in the Bering Sea, the "Polar High" pressure cell found over the Arctic Ocean (and associated "Greenland High") and the "Icelandic Low" found in the North Atlantic south of Greenland-Iceland. The pattern of weather systems that move around these features in essence create an inverted Omega Block for the North American Arctic and the relative intensity of each of these low and high pressure cells in any given summer will often determine whether cooler or warmer than normal air is able to penetrate into various regions of the North American Arctic over the brief summer melt period.

To investigate whether there are any patterns associated with cooler or normal summers, the melting degree (MD) records for each station and the years when the five lowest and five highest accumulated MDs were recorded for each station were reviewed. The results of this analysis are shown in Figure 26 and Figure 27.

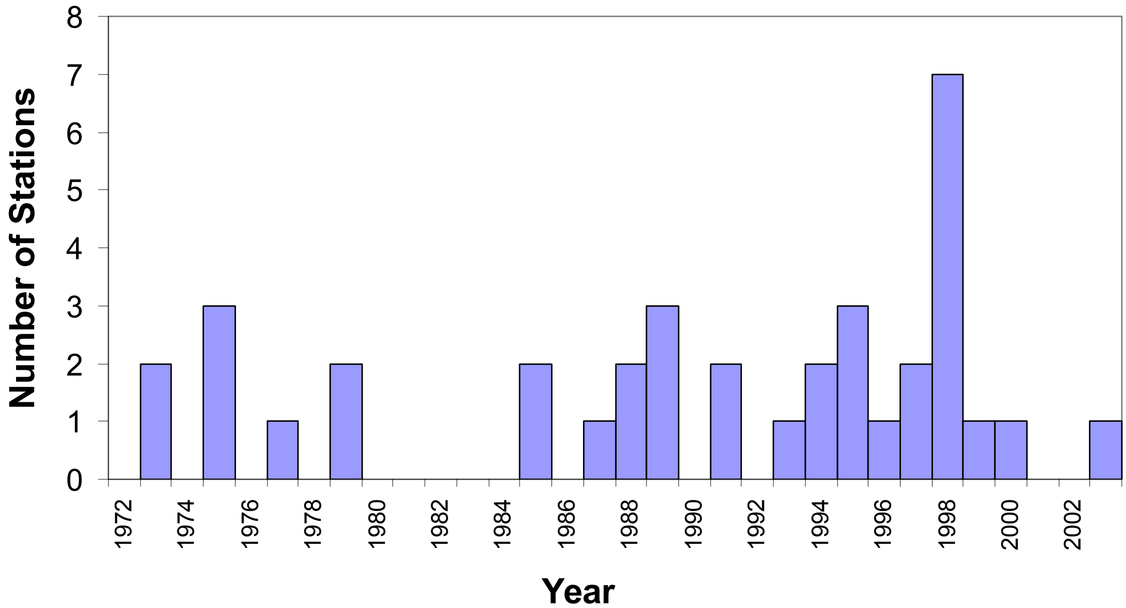

Figure 26: Number of Stations Reporting 5 Highest Cumulative Melting Degrees

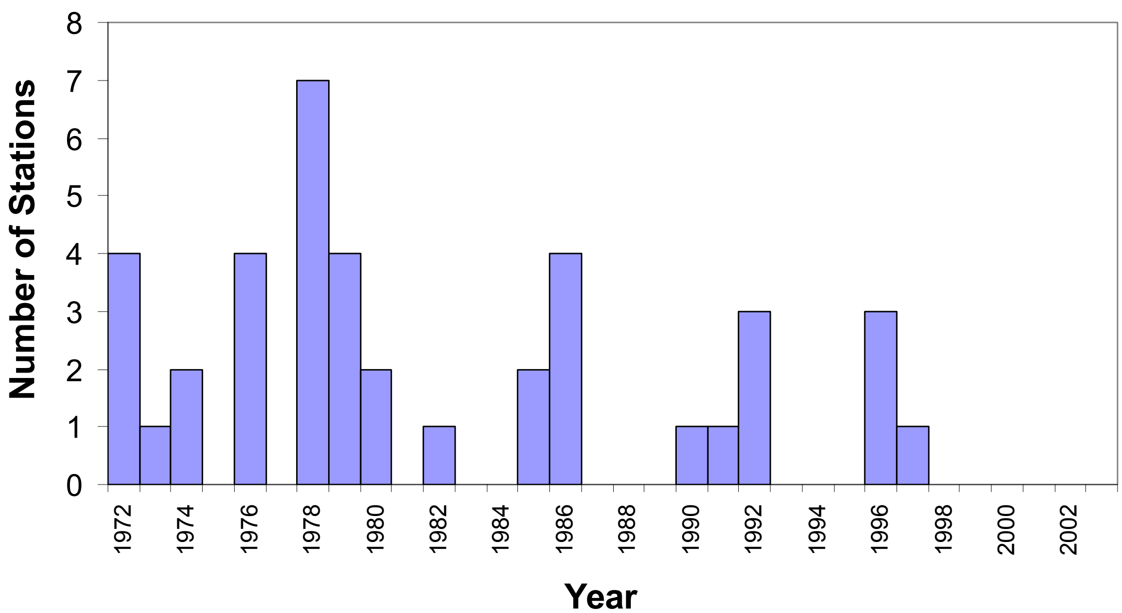

Figure 27: Number of Stations Reporting 5 Lowest Cumulative Melting Degrees

As can be seen from the Figures, below normal or above normal temperatures will often be reported by more than one station in any given summer, indicating that such trends are regional across a broad area of the Arctic rather than just in a local area. It can also be seen that cooler summers have tended to occur much more commonly in the 1970's and 1980's than in the 90's or in recent years and, conversely, there is a tendency for warmer summers in the 1990's. Such a trend is to be expected when a data record such as this is showing a steady increase in average summer temperatures over the period. Since several stations across the Arctic tend to report similar temperature trends over the data record, it is possible that there are larger global climate patterns at work that influence summer Arctic temperatures in any given year, including changes to the interaction between the Aleutian and Icelandic lows compared to the Polar High.

There is much discussion in the literature on the existence of the Arctic Oscillation (AO) and the influence this has on the climate of the Arctic region (Dickson et al 2000). It is generally agreed that the Arctic Oscillation is in fact part of the North Atlantic Oscillation (NAO) (Dickson et al 2000). The AO/NAO essentially refers to the difference in atmospheric pressure between the Polar High, the Icelandic Low and the Azores High, found west of Portugal. When the pressure differences are higher than the historical mean between these systems (i.e. when the gradient between the Polar and Azores high is steep compared to the Icelandic Low) then the AO/NAO is considered to be in a "positive" state and when the gradient is below the historical average the AO/NAO is considered to be in a "negative" state (that is, a weak Icelandic Low). During a strong positive AO/NAO the Icelandic Low is very strong, drawing down cold Arctic air along the Canadian East Coast and bringing warm moist air into Western Europe. Conversely, when the AO/NAO is negative, the Icelandic Low is weak keeping Polar air to the north and allowing warm air into eastern North America but cooler and drier air into Western Europe. The AO/NAO has its greatest influence during the winter months when the pressure gradient between the low and high pressure systems at its greatest. A study of ice conditions in the Gulf of St. Lawrence has found a close association between positive AO/NAO years and heavy winter ice conditions in the Gulf and, conversely, lighter ice conditions during negative AO/NAO conditions (Gorman 2000). This influence on regional weather is so strong that the British Met Office uses the AO/NAO indices as the basis for its long range weather forecast (Rodwell and Folland 2002).

There are no known studies available on the degree to which the AO/NAO influences weather or ice conditions in the Canadian Arctic. Figure 28 presents the AO/NAO pattern since 1950 as calculated by the British Met Office (the blue predicted line in the figure represents the test of skill of the British Met Office prediction system). The AO/NAO went through a long negative period during the 1960's and has trended towards positive since. Significant points along the observed curve include the trough of the negative cycle reached in 1969 followed by a positive period in the early to mid 1970's with the decade ending in a negative cycle. During the decade of the 1980's the AO/NAO generally trended upwards once again with a peak in 1989 and staying positive through most of the 1990's with the exception of 1996. The OA/NAO has trended near neutral in recent years.

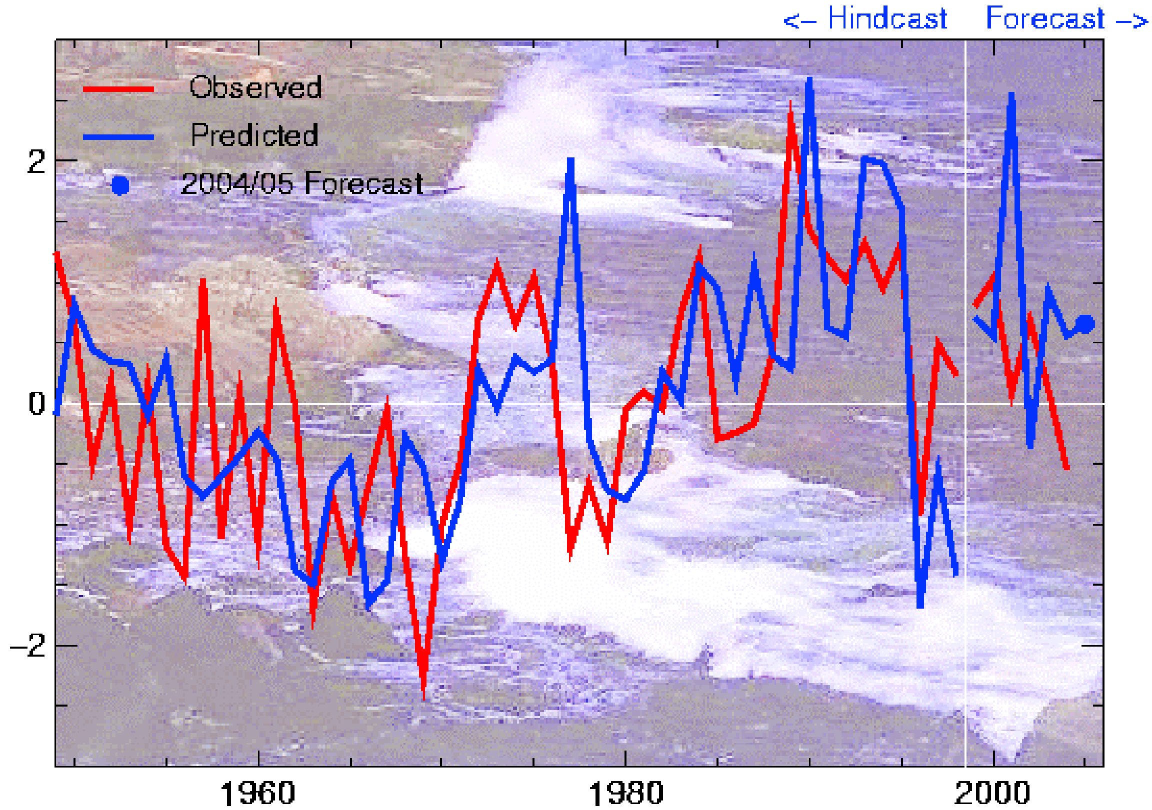

Figure 28: AO/NAO pattern since 1950 as calculated by British Met Office

If the years where three or more stations reported the highest MD accumulations are selected from our database, the years 1975, 1989, 1995 and 1998 stand out from the record. Figure 28 shows that in all four cases the AO/NAO was in a positive phase during these years. With a strong Icelandic Low, more warm air is able to penetrate into the Arctic pushing back the Polar High. If we do the same for years in our database with a least three or more stations reporting the lowest MD accumulations, the following years come to light; 1972, 1976, 1978, 1986, and 1992. The association with the AO/NAO is much less clear in these cases as it was positive for 1972, 1976 and 1992 but negative for 1978, 1979, 1986 and 1996. In recent years the AO/NAO has trended towards neutral and this has corresponded to less variability in summer Arctic temperatures since 2000.

It should be noted that the AO/NAO has its strongest influence in the winter months so the dates listed in Figure 28 represent the winter that preceded the summer of that year. An association can be made that positive AO/NAO's tend to produce warm summers in the Canadian Arctic and negative AO/NAO's produce cool summers, but this is a very weak association. The British Met Office data that was used to produce the figure above was based primarily on the analysis of the pressure difference between the Icelandic Low and the Azores Low. There may be an influence of the AO/NAO on summer conditions in the Arctic but this requires a much more detailed investigation involving a computation that includes the Polar High gradient. Such an analysis is well outside the scope of this present study.

A similar situation occurs in the Pacific Ocean relating to the El Niño Southern Oscillation (ENSO). ENSO refers to the cyclic pattern relating to the appearance of warmer than normal equatorial Pacific Ocean surface waters west of South America (the El Niño condition) or cooler than normal waters in the region (the La Niña condition). It is well documented that ENSO cycles have a significant effect on weather conditions experienced over North America.

During El Niño years the Polar Jet Stream that traverses North America splits in two, with a southern branch running across the southern United States and a northern branch running northward along the west coast of North America then plunging southward across the central and eastern portion of the continent. The consequence of this pattern is that western, central and south-eastern North America are placed into the sub-tropical air mass during an El Niño winter, creating much warmer and wetter conditions than usual. This means that Alaska and the Great Lakes should experience favourably warm weather conditions during an El Niño year. The Aleutian Low strengthens to dominate Alaska pushing back the Polar High and bringing warm air into the region. However, north-eastern North America, particularly the Labrador Coast, Hudson Strait and the eastern Arctic should experience colder to much colder than normal conditions. Figure 29 and Figure 30 map the temperature deviation over Canada during the previous El Niño winters of 1982/83 (Figure 29) and a strong El Niño in 1991/92 (Figure 30). It is quite clear, particularly from an analysis of Figure 30, that El Niño conditions provide for cold falls and winters to the eastern Canadian Arctic.

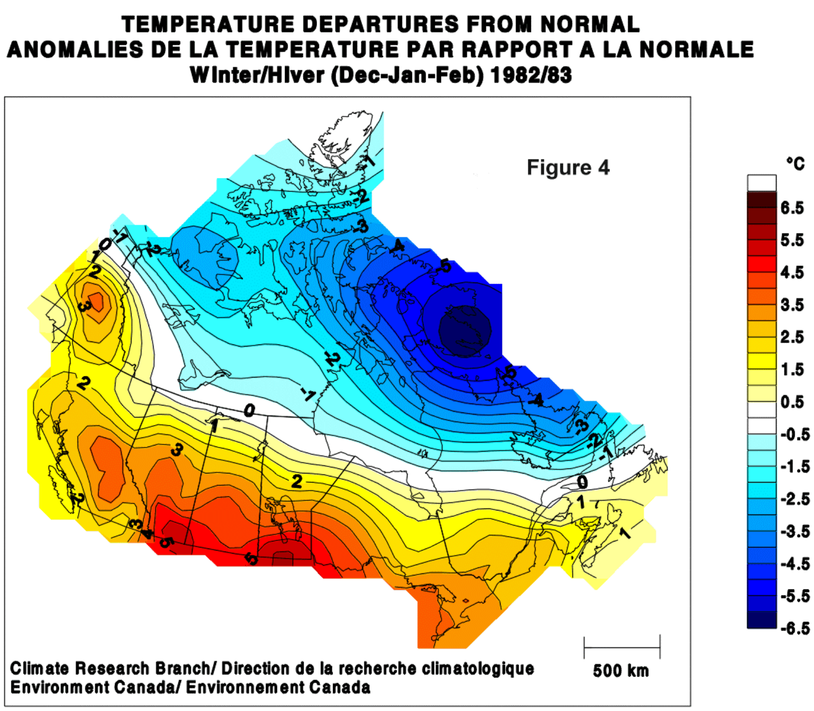

Figure 29: Temperature Deviation over Canada during the El Niño winter of 1982/83

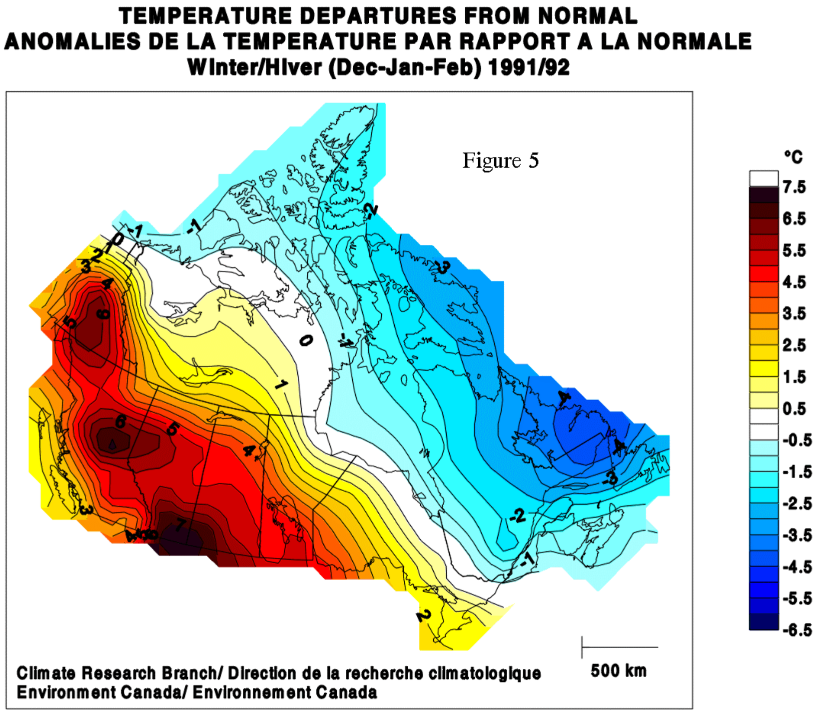

Figure 30: Temperature Deviation over Canada during the El Niño winter of 1991/92

However, during La Niña conditions, the situation is somewhat reversed. During La Niña winters, the intensity of the Polar Jet Stream increases and moves south to parallel the Canada/U.S. border. This brings colder, drier air into central North America providing colder winters over most of the continent.

Alaska suffers particularly colder than normal conditions during La Niñas, as does most of central North America and the Great Lakes. The Aleutian Low weakens allowing the Polar High to dominate over Alaska. However, the return air flow from the La Niña pattern actually provides warmer conditions into the eastern Canadian Arctic, although this air flow is rather weak. Therefore, La Niña conditions are more likely to provide milder and more favourable conditions to the Labrador Coast, Hudson Strait and the eastern Canadian Arctic. Alaska and the Beaufort Sea, however, will likely experience much worst than normal conditions in the fall of a La Niña year.

Given this general theory of how the ENSO behaves over North America, it can be looked at when El Niño and La Niña conditions have occurred and compare them to our database of summer Arctic Cumulative Melting Degrees (CMD). The years when El Niño and La Niña occurred concurrent with our data record are as follows:

El Niño years:

1969/70, 1972/73, 1982/83, 1986/87, 1991/92, 1994/95, 1997/98, 2002/03

La Niña years:

1970/71, 1973/74, 1975/76, 1985/86, 1987/88, 1995/96, 1999/2000

If we again look at our database of years where three or more stations reported the highest MD accumulations, we see that 1975, 1989, 1995 and 1998 stand out while our coolest years in the record are 1972, 1976, 1978, 1979, 1986, 1992 and 1996. Attempting to find a correlation of these years to ENSO events is a very complex problem as ENSO events are a gradual shifting phenomenon that can span one or more years. A detailed investigation of the ENSO relationship to Canadian Arctic summer temperatures is well beyond the scope of this present work but there are some observations that can be made.

The 1973 to 1976 La Niña was one of the strongest and longest lasting cool ENSO periods on record and contributed to extremely cold summers and heavy ice conditions in Alaska and the Beaufort Sea. In fact, the summer of 1975 was the worst on record for ice condition in the Beaufort Sea with the pack ice not clearing off the North Slope of Alaska all summer. In contrast, the strongest El Niño of 1997/98 contributed to the most extensive clearing in the Beaufort Sea. It is well understood that ice conditions in Alaska and the Beaufort Sea are strongly influenced by ENSO events. However, the relationship with Canadian Arctic ice conditions is less clear and it is possible that the ENSO and AO/NAO interact in a complex relationship that can only be identified with a rigorous analysis. For example, the 1997/98 El Niño led to the warmest year on record for all of Canada, including the Canadian Arctic that experienced the lightest ice conditions on record. This occurred during both a strong El Niño and moderate positive AO/NAO event and may have been related to these concurrent phenomenon.

The conclusion from this brief analysis is that the highly variable conditions seen in the Canadian Arctic temperatures may well be related to AO/NAO and ENSO events and that further research into this is warranted. This is particularly true in light of the fact that the AO/NAO and ENSO are the subject of ongoing investigations as to the role they play in climate change and finding a relationship between these phenomena and the Canadian Arctic would be an important link to understanding the implications of climate change on the region.

6. Methodology

As part of this project a new methodology was developed to analyze the impact of climate change and/or seasonal temperature variation on the veracity of the Zones and Dates used in the ZDS. The study focuses on the portion of the Canadian Arctic that covers the Northwest Passage as well as the access to the port of Churchill through Hudson Strait. The analysis examines the existing and potential changes to ice regimes in the Northwest Passage (NWP) and Hudson Strait shipping lanes due to the climate change. The length of the shipping season for colder than normal and warmer than normal summers is analyzed for each Zone by both the ZDS and the AIRSS. Both systems are then compared.

6.1 Data processing

Two sets of trajectories were defined. The first set of trajectories was defined as line segments approximately 125.5 km (Table 5). The trajectories in Zone 4 and Zone 12, Zone 11 and Zone 7, Zone 6 and Zone 13, and Zone 13 and Zone 9 were defined to assess how much the two neighboring Zones differ. The trajectories were also defined in Zone 14 and Zone 15. The route segments are shown in Figure 31.

Table 5: Length and locations of the first set

LOCATION	LENGTH (km)	ZONE
CAMBIDGE_BAY	125.002	ZONE 11
CAMBIDGE_BAY	125.187	ZONE 7
CORAL_HARBOUR	125.248	ZONE 14
IQALUIT	125.057	ZONE 15
POND_INLET	125.834	ZONE 13
POND_INLET	125.834	ZONE 9
RESOLUTE	125.124	ZONE 13
RESOLUTE	124.826	ZONE 6
TUKTOYAKTUK	125.539	ZONE 12
TUKTOYAKTUK	126.003	ZONE 4

The second set of trajectories consisted of actual navigation routes through the Northwest Passage, and through the approach to and across Hudson Bay (Figure 2). The Hudson Bay trajectory was defined with a Main route and an Alternative Route. These two routes are identical through the approach, but split east of Coats Island. The Alternative route curves northward around Coats Island, and the Main route curves Southward around Coats Island. The routes meet again at Churchill. These lines (trajectories) were buffered into 1 km wide polygons using ArcView GIS software. The trajectories have associated data attribute tables in ArcView consisting of fields describing the location of the trajectory (NWP East, NWP West, Hudson Strait, Hudson Bay Main route, Hudson Bay Alternate Route) and the Zone number. Digital Regional weekly ice charts issued by Canadian Ice Service (CIS) were also imported into ArcView and intersected with the trajectory maps (layers). The resulting layers' data attribute table contains attributes from both maps. Detailed description of data processing can be found in Appendix A.

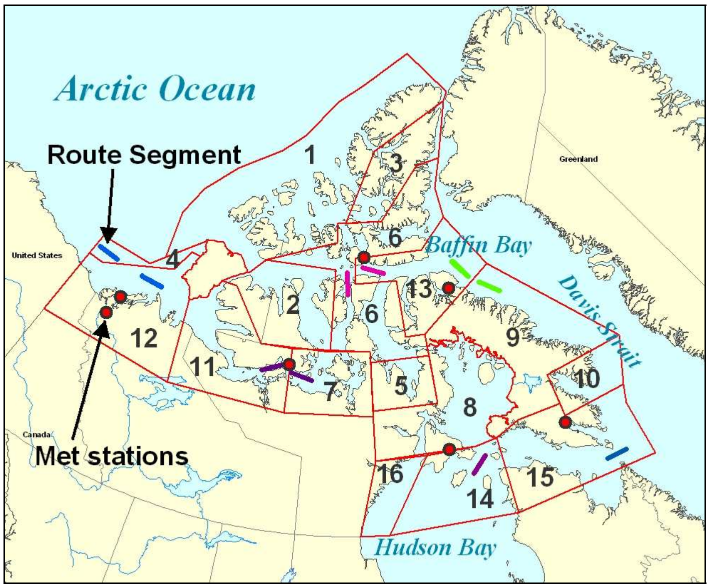

Figure 31: Route Segments in the Northwest Passage and in Hudson Strait

6.2 Data Analysis

It should be noted that the route remained fixed over all years of the analysis and no attempt was made to adjust the route to avoid ice. Such adjustment would have increased the complexity and difficulty of the analysis. In any case, the use of ice information and appropriate route planning is not a requirement of the Zone/Date component of ASPPR.

Figure 32 shows an example of the route crossing six different ice regimes in one Zone (Zone11). The Ice Numerals (IN) for Type B ice class vessel were calculated for each ice regime the shipping route crossed based on the ice information obtained from the egg code.

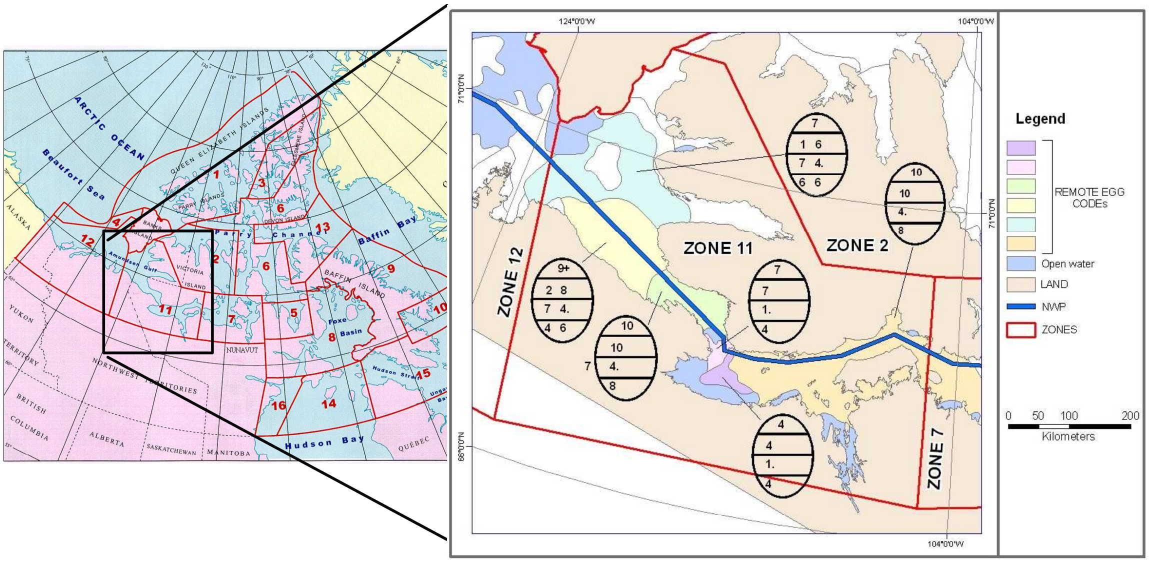

Figure 32: Northwest Passage route crossing six different ice regimes within Zone 11

The INs calculated throughout the whole year were compared to the Entry and Exit dates of the appropriate Zone. The ASPPR Type B ice class vessel was selected since this is the lowest ice class vessel allowed passage through all Control Zones that compose the Northwest Passage (Zones 12, 11, 7, 6, and 13). Table 6 shows Entry and Exit dates for Type B vessel as per the Zone/Date System. Zones 1, 2 and 5 do not allow access to Type B vessels, but since these Zones may also fall into the route plan of a vessel crossing the Northwest Passage they were analyzed as well. The IN calculations are based on the ice charts, which do not indicate ridging or decay, so neither ridging nor decay is reflected in the IN values. Satellite images were used to analyze and explain the ice movement and any peculiarities in results, for example a sudden drop in the IN value.

Table 6: Zone/Date Table for Type B vessel (Entry and Exit dates)

Zone No.	1	2	3	4	5	6	7	8	9	10	11	12	13	14	15	16
Entry Date	-	-	Aug 20	Aug 20	-	Aug 25	Aug 10	Aug 10	Aug 10	Aug 1	July 15	July 1	July 15	July 1	July 1	June 20
Exit Date			Sept 5	Sept 15		Sept 30	Oct 15	Oct 31	Oct 31	Oct 31	Oct 20	Oct 25	Oct 15	Nov 30	Nov 30	Nov 10

An example of analysis in comparing the two systems is shown in Figure 33 to Figure 36. Figure 33 and Figure 34 show the range of Ice Numerals in Zone 11 for cold and warm years, respectively. The circles represent the Ice Numerals calculated from the CIS ice charts. The Regional ice charts for the Canadian Arctic are issued monthly in the winter/spring season and weekly in the summer/fall season. The lowest values of Ice Numerals and the highest values of Ice Numerals are connected by a line to highlight the range of Ice Numerals throughout the whole year. In some instances the values of Ice Numerals are superimposed; therefore a number indicating a count of Ice Numerals at that particular value was printed on the circle. Circles without numbers represent a single

Ice Numeral for that particular value. The green rectangle represents the Zone/Date shipping season for Type B vessel in Zone 11 (July 15 to October 20).

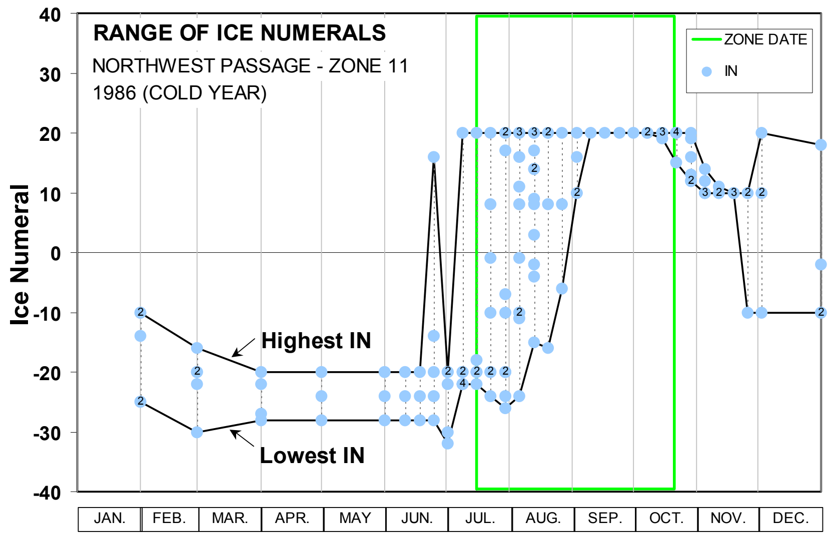

Figure 33: Range of Ice Numerals calculated from CIS ice charts for NWP shipping route in Zone 11, throughout year 1986 (colder than normal in period 1968-2004)

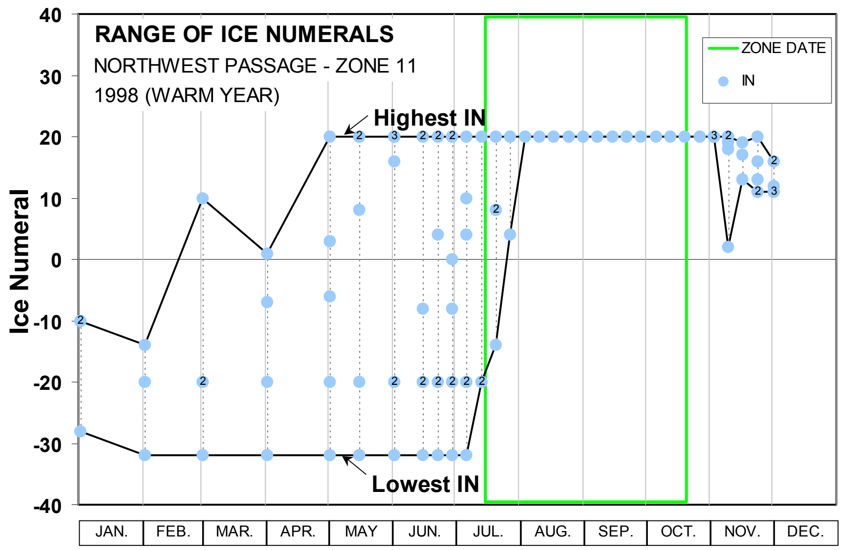

Figure 34: Range of Ice Numerals Calculated from CIS ice charts for NWP shipping route in Zone 11, throughout year 1998 (warmer than normal in period 1968-2004)

The sudden drop in the value of the IN in Figure 33 (cold year 1986) is due to the high concentrations of Thick First-Year ice in eastern Amundsen Gulf. Coronation Gulf was still fast with Thick First-Year ice.

Data shown in Figure 33 and Figure 34 are further analyzed in Figure 35 and Figure 36, respectively. These Figures (Figure 35 and Figure 36) show a count of negative and positive Ice Numerals for cold and warm years, respectively. The purpose of this plot is to illustrate the number of positive (passage allowed) or negative (passage restricted) Ice Numerals. The triangle symbol represents the number of ice regimes for which the Ice Numeral was negative. The square symbol represents the number of ice regimes for which the Ice Numeral was positive. The negative and positive counts are connected by lines for better visual observation and easier comparison with the Zone/Date window (bold rectangle indicating the shipping season for Type B vessel in Zone 11).

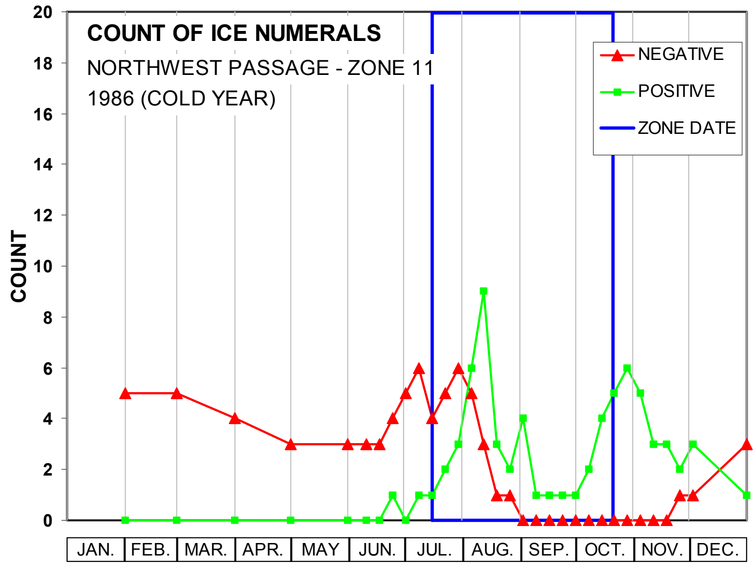

Figure 35: Count of negative and positive Ice Numerals calculated from data plotted in Figure 5 - NWP shipping route in Zone 11, throughout year 1986 (colder than normal in period 1968-2004)

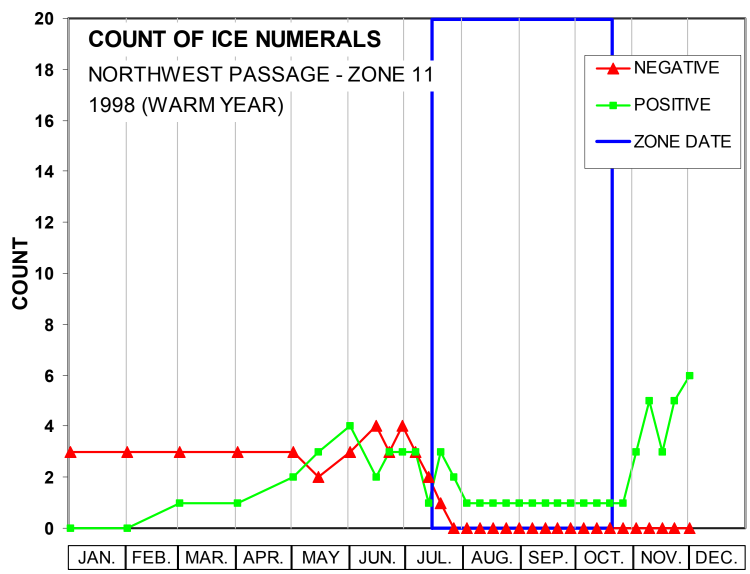

Figure 36: Count of negative and positive Ice Numerals calculated from data plotted in Figure 6 - NWP shipping route in Zone 11, throughout year 1998 (warmer than normal in period 1968-2004)

Zone 11 covers the portion of the Northwest Passage that includes Amundsen and Coronation Gulfs. The analysis of data plotted in Figure 33 to Figure 36 showed that negative Ice Numerals are encountered early in the Type B season for both colder as well as warmer than normal summers in Zone 11. This stems from the fact that the season for a Type B vessel in Zone 11 starts prior to the completion of melt of the Thick first year ice and Old Ice in Amundsen Gulf in July and early August. However, positive numerals are maintained in both the cool and warm summers well into November, more than a month beyond the Type B closing. This is because the limiting ice type of medium first year ice does not form in Amundsen Gulf until late November. Figure 37 and Figure 38 show the Zone/Date window (bold dashed rectangle), modified to reflect the actual ice conditions in the colder than normal and warmer than normal year, respectively. The analysis suggests shifting the opening and closing dates to early August to Mid-November for a Type B vessel in Zone11.

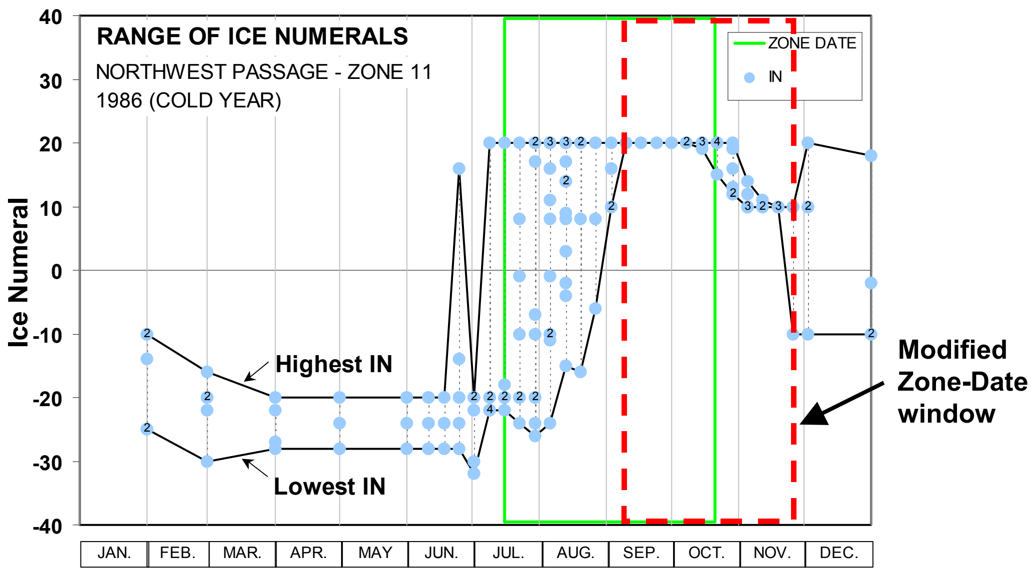

Figure 37: Corrected Zone/Date window (bold dashed rectangle), modified to reflect the actual ice conditions in the NWP shipping route in Zone 11, throughout year 1986 (colder than normal in period 1968-2004)

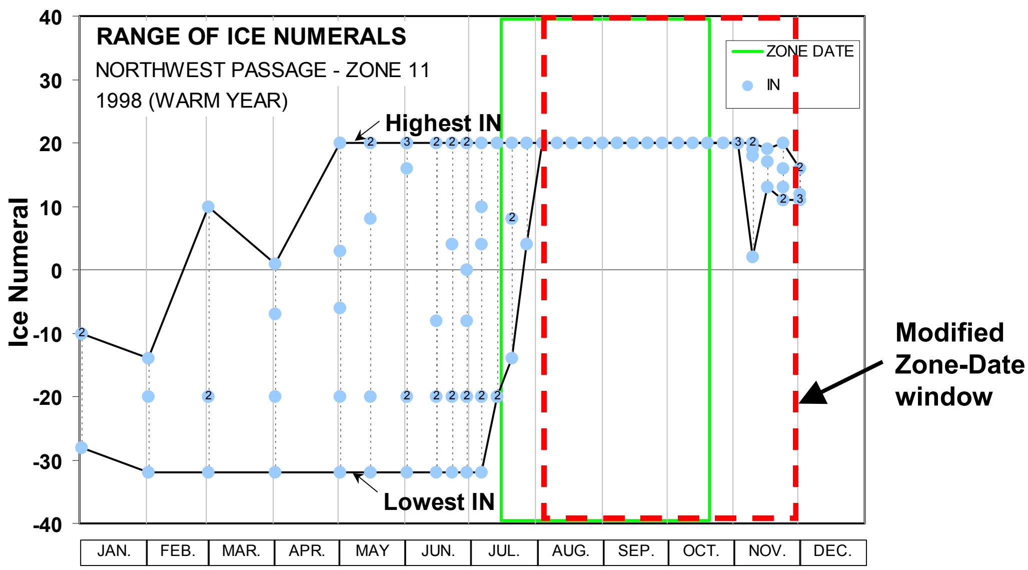

Figure 38: Corrected Zone/Date window (bold dashed rectangle), modified to reflect the actual ice conditions in the NWP shipping route in Zone 11, throughout year 1998 (warmer than normal in period 1968-2004)

Similar analysis was done for each Zone of the NWP route, for the access routes to the Port of Churchill in Hudson Strait, and for the route segments in neighboring Zones (the trajectories in Zone 4 and Zone 12, Zone 11 and Zone 7, Zone 6 and Zone 13, Zone 13 and Zone 9) and route segment in Zone 15, and in Zone 14. The plots for each Zone analyzed are listed in the Appendix B. Appendix C explains the reasons for sudden changes in values of the Ice Numerals.

7. Analysis of the Northwest Passage

The Northwest Passage is a sea route linking the Atlantic and Pacific Oceans. It provides an alternative and shorter passage from Europe to Asia, however, due to the ice conditions, the route cannot be used throughout the whole year. With potential global warming the ice cover in the NWP will decrease, which will increase the volume of traffic. At the same time the melt of the ice in the Canadian Arctic Archipelago will allow more Old Ice to reach the NWP, which will make shipping in the NWP challenging and hazardous. The existing Regulatory Zone/Date System was analyzed and evaluated to determine if it truly represents the existing ice conditions. Two years, warmer than normal and colder than normal, were analyzed to see how the climate change would affect the veracity of the Zone/Date System. The ice conditions in the shipping lane in all Control Zones that compose the Northwest Passage (Zones 4, 12, 11, 7, 6, and 13) were analyzed for Type B vessel. Zones 1, 2 and 5 do not allow access to Type B vessels, but since these Zones may also fall into the route plan of a vessel crossing the Northwest Passage they were analyzed as well. Also the Entry and Exit dates in each Zone were analyzed.

7.1 Zones 4 and 12

Zones 4 and 12 cover the Canadian Beaufort Sea portion of the Northwest Passage. During cooler than normal summers in the eastern Beaufort Sea, the southern limit of the pack ice occurs across Zone 4 and into the northern reaches of Zone 12 for most of the summer. This results in high concentrations of Thick first year ice and Old Ice in these zones with the consequence that a Type B vessel encounters negative numerals within Zones 4 and 12 throughout the opening dates for the zones, as was the case in 1986.

In a warmer than normal summer the pack ice retreats northward sufficiently that it clears Zone 4 and Zone 12 allowing a broad access window for a Type B vessel, almost one month longer than that allowed by the existing Zone Date system, as was the case in the very warm summer of 1998. However, in Zone 12, even in many warmer than normal summers, negative numerals can be encountered by a Type B vessel within the Zone 12 dates. This is due to the southward flux of the Beaufort pack ice edge along the west coast of Banks Island across the western entrance to Amundsen Gulf. The satellite image from September 28, 2003, shows this incursion of Thick first year ice and Old Ice across the eastern section of Zone 12 (Figure 39).

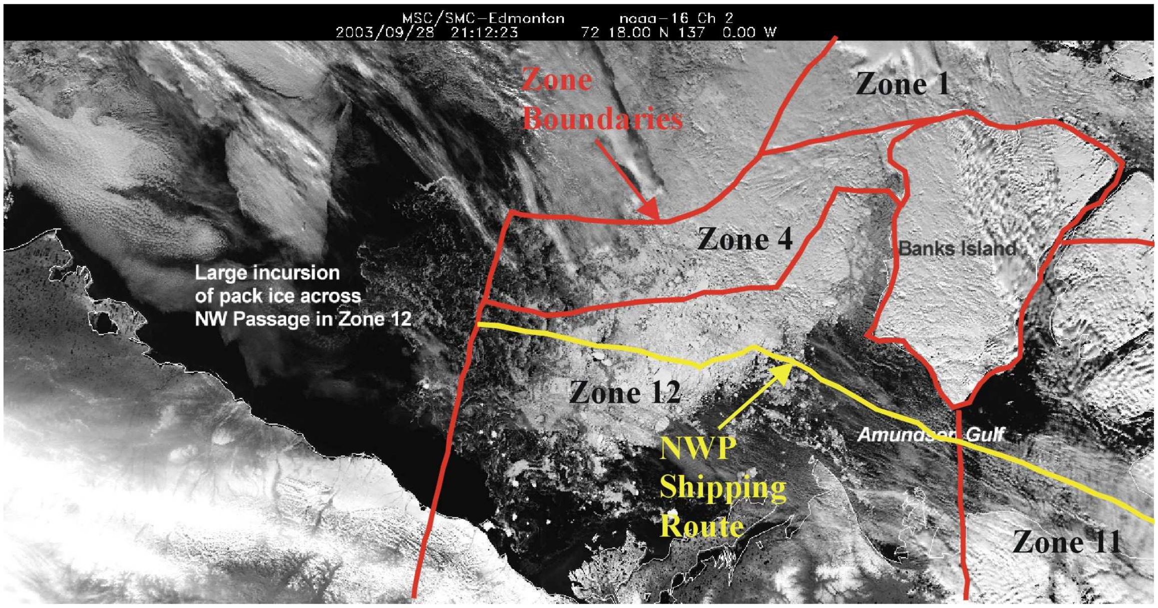

Figure 39: The satellite image from September 28, 2003, showing the incursion of Thick first year ice and Old ice across the eastern section of Zone 12. Note that the route through the Beaufort Sea is limited to narrow sounded tracks through the Pingo field. The Figure shows a sketch of Zones boundaries and Northwest Passage shipping route.

This incursion of ice along the west coast of Banks Island has occurred more frequently in recent summers and may be due to a change in the circulation of the Beaufort Gyre. In addition, the occurrence of this ice is unrelated to summer temperatures, occurring in both cold, average and above average summers.

The conclusion from this analysis is that the Zone date system for Type B vessels does not adequately reflect the tendency for negative numerals in Zone 12, even in warmer than normal summers. This trend of negative numerals is projected to continue to be a problem in Zone 12 even in a warming Arctic this century.

7.2 Zone 11 and 7

Zones 11 and 7 cover the portion of the Northwest Passage that includes Amundsen, Coronation and Queen Maud Gulfs.

The results show that the opening and closing dates of Zones 11 and 7 for Type B vessel do not agree with the observation. Negative numerals are encountered early in the Type B season for both cool as well as warmer than normal summers in Zone 11. This stems from the fact that the season for a Type B vessel in Zone 11 starts prior to the completion of melt of the Thick first year ice and Old Ice in Amundsen Gulf in July and early August. However, positive numerals are maintained in both the cool and warm summers well into November, more than a month beyond the Type B closing. This is because the limiting ice type of medium first year ice does not form in Amundsen Gulf until late November.

Negative numerals for a Type B vessel also occur in Zone 7 in both cool and warmer summers. These numerals result from the southward drift of Thick first year and Old Ice from M'Clintock Channel and Franklin Strait into southern Larsen Sound and through Icebreaker Channel into northern Queen Maud Gulf. M'Clintock Channel and Larsen Sound form the southern terminus of old and Thick first year ice drifting south through the Queen Elizabeth Islands. In cool to average summers there is insufficient warmth to completely melt this ice and the entire northern reaches of Zone 7 will contain high concentrations of this ice. Even in a warmer than normal summer not all of this ice will melt, particularly late in the Type B season for Zone 7 (in early October) when falling temperatures prevent the further melt of the ice that drifts into Zone 7 from M'Clintock Channel in Zone 2.

The satellite image from September 28, 2004, illustrates the accumulation of Thick first year ice and Old Ice in central and southern Larsen Sound in the northern extents of Zone 7 and the southern extents of Zone 6 (Figure 40). This ice creates an ice regime beyond the capabilities of a Type B vessel despite the fact that these zones are open to this ice class during this period. The ice conditions illustrated in the image below are typical for this region of the Canadian Arctic and represent the limiting ice conditions for ships attempting a transit of the Northwest Passage.

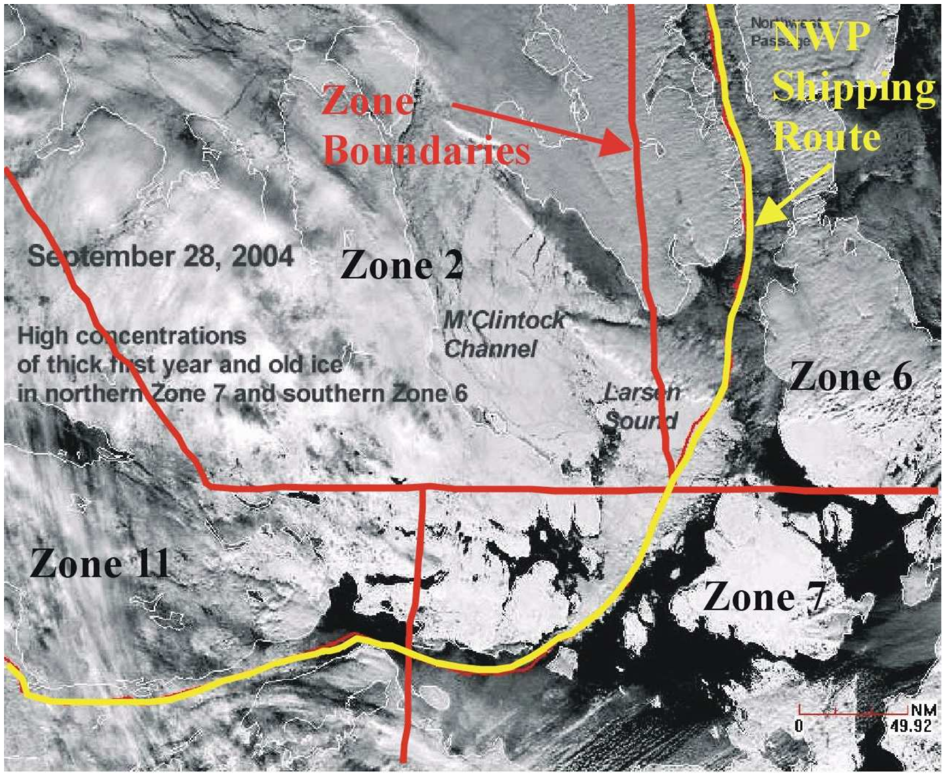

Figure 40: Satellite image from September 28, 2004, illustrating the accumulation of Thick first year ice and Old ice in central and southern Larsen Sound in the northern extents of Zone 7 and the southern extents of Zone 6. Note that available soundings limit the route a vessel can follow through this area to avoid ice. The Figure shows a sketch of Zones boundaries and Northwest Passage shipping route.

The area in central Larsen Sound where the three zones of 2, 6 and 7 meet represents a weakness in the Zone/Date system as it pertains to the Northwest Passage. This area of Larsen Sound represents a fairly homogeneous ice regime of Thick first year and Old Ice even in warmer than average summers. The boundary between Zone 6 and 7 results in a Type B vessel having an access window through this portion of the Northwest Passage spanning from August 25 to September 30 (the Zone 6 dates) when, in fact, a Type B vessel would have great difficulties navigating through this area in any given summer. The northern boundary of Zone 7, the southern boundary of Zone 6 and the southern boundary of Zone 2 all need revisions in this area to properly reflect the ice conditions that occur in this area. The ice conditions in southern and central Larsen Sound are most appropriately placed in Zone 2 (the same zone that presently covers M'Clintock Channel), even if we see warmer summers in the years to come.

7.3 Zone 6

Zone 6 is a broad zone spanning from northern Baffin Bay across Jones Sound into northern Viscount Melville Sound and southward through Peel Sound into central Larsen Sound. The difficulties with Type B vessel access in the Larsen Sound region of Zone 6 were already discussed in the previous section. However, there are also difficulties in the region of Zone 6 in central Barrow Strait south of Resolute. Thick first year ice and Old Ice drift eastward from Viscount Melville Sound into central Barrow Strait north of Peel Sound each summer following break-up in late July and August. As summer temperatures increase this ice melts as it drifts eastward. However, when temperatures are not sufficiently high enough in cooler summers this ice does not melt and presents the potential for negative numerals for a Type B vessel transiting the Northwest Passage. It is anticipated that warmer temperatures in future may reduce the possibility of this occurring.

The satellite image from August 28, 2002, shows the movement of Thick first yearice and Old Ice across the northern entrance to Peel Sound into central Barrow Strait across the Northwest Passage (Figure 41). Such a condition would result in negative numerals for a Type B ship at the August 25 opening of the zone.

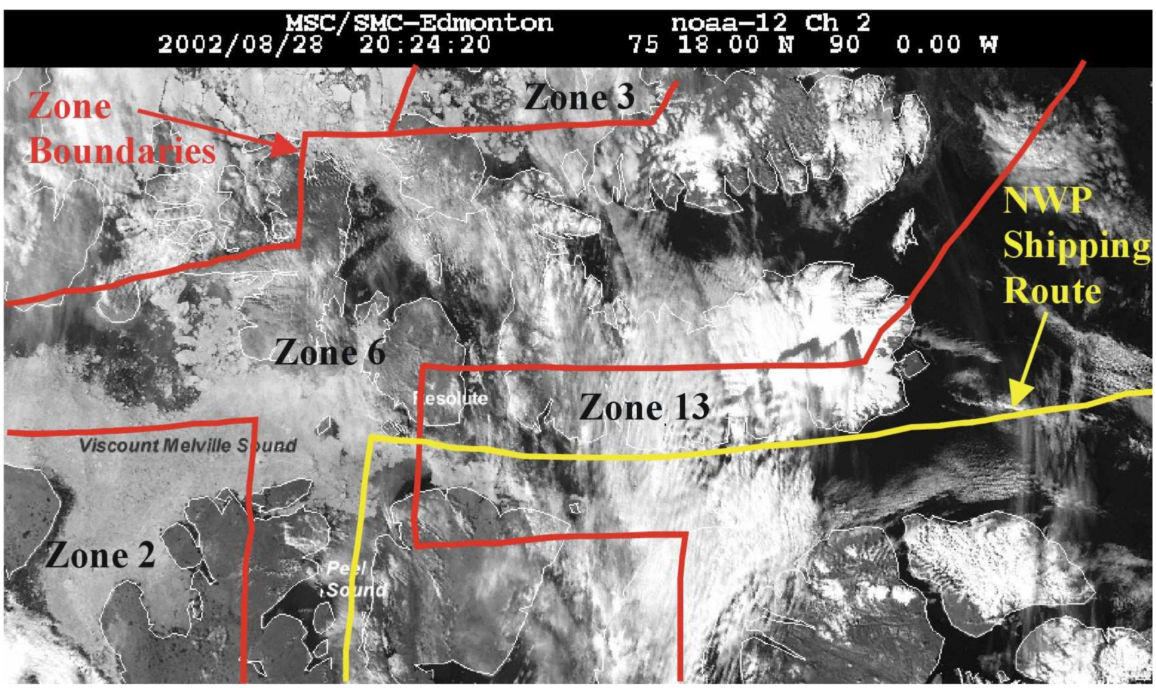

Figure 41: Satellite image from August 28, 2002, showing the movement of Thick first year ice and Old ice across the northern entrance to Peel Sound into central Barrow Strait across the Northwest Passage. The Figure shows a sketch of Zones boundaries and Northwest Passage shipping route.

7.4 Zone 13

Zone 13 covers the eastern entrance to the Northwest Passage from Baffin Bay westward through Lancaster Sound to eastern Barrow Strait west to Resolute. In cooler than normal summers Thick first year and Old Ice that drift eastward from central Barrow Strait and Viscount Melville Sound occur across eastern Barrow Strait causing negative numerals for a Type B vessel, as happened in the cool summer of 1986. Even in warmer than normal summers, the Old Ice that drifts south from Wellington Channel into eastern Barrow Strait or from Northern Baffin Bay from Nares Strait into eastern Lancaster Sound can create negative numerals for a Type B vessel within the Zone Dates, as happened in the very warm summer of 1998. This situation will persist even if summer temperatures increase in the Canadian Arctic over this century.

8. Analysis of Access Route to Churchill

The Port of Churchill located on the Western shore of Hudson Bay connects the Canadian railway system with the shipping system and is an important seaport for shipment of mining materials, grain, and manufactured goods. The access route from Labrador Sea to the Port of Churchill leads through the Hudson Strait and Northern portion of the Hudson Bay. The Ice conditions and the Entry and Exit dates in the Control Zones that are crossed by the shipping route were analyzed in the same manner as those comprising the Northwest Passage.

8.1 Zone 15 (Main and Alternate Routes)

Zone 15 covers Hudson Strait in the access to the Port of Churchill. One of the last areas to clear of ice in Zone 15 is the eastern entrance to Hudson Strait in the Labrador Sea. Thick first year ice and Old Ice drifting southward from Davis Strait and the northern Labrador Sea enters eastern Hudson Strait and will often persist in the region well into July after the start of the Type B season for Zone 15. The presence of this ice results in negative numerals for a Type B vessel early in the navigation season, and this occurs even in a warmer than normal summer. Consequently, this difficulty will persist into the future even with a warming Arctic.

The satellite image from July 28, 1983 shows the persistence of this ice in eastern Hudson Strait late into July in a cool summer (Figure 42).

8.2 Zone 14 (Main and Alternate Routes)

Zone 14 covers northern Hudson Bay south of Southampton Island. In average to cooler than average summers, high concentrations of Thick first year ice persist in northern Hudson Bay well into July producing negative numerals for Type B vessels during this period. Evidence of this persistent pack ice in Zone 14 can be seen at the extreme western edge of the satellite image above. Even in a warmer than normal summer, such as in 2004, high concentrations of Thick first year ice can persist into July in Zone 14, as evident in the satellite image from July 7, 2000 (Figure 43). Only in an exceptionally warm summer, as was the case for the summer of 1998, would the ice clear sufficiently as to generate positive numerals for a Type B vessel across Zone 14. The implication of this is that it will take many decades of continual warming of the region to get to the situation where the conditions of 1998 would be considered normal for the region.

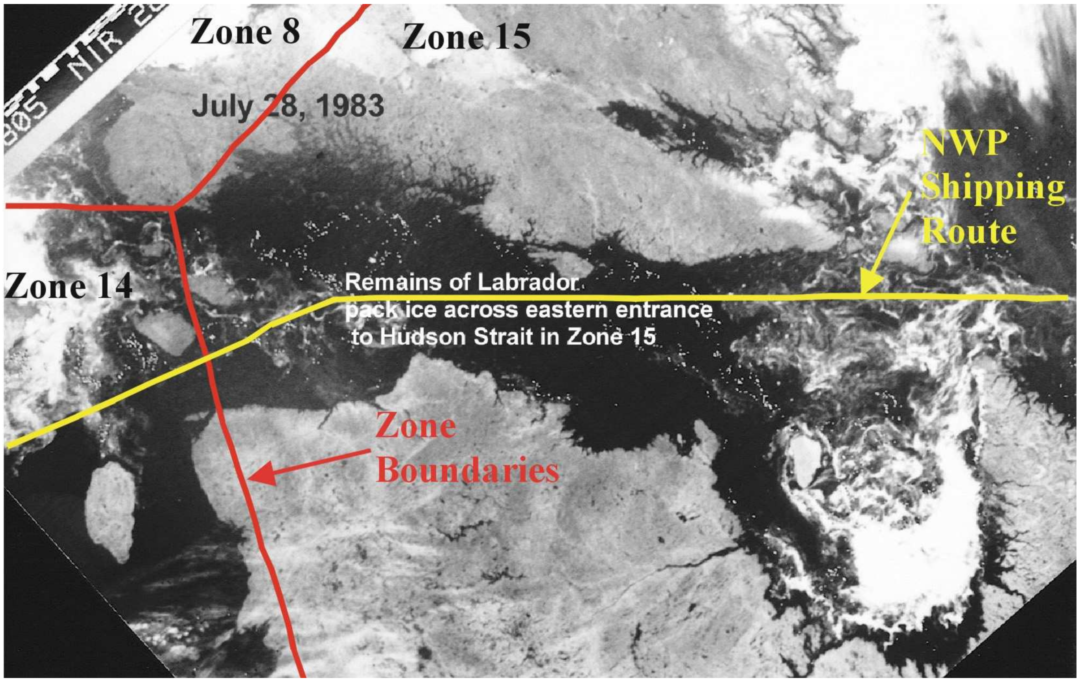

Figure 42: Satellite image from July 28, 1983 showing the persistence of the ice in eastern Hudson Strait late into July in a cool summer. The Figure shows a sketch of Zones boundaries and approach route to the Port of Churchill.

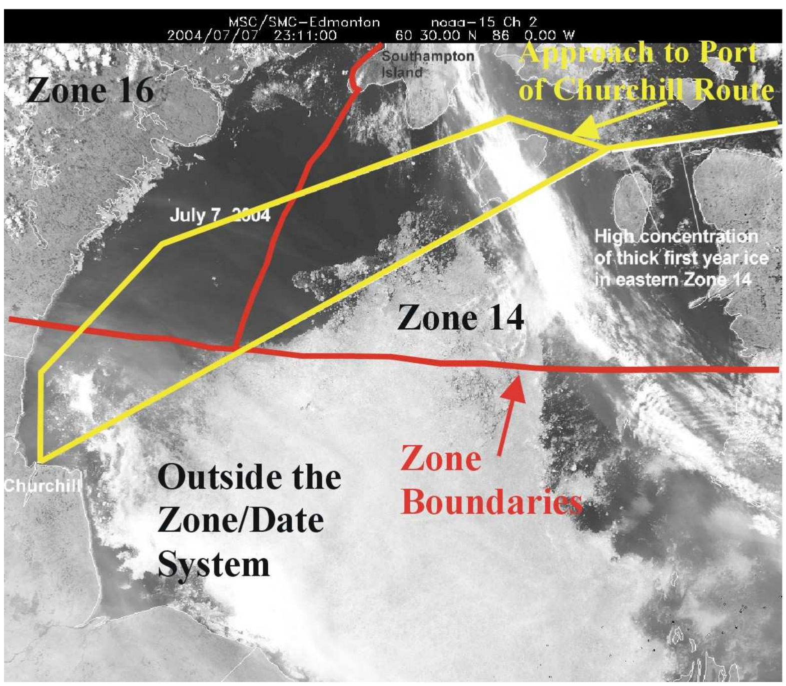

Figure 43: Satellite image from July 7, 2000, showing high concentrations of Thick first year ice persisting into July in Zone 14. The Figure shows a sketch of Zones boundaries The Figure shows a sketch of Zones boundaries and approach route to the Port of Churchill.

8.3 Zone 16 (Alternate Route)

Zone 16 covers the western shore of Hudson Bay north of 60°N. This zone was created to reflect the fact that the first ice to clear in Hudson Bay is the north-west quadrant due to the prevailing north-west winds in the region. This early clearing is evident in the satellite image above. Vessels attempting access to Churchill early in the shipping season will often take the alternate "northern" route across the south coast of Southampton Island and southward along the west coast of Hudson Bay avoiding the pack ice in the central portion. However, in normal to cooler than normal summers, such as occurred in 1992, the clearing of western Hudson Bay can be delayed well into July resulting in negative numerals for a Type B vessel. Only in warmer than normal summers, such as occurred in 1998 would positive numerals for a Type B vessel be expected in Zone 16 in early July.

9. Potential Damage to Vessels

Canadian Hydraulics Centre (CHC) of the National Research Council of Canada in Ottawa developed a comprehensive Ice Regime System (IRS) database (Timco and Morin, 1998; Timco and Kubat, 2002). This database contains information related to occurrences of both damage and non-damage events, where each event is characterized by 79 fields that relate to vessel characteristics, route, climate, ice conditions, and damage.

Damage in the CHC/IRS database was categorized according to its type and severity as described in Table 7. These categories were described in the database by a Damage Severity (DS) number as shown in the Table. A Damage Severity number greater than three was used to indicate that the damage had the potential for causing pollution.

Table 7: Definition of Damage Severity number.

Damage Severity Number	Description
0	No damage
1	High measured stress
2	slight deformation of hull, denting, propeller
3	small puncture or fracture, extensive denting
4	large hole
5	vessel sank

Kubat and Timco (2003) analyzed 125 IRS database events that caused damage to vessels in Arctic waters. The analysis showed that there was multi-year ice present in the ice regime in 73% of the damage events. For Canadian Arctic Class (CAC) vessels, designed to operate in severe ice conditions, there are few damage events, but virtually all those that did occur had ice regimes with multi-year ice present. The ice regime represents a region consisting of the same ice conditions, i.e. ice type and ice concentration. For Type vessels, designed to operate in more moderate first-year ice conditions, 66% of the damage events occurred in ice regimes which contained multi-year ice. The data also showed that damage is more severe in ice regimes that contain multi-year ice.

The analysis mentioned above illustrates the damage potential and hazards presented by multi-year (MY) ice, therefore the occurrence of MY ice in the shipping lanes in the Northwest Passage was analyzed. The concentration of MY ice in each ice regime within one Zone was normalized in order to calculate MY ice coverage of the shipping lane in that particular Zone. The results of this calculation for Zone 11 during the week of July 22 to July 28, 1986 are given in Table 8. Figure 44 shows 7 ice regimes that formed Zone 11 during the week of July 22 to July 28, 1986. The first column in the Table 8 lists the ice regimes, the second column indicates the area of the shipping route crossing the corresponding ice regime (i.e. trajectories buffered into 1 km wide polygons in the ArcView), the third column indicates the concentration of MY ice in tenth in the ice regime, the fourth column gives the area covered by MY ice in km^2 in each ice regime, and the fifth column gives the normalized percentage of the MY ice coverage to the whole length of the shipping route in the Zone. The last row in the Table 8 gives the Totals.

Table 8: Multi-year ice coverage in the Northwest Passage shipping lane in Zone 11 during week of July 22 – July 28, 1986

Ice Regime	Area Coverage (km^2)	MY ice coverage (tenth)	MY ice coverage (km^2)	MY ice % normalized
1	96.5	1	9.7	1.2
2	160.0	2	32.0	4.1
3	144.4	0.3 (trace)	4.3	0.6
4	9.8	Open Water	0	0
5	23.7	0	0	0
6	9.0	0	0	0
7	334.7	0	0	0
TOTAL	**778.1**	**N/A**	**46.0**	**5.9**

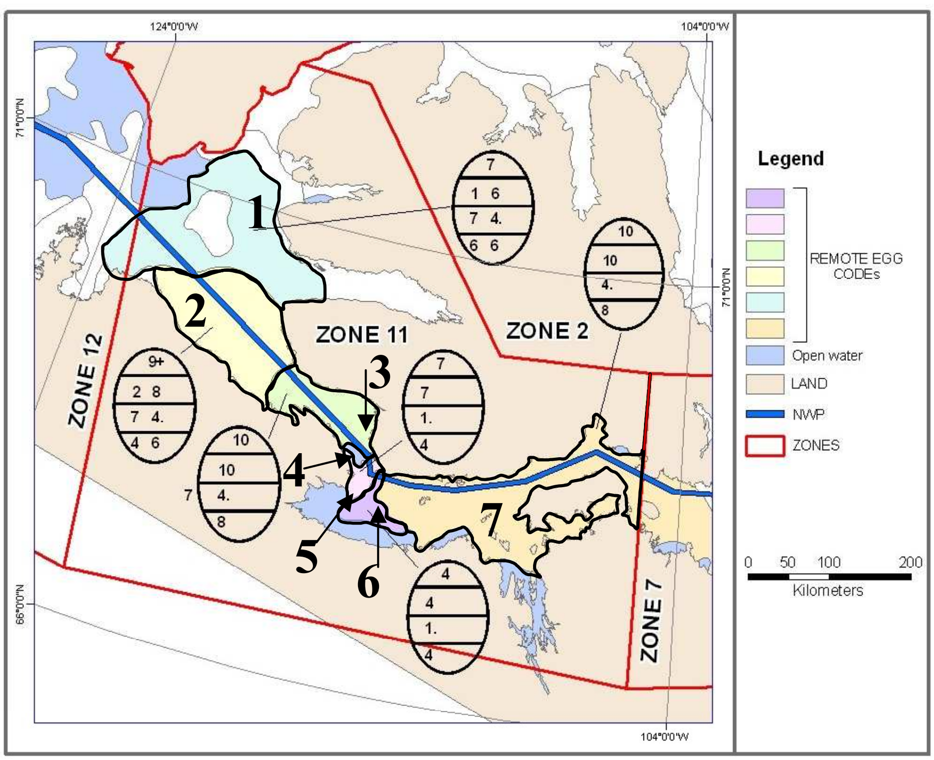

Figure 44: Ice regimes that formed Zone 11 during the week of July 22 to July 28, 1986

The same analysis was done for First-year ice coverage. The results are presented in Table 9.

Table 9: First-year ice coverage in the Northwest Passage shipping lane in Zone 11 during week of July 22 – July 28, 1986

Ice Regime	Area Coverage (km^2)	FY ice coverage (tenth)	FY ice coverage (km^2)	FY ice % normalized
1	96.5	6	57.9	7.4
2	160.0	8	128.0	16.5
3	144.4	10	144.4	18.6
4	9.8	Open Water	0	0
5	23.7	7	16.6	2.1
6	9.00	4	3.6	0.5
7	334.7	10	334.7	43.0
TOTAL	**778.1**	**N/A**	**685.2**	**88.1**

The analysis shows that the Zone 11 during the week of July 22 to July 28, 1986 was mainly covered by first-year ice, the multi-year ice was present in the western portion of the Zone 11 in the Amundsen Gulf, and Dolphin and Union Strait. The ice concentration in that region is high and with the presence of MY ice indicates potential danger to vessels, mainly to Type class vessels. Figure 45 and Figure 46 show the ice coverage in the Zone 11 throughout the warmer and colder than normal year, respectively. The ice coverage is presented in percents and is split into the Old Ice and First-year ice coverage. The line with the circle symbol represents the coverage by Old Ice, the line with the triangle symbol represents the total coverage by Old Ice and FY ice. The green rectangle represents the Zone/Date shipping season for Type B vessel in Zone 11 (July 15 to October 20). Figure 45 shows that there was no Old Ice present during the Type B vessel shipping season in the shipping lane. However in a colder than normal year the Old Ice is present in the shipping lane well into the end of the August and this presents a high potential for damage to low ice-strengthened vessels. The low percentage of ice coverage might tempt a vessel to travel with higher speed through the ice regime. This could result in a collision with the Old Ice floe that could cause considerable damage.

The same analysis was done for Zone 12, 7, 2, 6, and 13 (Zones comprising the Northwest Passage (NWP)) and Zones 15, 14, and 16 (approach to Port of Churchill through the Hudson Strait and Hudson Bay). The figures showing the ice coverage in these Zones throughout the warmer and colder than normal year are plotted in Appendix D.

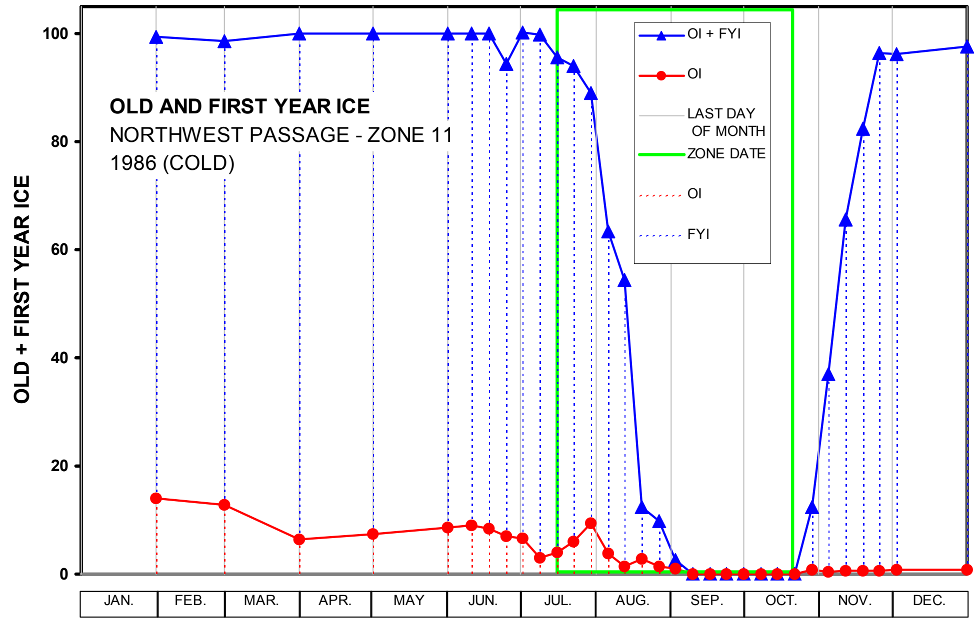

Figure 45: The ice coverage in the Zone 11 throughout the colder than normal year

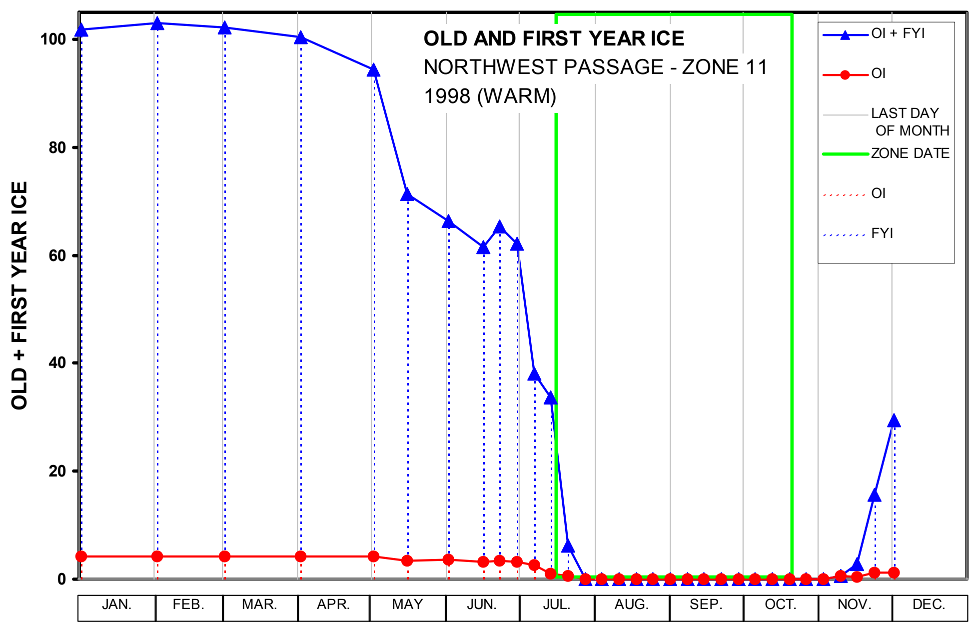

Figure 46: The ice coverage in the Zone 11 throughout the warmer than normal year

9.1 Ice Conditions in the Northwest Passage

The ice conditions vary from year to year. In some years Old Ice is present heavily in the Northwest Passage during the shipping season, in others it's not. The results from analyzing the warmer than normal year and colder than normal year showed that there is no Old Ice present in the Zone 12 shipping season for Type B vessel and less than 5% in the Zone 13 shipping season. In Zone 6 and Zone 7 the Old Ice is present at the beginning of the shipping season. Cautious travel is still required since Old Ice is difficult to detect and can cause considerable damage to a vessel.

It is interesting to notice that outside the shipping season there is a higher percentage of Old Ice coverage in warmer than normal year compared to colder than normal year in Zones 2, 7, and 13, which is due to the previous year ice conditions, i.e. the warmer temperatures in year 1998 were preceded by cooler temperatures in year 1997 in these regions; The cooler temperatures in year 1986 were preceded by warmer temperatures in year 1985 in these regions.

During the colder than normal year all Zones comprising the NWP experienced the presence of Old Ice well into the Type B vessel shipping season. The most severe ice conditions were in Zone 6 followed by Zone 7. Both Zones experienced about 20% coverage by Old Ice. The shipping lane in Zone 6 was covered by ice (combination of Old Ice and FY ice) in 90% and shipping lane in Zone 7 in 50%. Unless the vessel proceeds with extreme caution in such conditions the potential for damage is very high.

9.2 Ice Conditions in the Hudson Strait and Hudson Bay

The analysis of ice conditions for both main and alternate approach routes to the Port of Churchill during warmer than normal year indicates that the ice regimes that comprise the shipping routes are clear of ice during the shipping season (Zone/Date shipping window for Type B vessel). During the colder than normal year the shipping routes in all three Zones are covered in 50% by FY ice for the whole months of July. Zone 15 also experienced some Old Ice during the month of July, and Zone 14 old and FY ice for the whole month of November. Because of the presence of the Old Ice in Zone 14 in November, vessels must proceed through this region with an extreme caution at the end of the shipping season.

10. Conclusions and Recommendations

The purpose of this project was to assess the impact of climate change on the likelihood and severity of damage to vessels operating in Arctic waters, and address the impacts of climate change on the pollution prevention regulations governing ship traffic in the Arctic. The areas of concern for shipping in the north due to climate change were identified. This provides information which shipping companies can use to evaluate the length of the shipping season and to evaluate the type of ice-strengthened vessels that they will need to meet the pollution regulations.

Daily air temperatures measured at the meteorological stations representing the communities that lie along the Northwest Passage and in the approaches to Churchill were used to identify the changes that have occurred in the regions during years 1968-2004. Annual cumulative melting degrees for each station and average annual cumulative melting degrees for the whole Arctic were calculated. The results showed that there is a slight increase in cumulative melting degrees with high interannual variability in both the individual stations and the whole Arctic. This trend, therefore, has a low significance. Also the 36-year period is not long enough to make reliable conclusions.

The interannual variability in cumulative melting degrees was compared to Atlantic Oscillation (AO), which is a part of the North Atlantic Oscillation (NAO), and to the El Niño Southern Oscillation (ENSO). The conclusion from this brief analysis is that the highly variable conditions seen in the Canadian Arctic temperatures may well be related to AO/NAO and ENSO events. This is particularly true considering the fact that the AO/NAO and ENSO are the subject of ongoing investigations as to the role they play in the climate change. Finding a relationship between these phenomena and the Canadian Arctic would be an important link to understanding the implications of climate change on the region.

A methodology has been developed to compare and analyze two regulatory shipping systems, Zone/Date System and AIRSS, across the control zones that compose the Northwest Passage and the access routes to the Port of Churchill in Hudson Strait. In this analysis, two years were investigated representing colder than normal and warmer than normal summers in the period between 1968 and 2004. This analysis has, for the first time, allowed a direct comparison of the two systems. Satellite images were used to analyze and explain the ice movement and any peculiarities in results.

The results suggest shifting the opening and closing dates in most of the Zones for Type B vessel. Type B vessel was selected for the analysis since it is the lowest class of the vessel allowed to proceed through all zones comprising the NWP. Type B vessel does not adequately reflect the tendency for negative ice numerals in some Zones, even in warmer than normal summers, i.e. even if temperatures increase in the Canadian Arctic over this century. On the other hand, the shipping season for Type B vessel in some Zones closes prior to the growth of the limiting ice type.

In our previous work a cause of damage to vessels in Arctic waters was analyzed. The analysis showed that multi-year ice was present in the ice regime in 73% of the damage events. Therefore in the current study the presence of MY ice in the shipping lanes in the Northwest Passage and approach routes to the Port of Churchill was analyzed. Results showed that during the colder than normal year all Zones comprising the NWP experienced the presence of Old Ice well into the Type B vessel shipping season. The most severe ice conditions were in Zone 6 (Franklin Strait, Peel Sound, Barrow Strait and Lancaster Sound) followed by Zone 7 (Queen Maud Gulf and Victoria Strait). Both Zones experienced about 20% coverage by Old Ice during the allowed shipping season. During the warmer than normal year the Old Ice was present in Zone 6 and Zone 7 at the beginning of the shipping season. The rest of the Zones comprising the NWP were free of the Old Ice. During the colder than normal year the shipping routes were covered in 50% by FY ice for the whole months of July, and the routes in Zone 14 (North of Hudson Bay) were also covered by Old Ice at the end of the Type B vessel shipping season in November. The analysis showed that the presence of Old Ice is influenced by the previous year ice conditions, therefore more than just two years have to be analyzed before the final recommendations can be made.

The present analysis uses the existing AIRSS definition of the Ice Numeral, but it could not include influence of ridging and decay since such information is not available on the ice charts. The research described by Timco et al (2004, 2005) provides an Ice Regime System that is more scientifically accurate. The modified approach takes into account decay and rewards the ice-strengthened vessels with reliable navigation equipment and experienced Masters. It is recommended to use this modified approach to verify the Zone/Date System. The high year-to-year variability in air temperature and ice conditions make it difficult to set the Zone boundaries when only two years of datasets are analyzed. All years for which the CIS ice charts are available should be included in the analysis. Full examination of the Zone/Date System, i.e. not only the shipping routes in the Zones, should be carried out. Such comprehensive analysis will provide a quantitative information on the impact of climate change on the Zones and Dates in the Zone/Date System and will be a good basis for providing advice to Transport Canada on the likelihood of the need for regulatory changes due to climate change.

11. Acknowledgement

The authors would like to acknowledge the support of Climate Change Impacts and Adaptation Directorate, the PERD Northern POL, and Transport Canada for funding this study. The authors would also like to thank Katherine Wilson of the Canadian Ice Service, for supplying the ice thickness and ice temperature data from meteorological stations and Janette Walsh from CHC, for analyzing the air temperature data.

12. References

AIRSS, 1996, Arctic Ice Regime Shipping System (AIRSS) Standards, Transport Canada, June 1996, TP 12259E, Ottawa, Ont., Canada.

Agnew, T.A., Alt, B., De Abreau, R., and Jeffers, S., 2001, The loss of decades old sea ice plugs in the Canadian Arctic Islands, Proceedings of the 6th Conference on Polar Meteorology and Oceanography, San. Diego, Calif., American Meteorological Society (AMS), Boston, Massachusetts, pp9-12

ASPPR, 1989, Proposals for the Revision of the Arctic Shipping Pollution Prevention Regulations. Transport Canada Report TP 9981, Ottawa. Ont., Canada.

Barnett, D.G., 1980, A long-Range Ice Forecasting Method for the North Coast of Alaska, Proceedings of Arctic Ice Dynamics Joint Experiment International Commission on Snow and Ice Symposium, R.S.Pritchard (Ed.), University of Washington, Press, Seattle, Washington, pp.360-372

Brown, R.D., and Cote, P., 1992, Interannual Variability of Landfast Ice Thickness in the Canadian High Arctic, 1950-89, Arctic**,** Vol.45, No.3, pp.273-284

Canadian Gazette, 1996, Regulations Amending the Arctic Shipping Pollution Prevention Regulations. p 1729, Ottawa, Ont., Canada.

Cavalieri, D.J., Gloersen, P., Parkinson, C.L., Comiso, J.C., and Zvally, H.J., 1997, Observed Hemispheric Asymmetry in Global Sea Ice Changes. Science. Vol. 278, pp.1104-1106.

Comiso, J.C., 2002, A Rapidly Declining Perennial Sea Ice Cover in the Arctic. Geophysical Research Letters. Vol.29, No.20, pp.17-1 – 17-4.

Crocker, G., and Carrieres, T., 2000a, Documentation for the Canadian Ice Service Digital Sea Ice Database, Ballicater Consulting Ltd. Contract Report 00-02, March 2000.

Crocker, G., and Carrieres, T., 2000b, The Canadian Ice Service Digital Sea Ice Database – Assessment of Trends in the Gulf of St.Lawrence and Beaufort Sea Regions, Ballicater Consulting Ltd. Contract Report 00-04, March 2000.

Crocker, G.B., Carrieres, T., Chagnon, R., Mccourt, S., Agnew, T., and Lewis, J.E., Analysis of the Canadian Ice Service Digital Charts Database for Ice Climate Trends in Canadian Waters, in press.

DF Dickins Associated Ltd., 1998, A Study of the Technical Aspects of Deep Draft Shipping to the Western Arctic, Report prepared for Planning Division Department of Transportation Government of the Northwest Territories. September 30, 1998, pp.66

Dickson, R.R., Osborn, T.J., Hurrell, J.W., Meincke, J., Blindheim, J., Adlandsvik, B., Vinje, T., Alekseev, G., Maslowski, W., 2000, The Arctic Ocean Response to the North Atlantic Oscillation. American Meteorological Society. Journal of Climate Volume 13, pages 2671 – 2696.

Dumas, J., Carmack, E., and Melling, H., 2004, Climate Change Impacts on the Beaufort Shelf Land-fast Ice. Cold Regions Science and Technology. (In press)

Equivalent Standards for the Construction of the Arctic Class Ships, 1995, Transport Canada Report TP-12260, Ottawa, Ont., Canada.

Falkingham, J.C., Chagnon, R., and McCourt, S., 2001, Sea Ice in the Canadian Arctic in the 21st Century. Proceedings 16th International Conference on Port and Ocean Engineering under Arctic Conditions, pp 1191-1200, Ottawa, Ontario, Canada.

Falkingham, J.C., Chagnon, R., and McCourt, S., 2002, Trends in Sea Ice in the Canadian Arctic. Proceedings 16th IAHR International Symposium on Sea Ice. Vol.1, pp 352-359. Dunedin, New Zealand.

Falkingham, J.C., 2002, Canadian Arctic Ice Coverage Trends 1969 to 2001 Based on weekly ice charts produces by the Canadian Ice Service. PowerPoint presentation given at the IAHR Symposium on Sea Ice in Dunedin, New Zealand, in the fall of 2002.

Flato, G.M., and Brown, R.D., 1996, Variability and Climate Sensitivity of Land-fast Arctic Sea Ice, Journal of Geophysical Res., Vol.101, No.C10, pp.25,767-25,777.

Flato, G.M., and Boer, G.J., 2001, Warming Asymmetry in Climate Change Simulations, Geophysical Research Letters, Vo.28, No.1, pp.195-198

Gorman, R., 2000, Improving Methodologies for Vessel Routing in the St. Lawrence System: Cost Benefit Analysis. Contract report for the Canadian Ice Service by Enfotec Technical Services.

Holoway, G., and Sou, T., 2001, Is Arctic Sea Ice Rapidly Thinning? Proceedings 16th International Conference on Port and Ocean Engineering under Arctic Conditions, pp 1201-1206, Ottawa, Ontario, Canada.

Howell, S.E.L., and Yackel, J.J., 2004, A Vessel Transit Assessment of Sea-ice Variability in the Western Arctic, 1969-2002: Implications for Ship Navigation. Canadian Journal of Remote Sensing. Vo.30, No.2, pp205-215.

Jeffers, S., Agnew, T.A., Alt, B.T., DeAbreu, R., and McCourt, S., 2001, Investigating the anomalous sea-ice conditions in the Canadian High Arctic (Queen Elizabeth Islands) during summer 1998, Annals of Glaciology, Vol.33, pp.507-512

Kubat, I. and Timco, G.W., 2003, Vessel Damage in the Canadian Arctic. Proceedings 17th International Conference on Port and Ocean Engineering under Arctic Conditions, pp 203-212, Trondheim, Norway.

Malasnik, J.A., Serreze, M.C., and Agnew, T., 1999, On the Record Reduction in 1998 Western Arctic Sea-Ice Cover, Geophysical Research Letters, Vol.26, No.13, pp.1905-1908

Melling, H., 2002, Sea ice of the Northern Canadian Arctic Archipelago. Journal of Geophysical Research 107(C11), 3181, doi:10.1029/2001JC001102, 21 pp

Melling, H., and Riedel, D.A., 2005, Trends in Thickness and Extent of Seasonal Pack Ice, Canadian Beaufort Sea, Geophysical Research Letters, in press.

Mysak, L.A., 1986, El Niño, Interannual Variability and Fisheries in the Northeast Pacific Ocean, Canadian Journal of Fisheries and Aquatic Sciences,Vol.43, pp.464-497

Mysak, L.A., and Manak, D.K., 1989, Arctic Sea-Ice Extent and Anomalies, 1953-1984, Atmosphere-Ocean, Canadian Meteorological and Oceanographic Society, Vol.27(2), pp. 376-405

Parkinson, C.L., Cavalieri, D.J., Gloersen, P., Zwally, H.J., and Comiso, J.C., 1999, Arctic Sea Ice Extents, Areas, and Trends, 1978-1996. Journal of Geophysical Research. Vol.104, NO.C9, pp.20,837-20,856.

Parkinson, C.L., 1992, Spatial Patterns of Increases and Decreases in the Length of the Sea Ice Season, Journal of Geophysical Research, Vol. 97, NO. C9, pp14,377-14,388.

Polyakov, I.V., Alekseev, G.V., Bekryaev, R.V., Bhatt, U.S., Colony, R., Johnson, M.A., Karklin, V.P., Walsh, D., and Yulin, A.V., 2003, Long-Term Ice Variability in Arctic Marginal Seas, Journal of climate, Vol.16, pp.2078-2085.

Rodwell, M., Folland, C.K., 2002, Atlantic air-sea interaction and seasonal predictability. Quarterly Journal Royal Meteorological Society , Vol 128, pp.1413-1443.

Rothrock, D.A., and Maykut, G.A., 1999, Thinning of the Arctic Sea-Ice Cover. Geophysical Research Letters. Vol.26, NO.23, pp.3469-3472.

Timco, G.W. and Frederking, R.M.W., 1996, A Methodology for Developing a Scientific Basis for the Ice Regime System. National Research Council of Canada Report HYD-TR-009, Ottawa, Canada.

Timco, G.W., Frederking, R.M.W., and Santos-Pedro, V.M., 1997, A Methodology for Developing a Scientific Basis for the Ice Regime System. Proceedings ISOPE'97, Vol II, pp 498-503, Honolulu, USA.

Timco, G.W. and Morin, I., 1998, Canadian Ice Regime System Database. Proceedings 8th International Offshore and Polar Engineering Conference ISOPE'98, Vol II, pp 586-591, Montreal, P.Q., Canada.

Timco, G.W. and Kubat, I., 2002,. Scientific Basis for Ice Regime System: Discussion Paper. NRC Report CHC-TR-002, TP 13916E, Ottawa, Ont., Canada.

Timco, G.W., Kubat, I. and Johnston, M., 2004, Scientific Basis for Ice Regime System: Final Report. NRC Report CHC-TR-020, Ottawa, Ont., Canada.

Timco, G.W., Kubat, I. and Johnston, M., 2005, Scientific Basis for the Canadian Ice Regime System. Proceedings 18th International Conference on Port and Ocean Engineering under Arctic Conditions, POAC'05, Potsdam, N.Y.,U.S.A. Vol.2, pp.663-672.

Wilson , K.J., Falkingham, J., Melling, H., and De Abreau, R., 2004, Shipping in the Canadian Arctic, Other Possible Climate Change Scenarios. Proceedings IGARSS International Geoscience and Remote Sensing Symposium, Anchorage, Alaska,

Zhang, X., Vincent, L.A., Hogg, W.D., and Niitsoo A., 2000, Temperature and Precipitation Trends in Canada during the 20th Century. Atmosphere Ocean, 38(3), pp.395-429.

APPENDIX A. Methodology to Evaluate Canadian Regulations – Data Processing

As part of the project a new methodology was developed to analyze the impact of climate change and/or seasonal temperature variation on the veracity of the Zones and Dates used in the Zone / Date System. This Appendix describes data processing in detail.

Two sets of trajectories were defined. The first set of trajectories was defined as line segments approximately 125.5 km (Table A-1). The trajectories in Zone 4 and Zone 12, Zone 11 and Zone 7, Zone 6 and Zone 13, and Zone 13 and Zone 9 were defined to assess how much the two neighboring Zones differ. The trajectories were also defined in Zone 14 and Zone 15. The route segments are shown in Figure A-1.

Table A-1: Length and locations of the first set

LOCATION	LENGTH (km)	ZONE
CAMBIDGE_BAY	125.002	ZONE 11
CAMBIDGE_BAY	125.187	ZONE 7
CORAL_HARBOUR	125.248	ZONE 14
IQALUIT	125.057	ZONE 15
POND_INLET	125.834	ZONE 13
POND_INLET	125.834	ZONE 9
RESOLUTE	125.124	ZONE 13
RESOLUTE	124.826	ZONE 6
TUKTOYAKTUK	125.539	ZONE 12
TUKTOYAKTUK	126.003	ZONE 4

Figure A-1: Route Segments in the Northwest Passage and in Hudson Strait

The second set of trajectories consisted of actual navigation routes through the Northwest Passage, and through the approach to and across Hudson Bay (Figure A-2). The Hudson Bay trajectory was defined with a Main route and an Alternative Route. These two routes are identical through the approach, but split east of Coats Island. The Alternative route curves northward around Coats Island, and the Main route curves Southward around Coats Island. The routes meet again at Churchill.

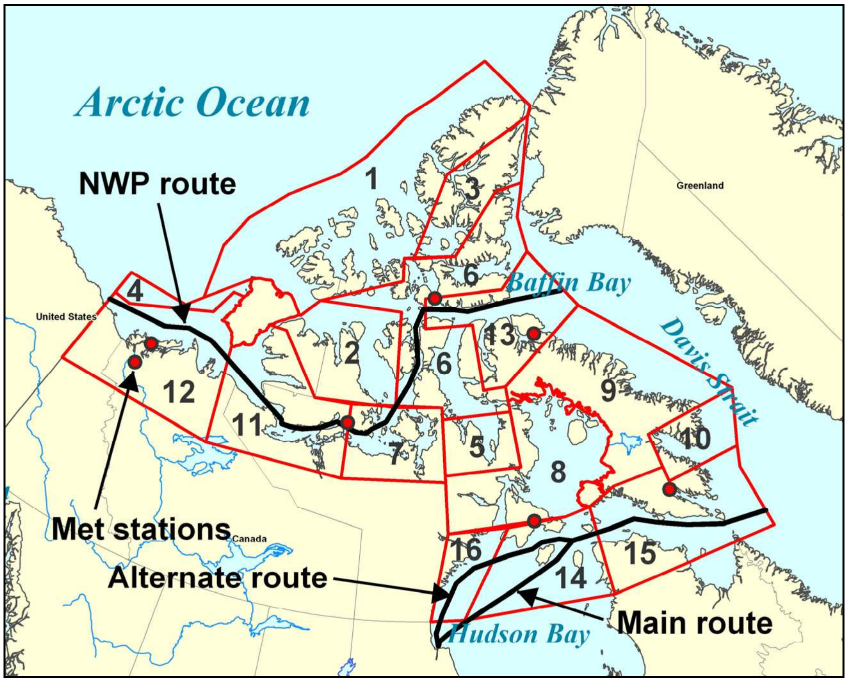

Figure A-2: Shipping Safety Control Zones in Canada, Meteorological Stations used for Air Temperature Analysis (from left on NWP route: Inuvik, Tuktoyaktuk, Cambridge Bay, Resolute, Pond Inlet; from left in Hudson Bay: Coral Harbour, Iqaluit), and Shipping Routes in Northwest Passage and in Hudson Bay

All the trajectories were first defined as 'arcs' or lines. These lines were buffered, such that the trajectories would subsequently be represented by polygons 1 km in width.

As for all data layers in Arc Map, the buffered trajectory layers have associated data attribute tables. In the case of the NWP trajectory, the attribute table contains fields describing the location of the trajectory, the Zone date code, as well as a code defining whether the location should be coded according to the Eastern Arctic Regional Ice Chart or according to the Western Arctic Regional Ice Chart. The Regional Ice Charts were obtained from the Canadian Ice Service in digital version. The other trajectories (the approach to and across Hudson Bay) do not cross 'Regional Ice Chart' boundaries, and thus do not require the latter code. Table A-2 illustrates the possible combinations of codes along the NWP trajectory.

Table A-2: Combinations of codes along the NWP trajectory

LOCATION	ZONE	EAST_WEST
NWP	ZONE 2	WEST
NWP	ZONE 6	EAST
NWP	ZONE 6	WEST
NWP	ZONE 7	WEST
NWP	ZONE 11	WEST
NWP	ZONE 12	WEST
NWP	ZONE 13	EAST

The dividing line between the 'WESTERN' and 'EASTERN' parts of the NWP trajectory was defined by looking at the 1998 set of Regional Ice Charts. Figure A-3 shows the typical data extents for the Eastern and Western Arctic Ice Charts in 1998. Examples of a Western Arctic (Figure A-4) and an Eastern Arctic (Figure A-5) Regional Ice Chart show that there is a data area common to both maps. The 1998 Eastern Arctic Regional Ice Charts have a sliver of data missing from the Northwestern corner. The eastern boundary of this sliver differs from map sheet to map sheet, and the most easterly boundary was selected for the division line. A yellow circle indicates the location of the detailed map of the division line (Figure A-6).

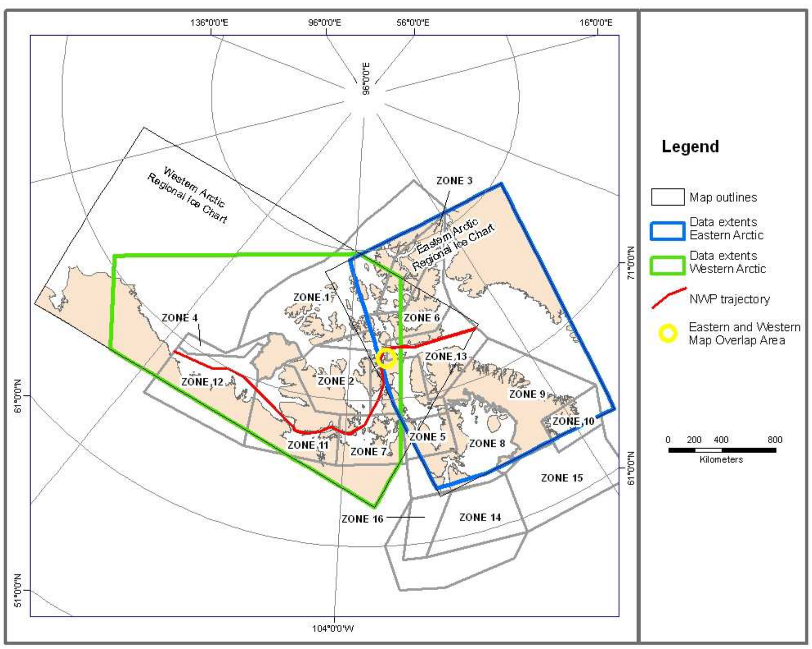

Figure A-3: Typical data extents for the Eastern and Western Arctic Ice Charts in 1998.

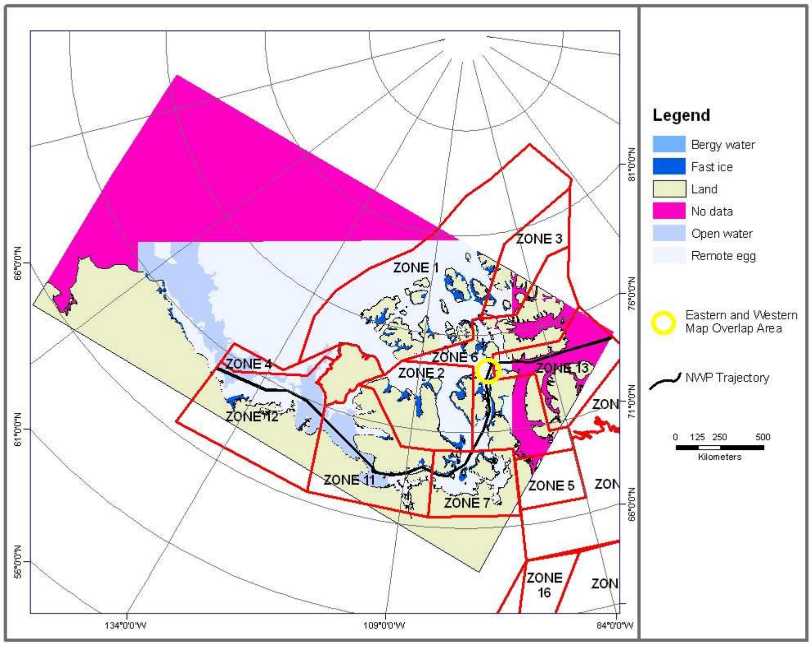

Figure A-4: Example of a Western Arctic Ice Chart for 1998 (Nov. 09). The division, east of which the NWP trajectory will be coded using data from the Eastern Arctic Ice Chart is located within the yellow circle

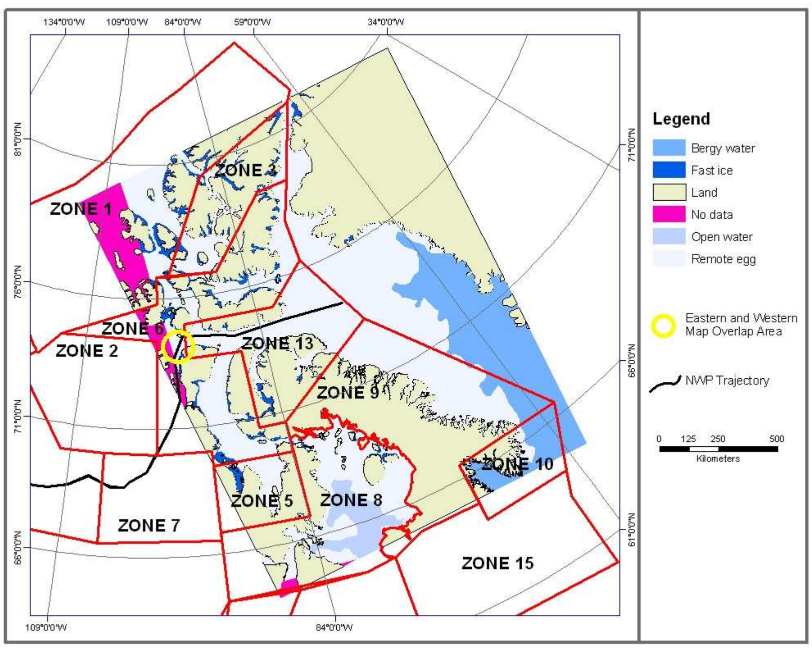

Figure A-5: Example of an Eastern Arctic Ice Chart for 1998 (Nov. 09). The division, west of which the NWP trajectory will be coded using data from the Western Arctic Ice Chart is located within the yellow circle

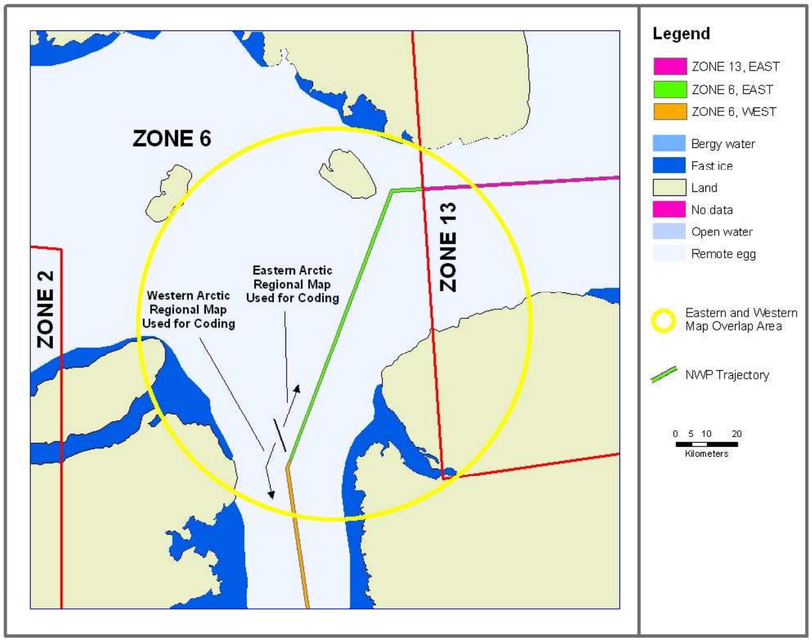

Figure A-6: Detailed map of the division line used to determine what areas of the NWP trajectory were to be coded using the Eastern Arctic Ice Chart and which were to be coded using the Western Arctic Ice Chart.

For the NWP trajectory, since the data are extracted from two adjacent Arctic Regional Ice Chart, there will probably be a duplication of codes on either side of the arbitrary break: For the Resolute trajectories, the ZONE 13 data were extracted from the Eastern Arctic Regional Ice Charts and the ZONE 6 data were extracted from the Western Arctic Regional Ice Charts.

Table A-3 presents CIS Regional Ice Chart (Sea Ice) Climate Format Data Description. An example of the type of information provided in the digital maps is shown in Table A-4. These data are illustrated in Figure A-7. Only land and the areas described in the Table A-4 are color coded in the map (Figure A-7). The rest of the map was left blank for simplicity. In this example the NWP trajectory intersects 4 different ice regimes, illustrated by coded eggs, and two regimes of open water. Note that in this area the NWP trajectory locations is coded 'NWP', the date zone is coded as 'ZONE 12' and Regional Ice Chart reference is coded as "West". Also, for better visibility, Figure A-6 and Figure A-7 depict the NWP buffer as 6 km wide. The egg code coding is explained in Figure A-8.

Table A-3: CIS Regional Ice Chart (Sea Ice) Climate Format Data Description

DATE_CARTE	valid date of chart
REGION	two letter identifier of the region
A_LEGEND	categorical representation of polygon coded as either: Bergy water, Fast ice, Open water, Ice free, Egg, Remote egg, No data or Land
E_CT	(EGG CODE) total concentration Ct
E_CA	(EGG CODE) partial concentration Ca
E_CB	(EGG CODE) partial concentration Cb
E_CC	(EGG CODE) partial concentration Cc
E_CD	(EGG CODE) partial concentration Cd
E_SO	(EGG CODE) stage of development of trace of ice thicker than Sa
E_SA	(EGG CODE) stage of development of ice reported by Ca
E_SB	(EGG CODE) stage of development of ice reported by Cb
E_SC	(EGG CODE) stage of development of ice reported by Cc
E_SD	(EGG CODE) stage of development of ice thinner than Sc
E_SE	(EGG CODE) stage of development of trace of ice thinner than Sd
E_FA	(EGG CODE) predominant floe size of ice type reported by Sa
E_FB	(EGG CODE) predominant floe size of ice reported by Sb
E_FC	(EGG CODE) predominant floe size of ice reported by Sc
E_FD	(EGG CODE) predominant floe size of ice reported by Sd
E_FE	(EGG CODE) predominant floe size of ice reported by Se

Table A-4: Egg code information extracted from the Western Arctic Regional Ice Chart for Nov. 09, 1998.

A_LEGEND	E_CT	E_CA	E_CB	E_CC	E_CD	E_SO	E_SA	E_SB	E_SC	E_SD	E_SE	E_FA	E_FB	E_FC	E_FD	E_FE
Open water																
Open water																
Remote egg	9	1	3	5			5	4	1			3	3	X		
Remote egg	6						1					X				
Remote egg	6						1					X				
Remote egg	9+	2	5	3			5	4	1			5	4	X		

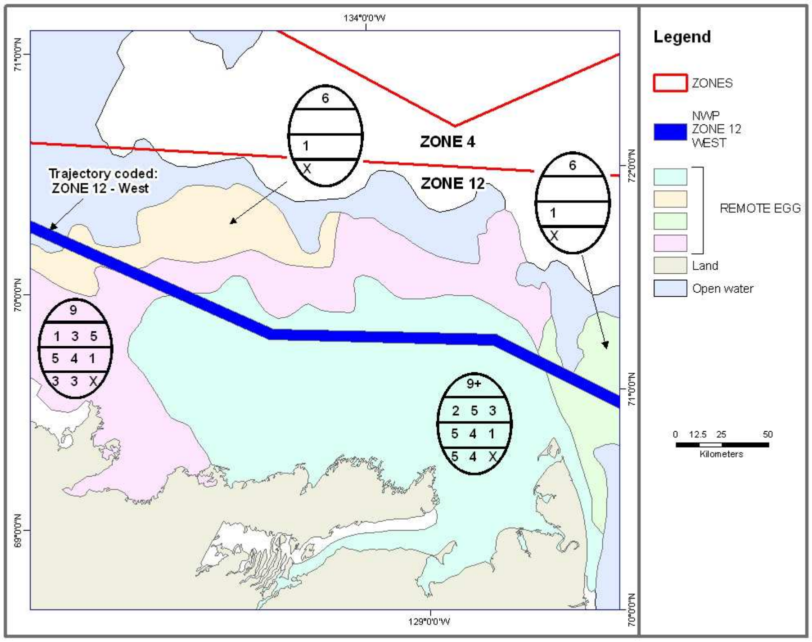

Figure A-7: Map that illustrates egg code data from Table 4.

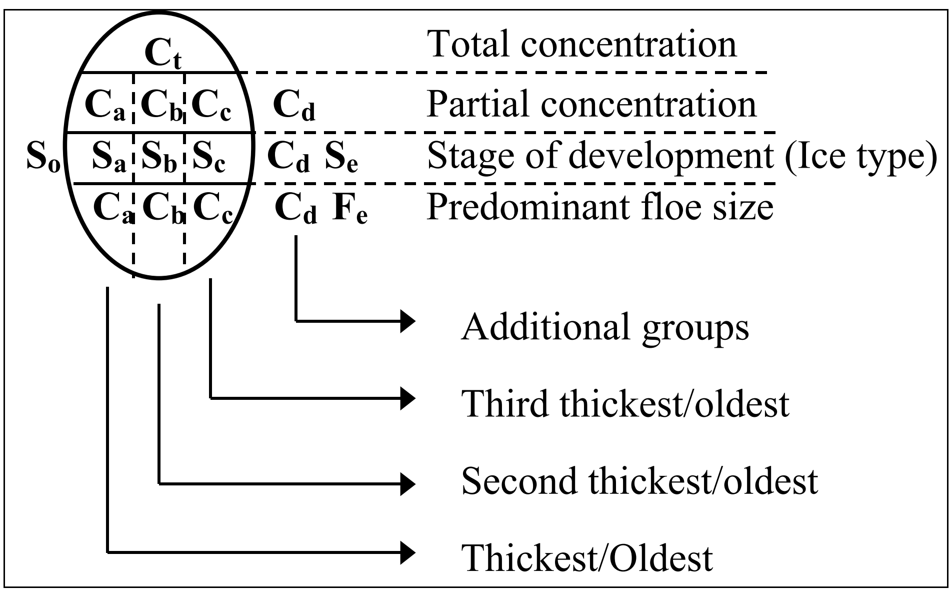

Figure A-8: Egg code description

Using ArcView, an intersect overlay operation can be performed that results in a map of the spatial intersection of both the Regional Ice Chart and the trajectory map. The resulting layer has a data attribute table that contains attributes from both the original maps. An excerpt of the data attribute table resulting from the present example can be seen in Table A-5.

Table A-5: Data extracted from the data attribute table of the map resulting from intersecting the Western Arctic Regional Ice Chart layer with the NWP trajectory layer.

LINE SEGMENT	ZONE	EAST_WEST	A_LEGEND	E_CT	E_CA	E_CB	E_CC	E_CD	E_SO	E_SA	E_SB	E_SC	E_SD	E_SE	E_FA	E_FB	E_FC	E_FD	E_FE
1	ZONE 12	WEST	Open water																
2	ZONE 12	WEST	Remote egg	6						1					X				
3	ZONE 12	WEST	Remote egg	9	1	3	5			5	4	1			3	3	X		
4	ZONE 12	WEST	Remote egg	9+	2	5	3			5	4	1			5	4	X		
5	ZONE 12	WEST	Remote egg	6						1					X				

This information is illustrated in Figure A-9.

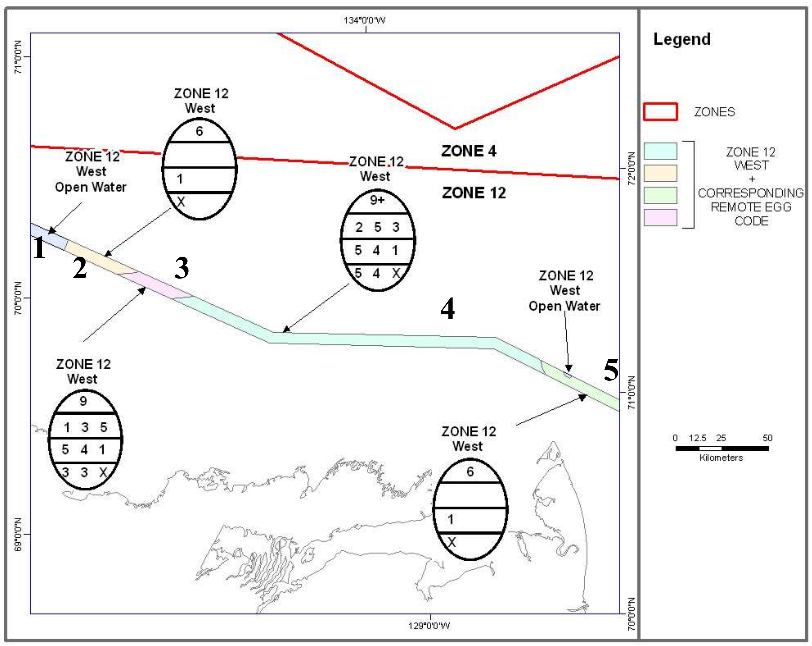

Figure A-9: Map that illustrates the intersection the Western Arctic Regional Ice Chart layer with the NWP trajectory layer. The data illustrated in this example can be seen in Table 5.

Personal Geodatabases were setup using ArcCatalog in which all the resultant intersection maps were stored. Since these Geodatabases are stored as MS-Access files, the data attribute tables are readily available for query. The data for each year were compiled into a single table. Data for particular Zones were extracted using queries, subsequently exported out of MS-ACCESS and imported into MS-EXCEL. Macros were setup in MS-EXCEL to calculate Ice Numerals (IN), and plot the data.

APPENDIX B. Range and Count of Ice Numerals

APPENDIX B-1. Northwest Passage

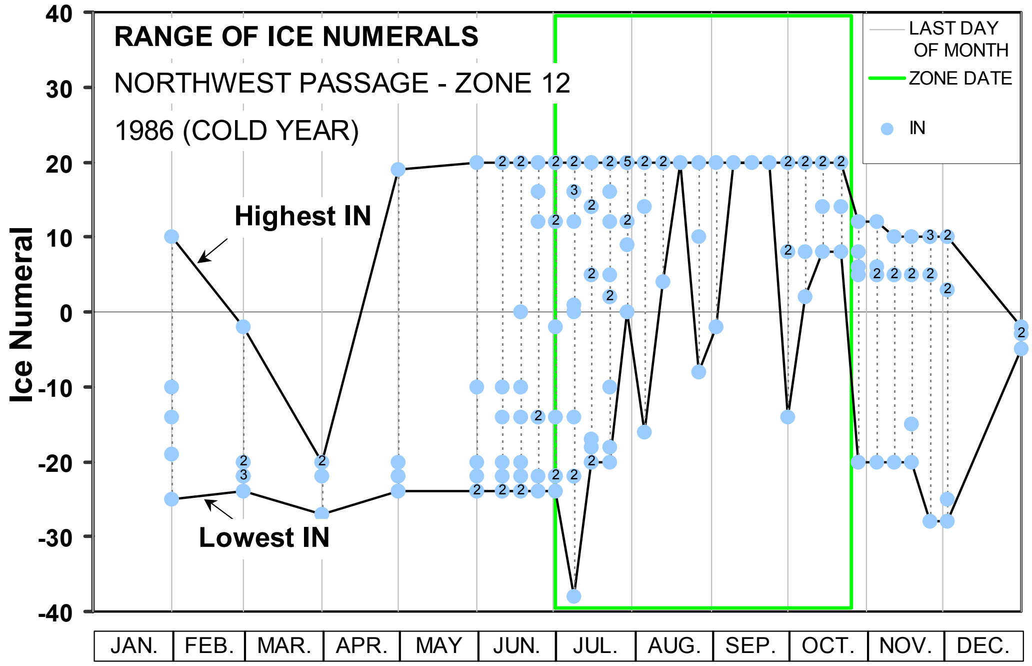

Figure B-1: Range of Ice Numerals calculated from CIS ice charts for NWP shipping route in Zone 12, throughout the colder than normal year

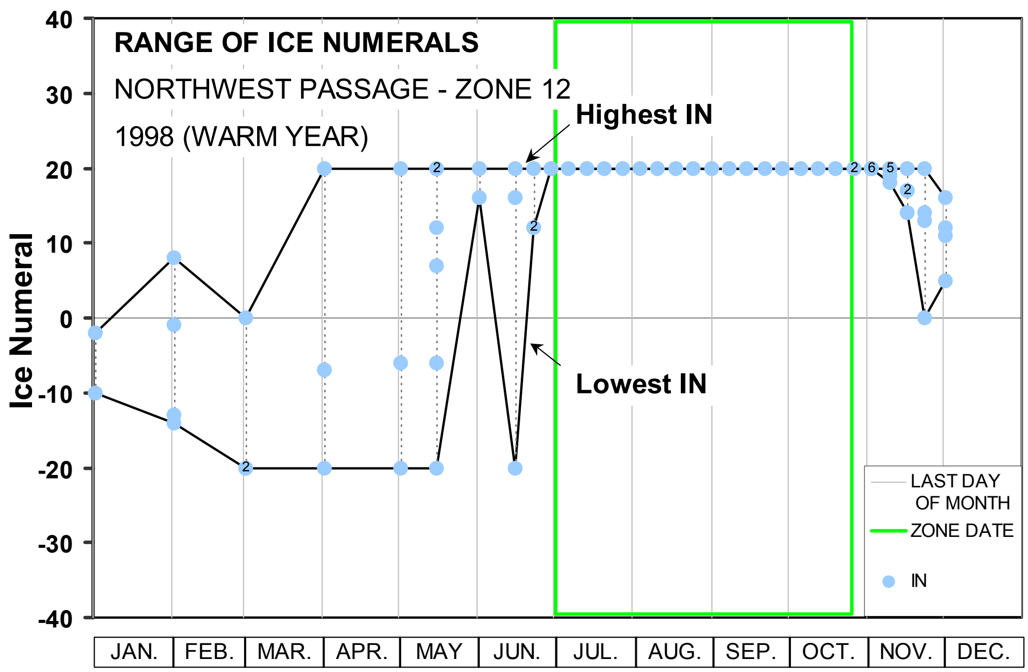

Figure B-2: Range of Ice Numerals calculated from CIS ice charts for NWP shipping route in Zone 12, throughout the warmer than normal year

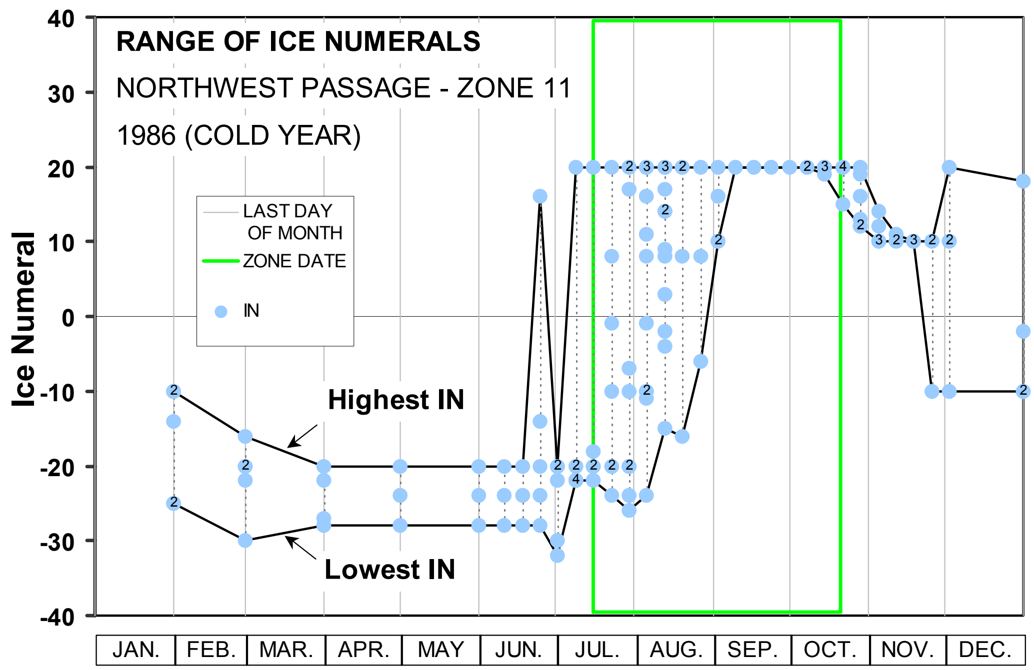

Figure B-3: Range of Ice Numerals calculated from CIS ice charts for NWP shipping route in Zone 11, throughout the colder than normal year

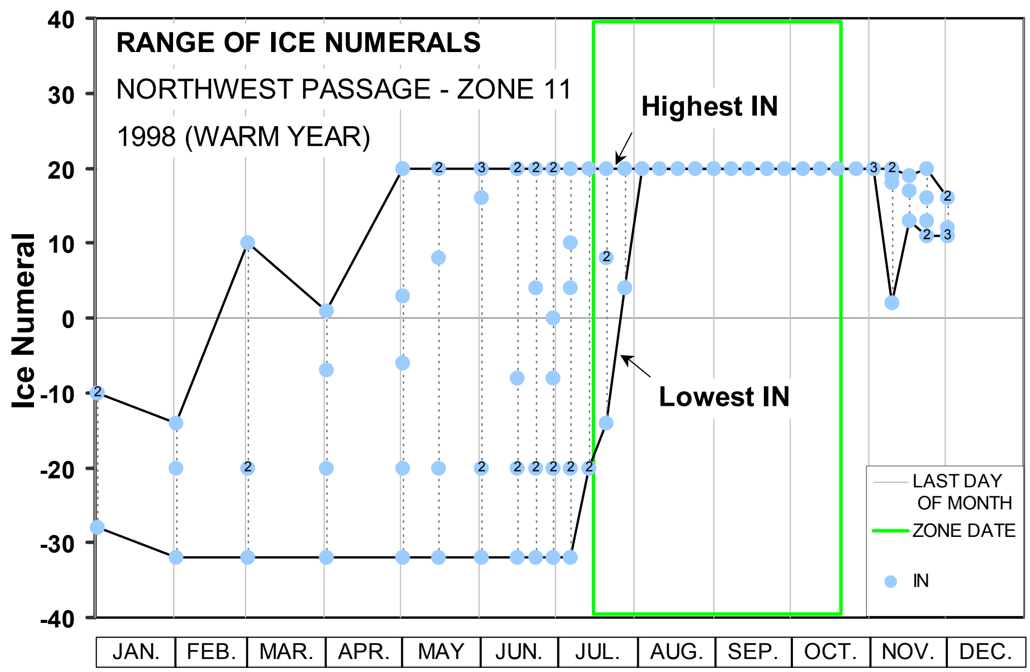

Figure B-4: Range of Ice Numerals calculated from CIS ice charts for NWP shipping route in Zone 11, throughout the warmer than normal year

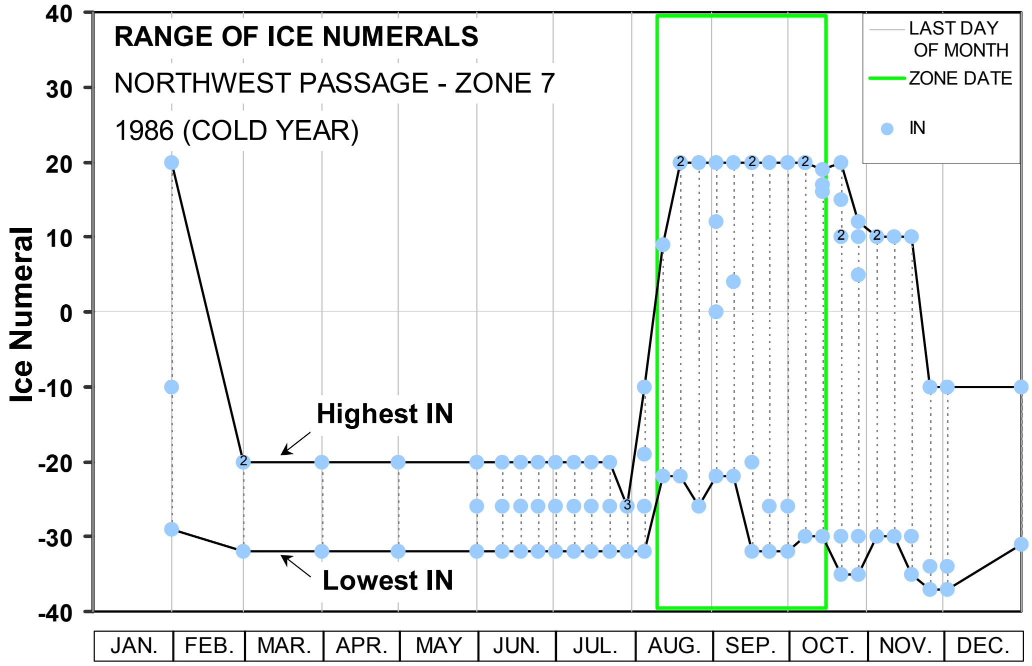

Figure B-5: Range of Ice Numerals calculated from CIS ice charts for NWP shipping route in Zone 7, throughout the colder than normal year

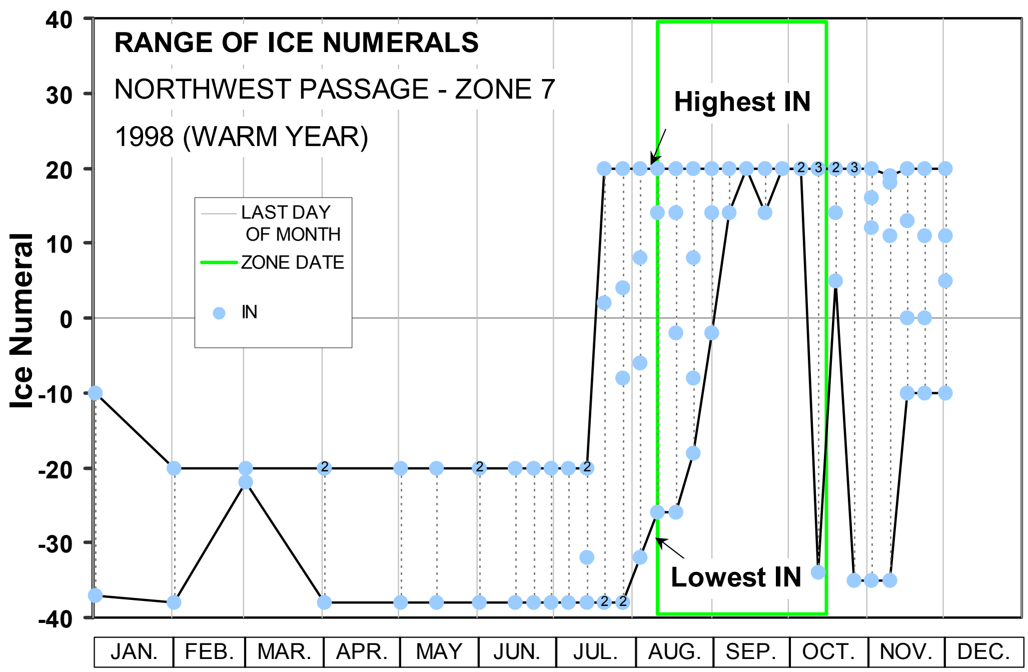

Figure B-6: Range of Ice Numerals calculated from CIS ice charts for NWP shipping route in Zone 7, throughout the warmer than normal year

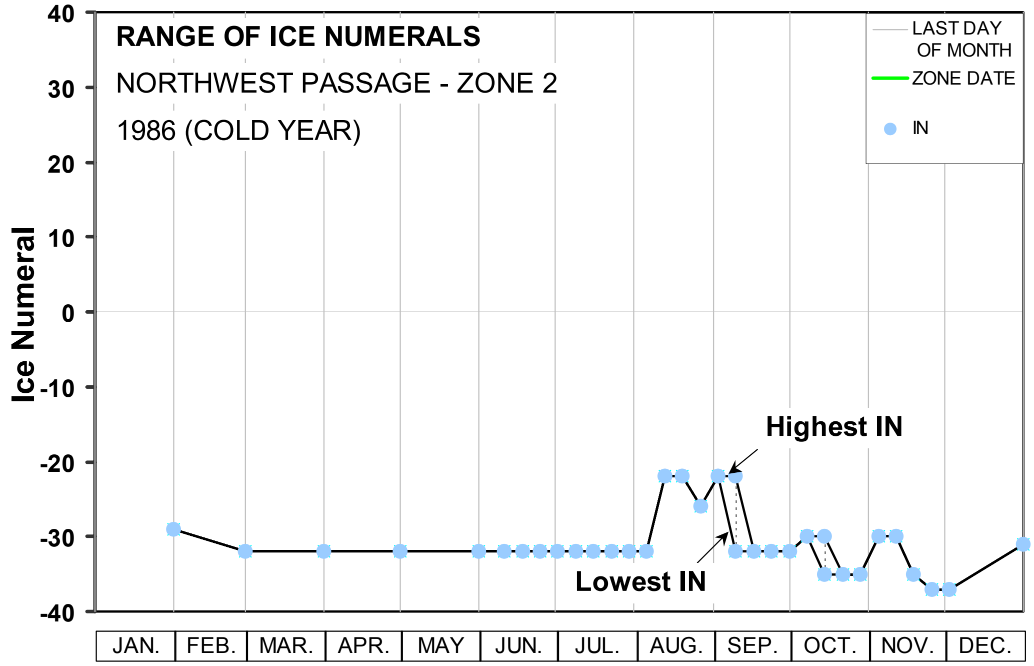

Figure B-7: Range of Ice Numerals calculated from CIS ice charts for NWP shipping route in Zone 2, throughout the colder than normal year

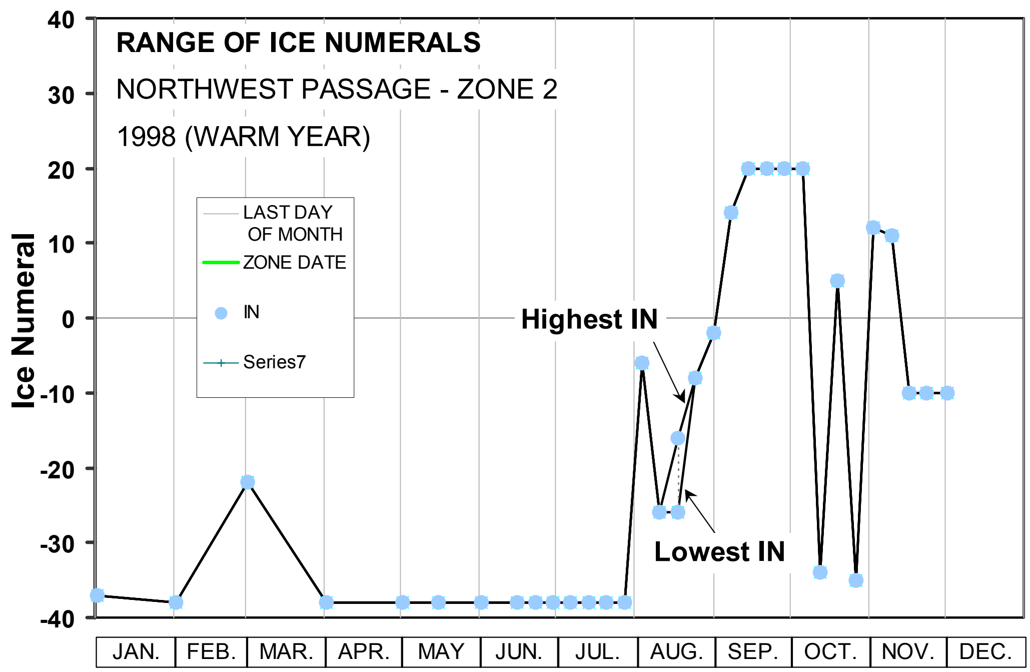

Figure B-8: Range of Ice Numerals calculated from CIS ice charts for NWP shipping route in Zone 2, throughout the warmer than normal year

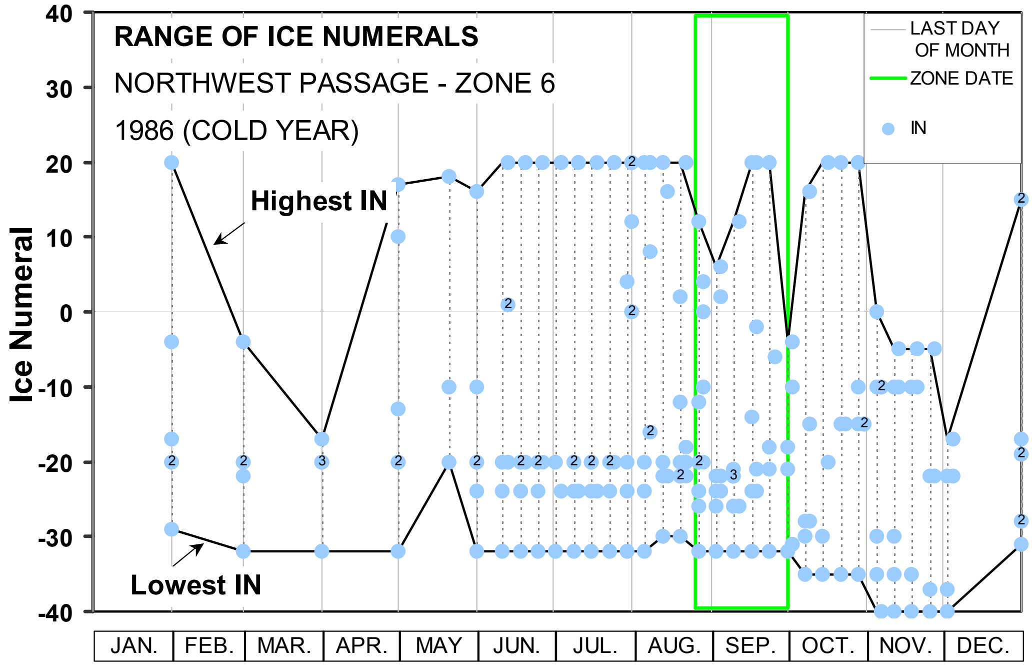

Figure B-9: Range of Ice Numerals calculated from CIS ice charts for NWP shipping route in Zone 6, throughout the colder than normal year

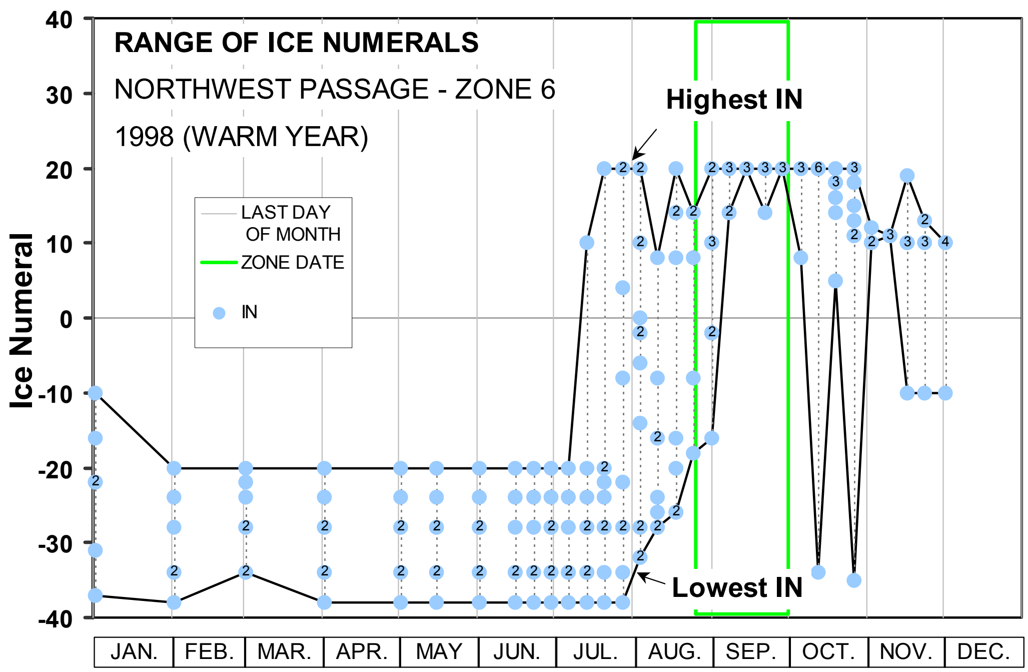

Figure B-10: Range of Ice Numerals calculated from CIS ice charts for NWP shipping route in Zone 6, throughout the warmer than normal year

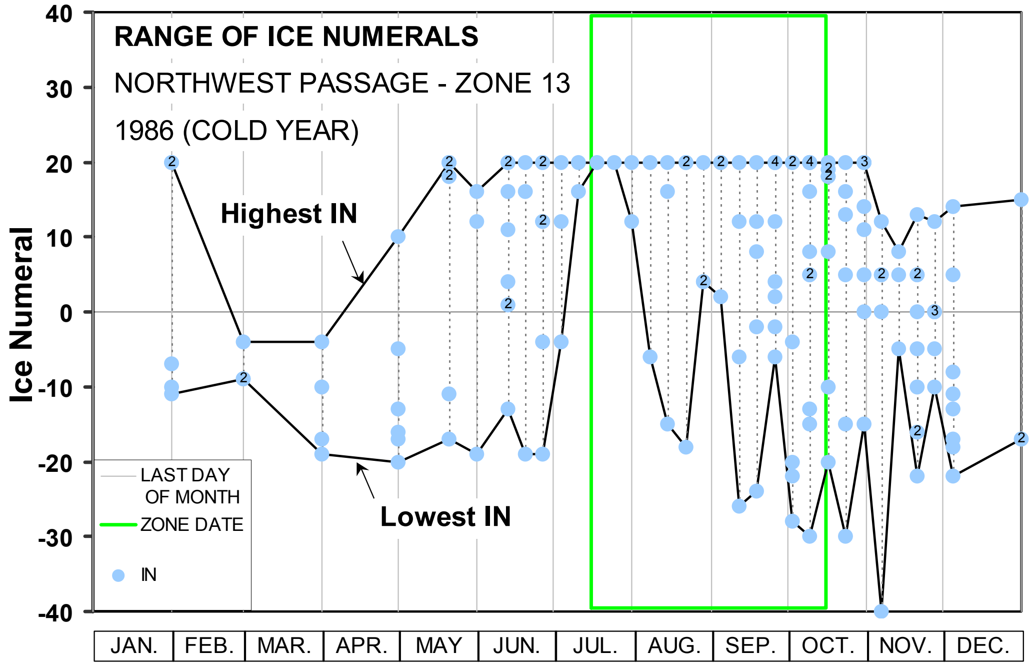

Figure B-11: Range of Ice Numerals calculated from CIS ice charts for NWP shipping route in Zone 13, throughout the colder than normal year

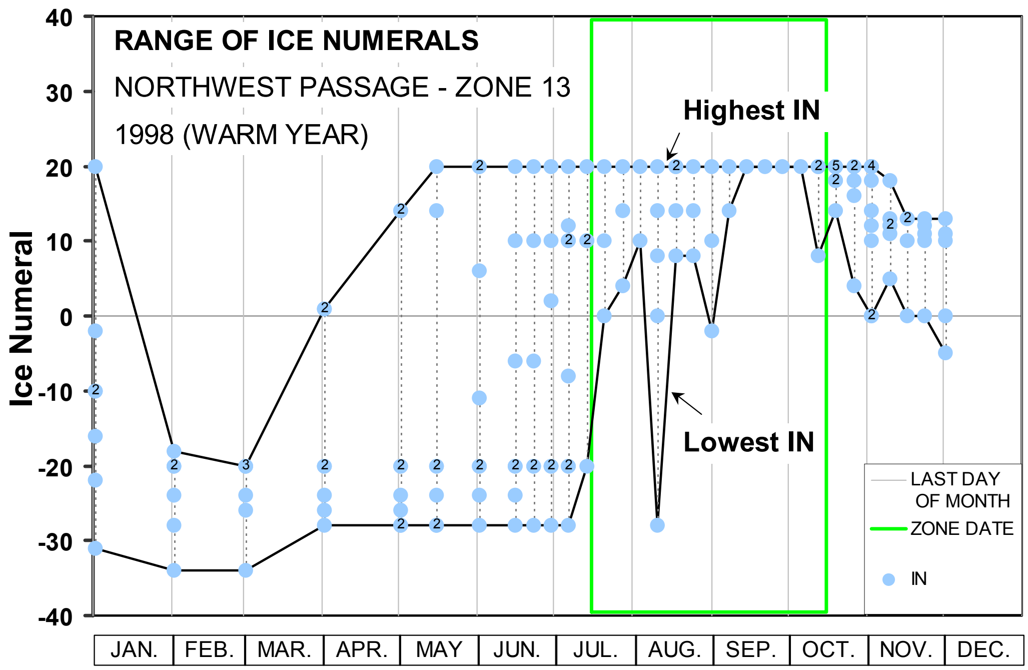

Figure B-12: Range of Ice Numerals calculated from CIS ice charts for NWP shipping route in Zone 13, throughout the warmer than normal year

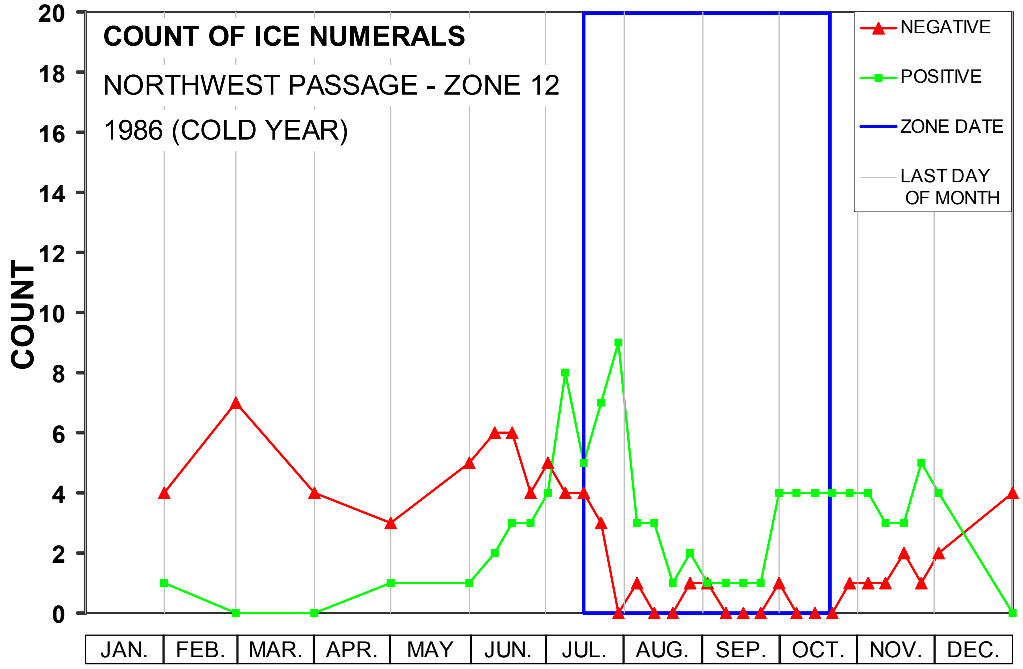

Figure B-13: Count of negative and positive Ice Numerals calculated from data plotted in Figure B-1 - NWP shipping route in Zone 12 throughout the colder than normal year

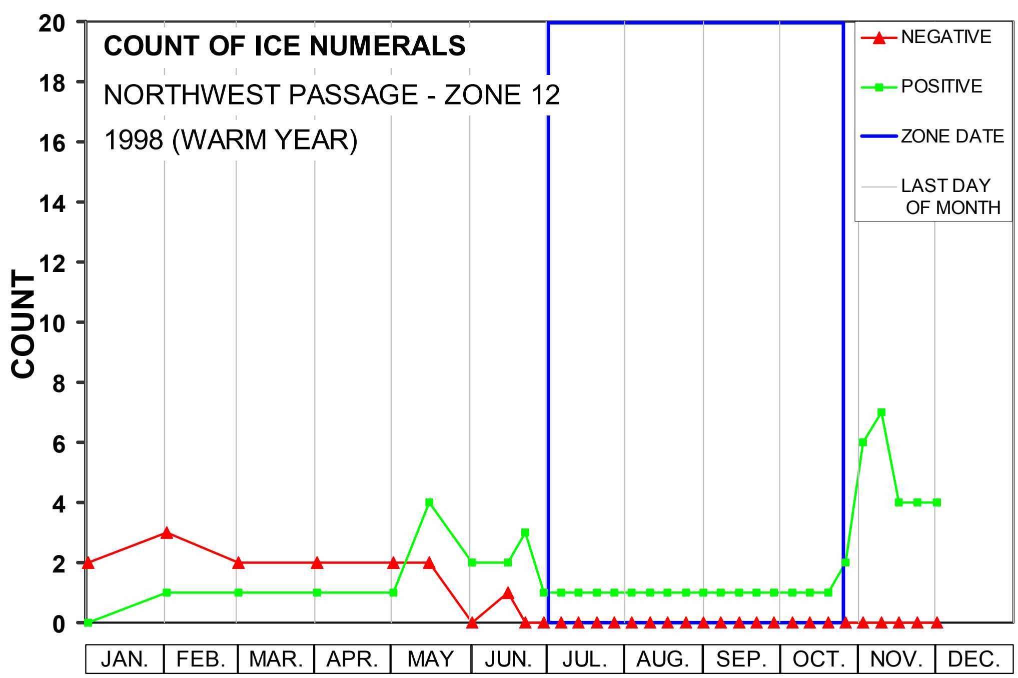

Figure B-14: Count of negative and positive Ice Numerals calculated from data plotted in Figure B-2 - NWP shipping route in Zone 12 throughout the warmer than normal year

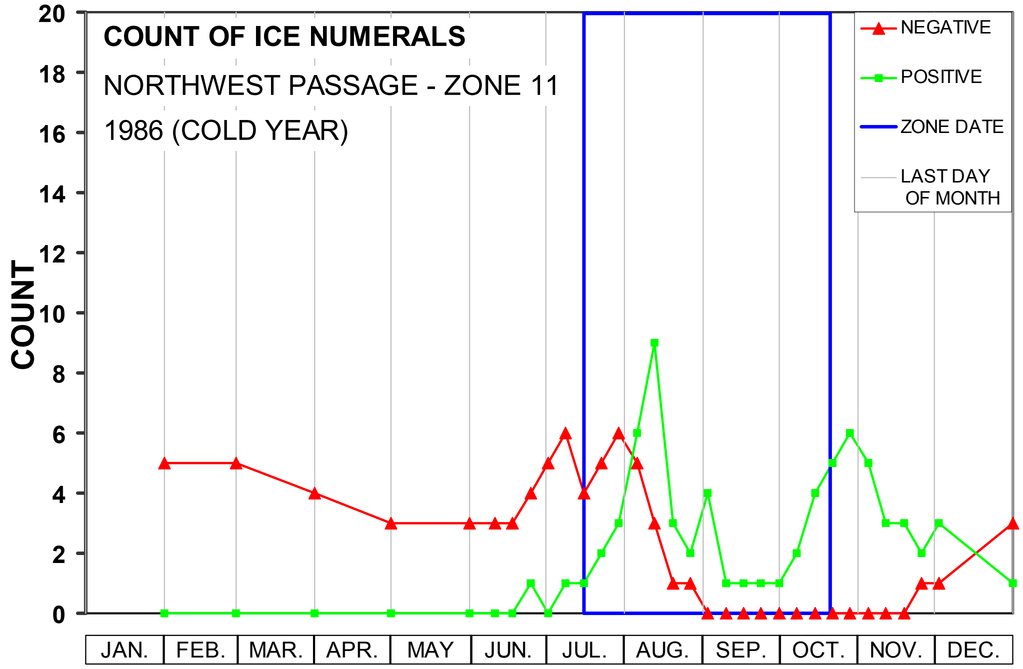

Figure B-15: Count of negative and positive Ice Numerals calculated from data plotted in Figure B-3 - NWP shipping route in Zone 11 throughout the colder than normal year

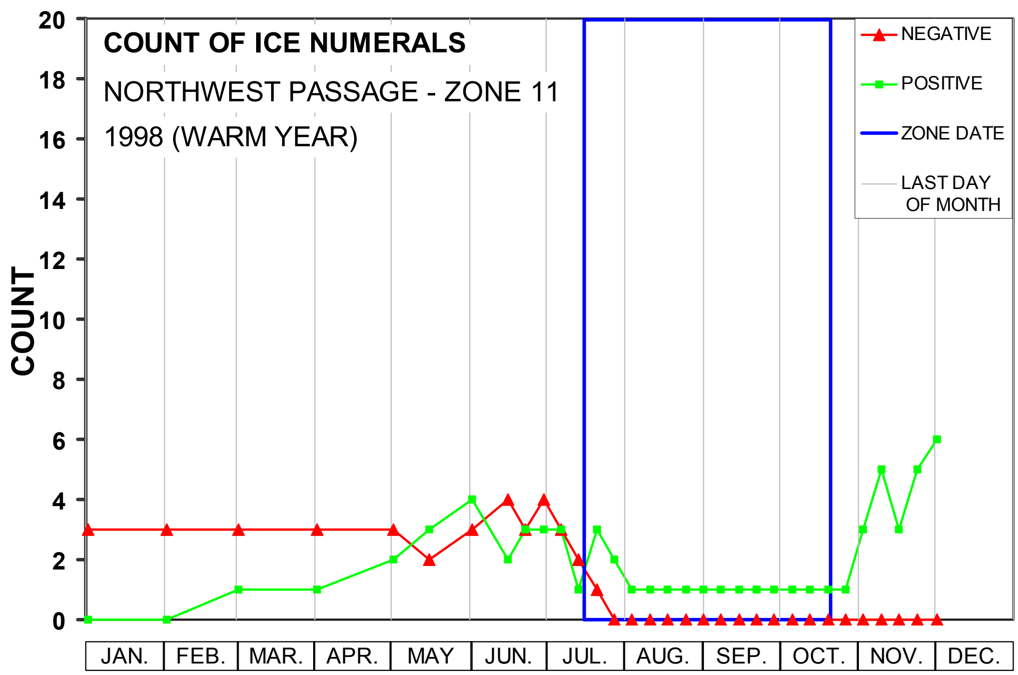

Figure B-16: Count of negative and positive Ice Numerals calculated from data plotted in Figure B-4 - NWP shipping route in Zone 11 throughout the warmer than normal year

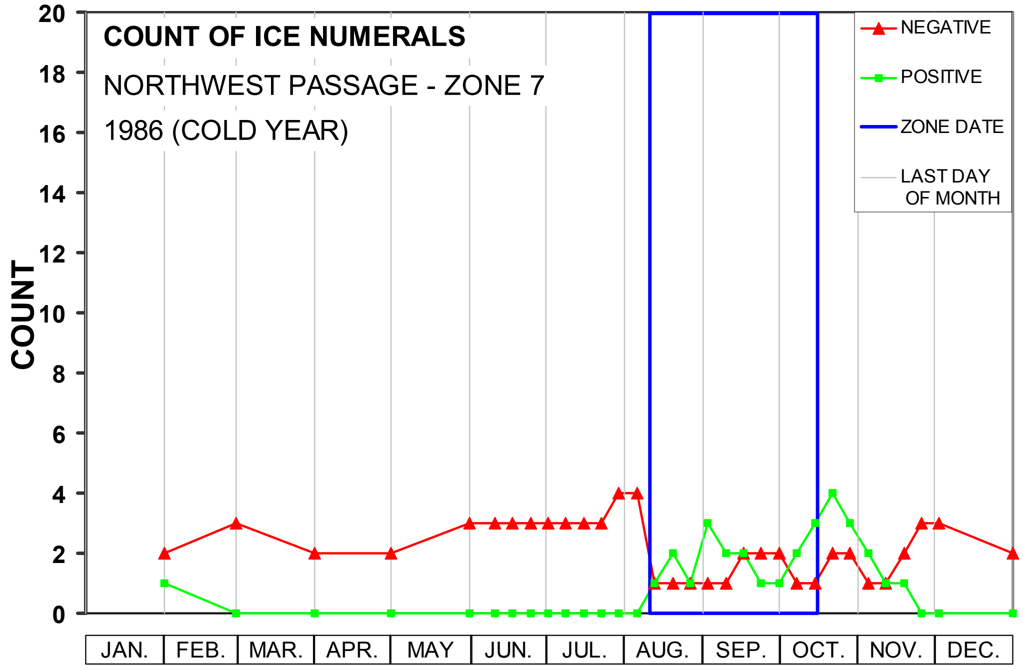

Figure B-17: Count of negative and positive Ice Numerals calculated from data plotted in Figure B-5 - NWP shipping route in Zone 7 throughout the colder than normal year

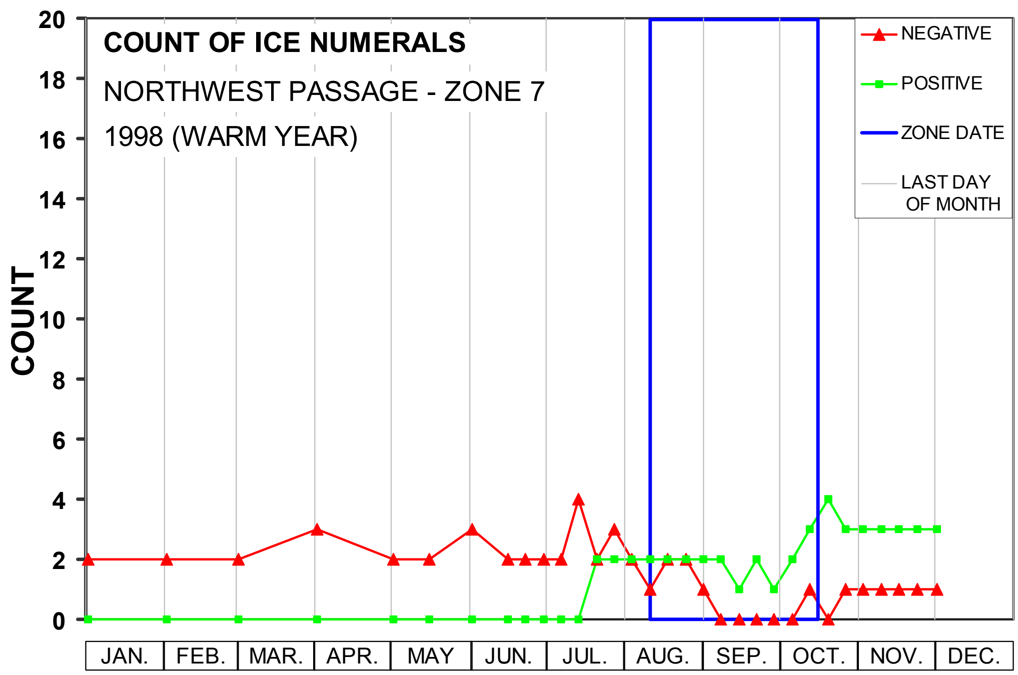

Figure B-18: Count of negative and positive Ice Numerals calculated from data plotted in Figure B-6 - NWP shipping route in Zone 7 throughout the warmer than normal year

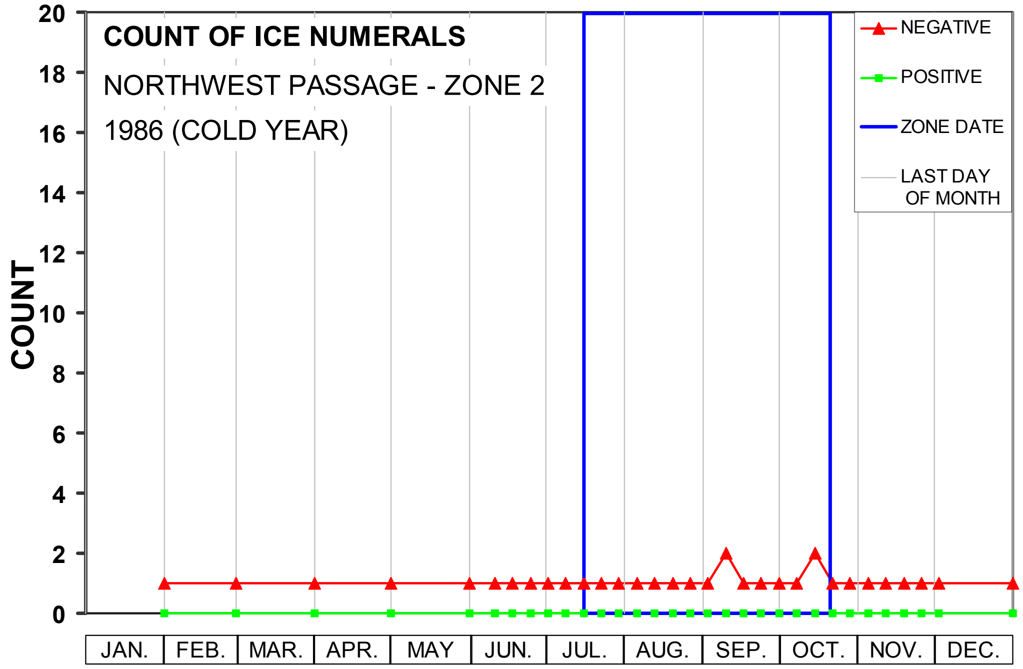

Figure B-19: Count of negative and positive Ice Numerals calculated from data plotted in Figure B-7 - NWP shipping route in Zone 2 throughout the colder than normal year

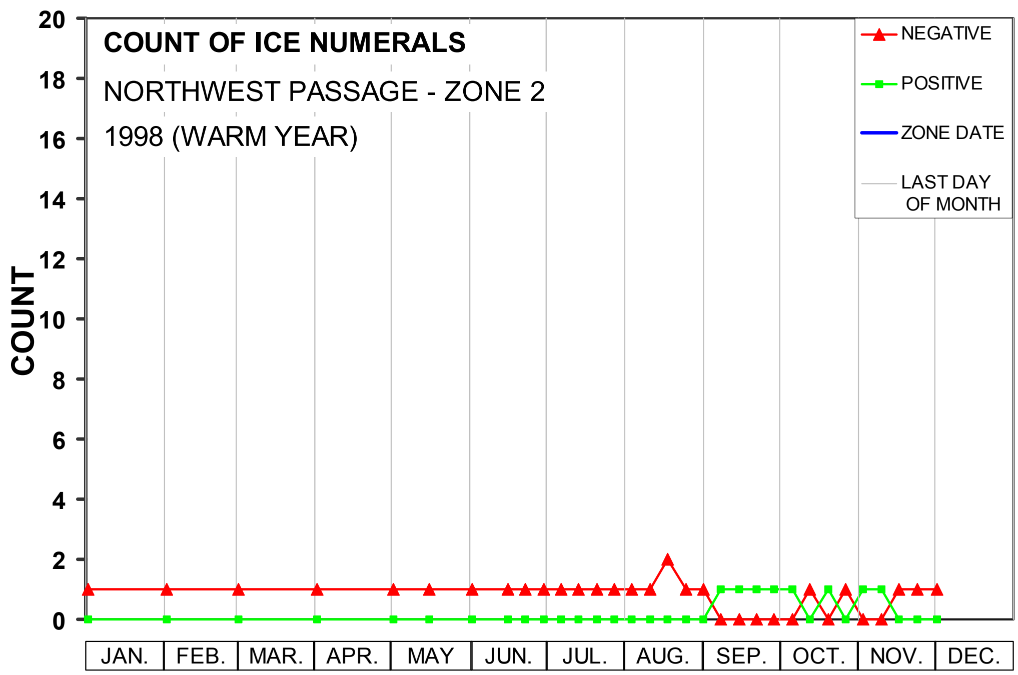

Figure B-20: Count of negative and positive Ice Numerals calculated from data plotted in Figure B-8 - NWP shipping route in Zone 2 throughout the warmer than normal year

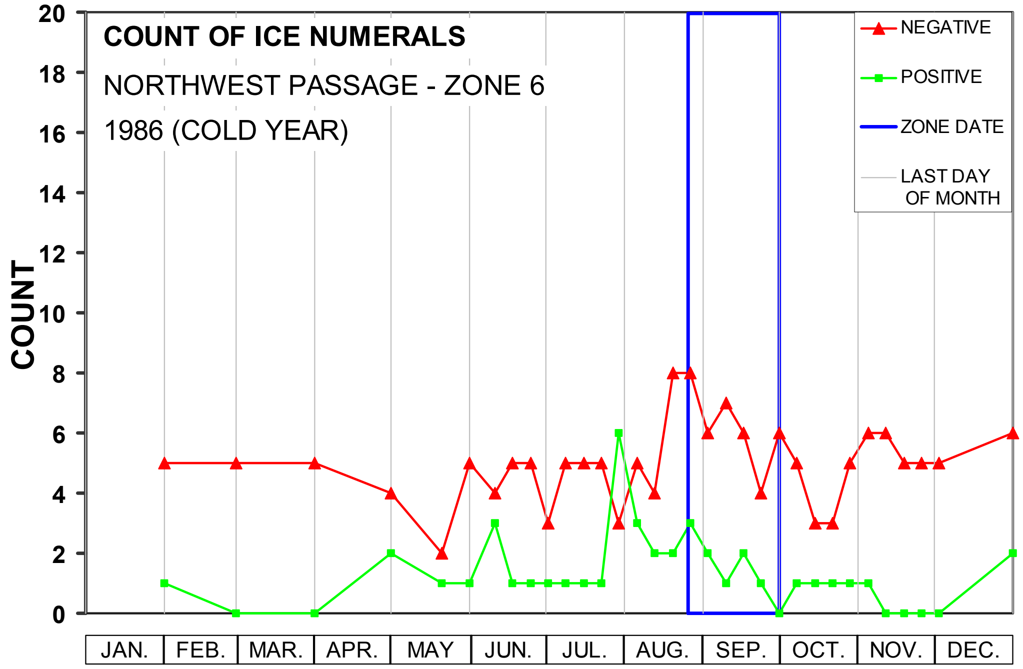

Figure B-21: Count of negative and positive Ice Numerals calculated from data plotted in Figure B-9 - NWP shipping route in Zone 6 throughout the colder than normal year

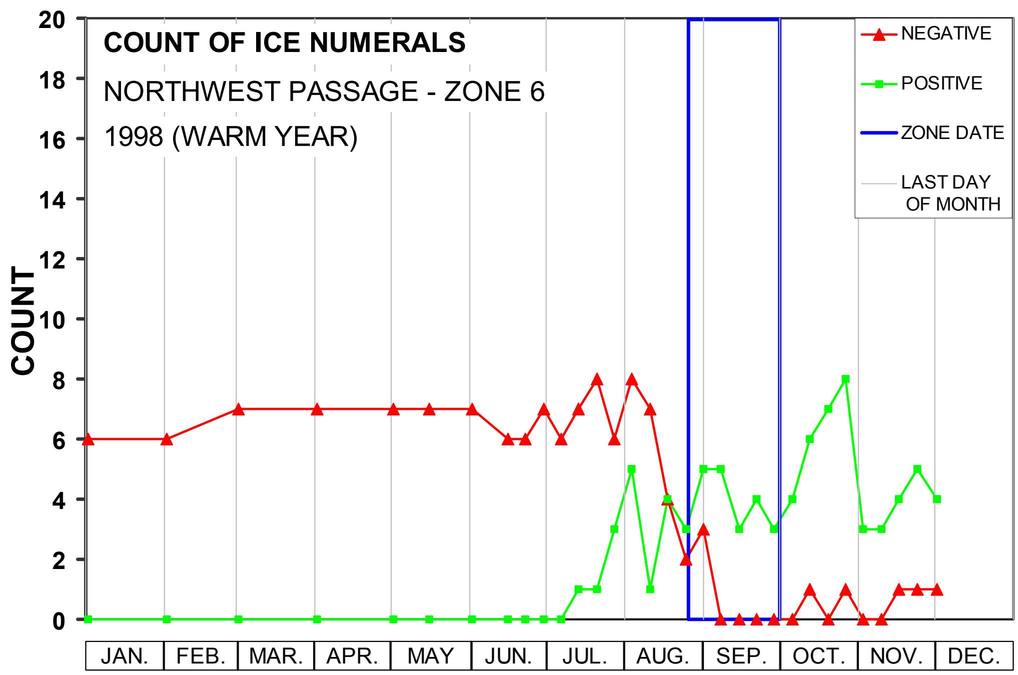

Figure B-22: Count of negative and positive Ice Numerals calculated from data plotted in Figure B-10 - NWP shipping route in Zone 6 throughout the warmer than normal year

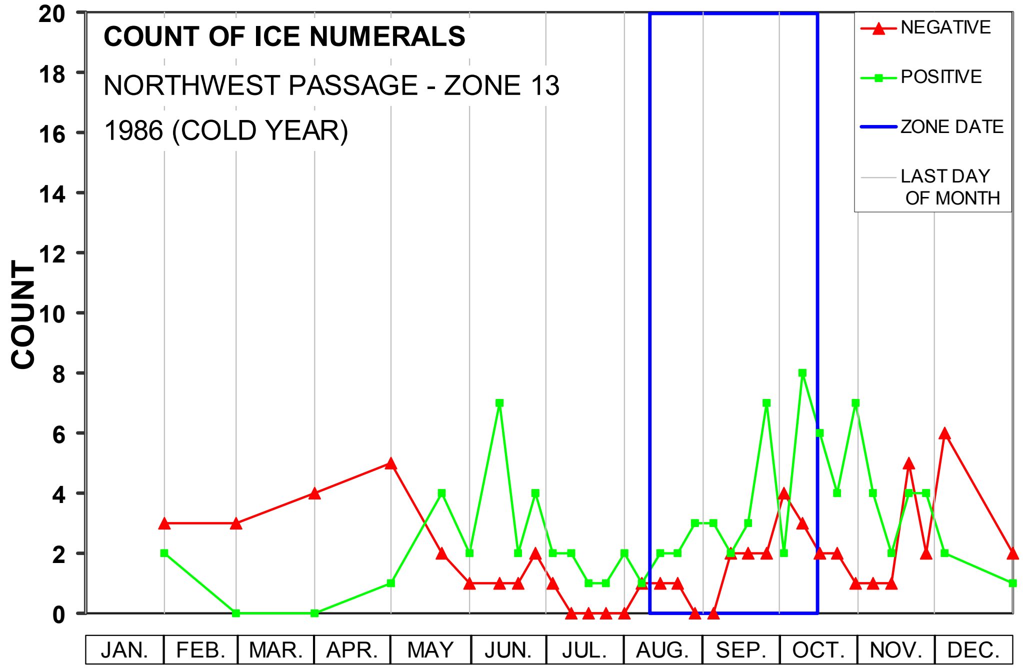

Figure B-23: Count of negative and positive Ice Numerals calculated from data plotted in Figure B-11 - NWP shipping route in Zone 13 throughout the colder than normal year

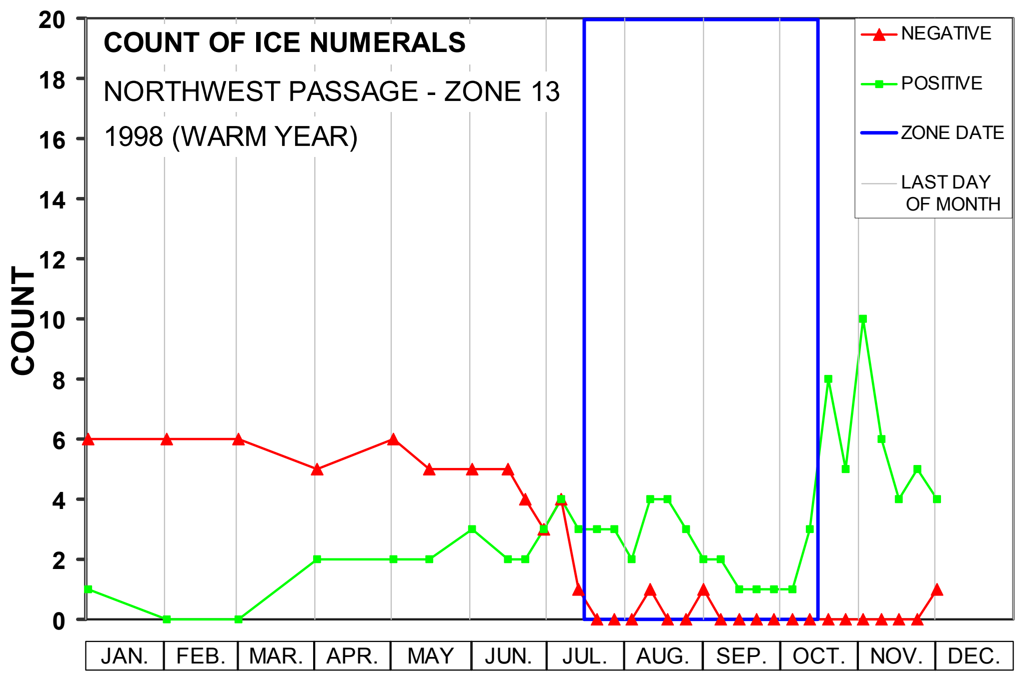

Figure B-24: Count of negative and positive Ice Numerals calculated from data plotted in Figure B-12 - NWP shipping route in Zone 13 throughout the warmer than normal year

APPENDIX B-2. Access Routes to Port of Churchill

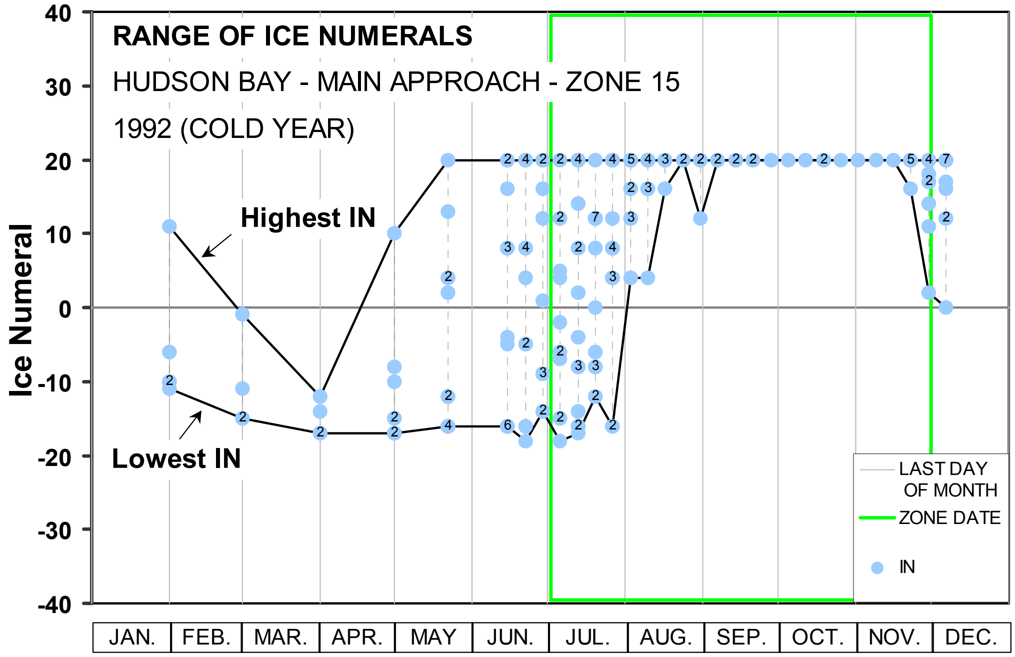

Figure B-25: Range of Ice Numerals calculated from CIS ice charts for the access route to the Port of Churchill in Zone 15 - main approach, throughout the colder than normal year

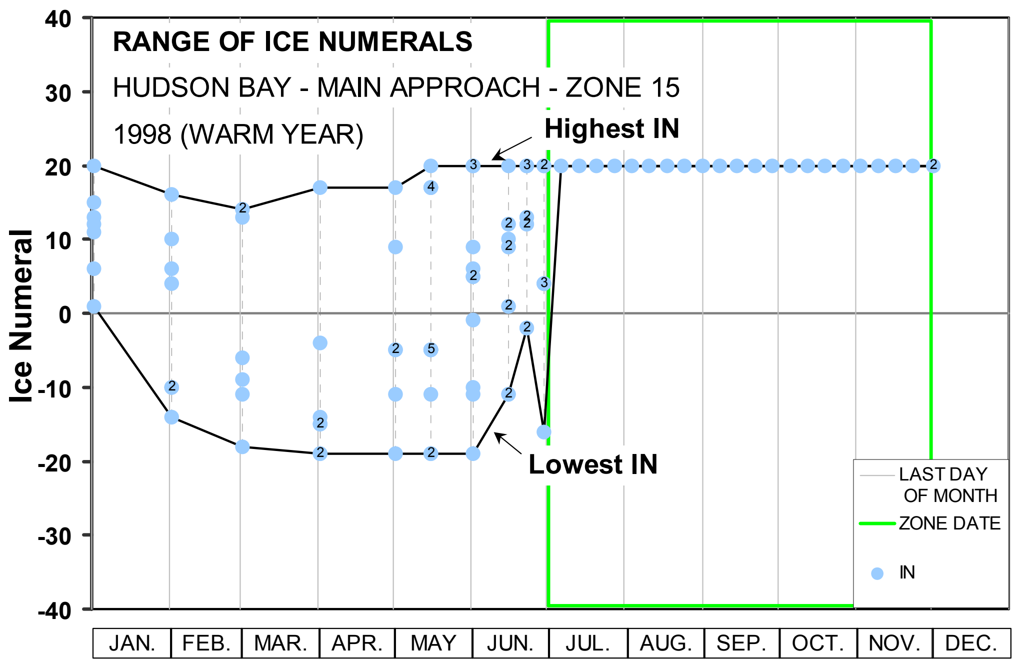

Figure B-26: Range of Ice Numerals calculated from CIS ice charts for the access route to the Port of Churchill in Zone 15 - main approach, throughout the warmer than normal year

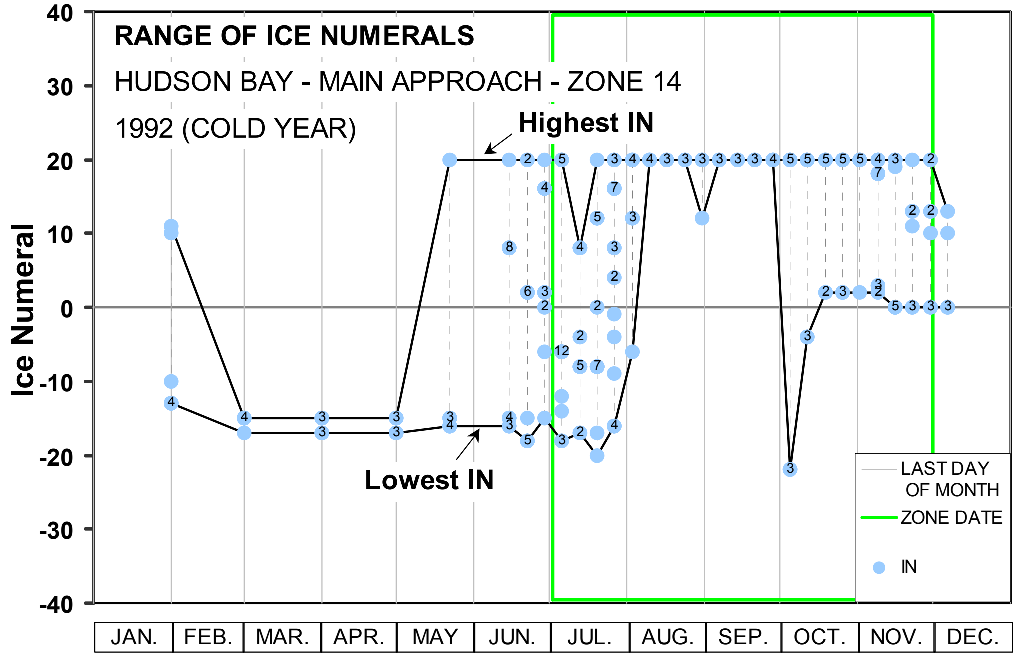

Figure B-27: Range of Ice Numerals calculated from CIS ice charts for the access route to the Port of Churchill in Zone 14 - main approach, throughout the colder than normal year

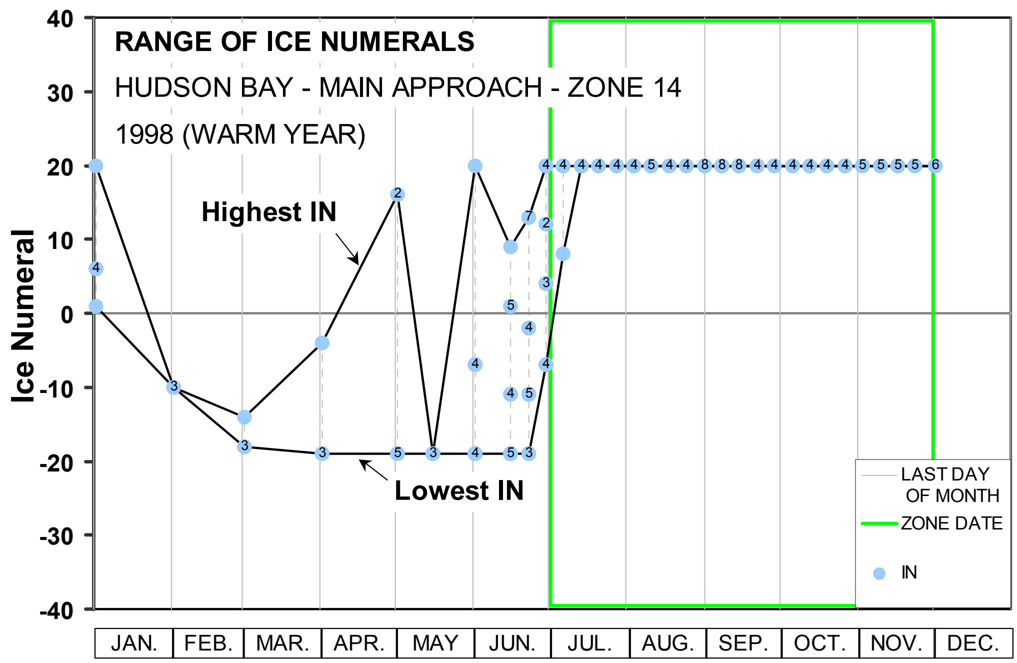

Figure B-28: Range of Ice Numerals calculated from CIS ice charts for the access route to the Port of Churchill in Zone 14 - main approach, throughout the warmer than normal year

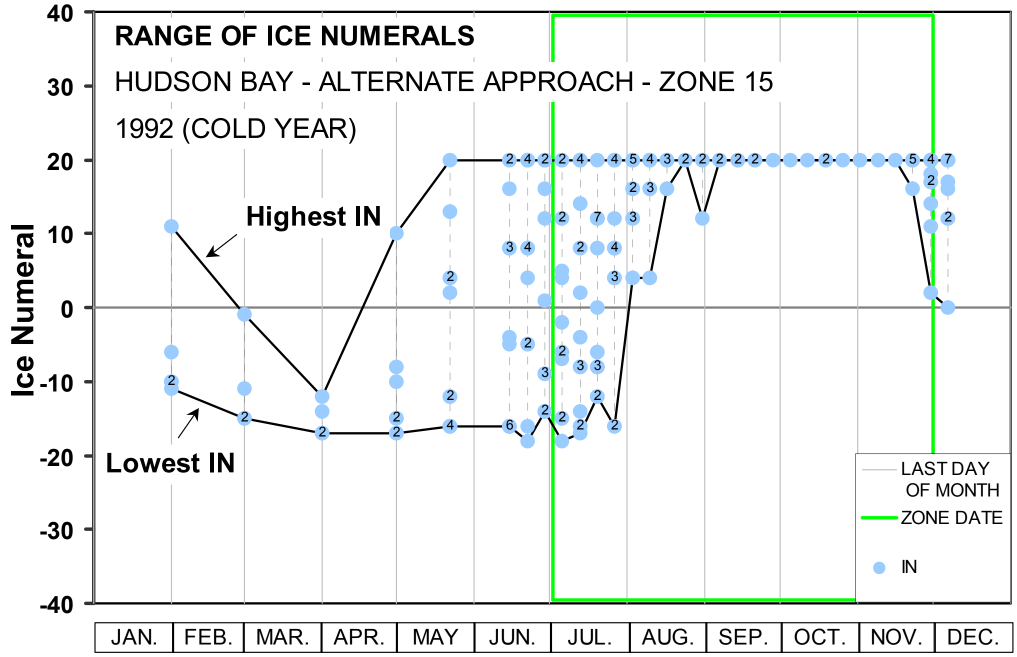

Figure B-29: Range of Ice Numerals calculated from CIS ice charts for the access route to the Port of Churchill in Zone 15 - alternate approach, throughout the colder than normal year

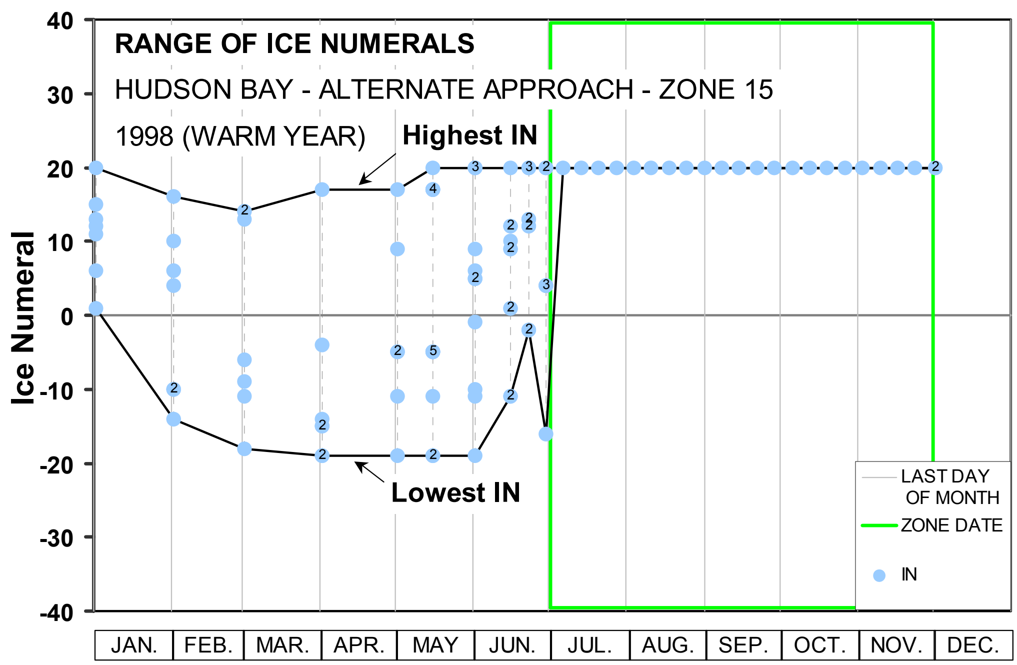

Figure B-30: Range of Ice Numerals calculated from CIS ice charts for the access route to the Port of Churchill in Zone 15 - alternate approach, throughout the warmer than normal year

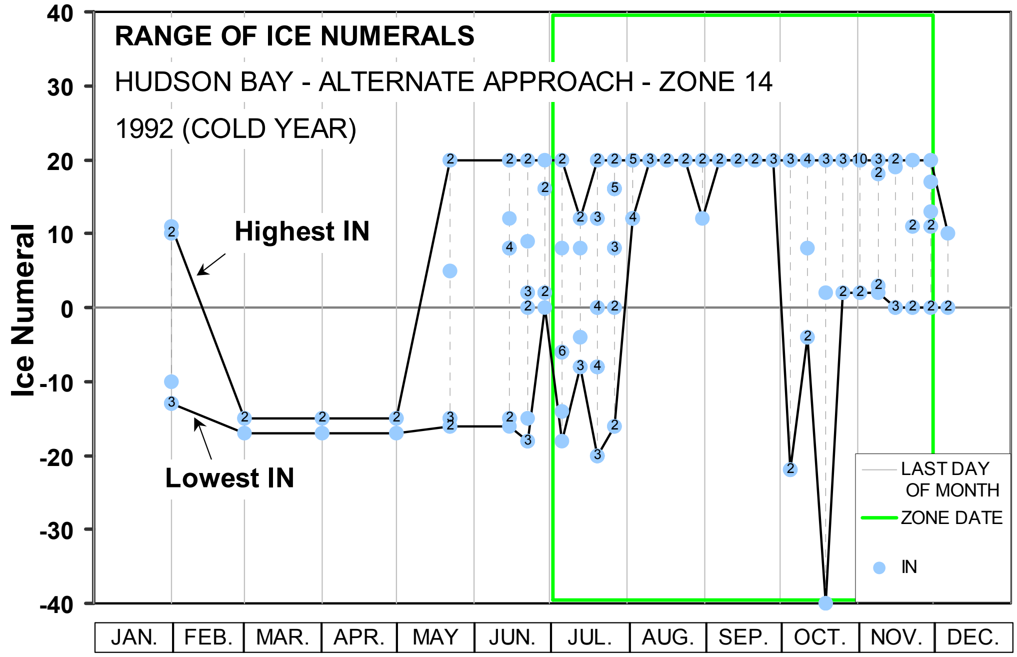

Figure B-31: Range of Ice Numerals calculated from CIS ice charts for the access route to the Port of Churchill in Zone 14 - alternate approach, throughout the colder than normal year

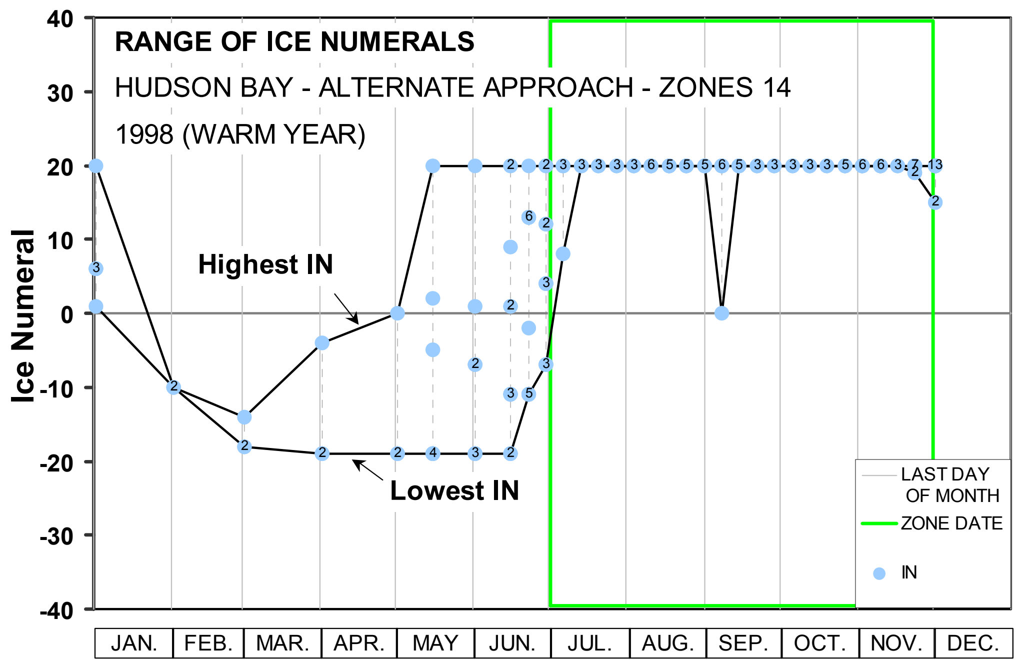

Figure B-32: Range of Ice Numerals calculated from CIS ice charts for the access route to the Port of Churchill in Zone 14 - alternate approach, throughout the warmer than normal year

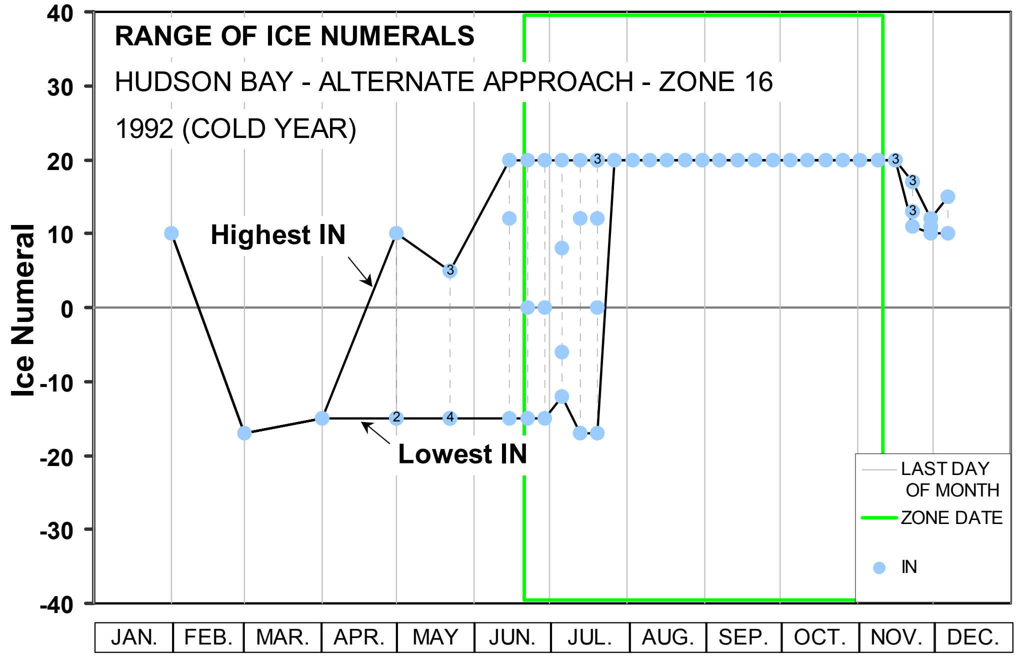

Figure B-33: Range of Ice Numerals calculated from CIS ice charts for the access route to the Port of Churchill in Zone 16 - alternate approach, throughout the colder than normal year

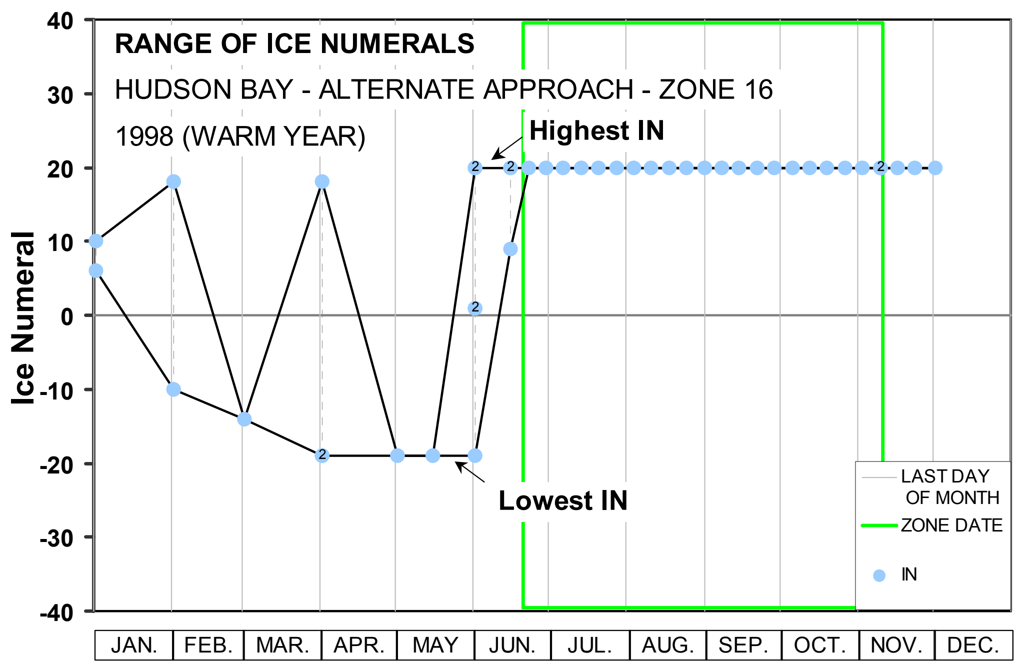

Figure B-34: Range of Ice Numerals calculated from CIS ice charts for the access route to the Port of Churchill in Zone 16 - alternate approach, throughout the warmer than normal year

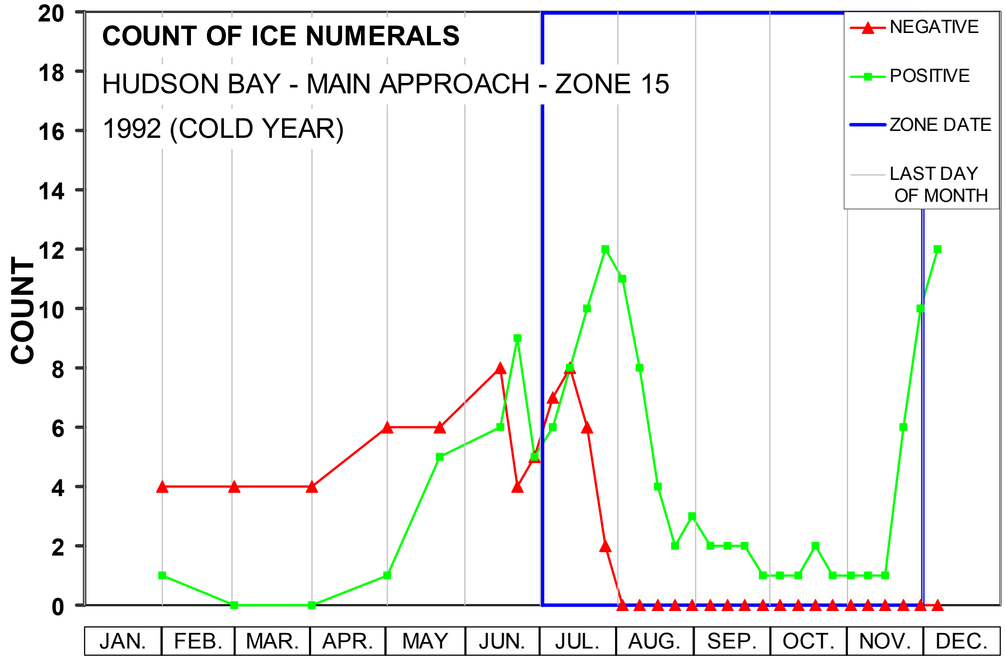

Figure B-35: Count of negative and positive Ice Numerals calculated from data plotted in Figure B-25 - the access route to the Port of Churchill in Zone 15 - main approach, throughout the colder than normal year

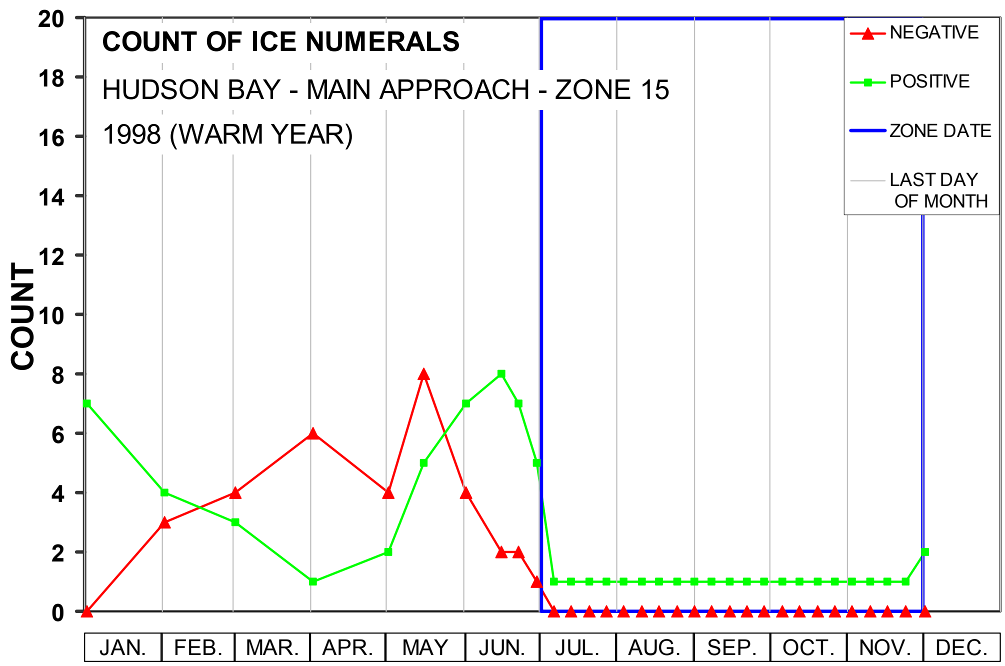

Figure B-36: Count of negative and positive Ice Numerals calculated from data plotted in Figure B-26 - the access route to the Port of Churchill in Zone 15 - main approach, throughout the warmer than normal year

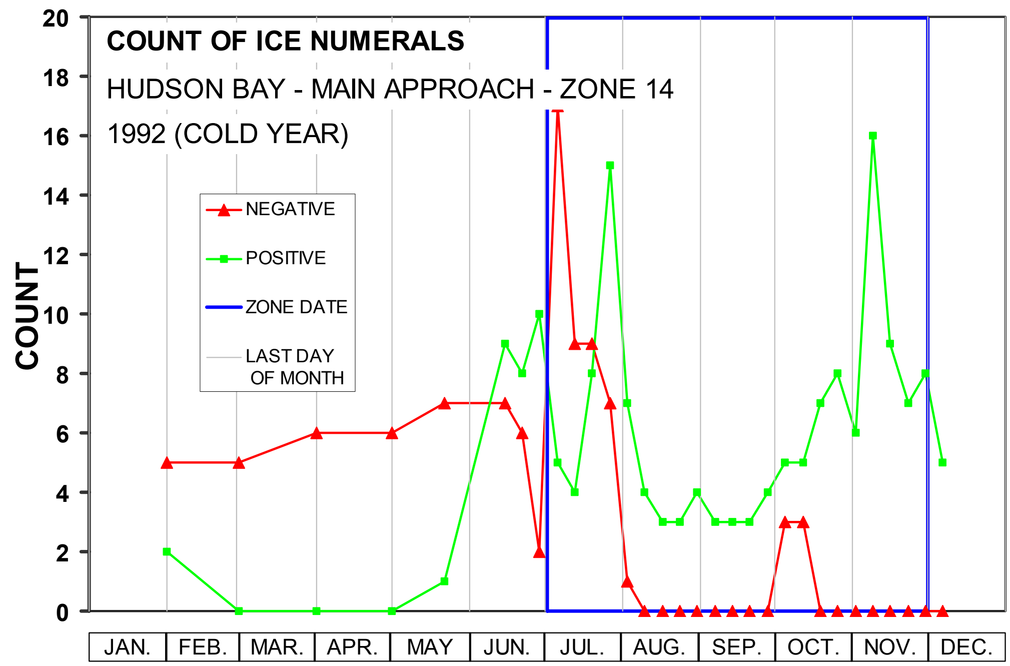

Figure B-37: Count of negative and positive Ice Numerals calculated from data plotted in Figure B-27 - the access route to the Port of Churchill in Zone 14 - main approach, throughout the colder than normal year

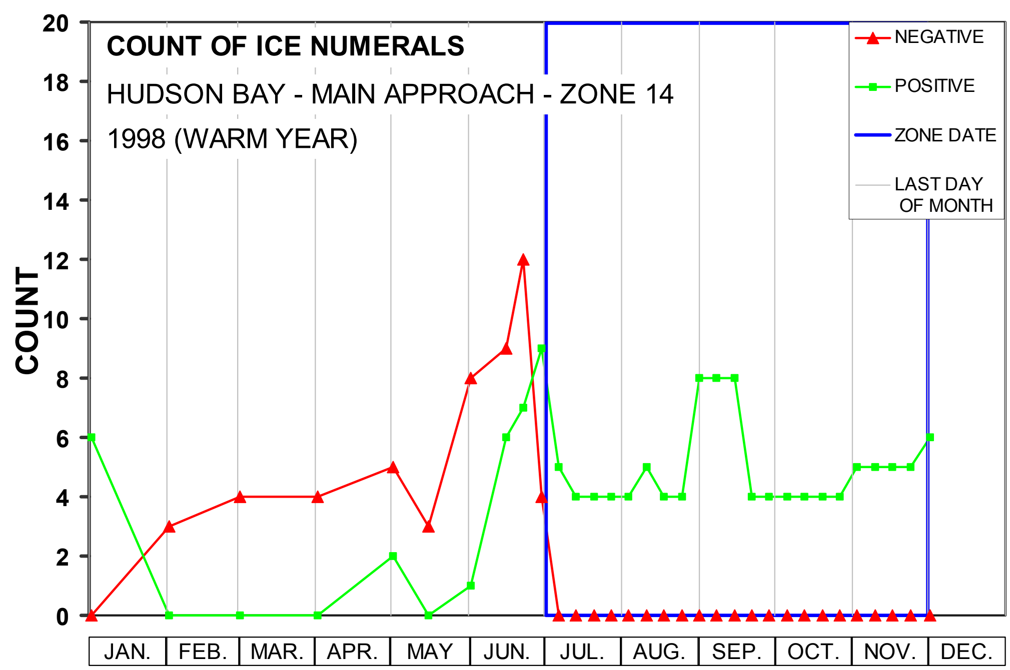

Figure B-38: Count of negative and positive Ice Numerals calculated from data plotted in Figure B-28 - the access route to the Port of Churchill in Zone 14 - main approach, throughout the warmer than normal year

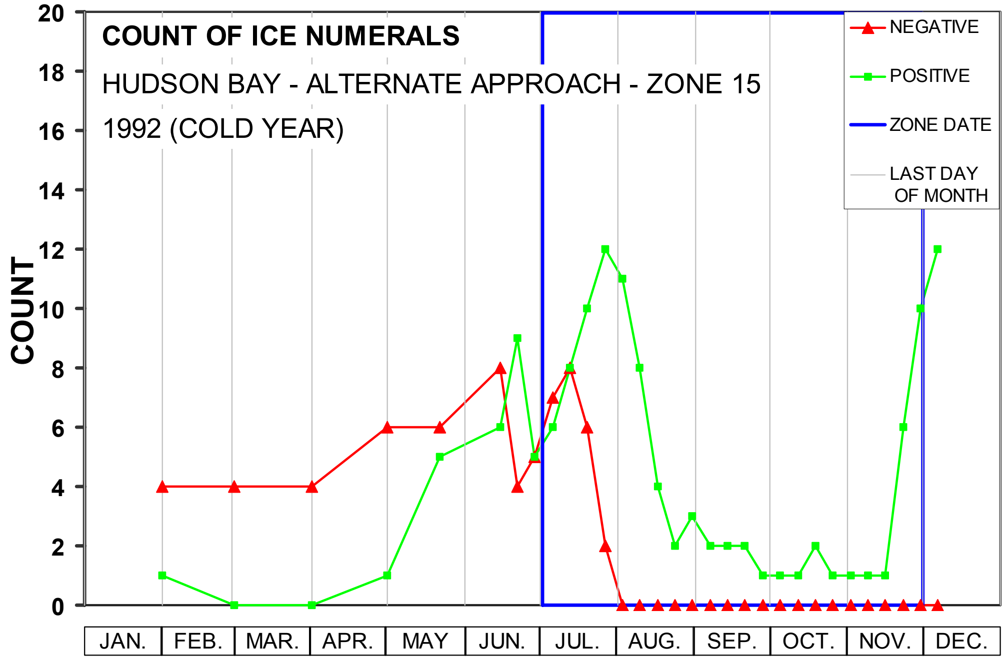

Figure B-39: Count of negative and positive Ice Numerals calculated from data plotted in Figure B-29 - the access route to the Port of Churchill in Zone 15 - alternate approach, throughout the colder than normal year

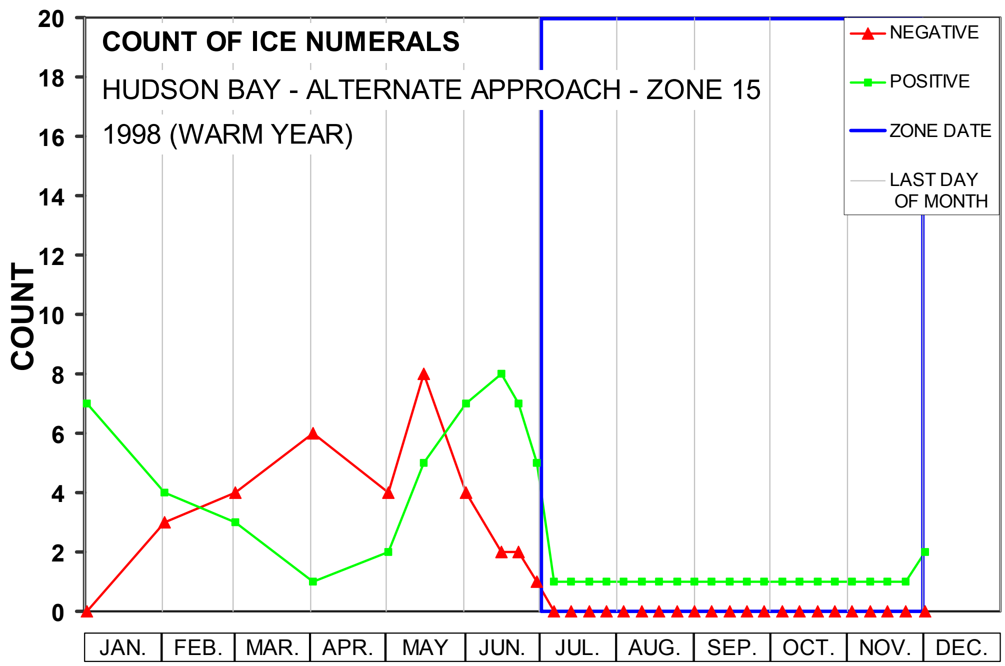

Figure B-40: Count of negative and positive Ice Numerals calculated from data plotted in Figure B-30 - the access route to the Port of Churchill in Zone 15 - alternate approach, throughout the warmer than normal year

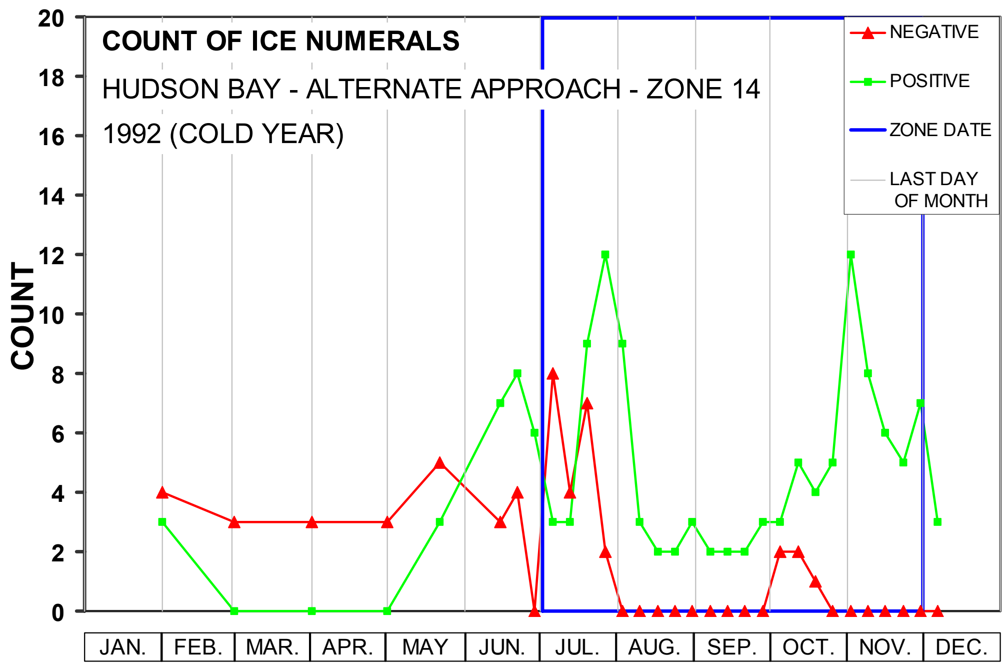

Figure B-41: Count of negative and positive Ice Numerals calculated from data plotted in Figure B-31 - the access route to the Port of Churchill in Zone 14 - alternate approach, throughout the colder than normal year

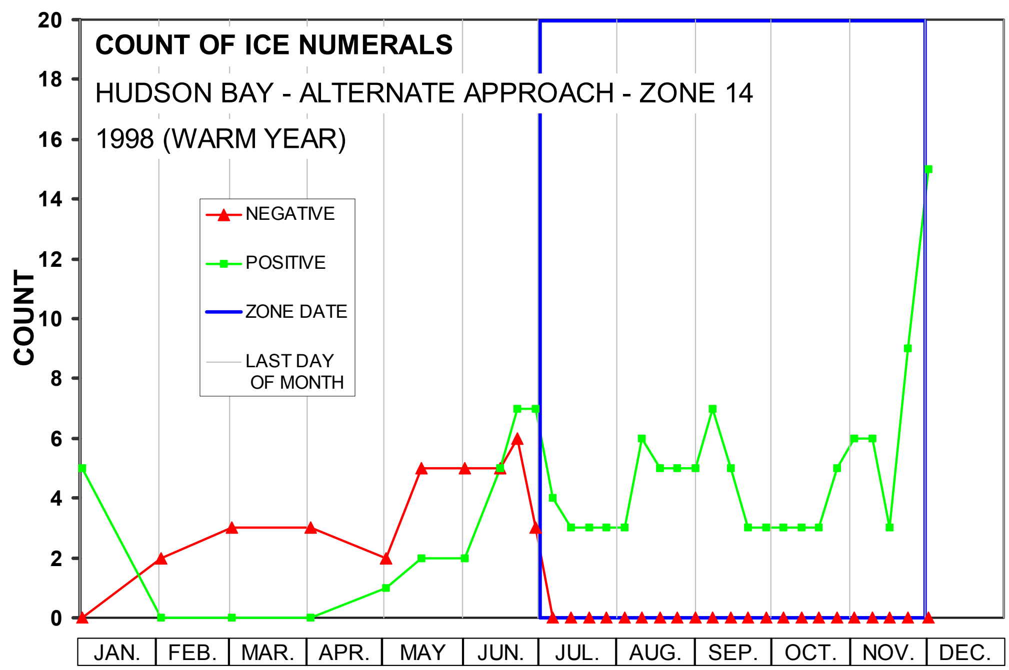

Figure B-42: Count of negative and positive Ice Numerals calculated from data plotted in Figure B-32 - the access route to the Port of Churchill in Zone 14 - alternate approach, throughout the warmer than normal year

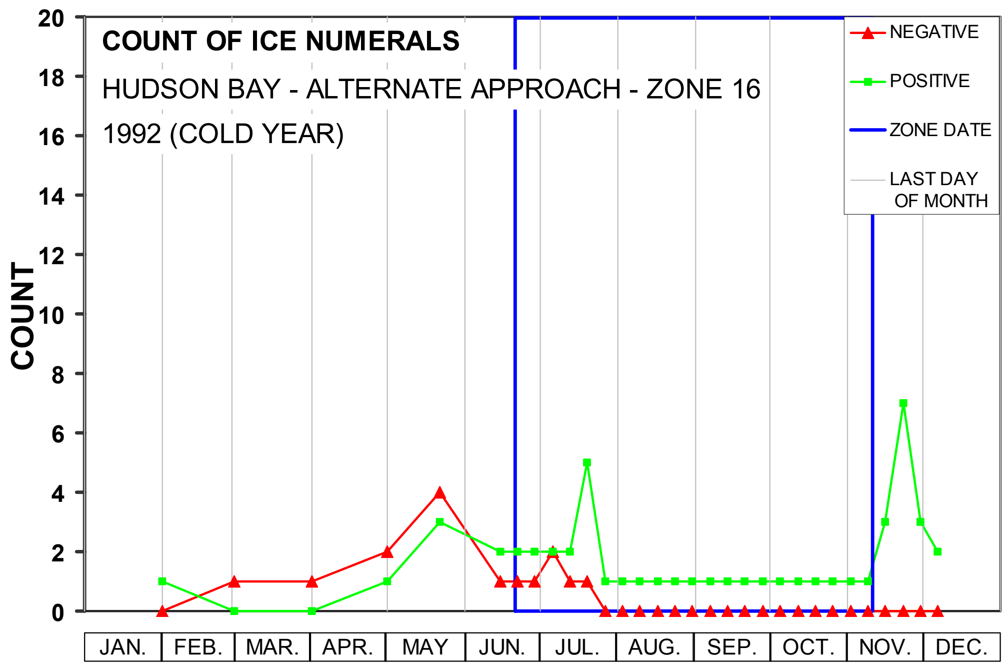

Figure B-43: Count of negative and positive Ice Numerals calculated from data plotted in Figure B-33 - the access route to the Port of Churchill in Zone 16 - alternate approach, throughout the colder than normal year

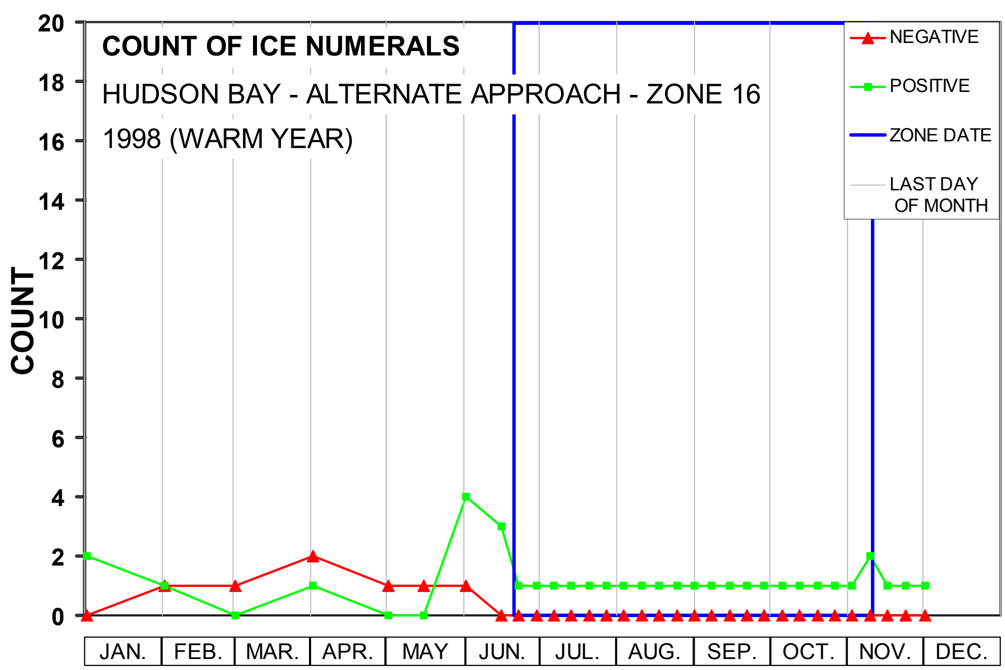

Figure B-44: Count of negative and positive Ice Numerals calculated from data plotted in Figure B-34 - the access route to the Port of Churchill in Zone 16 - alternate approach, throughout the warmer than normal year

APPENDIX B-3. Segment Routes

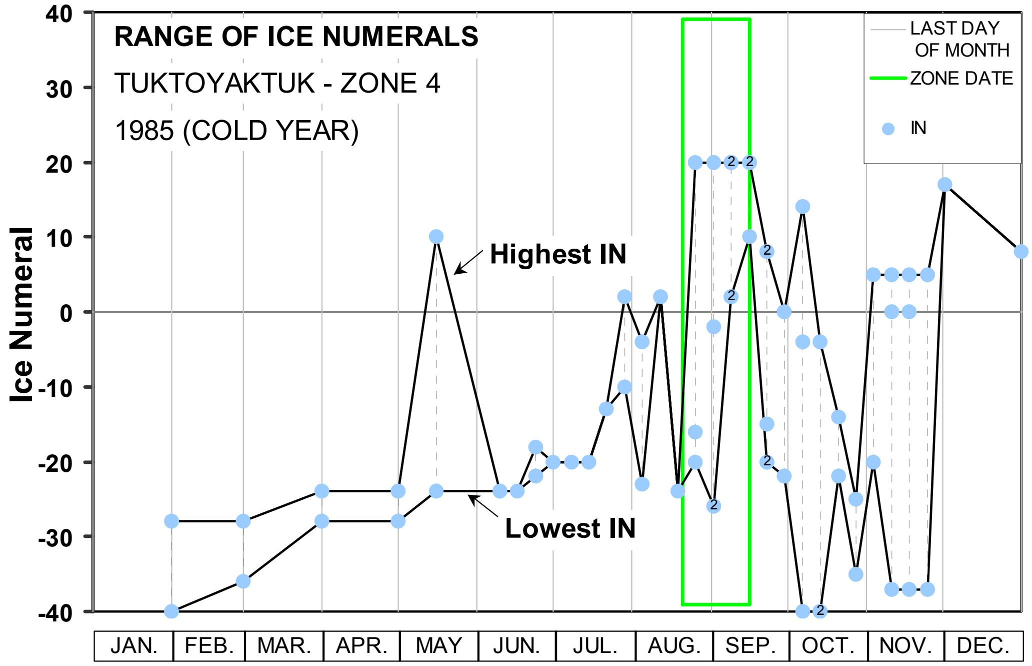

Figure B-45: Range of Ice Numerals calculated from CIS ice charts for a segment route in Zone 4, throughout the colder than normal year

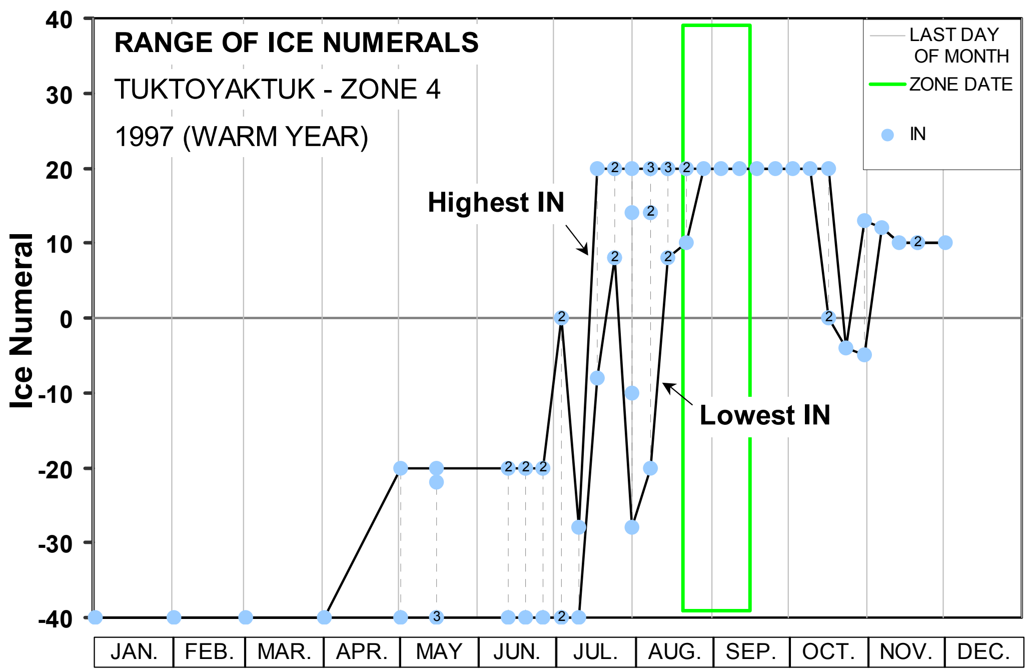

Figure B-46: Range of Ice Numerals calculated from CIS ice charts for a segment route in Zone 4, throughout the warmer than normal year

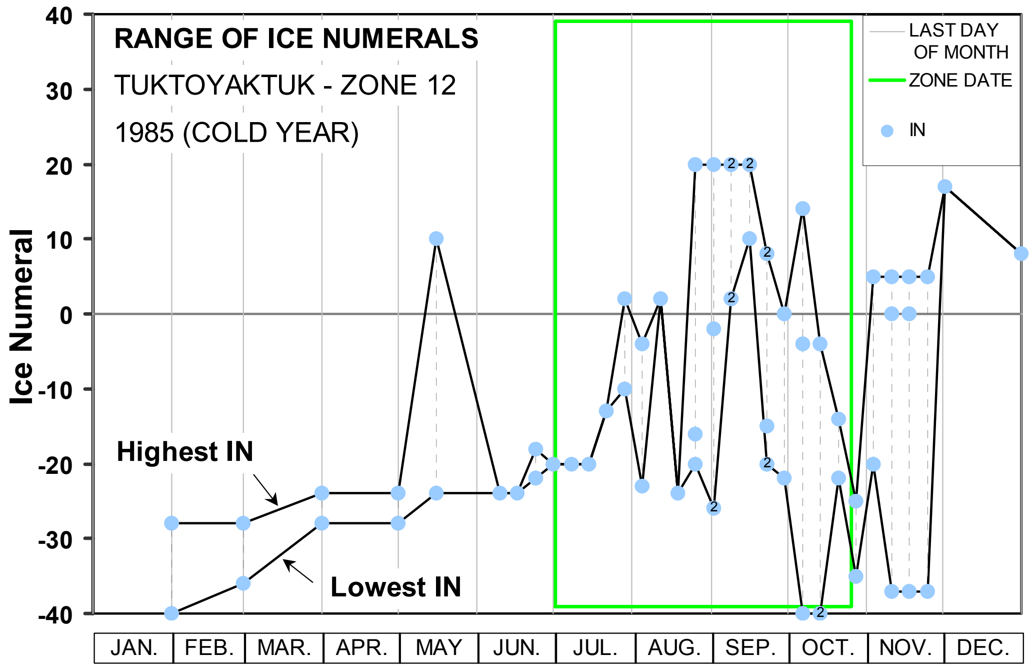

Figure B-47: Range of Ice Numerals calculated from CIS ice charts for a segment route in Zone 12, throughout the colder than normal year

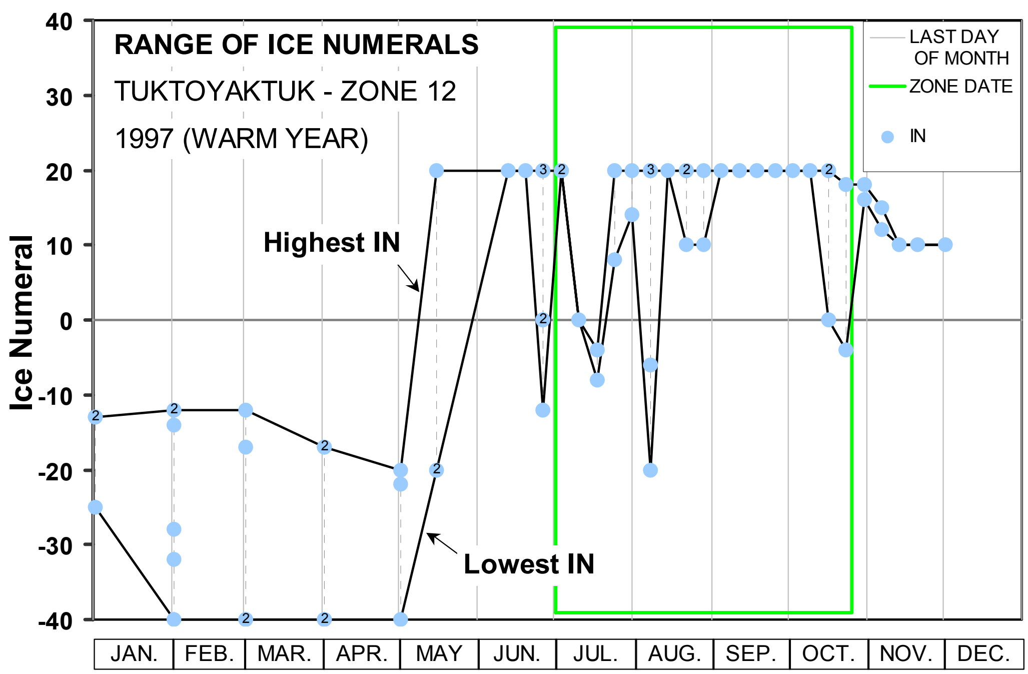

Figure B-48: Range of Ice Numerals calculated from CIS ice charts for a segment route in Zone 12, throughout the warmer than normal year

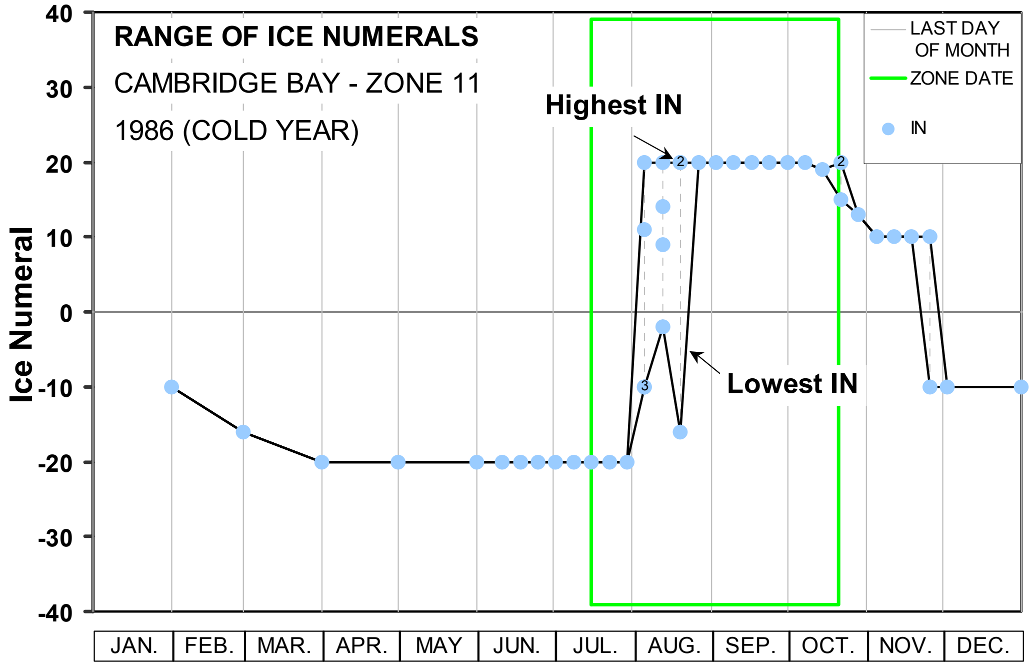

Figure B-49: Range of Ice Numerals calculated from CIS ice charts for a segment route in Zone 11, throughout the colder than normal year

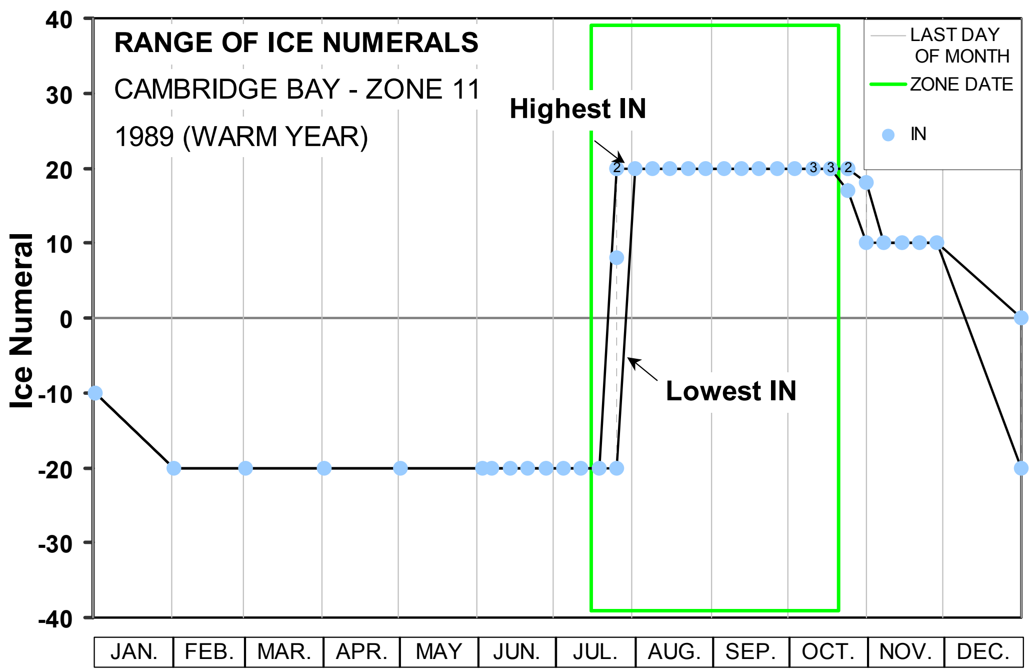

Figure B-50: Range of Ice Numerals calculated from CIS ice charts for a segment route in Zone 11, throughout the warmer than normal year

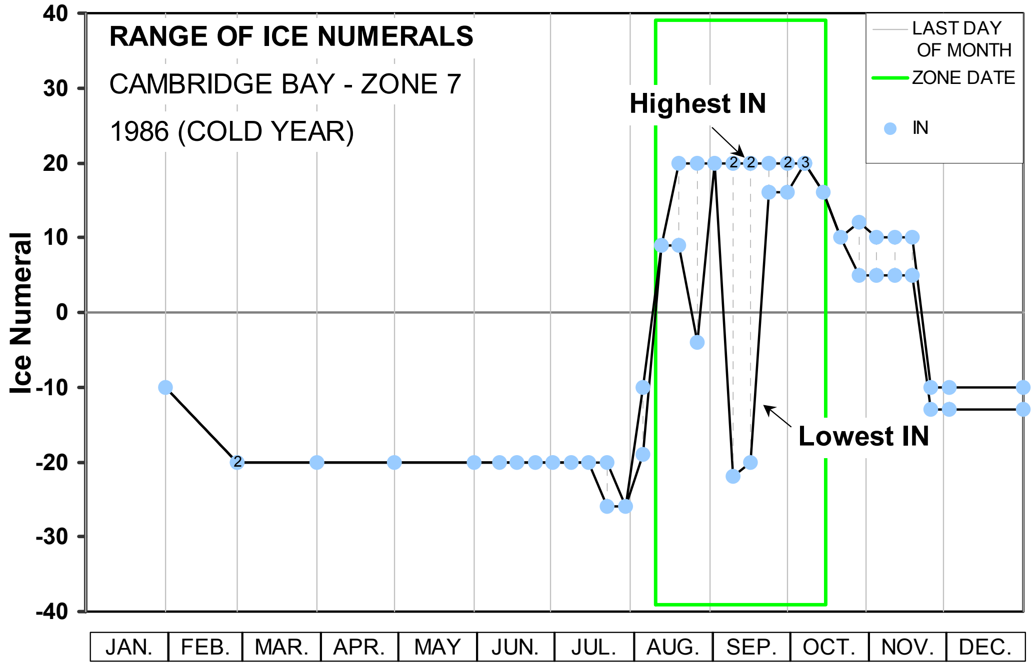

Figure B-51: Range of Ice Numerals calculated from CIS ice charts for a segment route in Zone 7, throughout the colder than normal year

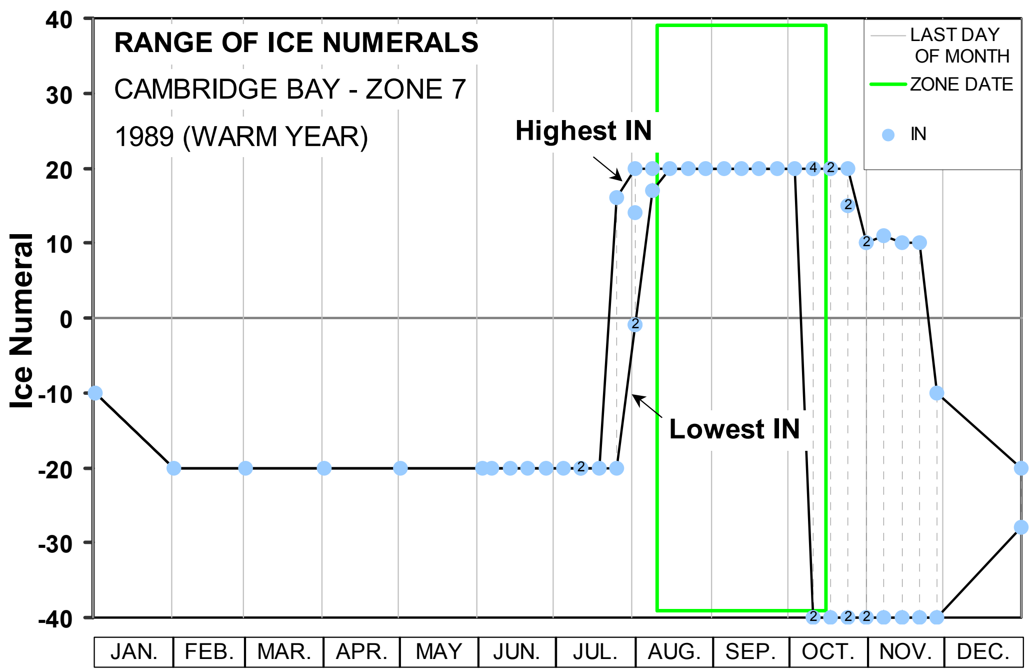

Figure B-52: Range of Ice Numerals calculated from CIS ice charts for a segment route in Zone 7, throughout the warmer than normal year

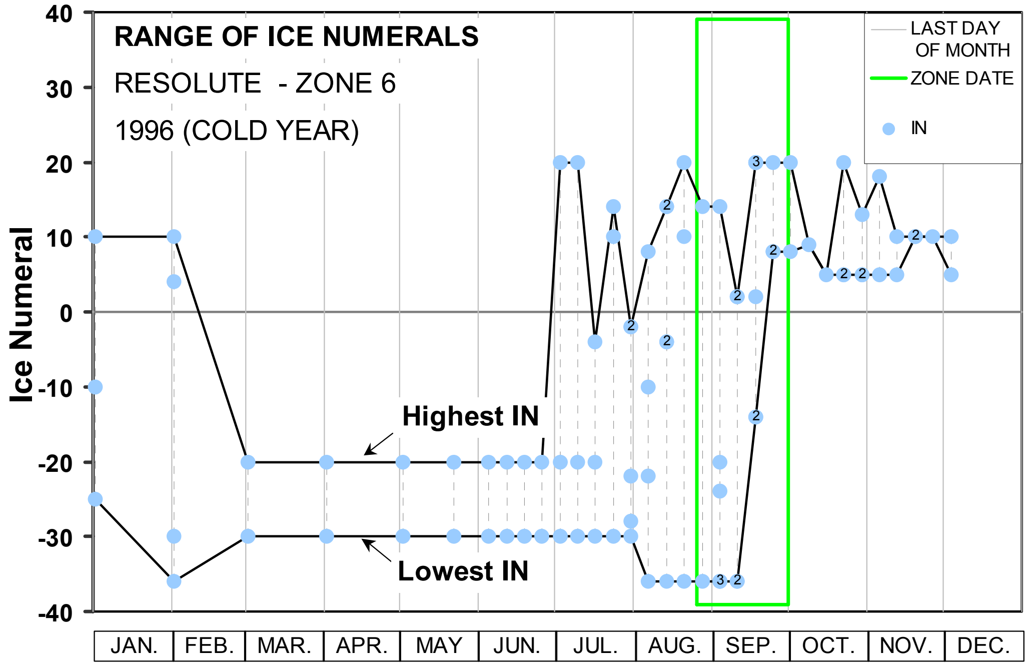

Figure B-53: Range of Ice Numerals calculated from CIS ice charts for a segment route in Zone 6, throughout the colder than normal year

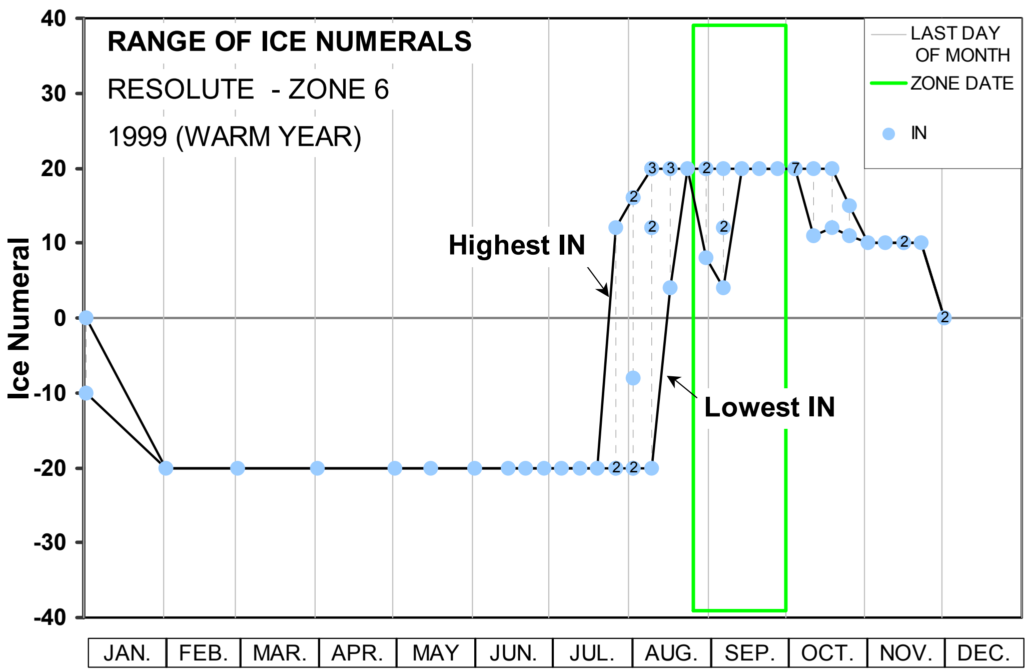

Figure B-54: Range of Ice Numerals calculated from CIS ice charts for a segment route in Zone 6, throughout the warmer than normal year

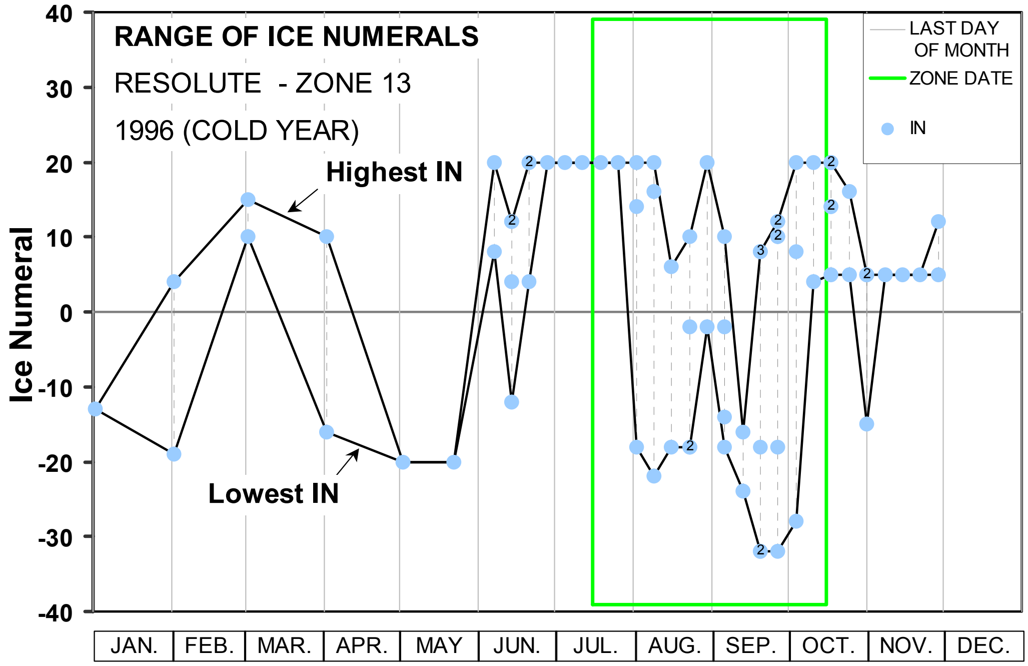

Figure B-55: Range of Ice Numerals calculated from CIS ice charts for a segment route in Zone 13, throughout the colder than normal year

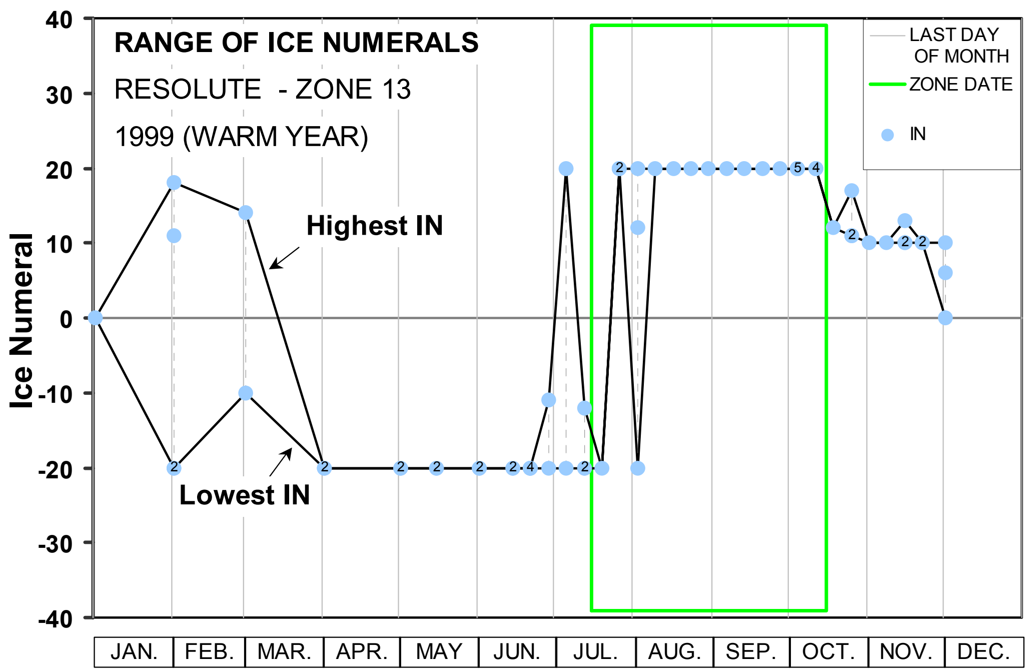

Figure B-56: Range of Ice Numerals calculated from CIS ice charts for a segment route in Zone 13, throughout the warmer than normal year

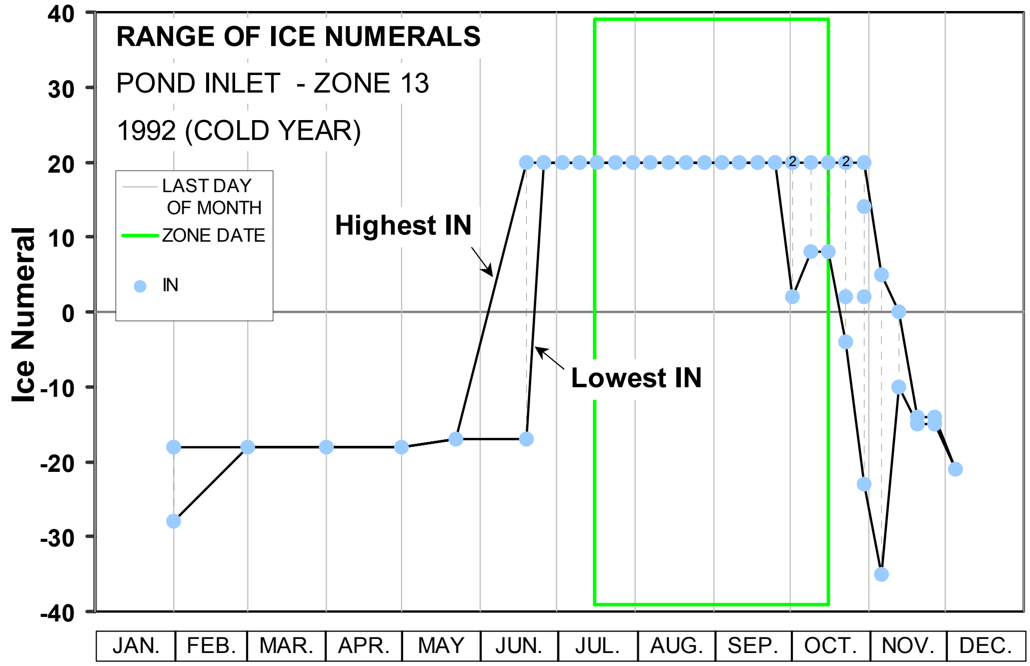

Figure B-57: Range of Ice Numerals calculated from CIS ice charts for a segment route in Zone 13, throughout the colder than normal year

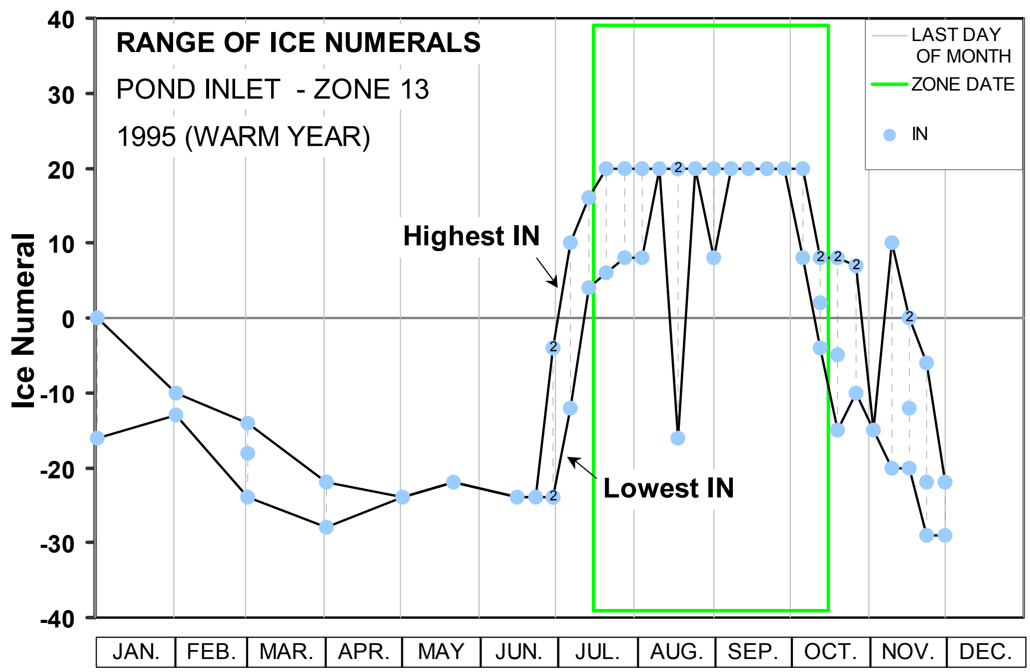

Figure B-58: Range of Ice Numerals calculated from CIS ice charts for a segment route in Zone 13, throughout the warmer than normal year

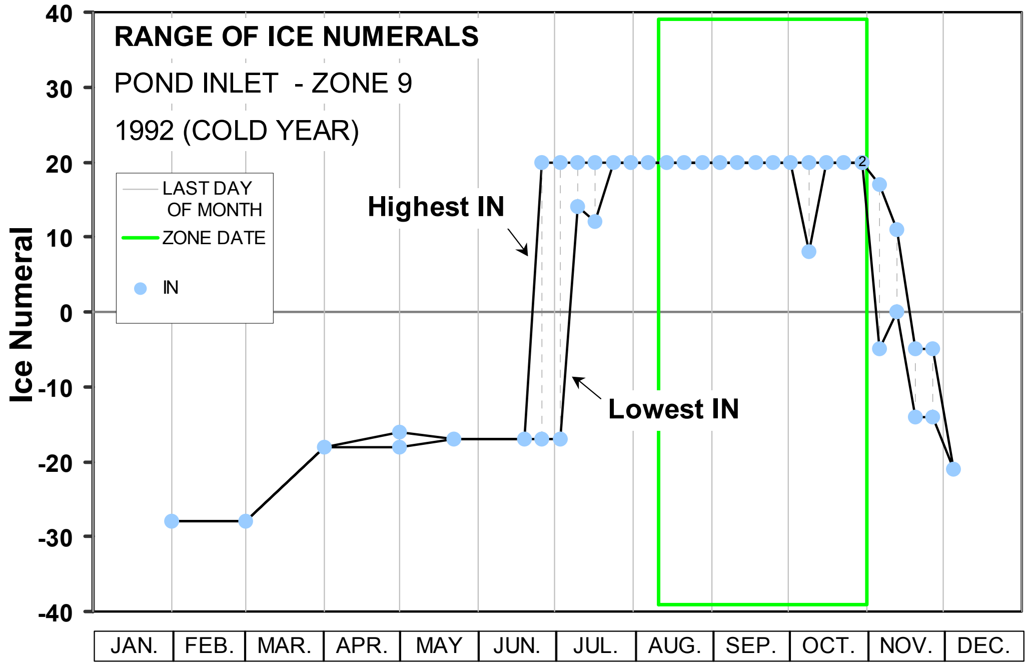

Figure B-59: Range of Ice Numerals calculated from CIS ice charts for a segment route in Zone 9, throughout the colder than normal year

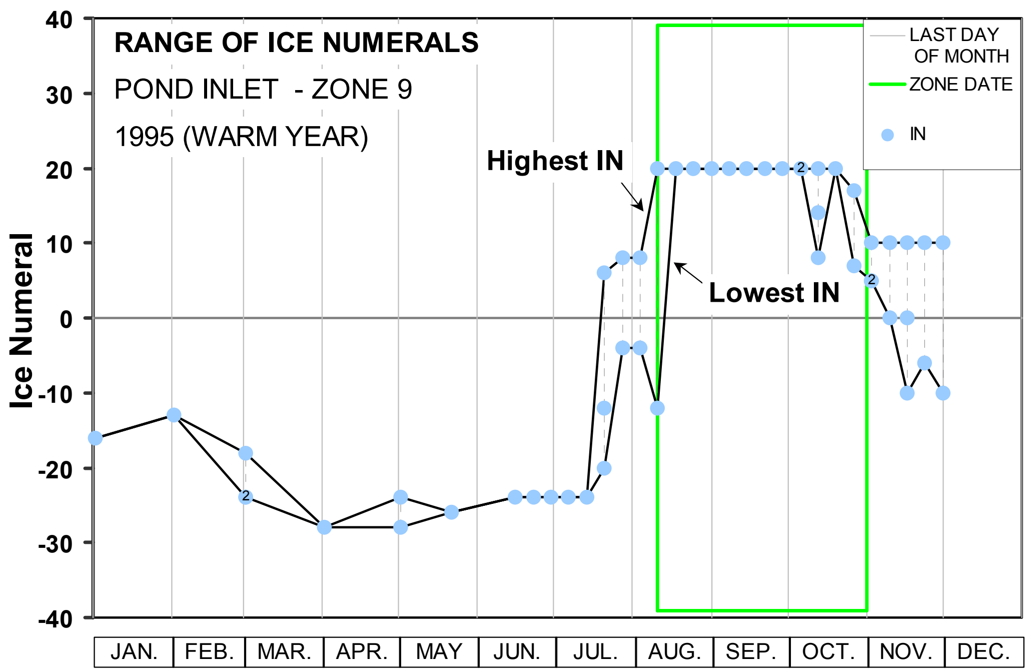

Figure B-60: Range of Ice Numerals calculated from CIS ice charts for a segment route in Zone 9, throughout the warmer than normal year

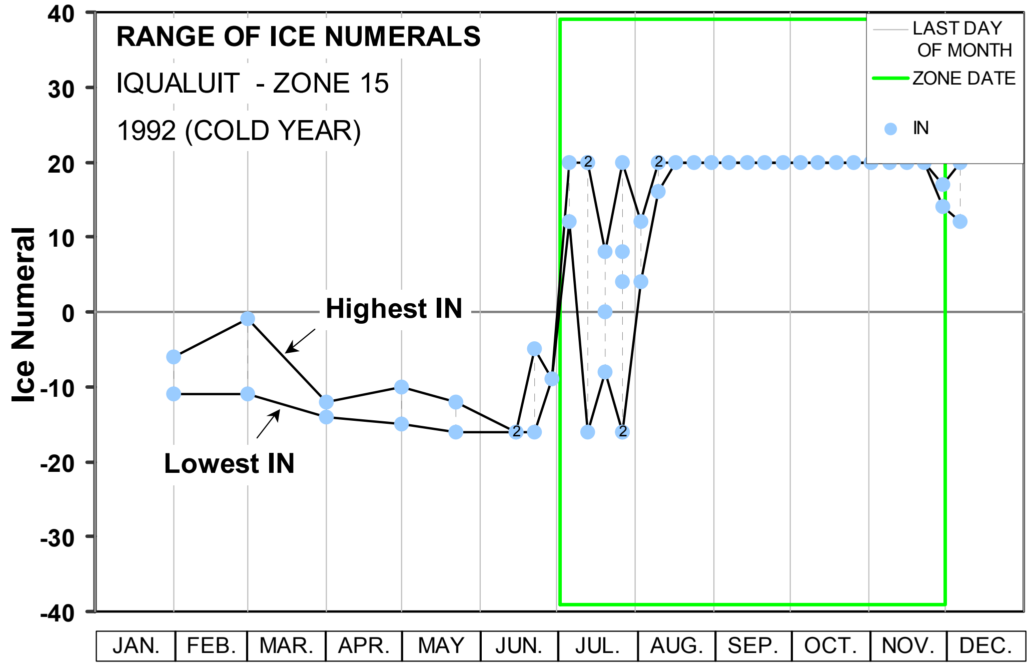

Figure B-61: Range of Ice Numerals calculated from CIS ice charts for a segment route in Zone 15, throughout the colder than normal year

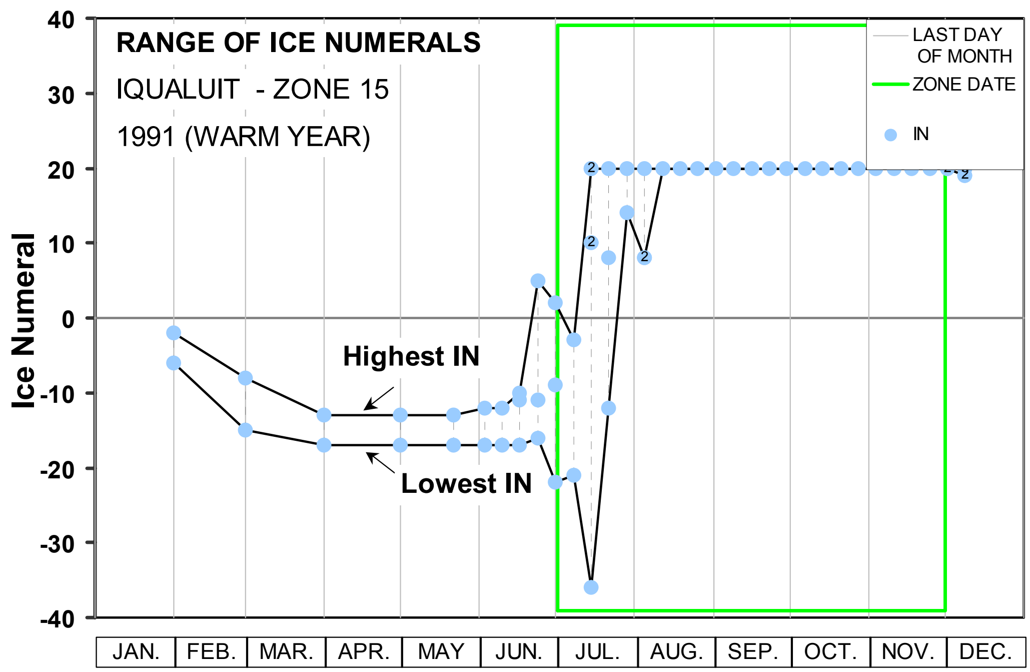

Figure B-62: Range of Ice Numerals calculated from CIS ice charts for a segment route in Zone 15, throughout the warmer than normal year

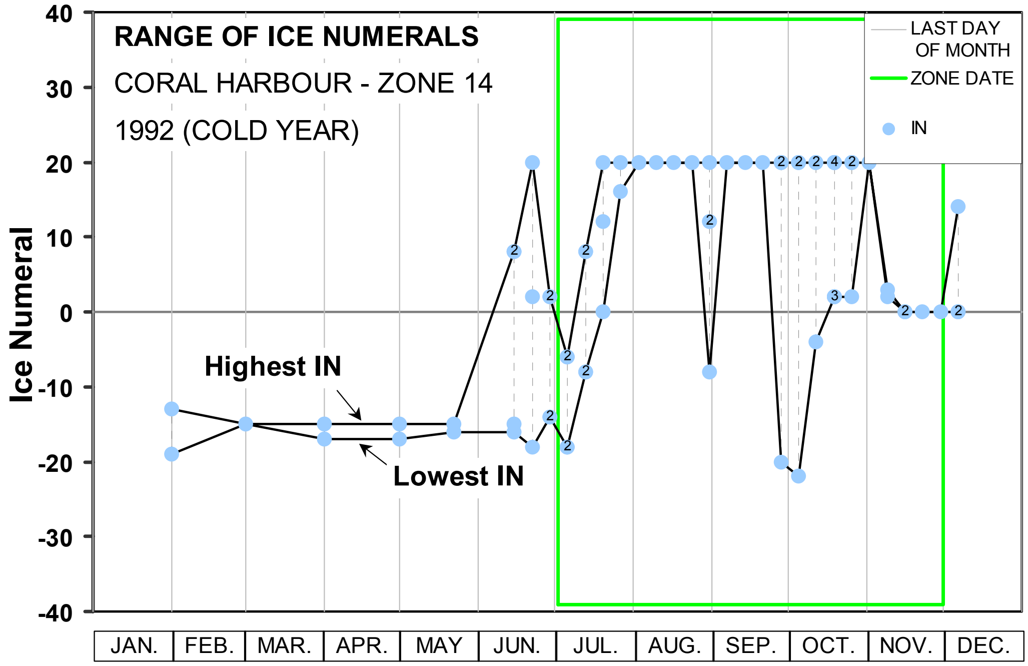

Figure B-63: Range of Ice Numerals calculated from CIS ice charts for a segment route in Zone 14, throughout the colder than normal year

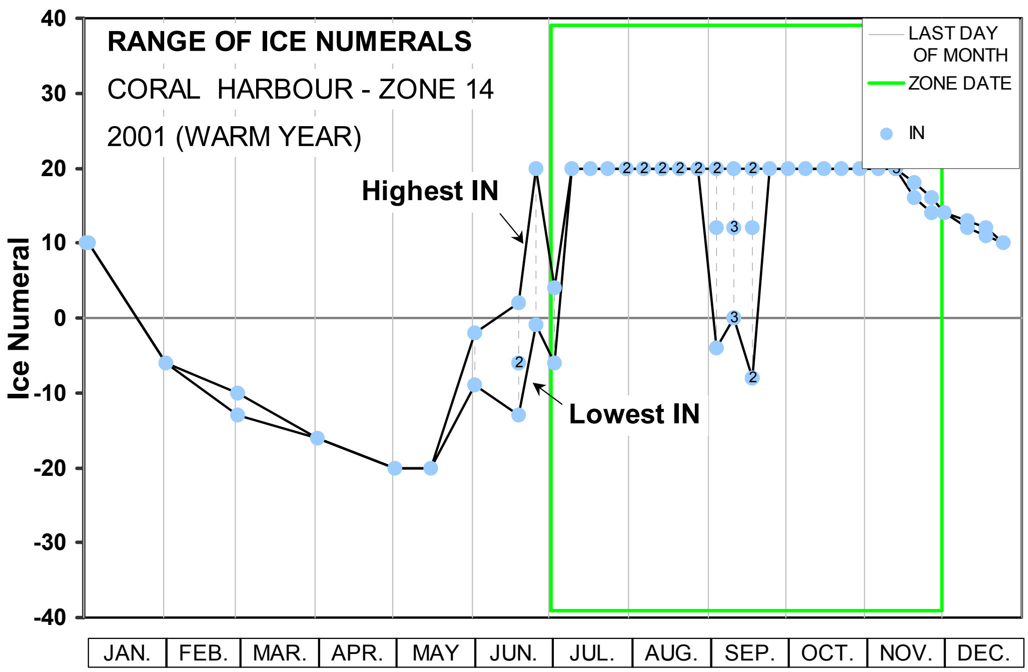

Figure B-64: Range of Ice Numerals calculated from CIS ice charts for a segment route in Zone 14, throughout the warmer than normal year

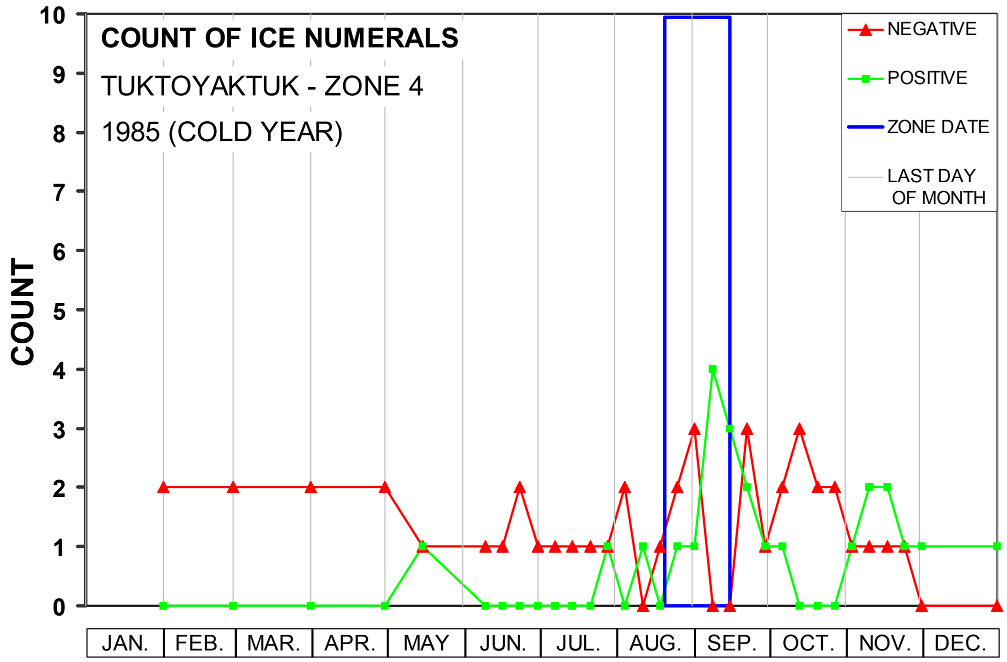

Figure B-65: Count of negative and positive Ice Numerals calculated from data plotted in Figure B-45 - the segment route in Zone 4, throughout the colder than normal year

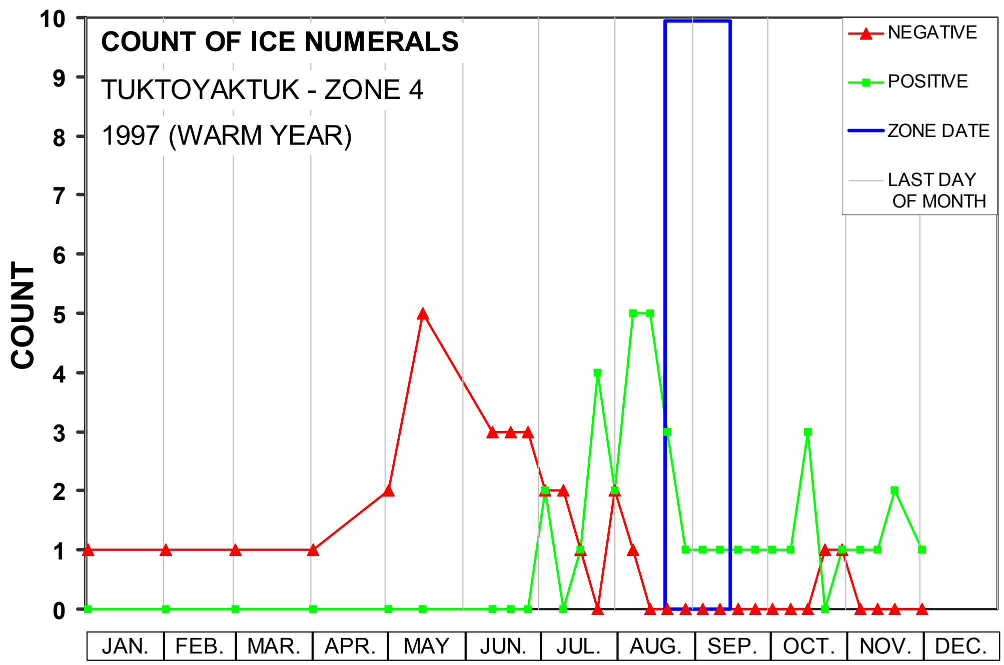

Figure B-66: Count of negative and positive Ice Numerals calculated from data plotted in Figure B-46 - the segment route in Zone 4, throughout the warmer than normal year

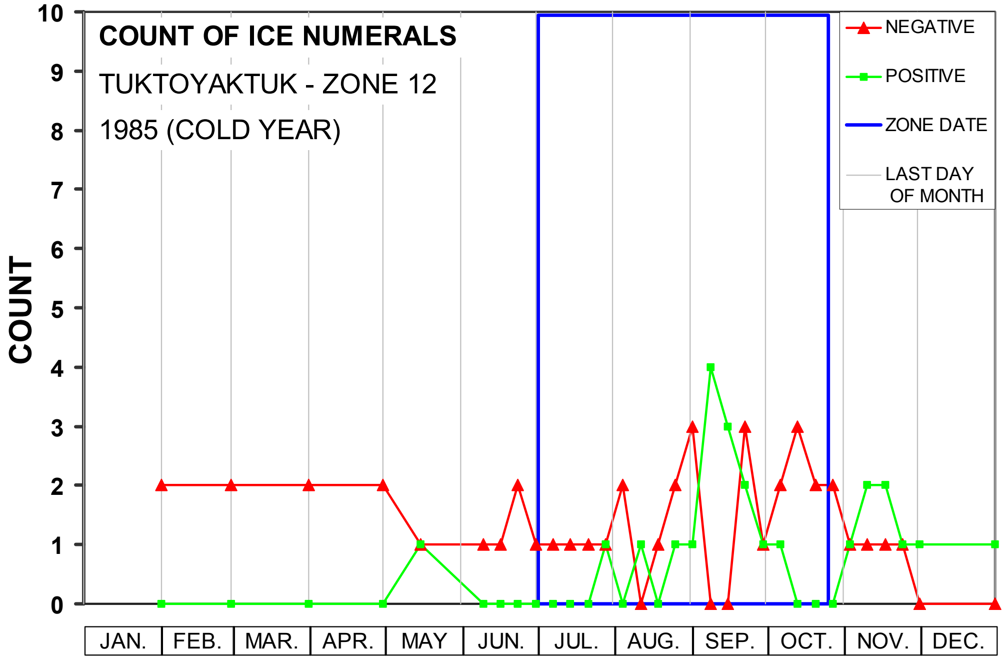

Figure B-67: Count of negative and positive Ice Numerals calculated from data plotted in Figure B-47 - the segment route in Zone 12, throughout the colder than normal year

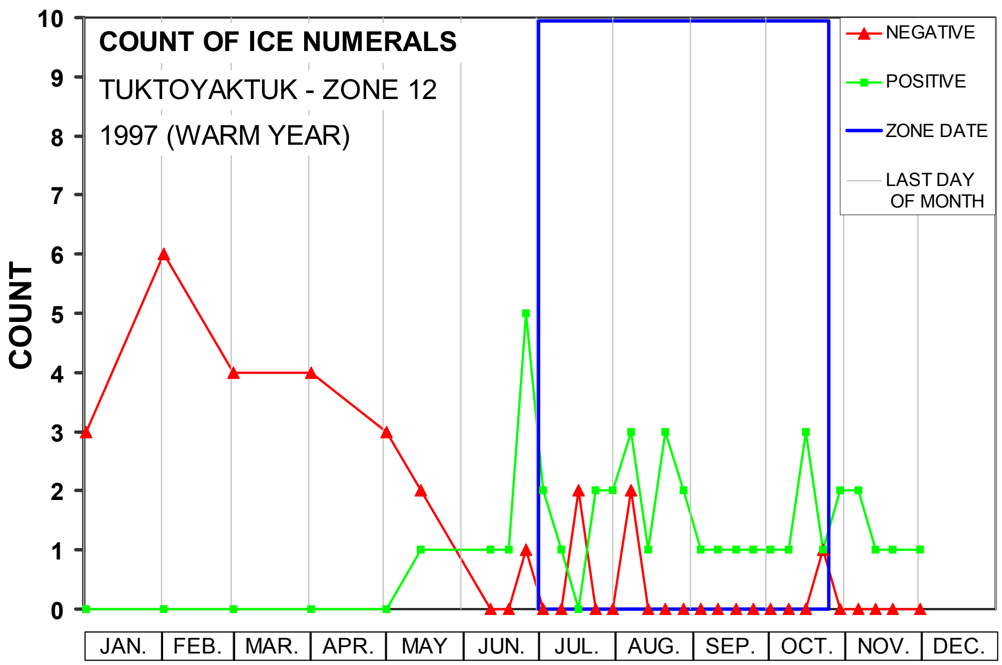

Figure B-68: Count of negative and positive Ice Numerals calculated from data plotted in Figure B-48 - the segment route in Zone 12, throughout the warmer than normal year

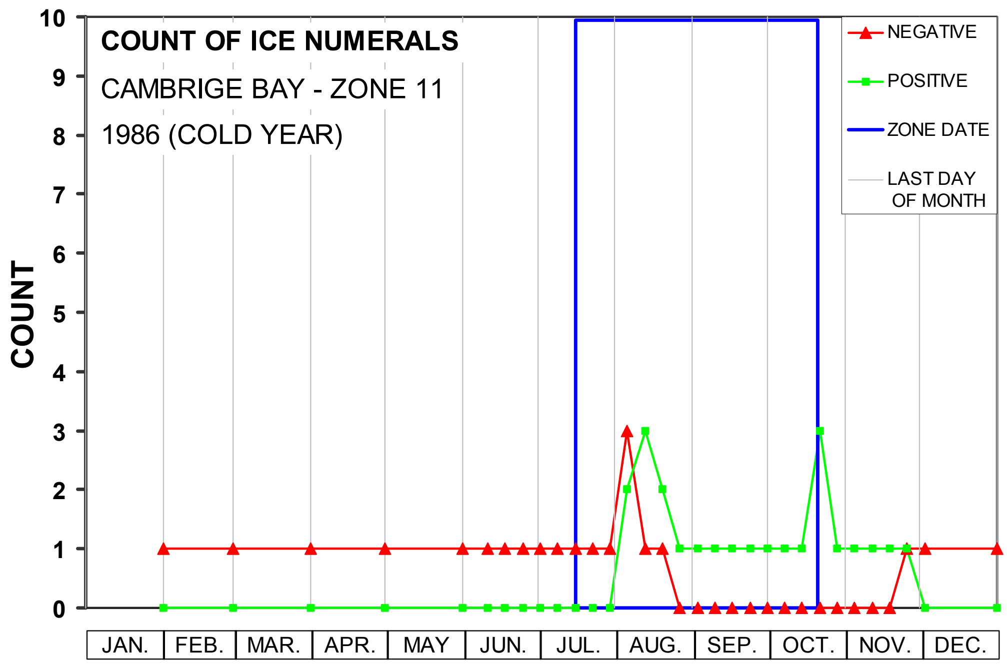

Figure B-69: Count of negative and positive Ice Numerals calculated from data plotted in Figure B-49 - the segment route in Zone 11, throughout the colder than normal year

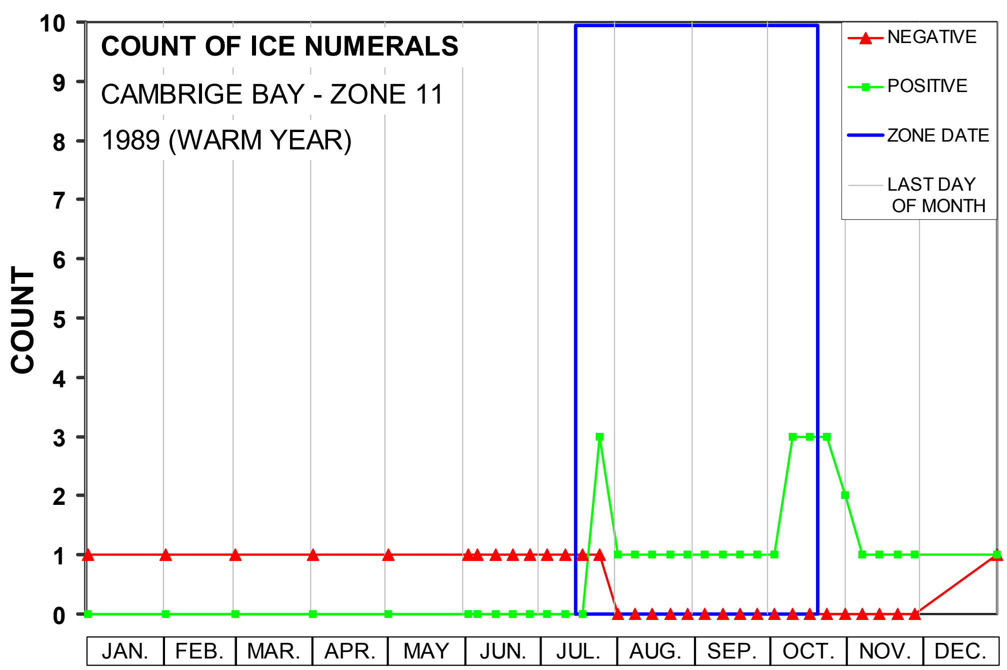

Figure B-70: Count of negative and positive Ice Numerals calculated from data plotted in Figure B-50 - the segment route in Zone 11, throughout the warmer than normal year

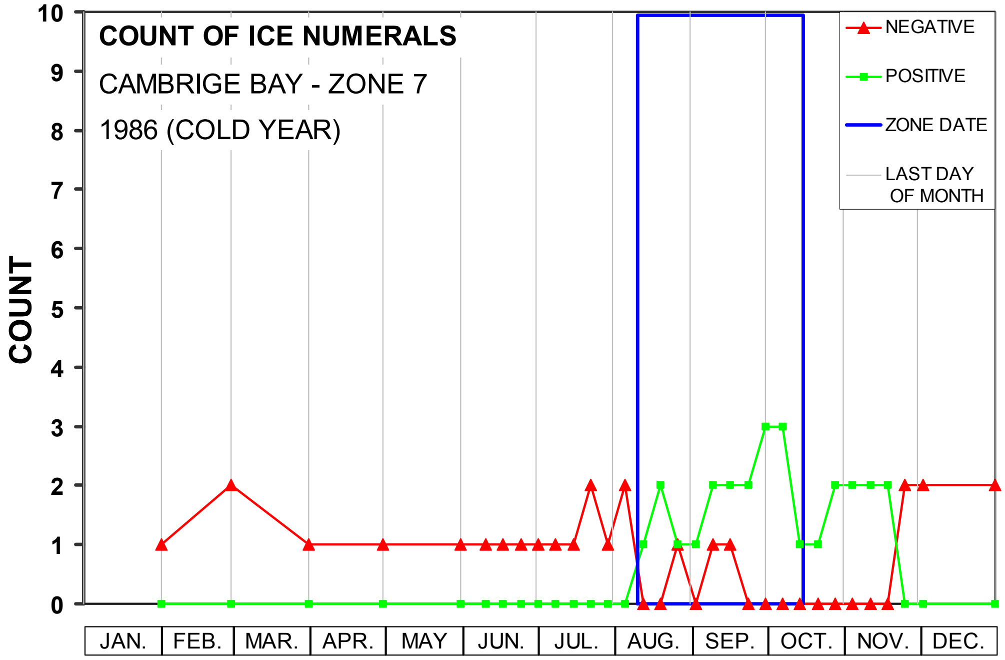

Figure B-71: Count of negative and positive Ice Numerals calculated from data plotted in Figure B-51 - the segment route in Zone 7, throughout the colder than normal year

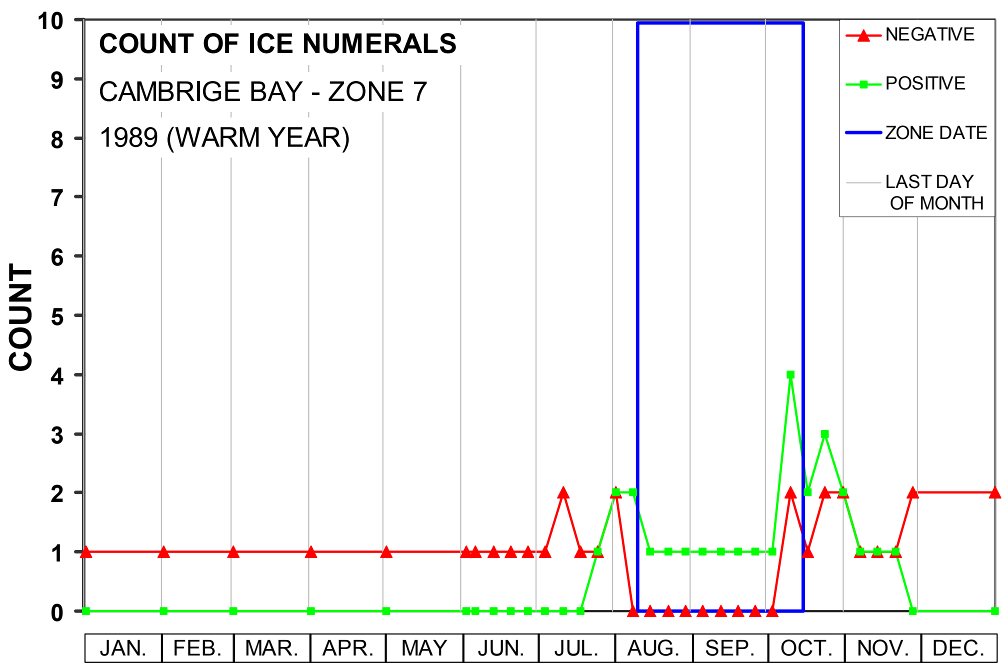

Figure B-72: Count of negative and positive Ice Numerals calculated from data plotted in Figure B-52 - the segment route in Zone 7, throughout the warmer than normal year

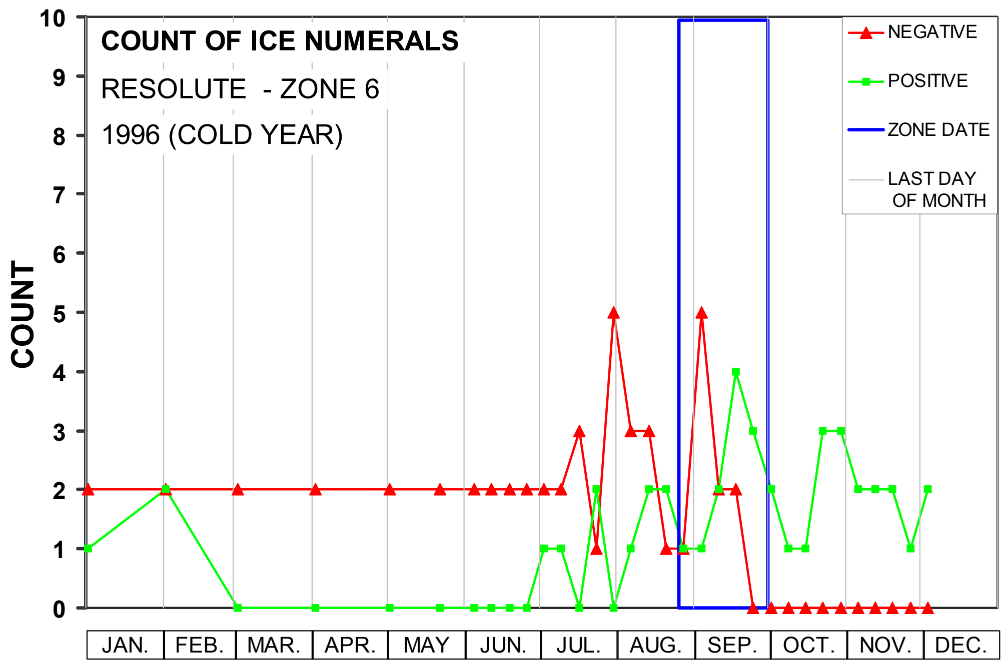

Figure B-73: Count of negative and positive Ice Numerals calculated from data plotted in Figure B-53 - the segment route in Zone 6, throughout the colder than normal year

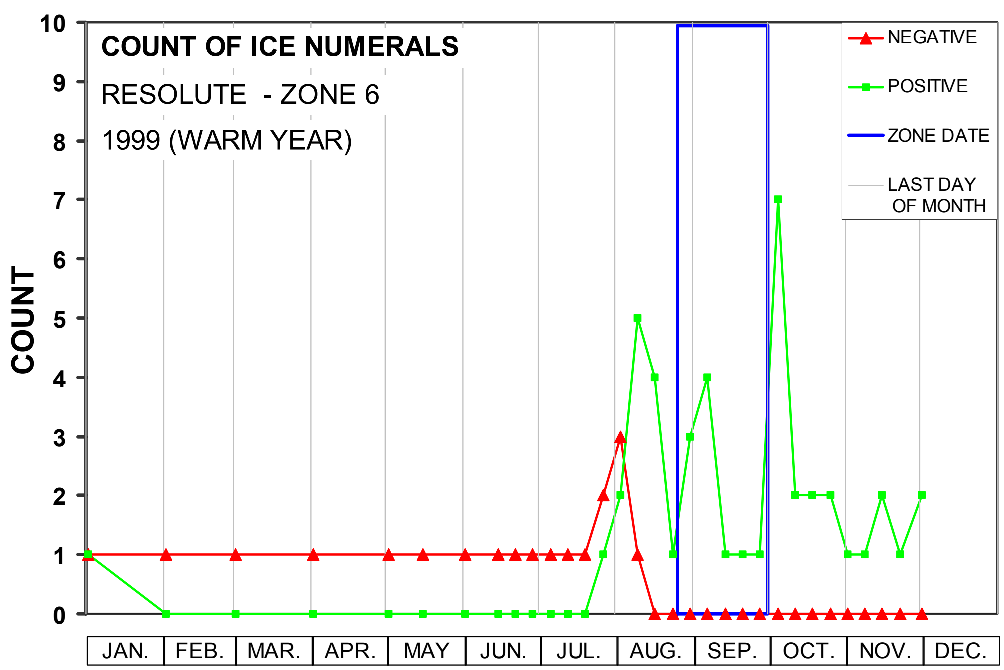

Figure B-74: Count of negative and positive Ice Numerals calculated from data plotted in Figure B-54 - the segment route in Zone 6, throughout the warmer than normal year

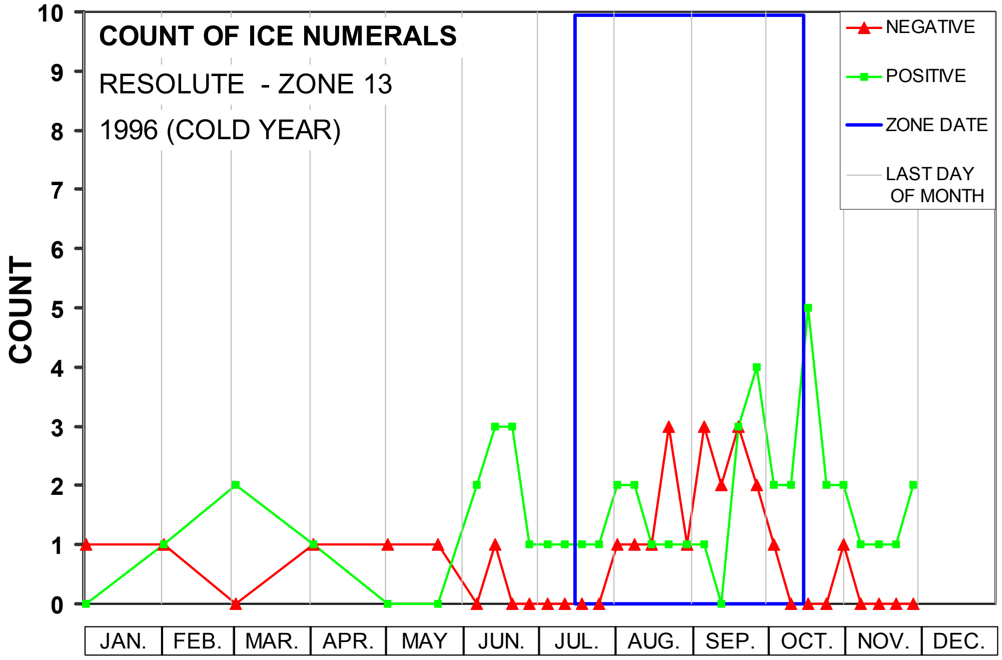

Figure B-75: Count of negative and positive Ice Numerals calculated from data plotted in Figure B-55 - the segment route in Zone 13, throughout the colder than normal year

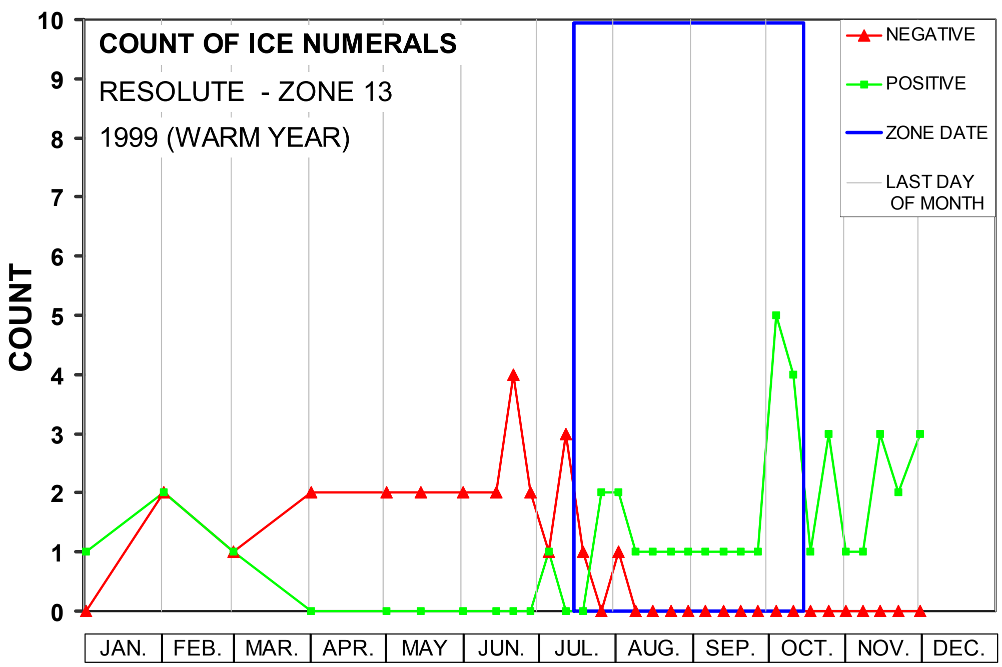

Figure B-76: Count of negative and positive Ice Numerals calculated from data plotted in Figure B-56 - the segment route in Zone 13, throughout the warmer than normal year

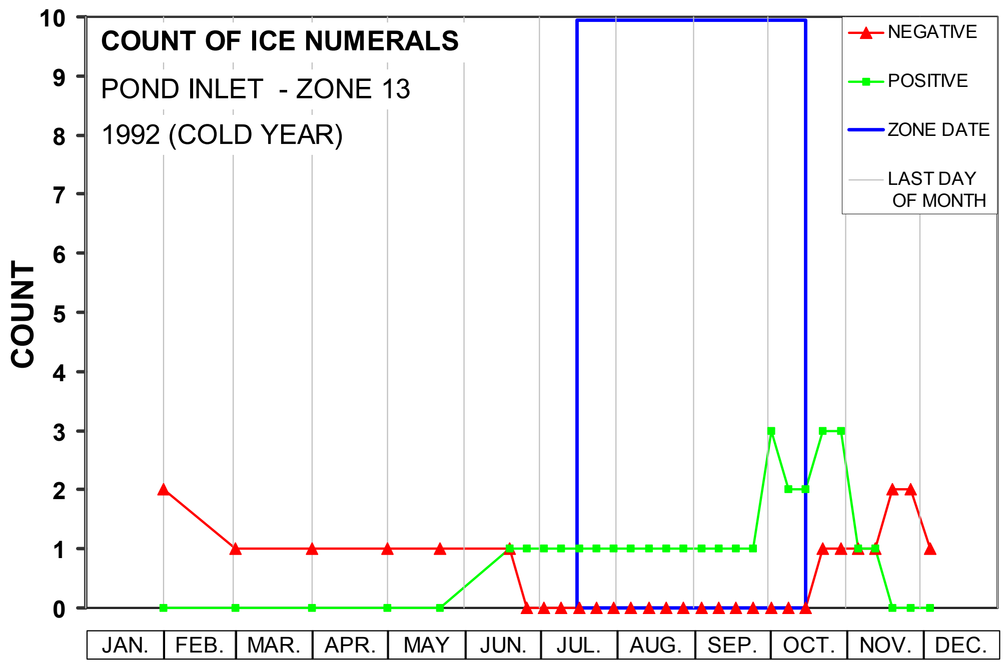

Figure B-77: Count of negative and positive Ice Numerals calculated from data plotted in Figure B-57 - the segment route in Zone 13, throughout the colder than normal year

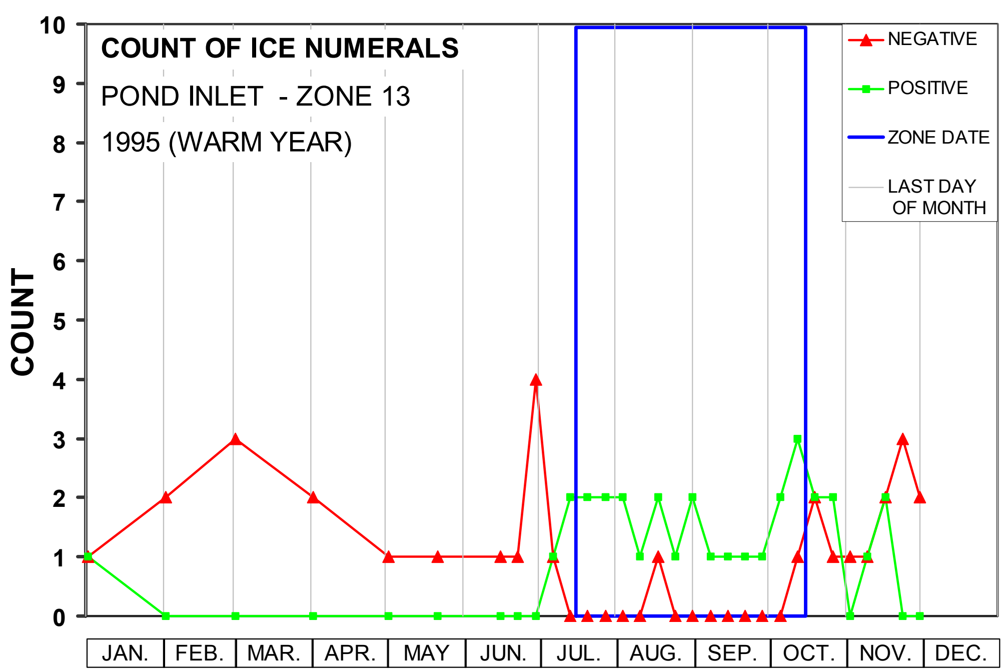

Figure B-78: Count of negative and positive Ice Numerals calculated from data plotted in Figure B-58 - the segment route in Zone 13, throughout the warmer than normal year

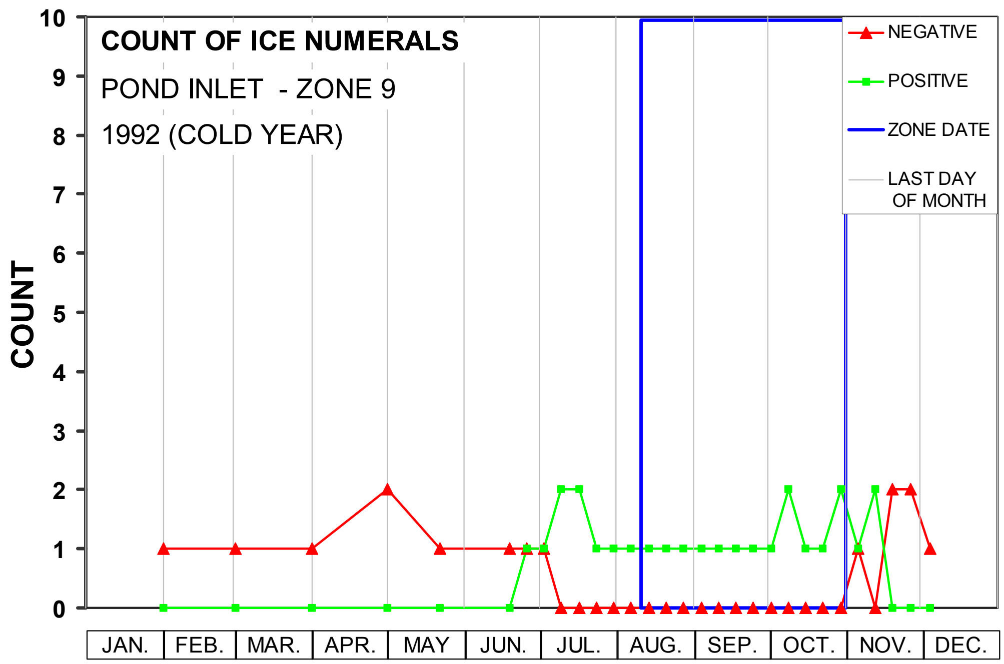

Figure B-79: Count of negative and positive Ice Numerals calculated from data plotted in Figure B-59 - the segment route in Zone 9, throughout the colder than normal year

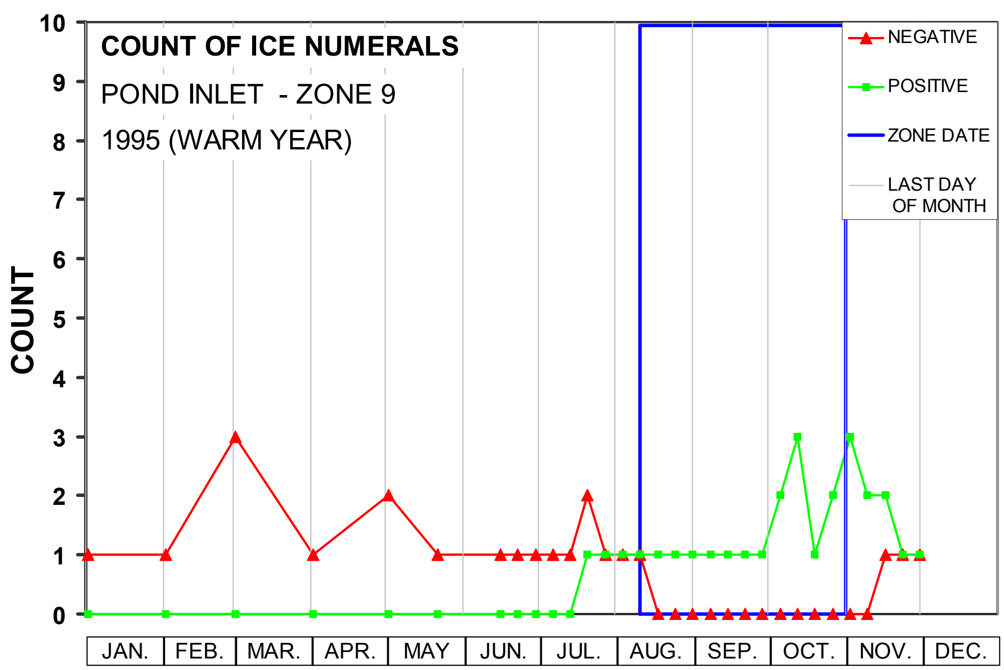

Figure B-80: Count of negative and positive Ice Numerals calculated from data plotted in Figure B-60 - the segment route in Zone 9, throughout the warmer than normal year

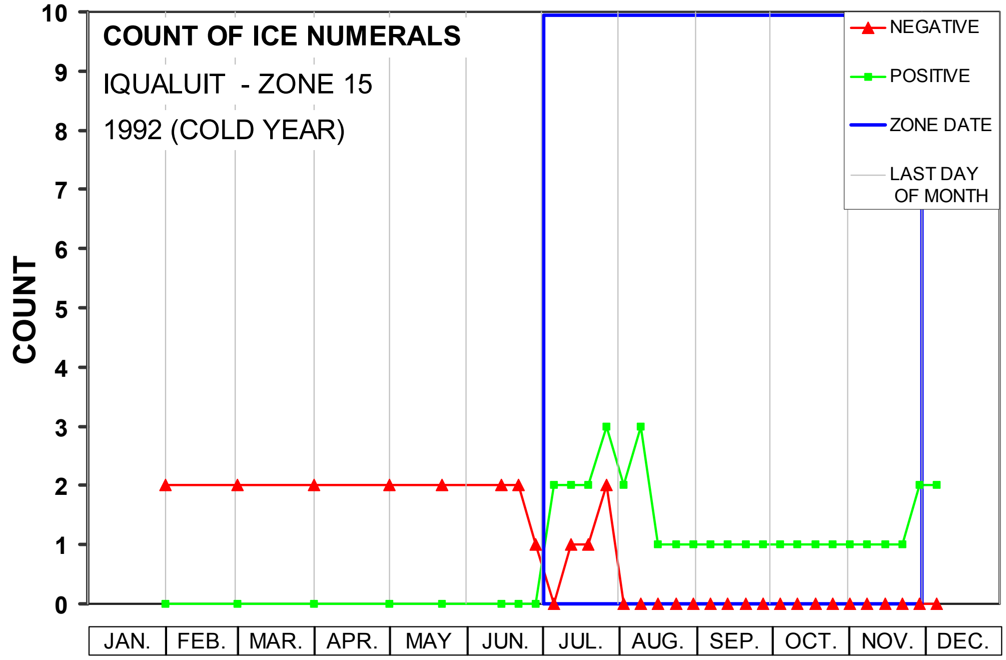

Figure B-81: Count of negative and positive Ice Numerals calculated from data plotted in Figure B-61 - the segment route in Zone 15, throughout the colder than normal year

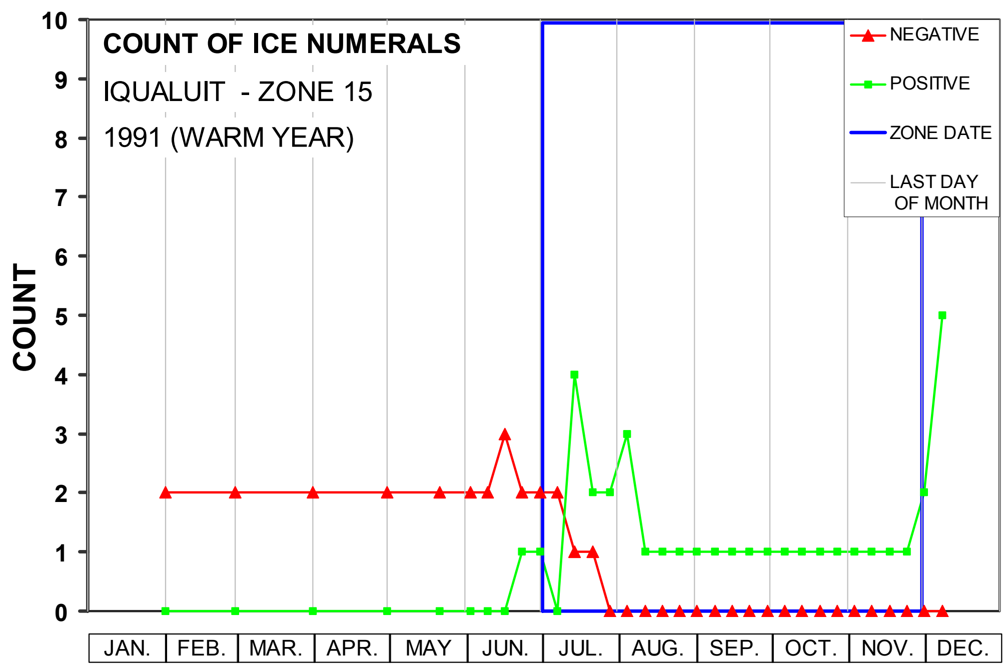

Figure B-82: Count of negative and positive Ice Numerals calculated from data plotted in Figure B-62 - the segment route in Zone 15, throughout the warmer than normal year

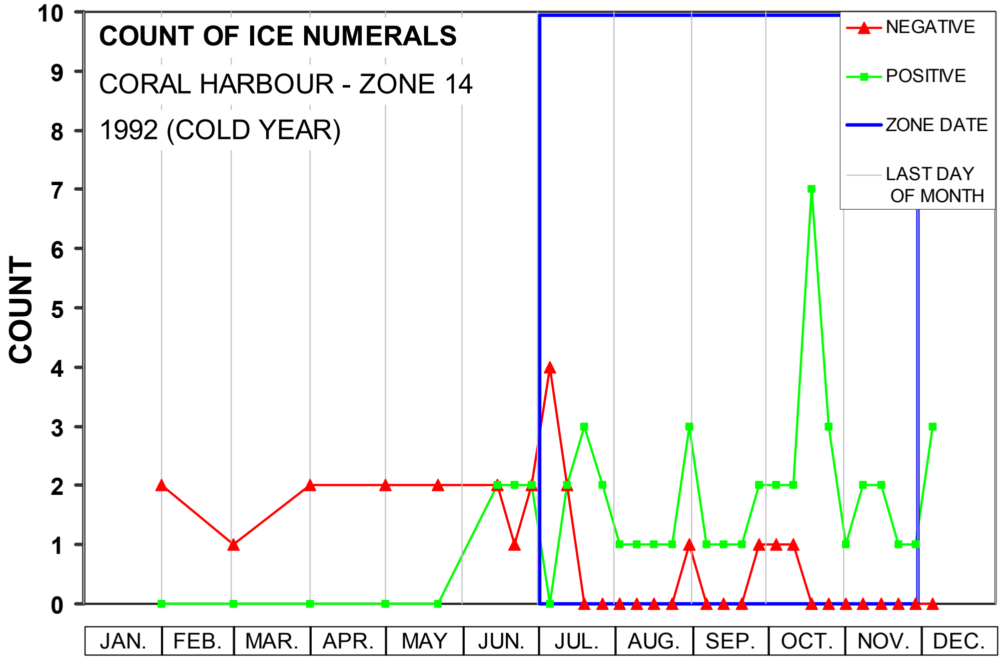

Figure B-83: Count of negative and positive Ice Numerals calculated from data plotted in Figure B-63 - the segment route in Zone 14, throughout the colder than normal year

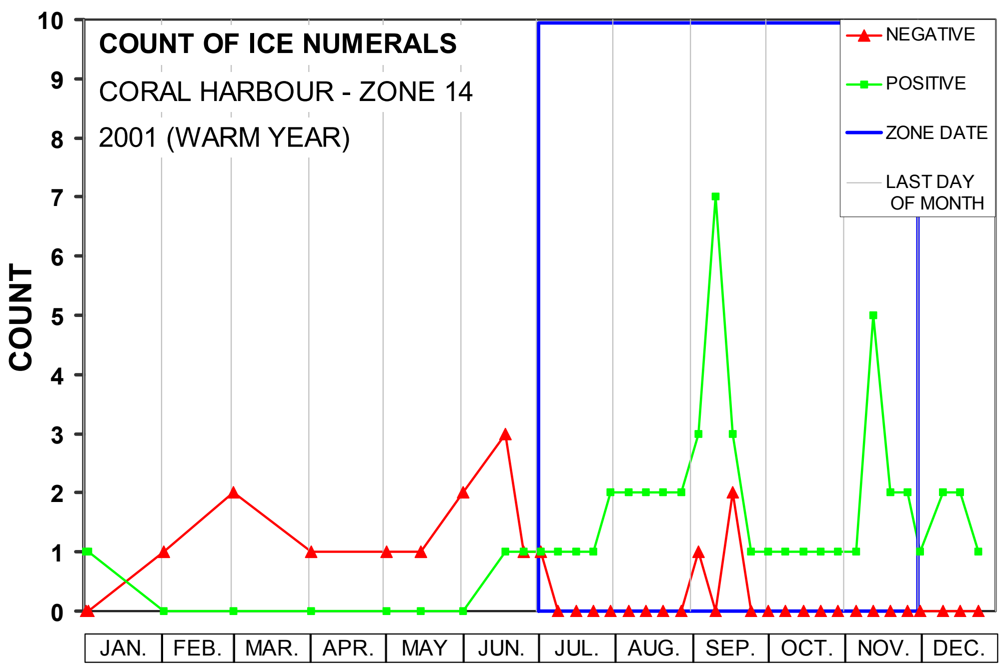

Figure B-84: Count of negative and positive Ice Numerals calculated from data plotted in Figure B-64 - the segment route in Zone 14, throughout the warmer than normal year

APPENDIX C. Ice Conditions Causing Changes in IN Values

1. Tuktoyaktuk – Zone 12
1985 – 0.088

High raise in the value of IN in May was caused by Arctic pack moving away from east side of C. Bathurst.

2. Tuktoyaktuk – Zone 12
1997 – 0.912

High drop in the values of INs was caused by Arctic pack reaching into Franklin Bay.

3. Cambridge Bay – Zone 7
1986 – 0.083

High drop in the value of INs was due to the presence of Old Ice in Victoria Strait.

4. Resolute – Zone 13
1999 – 0.889

High drop in the value of IN at the beginning of August was caused by Thick First-Year ice in Barrow Strait.

5. Pond Inlet – Zone 13
1995 – 0.931

High drop in the value of IN in the middle of August was due to that Old Ice has moved south from Kennedy Channel across the eastern entrance to Lancaster Sound.

6. Iqaluit – Zone 15
1991 – 0.889

A drop in the value of IN in the middle of July was caused by Old Ice beginning to move across the entrance to Frobisher Bay.

7. Coral Harbour – Zone 14
1992 – 0.083

The high drops in the values of INs at the end of August and at the end of September were due to high concentrations of Second-Year Ice moving southward from their location east of Southampton Island.

8. Coral Harbour – Zone 14
2001 – 0.889

High drops in the values of INs were due to circumvention of Ice in Evans Strait, south of Southampton Island.

9. Hudson Bay – Main Approach – Zone 14
1992 (Cold)

High drop in the value of INs at the beginning of October was due to high concentrations of Second-Year Ice between Southampton Island and Mansel Island (same time and place as 7 above).

10. Hudson Bay – Alternate Approach – Zone 14
1992 (Cold)

High drop in the values of INs in October was due to a tongue of Old and Thick First-Year ice drifting around the eastern portion of Southampton Island from the Foxe Basin.

11. Northwest Passage - Zone 12
1986 (cold)

The drops in the value of INs were caused by Beaufort Sea ice pack that was approaching Cape Bathurst in August.

12. Northwest Passage - Zone 12
1998 (warm)

High drop in the value of the IN in the middle of June was due to Thick First-Year ice present west of Herschel Island.

13. Northwest Passage - Zone 11
1986 (cold)

High drop in the value of the INs in the beginning of July was caused by high concentrations of Thick First-Year ice in eastern Amundsen Gulf. The Coronation Gulf was still fast with Thick First-Year ice.

14. Northwest Passage - Zone 13
1998 (warm)

High drop in the value of IN in August was caused by the southward drift of Old Ice from Wellington Channel into the northern reaches of eastern Barrow Strait east of Resolute.

APPENDIX D. Ice Coverage in Shipping Routes

APPENDIX D-1. Northwest Passage

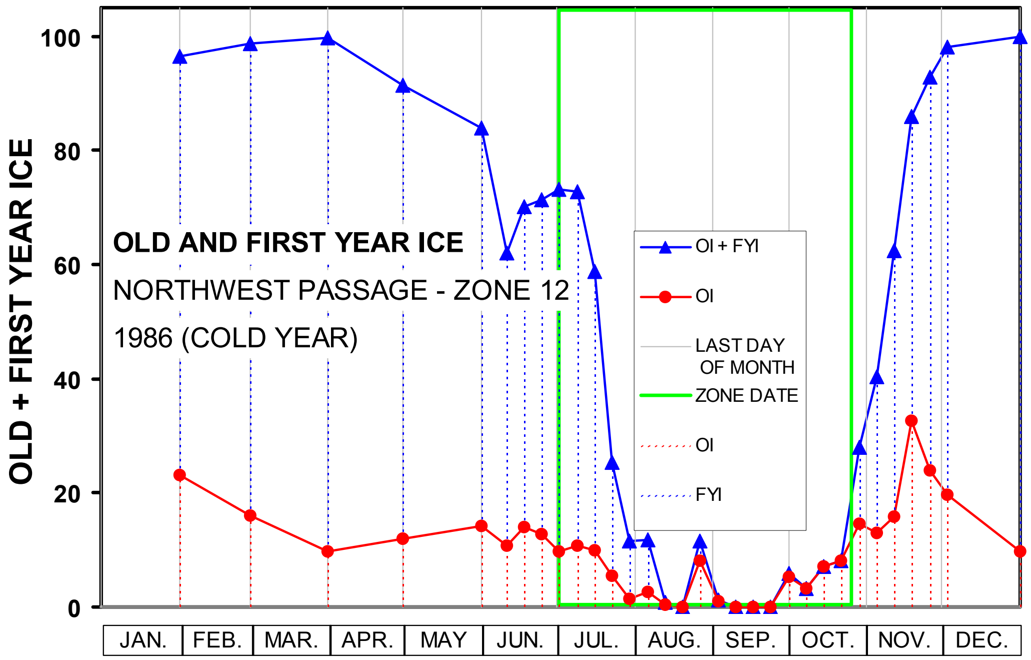

Figure D-1: The ice coverage in the NWP in Zone 12 throughout the colder than normal year

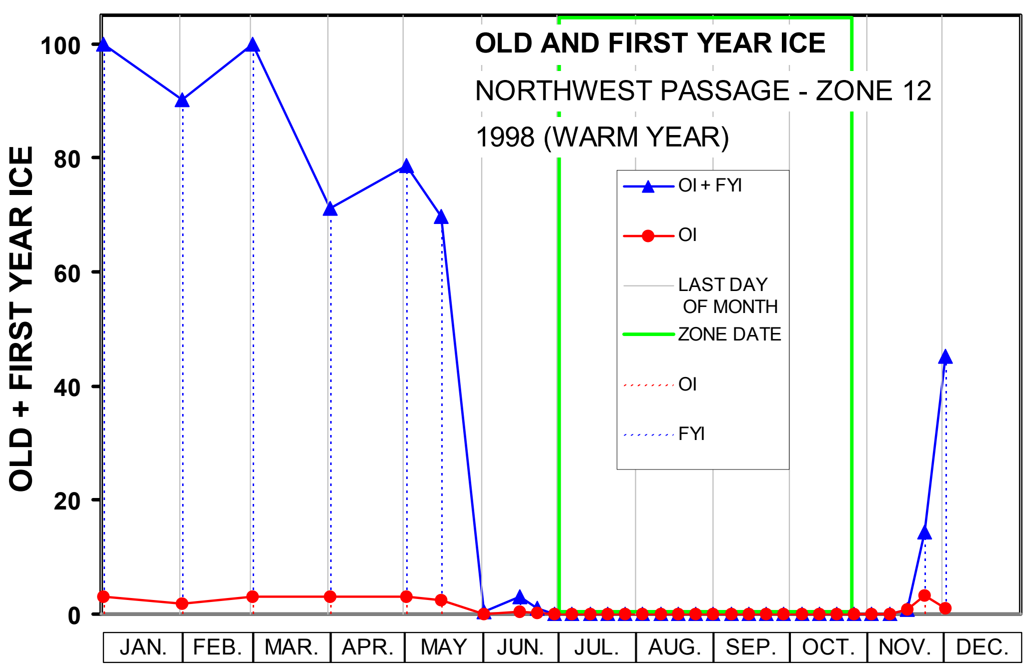

Figure D-2: The ice coverage in the NWP in Zone 12 throughout the warmer than normal year

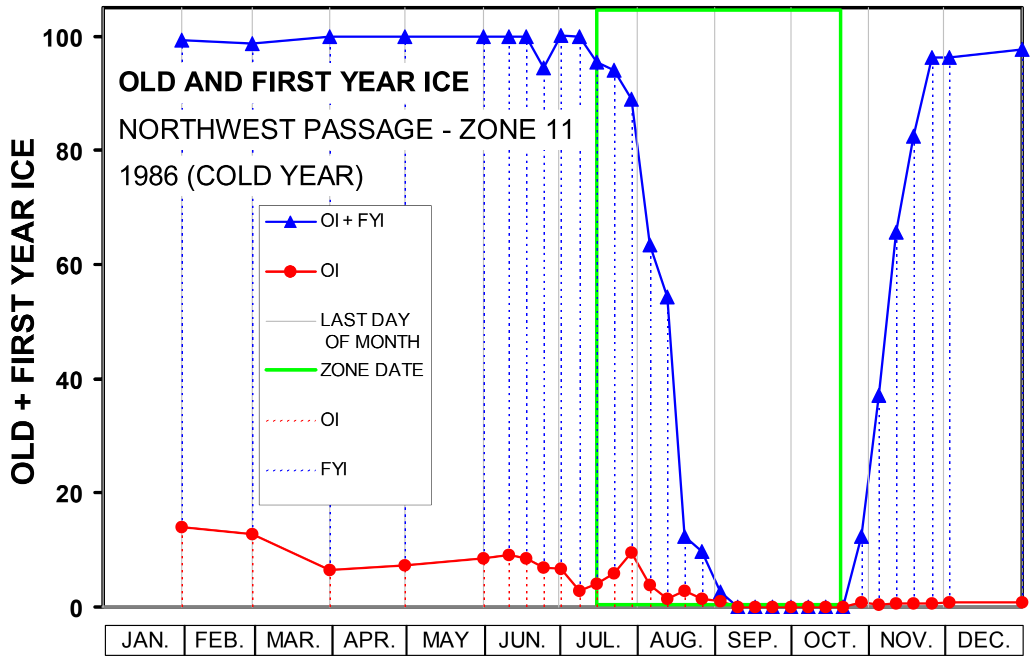

Figure D-3: The ice coverage in the NWP in Zone 11 throughout the colder than normal year

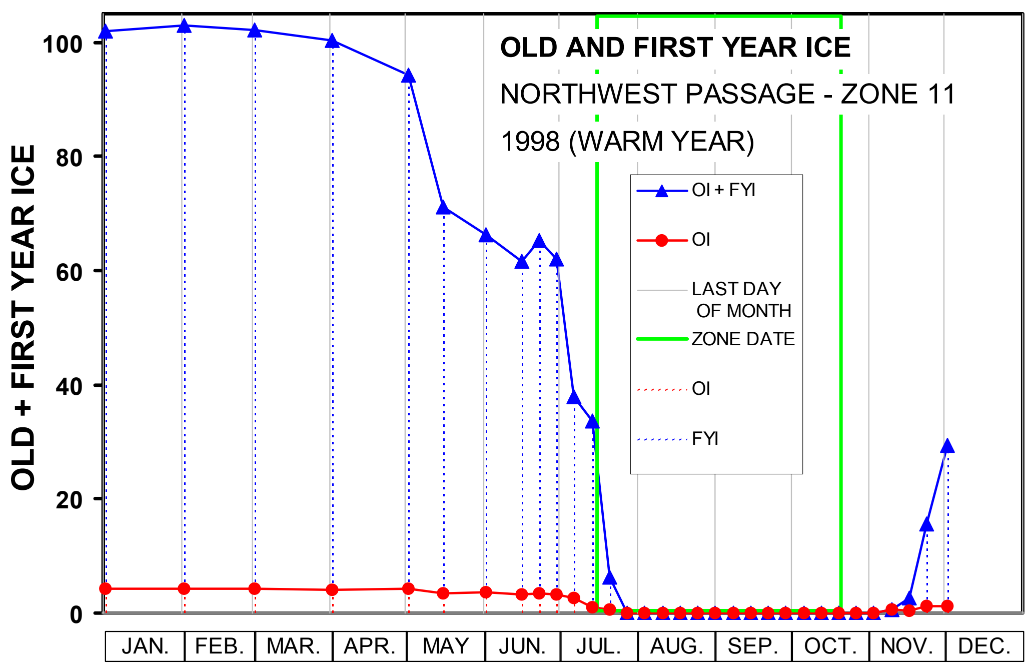

Figure D-4: The ice coverage in the NWP in Zone 11 throughout the warmer than normal year

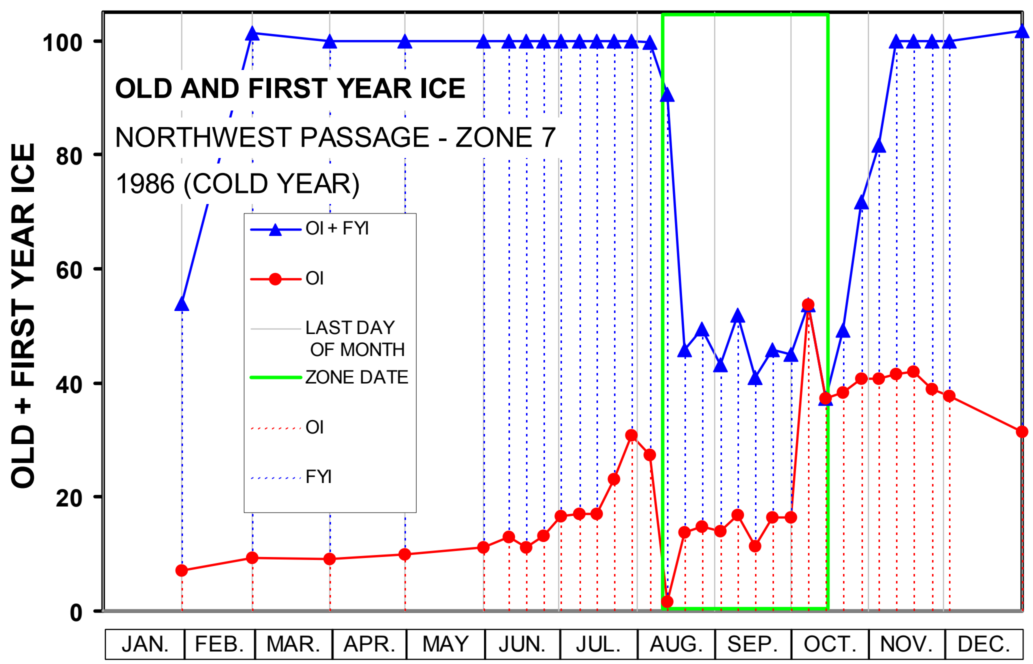

Figure D-5: The ice coverage in the NWP in Zone 7 throughout the colder than normal year

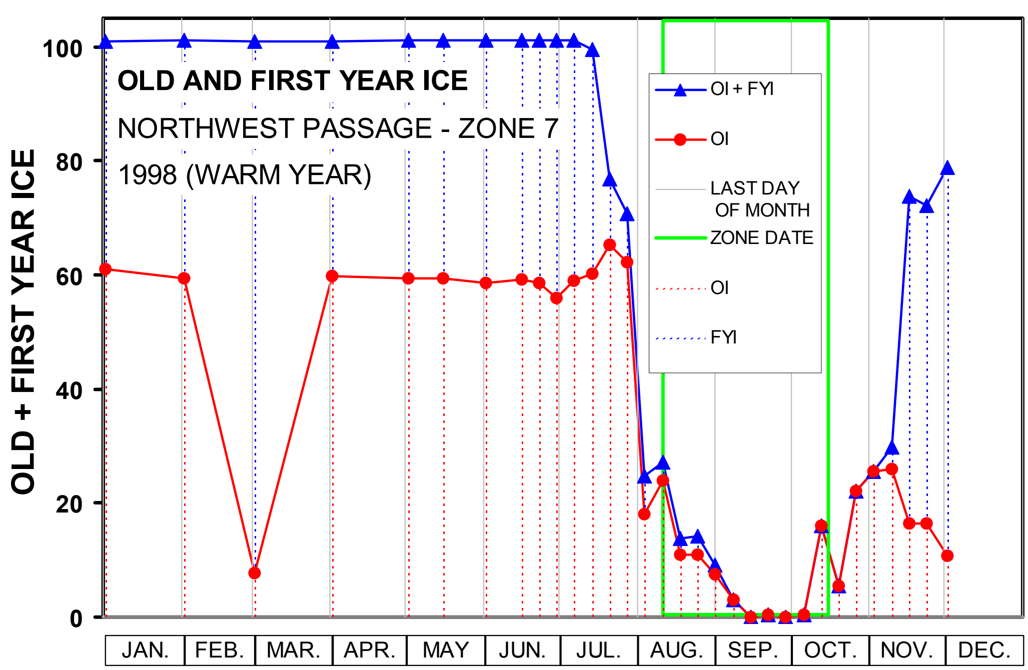

Figure D-6: The ice coverage in the NWP in Zone 7 throughout the warmer than normal year

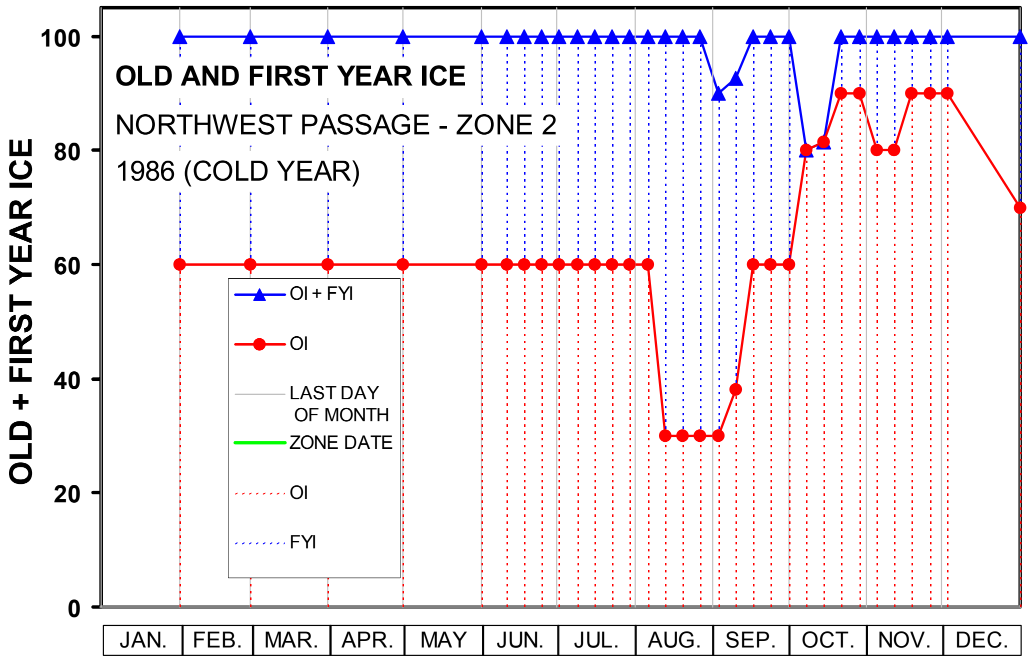

Figure D-7: The ice coverage in the NWP in Zone 2 throughout the colder than normal year

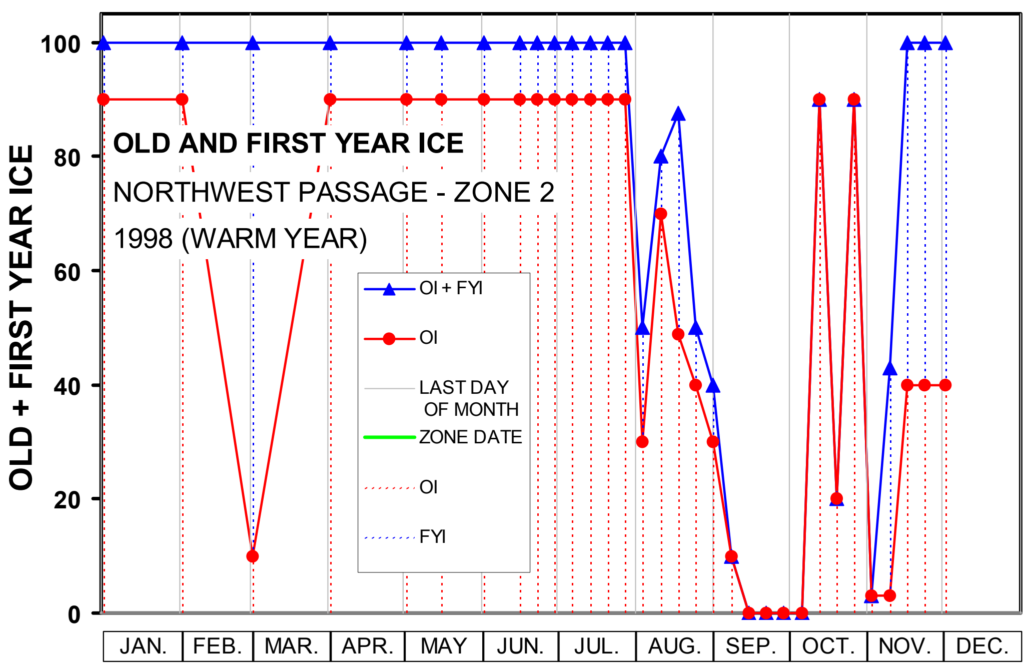

Figure D-8: The ice coverage in the NWP in Zone 2 throughout the warmer than normal year

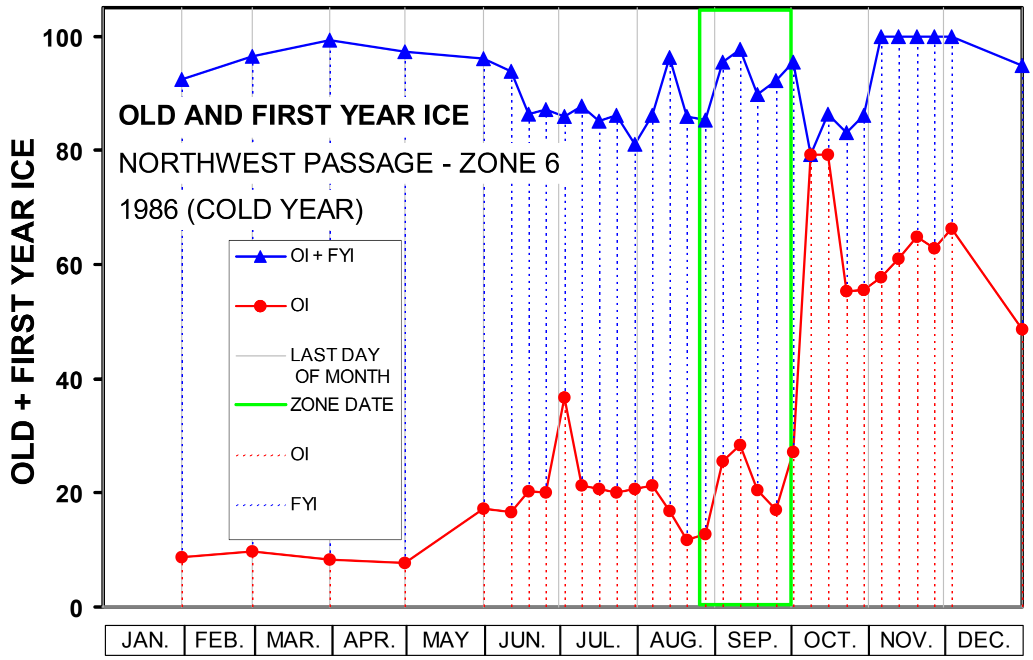

Figure D-9: The ice coverage in the NWP in Zone 6 throughout the colder than normal year

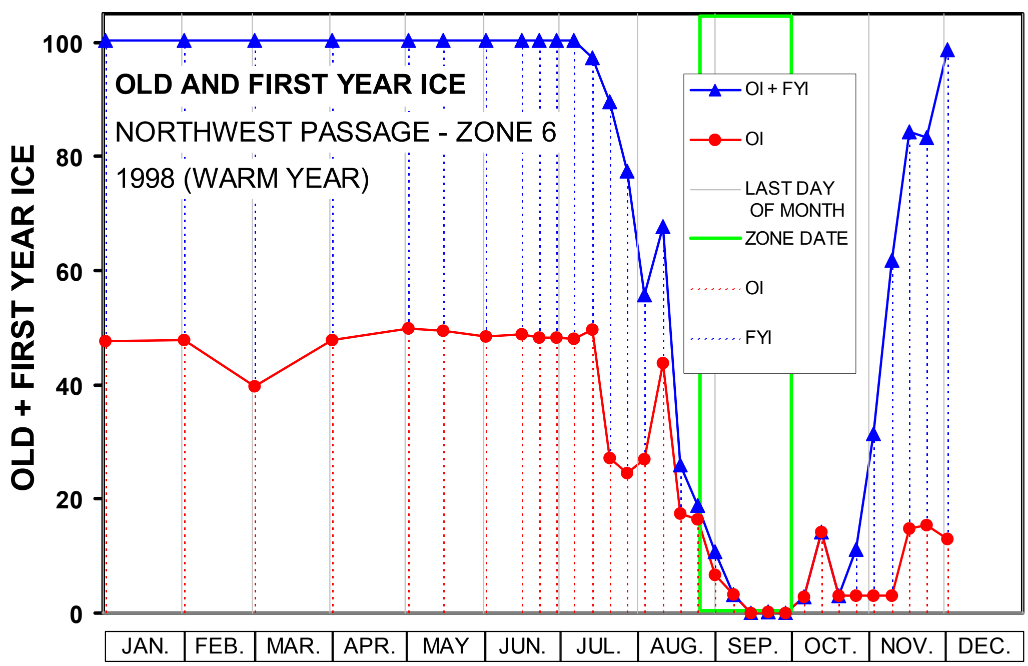

Figure D-10: The ice coverage in the NWP in Zone 6 throughout the warmer than normal year

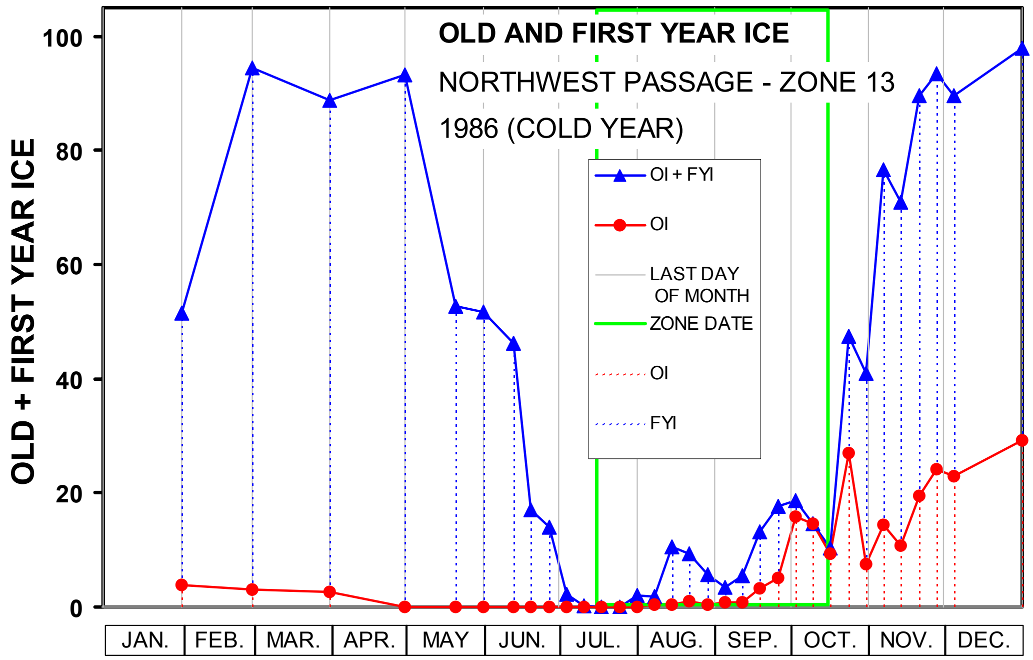

Figure D-11: The ice coverage in the NWP in Zone 13 throughout the colder than normal year

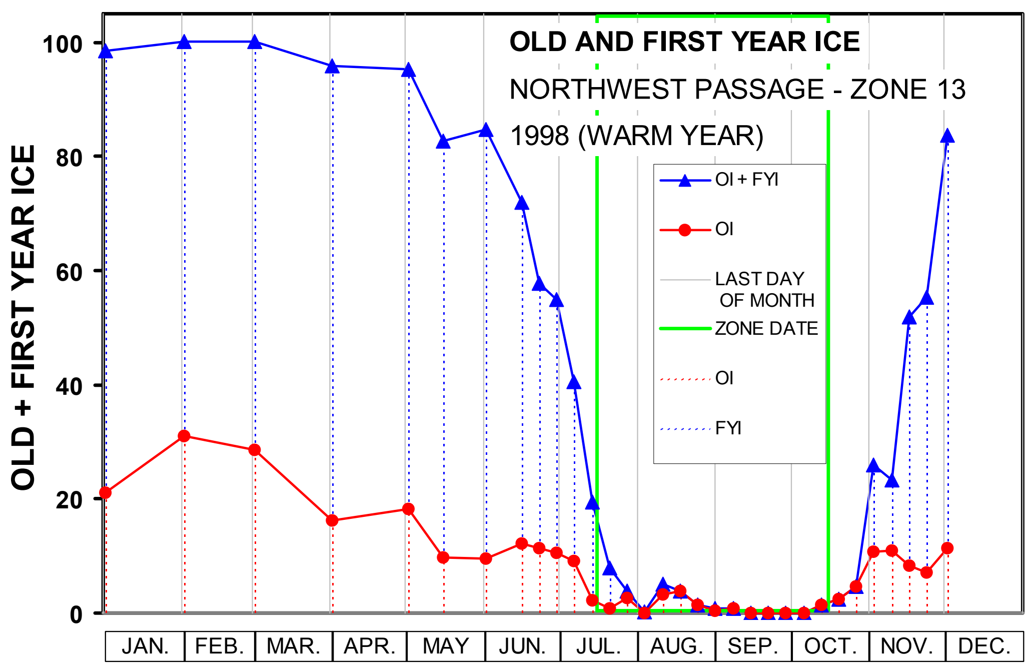

Figure D-12: The ice coverage in the NWP in Zone 13 throughout the warmer than normal year

APPENDIX D-2. Access Routes to Port of Churchill

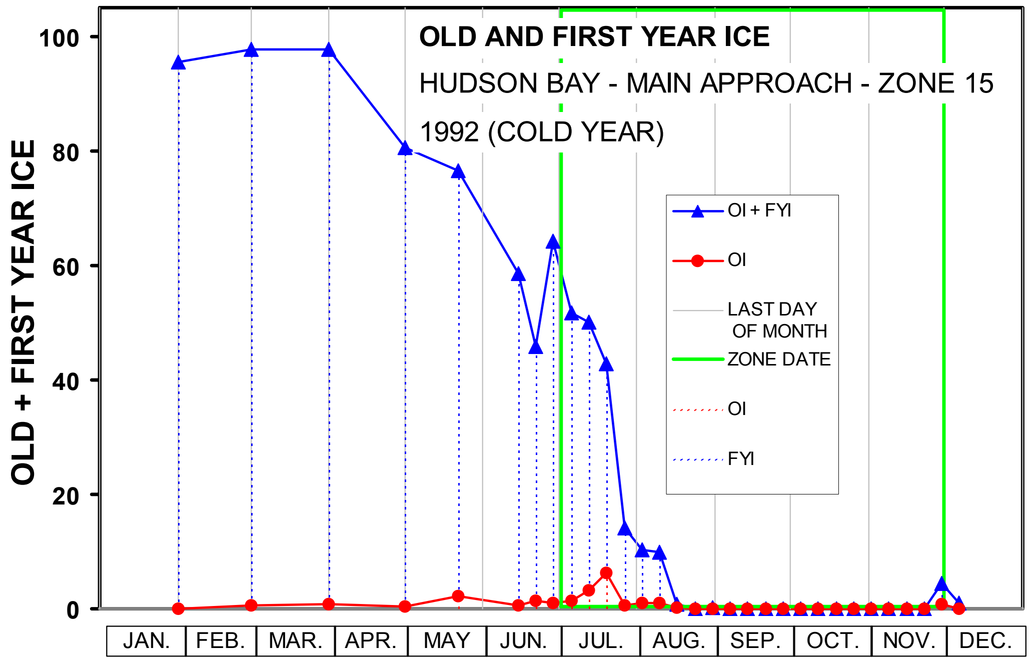

Figure D-13: The ice coverage in the access route to the Port of Churchill in Zone 15 - main approach, throughout the colder than normal year

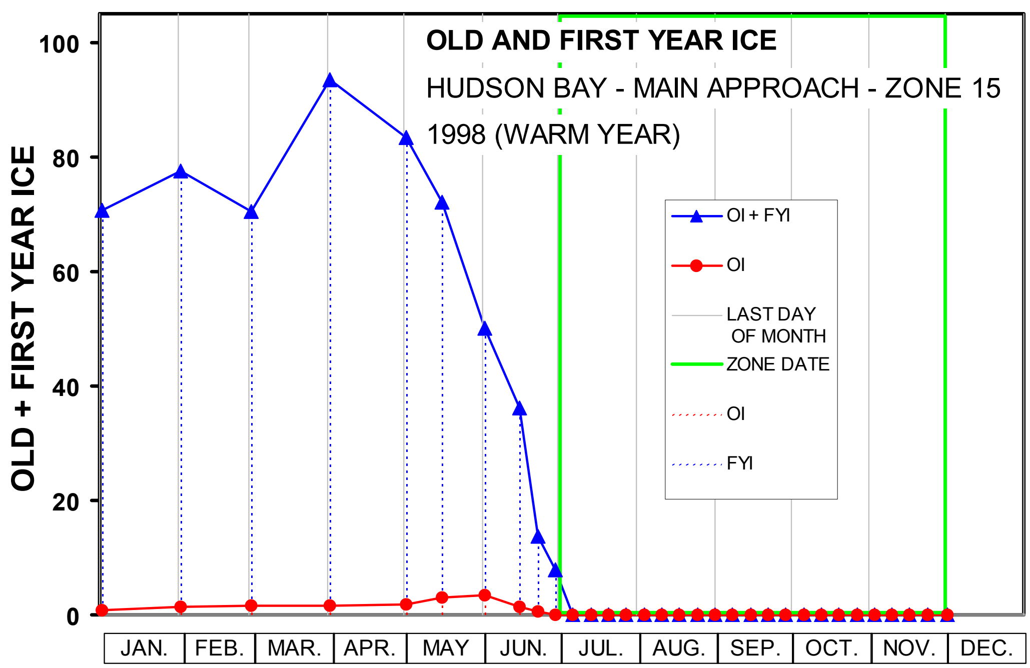

Figure D-14: The ice coverage in the access route to the Port of Churchill in Zone 15 - main approach, throughout the warmer than normal year

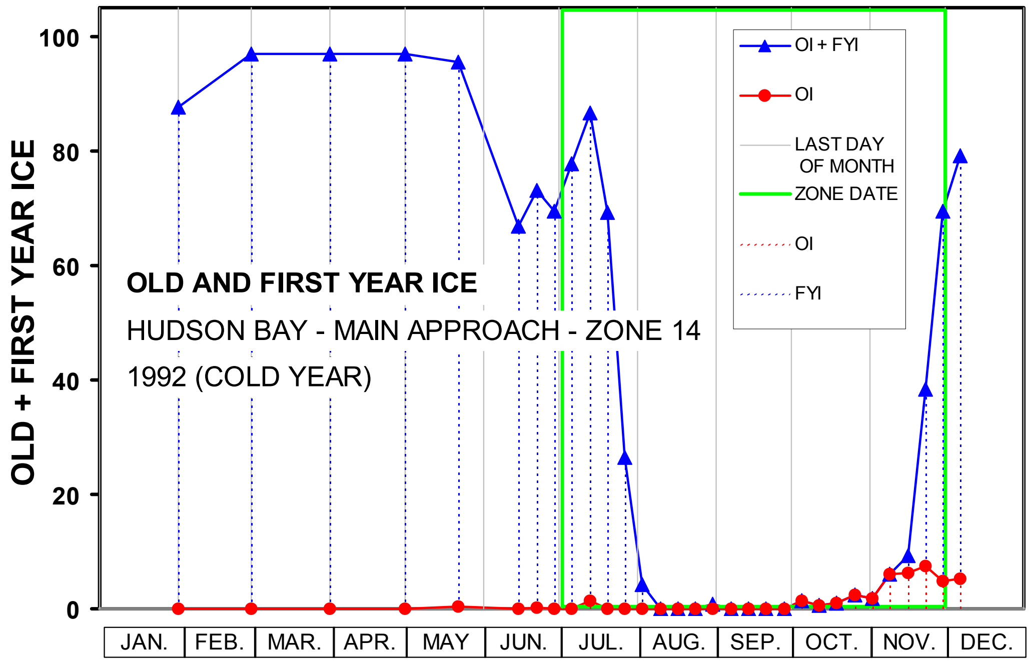

Figure D-15: The ice coverage in the access route to the Port of Churchill in Zone 14 - main approach, throughout the colder than normal year

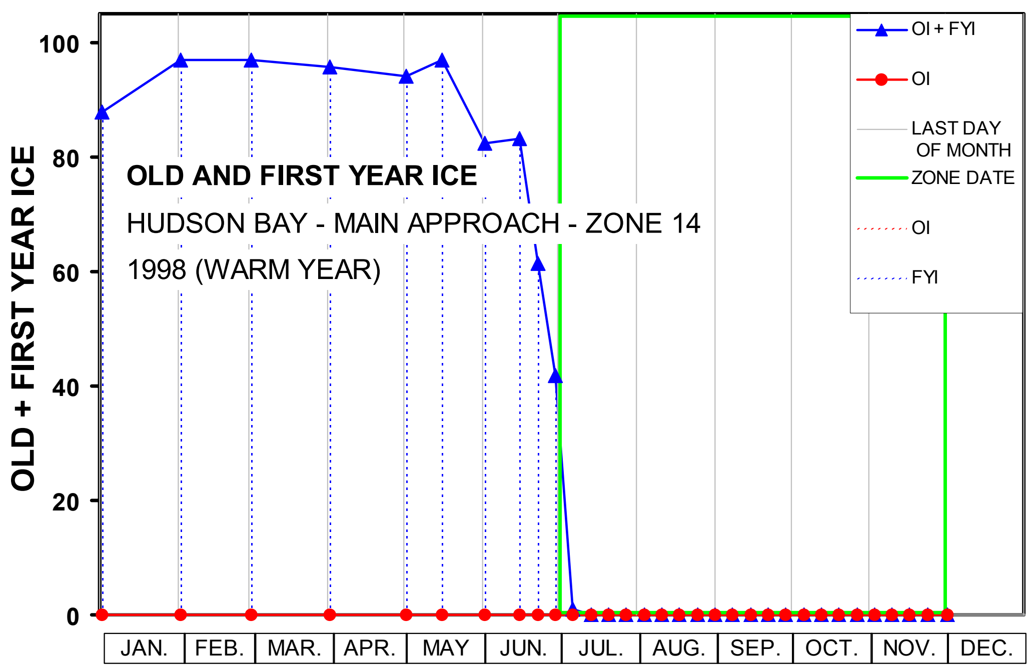

Figure D-16: The ice coverage in the access route to the Port of Churchill in Zone 14 - main approach, throughout the warmer than normal year

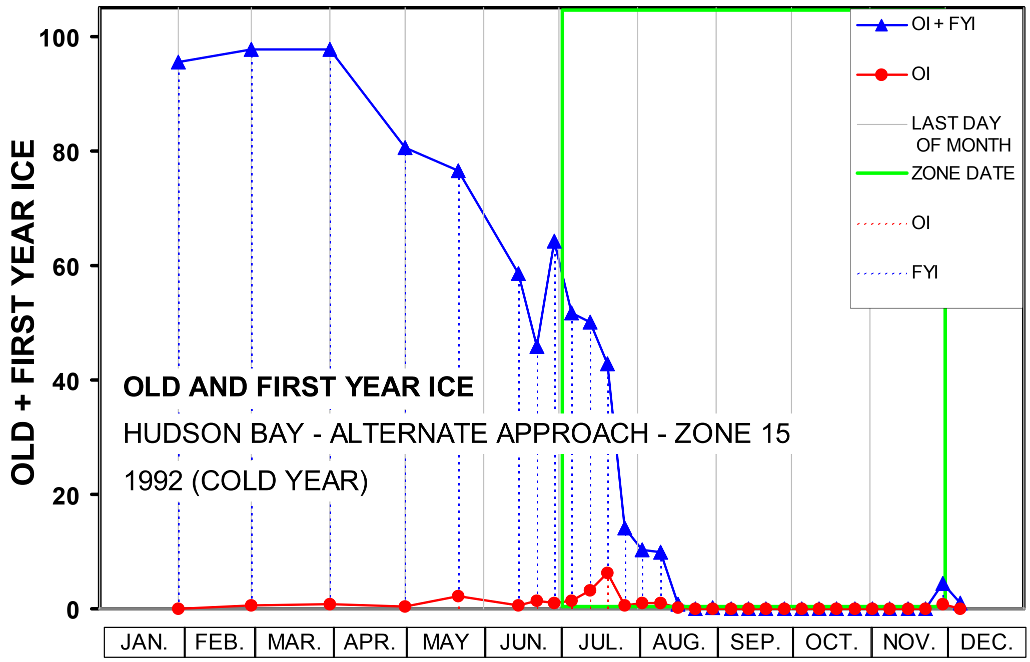

Figure D-17: The ice coverage in the access route to the Port of Churchill in Zone 15 - alternate approach, throughout the colder than normal year

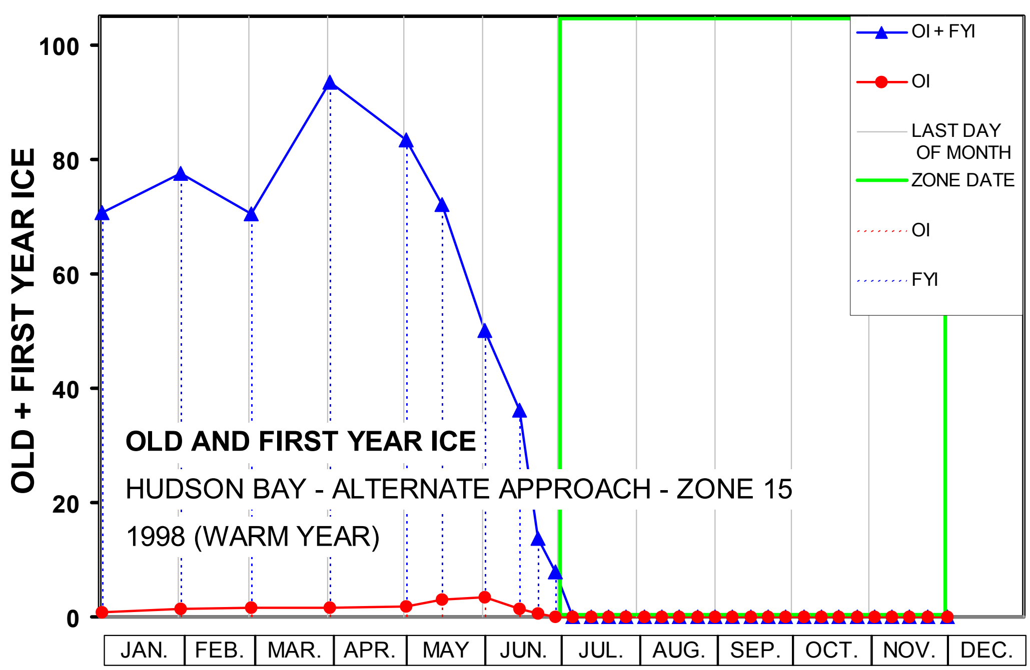

Figure D-18: The ice coverage in the access route to the Port of Churchill in Zone 15 - alternate approach, throughout the warmer than normal year

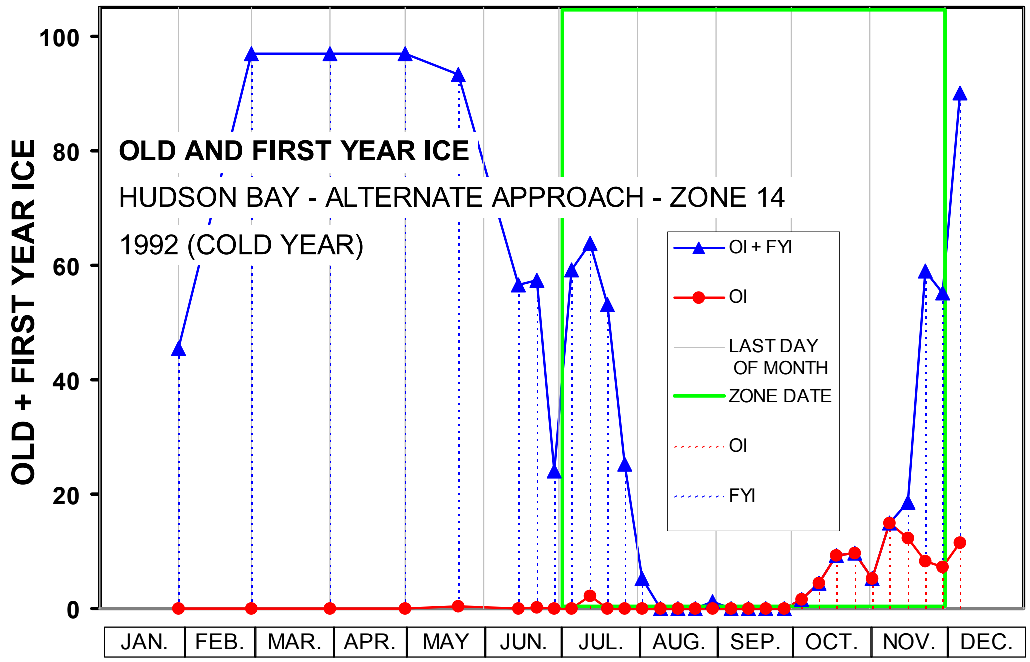

Figure D-19: The ice coverage in the access route to the Port of Churchill in Zone 14 - alternate approach, throughout the colder than normal year

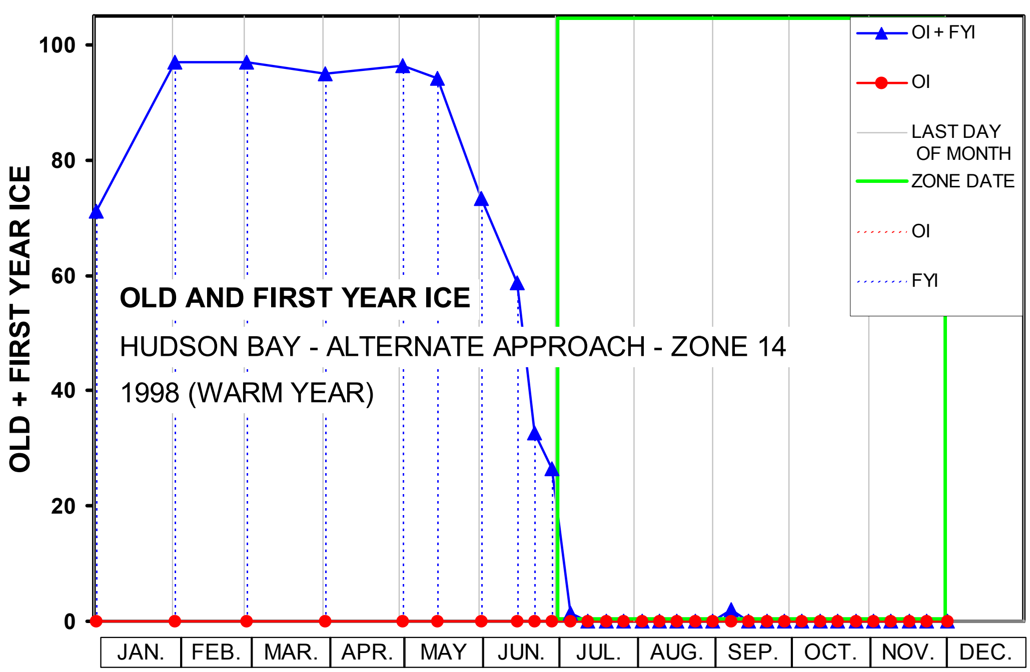

Figure D-20: The ice coverage in the access route to the Port of Churchill in Zone 14 - alternate approach, throughout the warmer than normal year

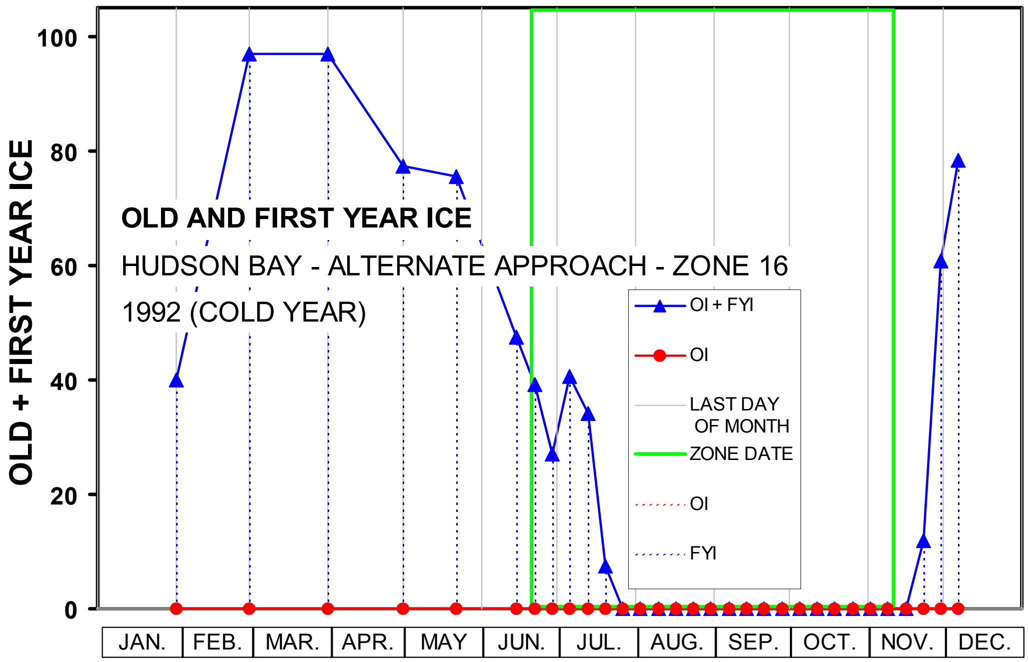

Figure D-21: The ice coverage in the access route to the Port of Churchill in Zone 16 - alternate approach, throughout the colder than normal year

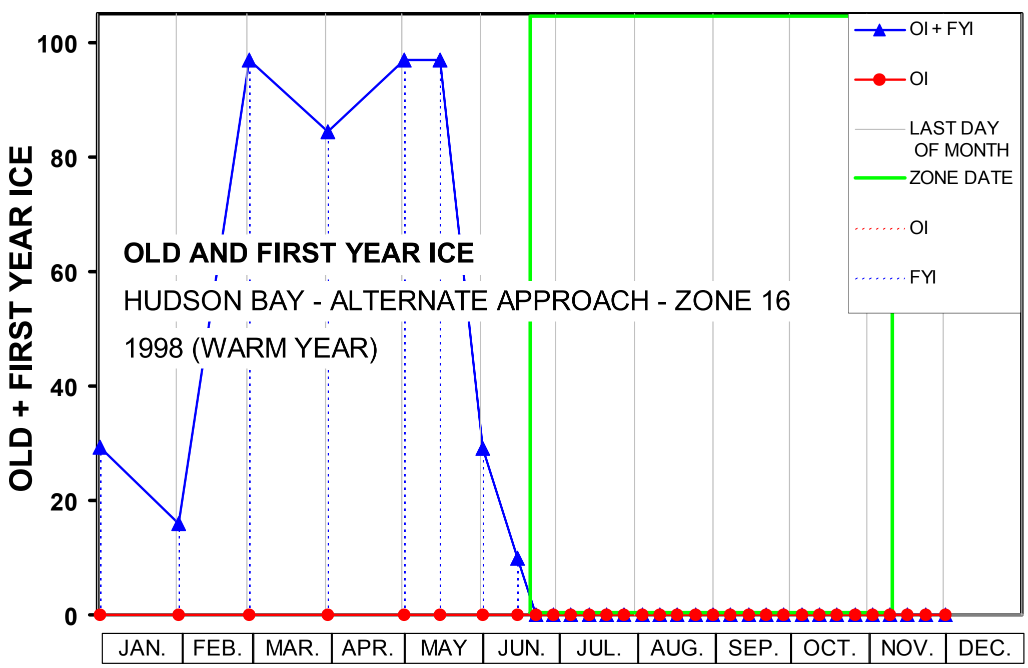

Figure D-22: The ice coverage in the access route to the Port of Churchill in Zone 16 - alternate approach, throughout the warmer than normal year